A biomechanical analysis of the trunk and spine during paediatric cerebral palsy gait.

Damien Kiernan B.E., M.Sc.
05169143

A thesis submitted to the University of Dublin in fulfilment of the Degree of Doctor of Philosophy

Department of Mechanical and Manufacturing Engineering
University of Dublin
Trinity College

Supervisor: Dr. Ciaran K. Simms
Internal Examiner: Prof. David Taylor
External Examiner: Prof. Richard Baker

June 2017

Declaration

I, Damien Kiernan, declare that this thesis has not been submitted as an exercise for a degree at this or any other university and it is entirely my own work.

I agree to deposit this thesis in the University's open access institutional repository or allow the library to do so on my behalf, subject to Irish Copyright Legislation and Trinity College Library conditions of use and acknowledgement.

Signed: _____

Damien Kiernan B.E., M.Sc.

Date: _____

If

If you can keep your head when all about you
are losing theirs and blaming it on you,
If you can trust yourself when all men doubt you,
But make allowance for their doubting too;
If you can wait and not be tired by waiting,
Or being lied about, don't deal in lies,
Or being hated, don't give way to hating,
And yet don't look too good, nor talk too wise:

If you can dream - and not make dreams your master;
If you can think - and not make thoughts your aim;
If you can meet with Triumph and Disaster
And treat those two impostors just the same;
If you can bear to hear the truth you've spoken
Twisted by knaves to make a trap for fools,
Or watch the things you gave your life to, broken,
And stoop and build 'em up with worn-out tools:

If you can make one heap of all your winnings
And risk it on one turn of pitch-and-toss,
And lose, and start again at your beginnings
And never breathe a word about your loss;
If you can force your heart and nerve and sinew
To serve your turn long after they are gone,
And so hold on when there is nothing in you
Except the Will which says to them: 'Hold on!'

If you can talk with crowds and keep your virtue,
Or walk with Kings - nor lose the common touch,
If neither foes nor loving friends can hurt you,
If all men count with you, but none too much;
If you can fill the unforgiving minute
With sixty seconds' worth of distance run,
Yours is the Earth and everything that's in it,
And - which is more - you'll be a Man, my son!

Rudyard Kipling

Abstract

Movement pathologies in the lower limbs of children with cerebral palsy are well established in the literature. However, movement pathologies of the upper body, in particular the trunk, are less well defined. Mechanical loads at the spine and the surrounding areas are influenced by gravity, inertia and externally applied loads and pathological motion patterns could result in mechanical changes in structural tissue surrounding the spine over time. Consequently, this thesis reports an investigation into the relationship between pathological movement of the trunk and loading at the lower lumbar spine. The specific impact of Trendelenburg and Duchenne type movement patterns on loading at the lower lumbar spine was also examined.

Prior to assessment, the role of gait analysis in the assessment of trunk and lower lumbar spinal loading was considered. This highlighted a number of issues relating to the kinematic and kinetic models that warranted further investigation. Specifically, those issues related to (1) the choice of body segment parameter set, (2) the choice of hip joint centre regression equation set, (3) the thorax kinematic protocol and (4) the lumbar segment kinematic protocol. Before data were collected to address the primary goals of the thesis, a number of preparatory studies were therefore conducted.

The first two preparatory studies identified the most suitable choice of body segment parameter and hip joint centre regression equation sets for the purposes of this thesis. Next, a thorax kinematic protocol was proposed to address some of the practical issues experienced when using other protocols during the assessment procedure. As a preliminary evaluation before use, the protocol was compared to two reference protocols from the literature and performed well and was later used in the thesis. A separate investigation into choice of lumbar segment kinematic protocol identified a skin surface protocol as suitable for studies where axial rotation may be a consideration and so was used in this thesis.

With the kinematic and kinetic models in place, 3-dimensional thoracic, lumbar and L5/S1 kinetics were measured in 52 children with cerebral palsy and 26 typically developed children. Differences were present for cerebral palsy children, most notably in the coronal plane for thorax kinematics and L5/S1 kinetics. Peak L5/S1 moment data were up to 21% higher than normal for GMFCS level one children and up to 90% higher than normal for GMFCS level two children. Moderate to strong correlations were evident between movement of the thorax and L5/S1 loading ($r = 0.52$). However, other factors may have contributed to this loading and further investigation was suggested, perhaps by means of forward dynamics, to determine other underlying factors that may contribute to this loading.

The final investigation of this thesis examined the impact of Duchenne and Trendelenburg type gait on loading at the lower lumbar spine in children with cerebral palsy. The same cohort of subjects was divided according to clinical presentation of each pattern. Trendelenburg gait had little impact on L5/S1 loading. However, increased loading was evident where Duchenne type movements were present.

To conclude, increased loading was evident at the lower lumbar spine during cerebral palsy gait. This loading was related to the position of the thorax. It is important that interventions relating to movement of the trunk during cerebral palsy gait, or specifically related to Duchenne or complex Trendelenburg-Duchenne type gait, are aimed at reducing trunk motion specifically in the coronal plane in order to reduce abnormal loading which could, in turn, impact the health of the spine in this population.

Funding Acknowledgements

Part funding was provided by the Scientific and Research Trust of the Central Remedial Clinic, Dublin.

Acknowledgements

Firstly, I would like to thank my supervisor Dr. Ciaran Simms for all his help and guidance throughout the course of this Ph.D. From the very beginning Ciaran's enthusiasm and interest in the project were evident and he was always available to offer suggestions and advice, usually over lunch in Kennedys or the Lincoln Inn, when needed. I have enjoyed my time working with Ciaran and hopefully we will collaborate on more projects in the future.

I would like to thank the Gait Laboratory team, without whom I would not have had the ability or confidence to proceed with this study. I have been part of the team for over 10 years and have learnt so much in that time. I would particularly like to thank Ailish and Prof. Tim O'Brien for their input on the clinical side of things when my engineering brain just wasn't getting it, and thanks to Niamh and Rory for all their help.

I would like to say a special thanks to all my subjects who provided me with the results I needed, your input is greatly appreciated, and all my proofreaders who, while probably not the most interesting way to spend an evening, painstakingly went through every word, figure and table.

I would like to thank my family, in particular my Mam and Dad for all their support and encouragement over the course of my education, my sisters Hazel and Selina for all their support, my brother Ciaran without whom this thesis would not have been possible, and of course my two beautiful daughters Clodie and Avie for keeping me focused on the more important things in life.

Finally, I would like to thank my wife Cleo for all her support throughout this process. I cannot put into words how much I appreciate you always being there.

List of Abbreviations

3DGA	Three-Dimensional Gait Analysis
AFO	Ankle Foot Orthosis
ASIS	Anterior Superior Iliac Spine
AJC	Ankle Joint Centre
BSP	Body Segment Parameters
CMC	Coefficient of Multiple Correlation
CMID	Clinically Meaningful Important Difference
CP	Cerebral Palsy
CRC	Central Remedial Clinic
CSF	Cerebrospinal Fluid
FBD	Free Body Diagram
FLoA	Functional Limits of Agreement
GCS	Global Coordinate System
GDI	Gait Deviation Index
GPS	Gait Profile Score
GRF	Ground Reaction Force
HJC	Hip Joint Centre
Hz	Hertz
IVH	Intraventricular haemorrhage
IJ	Incisura Jugularis
ISB	International Society of Biomechanics
ITB	Intrathecal Baclofen
KJC	Knee Joint Centre
LCS	Local Coordinate System
LL	Leg Length
LoA	Limits of Agreement
MAV	Mean Absolute Variability
MRI	Magnetic Resonance Imaging
N	Newtons
PD	Pelvic Depth
PiG	Plug in Gait (Vicon Movement Analysis Software)
PSIS	Posterior Superior Iliac Spine
PVHI	Periventricular Haemorrhage Infraction
PVL	Periventricular Leukomalacia
PW	Pelvic Width
RC	Rigid Cluster
RoM	Range of Motion
SD	Standard Deviation
SDR	Selective Dorsal Rhizotomy
SMA	Skin Movement Artefact
SS	Skin Surface
TD	Typically Developed
XP	Xypoid Process

Glossary of Terms

Cerebral Palsy	A group of permanent disorders of the development of movement and posture that are attributed to non-progressive disturbances that occurred in the developing fetal or infant brain
Kinematics	Angular movement of joints
Kinetics	Forces, moments and powers acting on joints
Joint Moment	The product of a force applied by its distance from the fulcrum. In gait, a joint moment represents the body's internal response to an external load
Joint Power	The scalar product of the joint moment and the angular velocity of the moving segment
Gait Analysis	The systematic measurement, description, and assessment of quantities that characterise a person's walking pattern
3-D Gait Analysis	A 3-dimensional reconstruction of a person's walking pattern using high speed motion analysis cameras, force platforms and mathematical algorithms
Gait Cycle	Traditionally defined as the time between the point of heel contact of the foot and the next heel contact of the same foot.
Ipsilateral	Occurring on the same side of the body
Contralateral	Occurring on the opposite side of the body
Dorsiflexion	Flexion of the foot in an upward direction in the sagittal plane
Plantarflexion	Flexion of the foot in a downwards direction in the sagittal plane
Equinus	Reduced dorsiflexion of the ankle – sometimes fixed.
Crouch	Mid-stance knee flexion of approximately 20^{o} or greater.

List of Publications

Journal Articles

Kiernan, D., Walsh, M., O'Sullivan, R., O'Brien, T. & Simms, C. K. 2014. *The influence of estimated body segment parameters on predicted joint kinetics during diplegic cerebral palsy gait*. J Biomech*,* 47**,** 284-288.

Kiernan, D., Malone, A., O'Brien, T. & Simms, C. K. 2014. *A 3-dimensional rigid cluster thorax model for kinematic measurements during gait.* J Biomech, 47, 1499-1505.

Kiernan, D., Malone, A., O'Brien, T. & Simms, C. K. 2015. *The clinical impact of hip joint centre regression equation error on kinematics and kinetics during paediatric gait*. Gait & Posture, 41, 175-179.

Kiernan, D., Malone, A., O'Brien, T. & Simms, C. K. 2015. *A quantitative comparison of two kinematic protocols for lumbar segment motion during gait.* Gait & Posture, 41, 699-705.

Kiernan, D., A. Malone, T. O'Brien, and C.K. Simms. 2016. *Children with cerebral palsy experience greater levels of loading at the low back during gait compared to healthy controls.* Gait & Posture, 48: p. 249-255

Kiernan, D., A. Malone, T. O'Brien, and C.K. Simms. 2017. *Three-dimensional lumbar segment movement characteristics during paediatric cerebral palsy gait.* Gait & Posture, 53: p. 41-47.

Kiernan, D.,O'Sullivan, R., Malone,A., O'Brien,T., and Simms, C.K.2017.*Pathological movements of the Pelvis and Trunk during gait in children with Cerebral Palsy: A cross-sectional study with 3-dimensional kinematics and lower lumbar spinal loading.* Physical Therapy. Accepted for publication.

Conference Proceedings

Kiernan, D., Walsh, M., O'Sullivan, R., O'Brien, T. & Simms, C. K. The influence of estimated body segment parameters on predicted joint kinetics during diplegic cerebral palsy gait. *22nd Annual meeting of the European Society for Movement Analysis in Adults and Children (ESMAC), Glasgow. Sept 5-7th 2013.*

Kiernan, D., Malone, A, O'Brien, T. & Simms, C. K. An alternative model for 3-dimensional thorax measurements during gait. *13th Annual meeting of the Clinical Movement Analysis Society UK and Ireland (CMAS),Oswestry. April 7-8th 2014.*

Kiernan, D., Malone, A, O'Brien, T. & Simms, C. K. The clinical impact of hip joint centre regression equation error on kinematics and kinetics during gait. *14th Annual meeting of the Clinical Movement Analysis Society UK and Ireland (CMAS),London, Oxford. April 16-17th 2015.*

Kiernan, D., Malone, A, O'Brien, T. & Simms, C. K. Trunk kinematics and lower lumbar spinal loading during paediatric cerebral palsy gait. *24th Annual meeting of the European Society for Movement Analysis in Adults and Children (ESMAC), Heidelberg, Germany. Sept. 10-12th 2015.*

Kiernan, D., Malone, A, O'Brien, T. & Simms, C. K. Are children with cerebral palsy more susceptible to greater levels of loading at the low back during gait compared to healthy controls? *15th Annual meeting of the Clinical Movement Analysis Society UK and Ireland (CMAS),Belfast. April 14-15th 2016.*

Table of Contents

Chapter 1: Introduction

1.1 Purpose of this study

The purpose of this study is to identify and describe characteristic trunk kinematic and lower lumbar spinal kinetic patterns during gait in children with cerebral palsy (CP) compared to typically developed (TD) controls. Differences between groups will be reported and the impact of aberrant trunk kinematics on lower lumbar spinal loading during CP gait will be investigated. The methodology required to achieve this will be assessed and further developed where necessary. Finally, a clinical application of these measurements will be presented where the effects of Trendelenburg and Duchenne movement patterns on lower lumbar spinal loading during CP gait will be discussed.

1.2 Justification for this study

The Gait Laboratory at the Central Remedial Clinic (CRC) is the national referral centre for adults and children with complex walking disabilities in the Republic of Ireland. The team consists of two consultant orthopaedic surgeons, four physiotherapists and one clinical engineer. A large percentage of clients referred to the laboratory have a diagnosis of CP. CP is defined as "*a group of permanent disorders of the development of movement and posture"* that are attributed to "*non-progressive disturbances that occurred in the developing fetal or infant brain"* (Rosenbaum et al., 2007) (please refer to Chapter 2 for a full description). CP is one of the most severe and common causes of physical disability in children and occurs in approximately 2 to 2.5 per 1000 live births in developed countries (Cans, 2000).

For the past ten years I have worked as clinical engineer within the gait laboratory assessing pathological gait using 3-dimensional movement analysis. Traditionally, gait analysis has focused on the lower limbs. However, in recent times the gait laboratory team have questioned the role of the trunk during CP gait. Studies reporting trunk biomechanics in

children with CP are limited in the literature and there is a limited knowledge regarding deviations during walking when compared to TD controls. At commencement of this study, only three groups had examined trunk kinematics in CP, with results indicating an increased range of motion (ROM) for the thorax in all 3 planes (Romkes et al., 2007, Pratt et al., 2012, Heyrman et al., 2013a). Of these three studies, two also reported an ipsilateral lateral bending of the thorax in stance and a contralateral bending in swing for one gait cycle, resulting in increased lateral thorax sway. In contrast, TD children maintained a neutral thorax position.

The need for further studies relating trunk kinematics with lower limb kinematics and kinetics has been warranted to further contribute to the understanding of the functional relationship between segments (Heyrman et al., 2013a). While limited information existed in relation to trunk kinematics during gait in CP, there were no studies examining kinetic profiles at the trunk in this cohort. In many cases the increased lateral thorax sway during gait in CP will result in a manipulation of the ground reaction force (GRF) for the purpose of aligning the GRF closer to the hip joint. This may be to compensate for hip abductor weakness and facilitate a better coronal plane pelvic position. It is feasible that this type of compensatory movement will alter the kinetic profiles at the lower trunk region. This compensatory pattern may be acceptable from a kinematic point of view, especially if the child demonstrates good levels of ambulation. However, exposure to increased reactive forces and moments at the lumbar region may result in changes to the structural tissue and may act as risk factor for low back pain in this population as they age.

It has been stated that a detailed analysis of gait from a 3-dimensional point of view (e.g. kinematics and kinetics etc.) can significantly enhance the understanding of a deficit (Patrick, 2003). Such an analysis forms the mainstay of the assessment and classification of gait in CP (Gough and Shortland, 2008). Consequently, there is a clinical need to measure and report characteristic trunk kinematic and kinetic patterns for a group of children with CP and compare to a TD group to determine whether deviations exist. It is of course possible that CP

subjects may not present increased reactive forces and moments at the trunk suggesting the increased trunk movement may be only mildly demanding in relation to increased tissue demand or risk of injury. However, gaining an appreciation of the loading of the lower level trunk will provide an additional tool in the assessment process that has not yet been reported for CP. The current limited knowledge regarding trunk kinematics in CP and the complete lack of knowledge regarding trunk kinetics in CP during gait provide the rationale for this study.

1.3 Outline of this Thesis – Thesis Roadmap

The flowchart detailed in Figure 1.1 demonstrates the structure of this thesis. The thesis is divided into 14 chapters in total. A background to CP and gait analysis and a literature review are provided in Chapters 2 and 3. Chapter 4 details the overall goals and specific objectives of the thesis. General methodology is described in Chapter 5. To achieve the objectives outlined in Chapter 4, the thesis contains a further 6 distinct but related chapters. The discussion and conclusion chapters, Chapter 12 and 13, draw together the findings of the thesis. Chapter 14 presents some areas of consideration for future work (Fig.1.1).

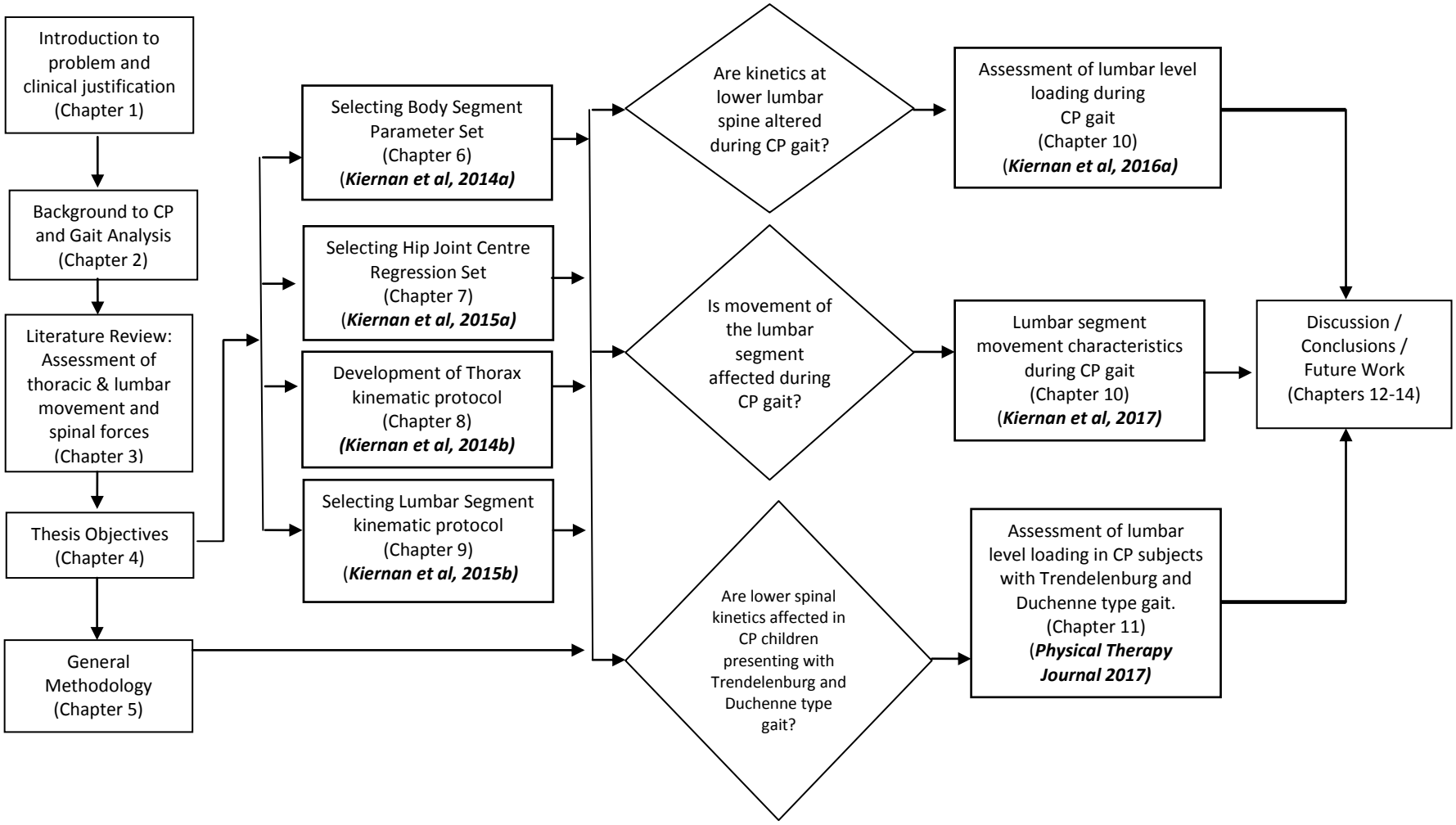

Figure 1.1: Flowchart demonstrating thesis structure

Chapter 2: Background to Cerebral Palsy and Gait Analysis

2.1 Introduction

This chapter provides a background to CP and examines the aetiology associated with the condition. Reference will be made to the clinical diagnosis and classifications currently in use in CP. The associated impairments from a movement analysis point of view and the management and prognosis of CP will also be discussed.

2.2 Background to Cerebral Palsy

2.2.1 Definition of Cerebral Palsy

The definition of CP has been revised on a number of occasions over the years due to the complexity of the condition. As early as 1843, CP has been attributed to the deformities and contractures associated with difficult deliveries (Little, 1844). One of the first definitions proposed in 1959 by the group "Little Club" described CP as " *a persistent but not unchanging disorder of movement and posture, appearing in the early years of life and due to a non-progressive disorder of the brain, the result of interference during its development*" (Mac Keith et al., 1959). The classic definition of CP proposed in 1964 was "*a disorder of movement and posture due to a deficit or lesion of the immature brain*" (Bax, 1964). It was also proposed at this time that disorders that are short in duration, due to progressive disease or solely due to mental deficiency should be excluded from CP (Bax, 1964, Bax et al., 2005). This particular definition focused on the motor aspects associated with the condition while other impairments such as sensory, cognitive or behavioural, were not formally included (Bax et al., 2005). Due to the diversity of the condition, another definition was put forward in later years describing the condition as "*an umbrella term covering a group of non-progressive, but often changing, motor impairment syndromes secondary to lesions or anomalies of the brain arising in the early stages of development*" (Mutch et al., 1992). It was felt this definition emphasized the motor impairment associated with the condition and excluded progressive disease (Bax et

al., 2005). A later definition, proposed to incorporate the emerging understanding of developmental neurobiology and changing concepts about impairments and functional status, was put forward in 2005. The updated definition defined the condition as "*Cerebral palsy (CP) describes a group of disorders of the development of movement and posture, causing activity limitation, that are attributed to non-progressive disturbances that occurred in the developing fetal or infant brain. The motor disorders of cerebral palsy are often accompanied by disturbances of sensation, cognition, communication, perception, and/or behaviour, and/or by a seizure disorder"* (Bax et al., 2005). This definition was later changed to define the "group of disorders" as "permanent" (Rosenbaum et al., 2007).

2.2.2 Prevalence of Cerebral Palsy

CP is one of the most severe and common causes of physical disability in children (Cans, 2000). While numerous epidemiological studies have been conducted in developed countries, few have been conducted in developing countries. The prevalence estimates for developed countries vary between studies. However, trends suggest that the instance of CP is approximately 2 to 2.5 per 1000 live births in developed countries (Cans, 2000, Liu et al., 1999, Pharoah et al., 1998, Stanley et al., 2000, Thorngren-Jerneck and Herbst, 2006). A number of studies demonstrated an increase in the prevalence of CP over time with higher rates of CP coincident with higher survival rates, most likely as a consequence of improved neonatal care (Cans, 2000, Liu et al., 1999, Stanley et al., 2000, Koman et al., 2004).

2.2.3 Classifications of Cerebral Palsy

The definition of CP allows for a wide range of clinical presentations and therefore it is necessary to further categorise individuals with CP into subgroups. However, in general, there has been a lack of consensus regarding exact classifications of CP. Traditionally, CP is classified according to the limbs involved and the characteristics of the neurological dysfunction (Kuban and Leviton, 1994):

- monoplegia - one lower limb is primarily involved
- diplegia - both lower limbs involved with minimal involvement of upper limbs
- hemiplegia - one lower limb and upper extremity involved
- triplegia - ipsilateral hemiplegia with contralateral monoplegia
- double hemiplegia – all four limbs involved (Ounpuu et al., 2009).

These terms usually carry the prefix "spastic" relating to the hypertonicity that can accompany the condition. Some patients have weakness rather than spasticity as a main feature. The most comprehensive classification system was proposed by Minear (Minear, 1956). This system includes the following categories: (A) Physiological, (B) Topographical, (C) Aetiological, (D) Trauma, (E) Supplemental, (F) Neuroanatomical, (G) Functional capacity and (H) Therapeutic, that are broken down into further sub-categories (Minear, 1956). In a recent surveillance survey of CP across Europe, reference was made to the wide variations in the use of such terms as spastic diplegia (Cans, 2000). Consequently, the authors of that survey proposed a simpler classification system:

(1) Spastic CP (characterised by at least two of the following):

- Abnormal pattern of posture and/or movement.
- Increased tone (not necessarily constant).
- Pathological reflexes (increased reflexes: hyperreflexia and/or pyramidal signs e.g. Babinski response).

Spastic CP may be either bilateral or unilateral

(2) Ataxic CP (characterised by both of the following):

- Abnormal pattern of posture and/or movement.

- Loss of orderly muscular coordination so that movements are performed with abnormal force, rhythm and accuracy.

(3) Dyskinetic CP (dominated by both):

- Abnormal pattern of posture and/or movement.
- Involuntary, uncontrolled, recurring, occasionally stereotyped movements.

Dyskinetic CP may be either dystonic or choreo-athetotic:

(3a) Dystonic CP (is dominated by both):

- Hypokinesia (reduced activity i.e. stiff movements).
- Hypertonia (tone usually increased).

(3b) Choreo-athetotic CP (is dominated by both):

- Hyperkinesia (increased activity, i.e. stormy movements).
- Hypotonia (tone usually decreased).

An alternative simplified classification was proposed subsequently with four major dimensions of classification (Bax et al., 2005). The four classifications were: (1) motor abnormalities, (2) associated impairments, (3) anatomic and radiological findings and (4) causation and timing. The purpose of this classification system was to remove the terms diplegia and hemiplegia due to inconsistency in definition and use (Bax et al., 2005). It has also become common practice to additionally classify children with CP according to function and in recent years the Gross Motor Function Classification System (GMFCS) has become widely used (Palisano et al., 1997). This allows for a measurement of gross motor function and is useful for the identification of the progress of a child at a particular point in time according to age and gross motor function (Ounpuu et al., 2009). Other methods of classification include classification by motion analysis (O'Byrne et al., 1998, Winters et al., 1987), in particular by knee kinematic pattern (O'Sullivan et al., 2010b). However, no particular classification system has become definitive. Depending

on the clinical situation, different combinations of characteristics may be more useful than others (Bax et al., 2005). In general, a mixture of topographical, gait and gross motor function classifications are used.

2.2.4 Aetiology of Cerebral Palsy

As previously discussed, the definition of CP refers to "*non-progressive disturbances that occurred in the developing fetal or infant brain".* In general, a broad spectrum of aetiologies can result in injury to the developing or fetal brain with the most common cause due to cerebrovascular injury (Du Plessis, 2009). The anatomic structure and functional immaturity of the cerebral vessels leave the brain vulnerable (Du Plessis, 2009), with Central Nervous System (CNS) haemorrhage (mechanical spinal cord or brainstem damage), CNS hypoxia (cerebral cortex) and irreversible ischaemia all associated with CP (Koman et al., 2004).

In the un-well preterm infant, instability of the cardiorespiratory system is common with fluctuations in systemic blood pressure that can result in a cerebral vasculature pressure-passivity (Soul et al., 2007). Consequently, fluctuations in systemic blood pressure are transmitted directly into the immature cerebral microvasculature. Increased pressure may consequently rupture vessels resulting in hypoxic-ischaemia damage of the arterial end zones of the periventricular white matter, referred to as "periventricular leukomalacia" or PVL for short (Du Plessis, 2009). Diplegia is associated with this type of brain lesion (Koman et al., 2004). "Periventricular haemorrhagic infraction" (PVHI) is another type of lesion that develops when intraventricular haemorrhage (IVH) impairs drainage of the blood through the terminal vein resulting in ischaemia through large areas of the cerebral hemisphere (Du Plessis, 2009). Hemiplegia is associated with single hemisphere injury in most cases (Koman et al., 2004). "Posthaemorrhagic hydrocephalus" is a complication of IVH where leakage of blood obstructs cerebrospinal fluid (CSF) pathways. This can result in compression of periventricular white matter. This lesion has similar effects as a PVL lesion (Du Plessis, 2009). Hydrocephalus

shunting is commonly used as a method to drain excessive CSF. It is possible for more than one of these types of lesion to be present in the preterm infant brain.

In the term infant there also exists a vulnerability to brain injury (Du Plessis, 2009). At term, the cerebral vasculature will have matured and is better capable of dealing with the demands of the cerebral pressure-flow auto regulation. However, the cerebral vasculature may have become pressure-passive by a moderate hypoxic-ischemic insult. Consequently, any lose of autoregularity function in combination with compromised myocardial function leaves the brain predisposed to cerebral injury (Du Plessis, 2009). The main cerebrovascular lesions that present in the term infant are due to global hypoxia-hypoperfusion insults to the entire brain, an example of such would be perinatal asphyxia (deprivation of oxygen during the period of childbirth), and cerebral infarction (stroke) due to the occlusion of one or more cerebral arteries (Du Plessis, 2009). Common perinatal factors associated with CP include maternal age, vaginal breech delivery, abrupt placentae, instrumented delivery and emergency caesarean delivery, smoking in early pregnancy, maternal insulin-dependent diabetes, low birth weight and gestational age and twin / multiple pregnancies (Thorngren-Jerneck and Herbst, 2006).

2.2.5 Clinical Diagnosis

The clinical manifestations as a result of this injury depend heavily on the extent, type and location of the CNS damage. Neuroimaging tests such as CT and MRI are required to examine the extent of the lesion (Koman et al., 2004). A complete birth history, physical examination and an assessment of the extent of movement disorders, ideally using instrumented gait analysis (Gough and Shortland, 2008, Patrick, 2003), are vital for diagnosis and management of CP.

2.2.6 Management of Cerebral Palsy

A number of management options are available for CP, primarily non-surgical, surgical, pharmacological and assistive device management. Over the years an abundance of studies have examined the effects of many different types of management strategy on CP with a variety of results. The purpose of this section is to give a brief overview of some of the various management strategies available.

2.2.6.1 Physiotherapy/ Conservative Management

Physiotherapy is usually one of the first management options recommended for the child with CP with the aim of improving mobility (Murr and Walt, 2009). The effects of spasticity are thought to take effect in the young child from the ages of 5 onwards with the development of fixed and bony deformities (Koman et al., 2004). Therefore, the intervention program of the child with CP will start at an early age where the child may respond with more positive results to physiotherapy management (Koman et al., 2004). Treatment interventions include stretching to maintain or improve range of motion, practice of functional activities with the aim of improving levels of activity and participation, strengthening to increase power, and gait training, possibly using an assistive device, to improve endurance and functional gait (Murr and Walt, 2009). The evidence around some conservative therapies remains inconclusive. A recent review examining the effects of passive stretching in children with CP reported conflicting results (Pin et al., 2006). On the other hand, positive results were reported regarding the effectiveness of strength training programmes and partial body-weight supported treadmill training (Dodd et al., 2002, Willoughby et al., 2009). In many cases, physiotherapy management may be used as a standalone treatment or in conjunction with other treatment modalities.

2.2.6.2 Pharmacological Management

Pharmacological management is commonly used to manage spasticity in CP and is divided across oral medications and more focal therapies such as botulinum toxin. Spasticity management in children with CP using oral medications has decreased in recent years due to alternative, and in some case more effective, options such as botulinum toxin or specific surgical techniques (Ward, 2009). Side effects and risks limit the usefulness of oral medications and often the utility of the medication is determined on a trial and error basis (Ward, 2009). The goals for treatment with oral medications differ depending on the child and the clinical situation. Oral medication can reduce spasticity and the frequency of muscle spasms. However, nearly all of these types of medication have side effects of sedation and cognitive impairment (Ward, 2009). Examples of oral medication include Benzodiazepines, Baclofen, Dantrolene sodium and Levodopa to name a few. All of these medications have been used for spasticity management in CP with varying results and side effects. A more recent development in spasticity management in CP is the use of Botulinum toxin type A, a neurotoxin that is injected directly into the muscle (Koman et al., 1993). This has the effect of temporary muscular denervation allowing for greater selective control of the muscle. Casting, day and night orthoses and physiotherapy are commonly used in conjunction with botulinum toxin to maintain the improved muscle length and to facilitate the carryover of improved motor control (Molenaers and Desloovere, 2009).

2.2.6.3 Surgical Management

Surgical management in CP involves procedures to reduce spasticity and orthopaedic procedures to correct deformities and contractures. The purpose of this section is to give a brief overview of some of the common procedures. To reduce spasticity from a surgical point of view, Intrathecal Baclofen (ITB) and Selective Dorsal Rhizotomy (SDR) have been used in CP. ITB involves the implantation of a pump and the site of action is at the spinal cord. The

effectiveness of baclofen has been shown to be limited when administered orally but when delivered intrathecally it can be given in lower doses with higher effectiveness (Krach, 2009). The ITB pump can then be programmed to work on a continuous basis, hourly or at set times during the day. Risks of using ITB involve infection, cerebrospinal fluid leaks and hardware faults. The use of SDR is a contentious issue due to the risk during and after treatment. SDR involves transection of dorsal rootlets arising from the spinal cord. Specifically, stimulation and transection of selective posterior rootlets or arbitrary transection of a specific proportion of rootlets, requiring a laminectomy at L2-L5 (Koman et al., 2004). The procedure is irreversible and due to muscle weakness and the need for long term follow up care, caution is needed in selection of the most suitable candidates. It is beyond the scope of the section to debate the pros and cons of this technique.

Orthopaedic management in CP include a variety of procedures such as muscle lengthening, arthrodesis (joint fusing), osteotomy (bone transection), tendon transfer and tenotomy (division of a tendon) and may involve one or a combination of these procedures (Koman et al., 2004).

2.2.6.4 Assistive Device Management

Several devices have been used in the management of CP and include kaye walkers, orthotics, splints and electrical stimulation. Ankle Foot Orthoses (AFOs) are the most commonly used assistive device during CP gait and can be divided into many types. These include rigid AFOs, hinged AFOs, ground reaction AFOs, posterior leaf spring orthoses and supramaleolar orthoses. Often in CP, weak plantarflexors, bony deformities, foot misalignment relative to the knee and unstable foot structure result in insufficient knee support during stance and poor push off leading into swing (Novacheck et al., 2009). The role of an AFO during gait is to improve or correct the resultant lever-arm misalignment. Functional Electrical Stimulation (FES), used at low intensity to electrically stimulate a muscle, is an alternative to

AFOs in some situations. The use of FES during drop foot is one such example where the tibialis anterior is stimulated during the swing phase to assist ground clearance. Walking aids such as kaye walkers or tripods are also commonly used as assistive devices during gait.

2.3 History of Movement Analysis

The first known written reference to the analysis of human walking was made by Aristotle (384-322 BC), however, it was not until the renaissance in Europe that the science and mathematics that form the basis of modern gait analysis were developed (Baker, 2007, Sutherland, 2001). Giovanni Alfonso Borelli (1608 – 1679) was accredited with performing the first experiment in gait analysis when he placed two poles a set distance apart and tried to walk towards them keeping one pole in front of the other (Baker, 2007). He concluded that the near pole always appeared to move from the left to the right suggesting that there must be a medio-lateral movement of the head during walking (Baker, 2007). In the late 18th century Braun and Fischer used Geissler tubes attached to limb segments to analyse movement (Sutherland, 2002). The subject would walk in total darkness and the illumination of the tubes would be interrupted at regular intervals and photographed. The subjects were protected from electrical shock by means of rubber suits and the whole assessment could take up to 10 hours, with months required for data reduction (Sutherland, 2002). The 19th century saw further advancement in gait analysis, in particular, when Guillaume Duchenne and Freiderich Trendelenburg described gait patterns related to hip abductor dysfunction (Duchenne, 1949, Trendelenburg, 1895). The next major step in the evolution of gait analysis was the development of force plates. Marey and Carlet developed a pneumatic system to measure in-shoe pressure (Marey, 1874), while a pneumatic force plate was later developed by Demeny and Marey to investigate the energetics of gait (Marey, 1883, Baker, 2007). This work was further advanced when Amar developed a three-component force plate to measure rehabilitation of injured arising from war (Amar, 1916). However, it was not until the 20th

century that major advances took place when Vern Inman and colleagues moved the science of gait analysis forward by the use of kinesiological electromyography, 3-D force and energy measurements (Sutherland, 2001). The methods of Inman were, however, massively labour intensive from both a data collection and computational point of view making the early adaption into clinical practice difficult (Baker, 2007, Sutherland, 2001). Developments in technology brought with them the development of gait analysis and with this the use of gait analysis as a clinical tool. Later 20th century developments in clinical gait analysis were mainly driven by David Sutherland and Jacquelin Perry in America and Jurg Baumann in Europe (Baker, 2007).

Clinical gait analysis is a widely used tool throughout the world. In Ireland, the Central Remedial Clinic (CRC) is a national referral centre for the Republic of Ireland which provides a full range of medical, social and technical services to adults and children with physical disabilities. The CRC gait laboratory was established in 1989 and was one of the first in Europe. Like many clinical gait labs, CP is the main referral population accounting for up to 70% of referrals per annum. Spina Bifida, Charcot-Marie Tooth, Idiopathic toe walking and query diagnosis are among the remaining referrals. The laboratory conducts upwards of 400 assessments per year. The CRC was one of the first laboratories to receive accreditation to Clinical Movement Analysis Society of UK and Ireland (CMAS) standards in 2011. Currently, across Ireland and the UK, there are 14 CMAS accredited laboratories.

2.4 Movement Analysis and Cerebral Palsy

2.4.1 Role of Movement Analysis in Cerebral Palsy

Three-dimensional movement analysis allows patterns of joint movement to be measured in 3 planes, namely sagittal, coronal and transverse. It is a clinical tool that allows increased understanding of movement patterns in both normal and pathological states (Patrick, 2003). Movement analysis has been shown to be effective in the identification and

management of gait pathologies in children with CP (Patrick, 1991, Gage, 1993, Sutherland et al., 1999, Patrick, 2003, Gough and Shortland, 2008, Chang et al., 2006). Reference has been made to the situation where children with CP have gained significant improvement by means of gait analysis prior to treatment (Patrick, 2003).

2.4.2 Normal Gait Patterns – An Overview

The gait cycle is defined as the time interval between two successive occurrences of one of the repetitive events of walking. Traditionally, the start of the gait cycle is defined as the point of heel contact of the foot while the end of the gait cycle is defined as the next heel contact of the same foot. The gait cycle is then divided into two phases, namely stance and swing. The stance phase constitutes approximately the first 60% of the gait cycle while the swing phase makes up the remaining 40%. The corresponding stick figure represents the most important parts of the gait cycle (Fig.2.1).

Initial Contact: Initial contact marks the first phase of the gait cycle. This phase prepares the heel for contact with the floor in preparation for weight acceptance. The ankle is in a neutral position, the knee is fully extended and the hip is flexed to approximately 25^{o} – 30^{o} (Fig.2.1).

Loading Response: Loading response marks the second phase of gait and occurs between 0 - 10%. Weight acceptance occurs during this phase and is accompanied by shock absorption primarily by the quadriceps muscle. Ankle plantarflexion occurs when the heel contacts the ground allowing the tibia to drop slightly aiding in shock absorption. The ankle plantarflexes to approximately 10^{o} with forefoot contact controlling the degree of tibia advancement. The knee moves into a flexed position and the hip prepares to extend. The quadriceps limits the degree of knee flexion (Fig.2.1).

Mid-Stance: Mid-stance marks the third phase of the gait cycle and occurs between 10 – 30%. The main tasks of this phase are restrained ankle dorsiflexion and single limb support, with the body progressing over the foot in a controlled manner. During this period there is controlled

tibial advancement and it is the period of flat foot to heel off where the tibia rotates about the ankle from a position of plantarflexion to dorsiflexion (Fig.2.1).

Terminal Stance: Terminal stance marks the fourth phase of the gait cycle and occurs between 30 - 50%. The main task during this period is single limb support as the body passes in front of the foot. During this phase the hip extends and reaches 10^0 to 15^0 of extension by the time of heel off. The phase ends with the opposite foot making contact with the ground (Fig.2.1).

Pre-Swing: Pre-swing marks the fifth phase of the gait cycle and occurs between 50 – 60%. The purpose of this phase is to prepare and position the leg for swing. The gastro-soleus complex completes push-off which flexes the knee and initiates hip flexion. As toe off approaches, the ground reaction force diminishes rapidly and finally disappears as the foot leaves the ground and enters the swing phase (Fig.2.1).

Initial Swing: Initial swing marks the sixth phase of the gait cycle and occurs between 60 – 75%. During this phase advancement of the swinging limb occurs. The leg is lifted by flexion of the hip and shortened by flexion of the knee and dorsiflexion of the ankle in order to achieve adequate ground clearance. The foot needs to move from a position of plantarflexion to a neutral position (Fig.2.1).

Mid-Swing: Mid-swing marks the seventh phase of the gait cycle and occurs between 75 – 90%. Limb advancement continues during this phase. Adequate foot clearance is still necessary and the ankle maintains its neutral position by activation of the tibialis anterior. Hip flexion reaches a maximum during this phase and at the end of this phase hamstring muscle activity is beginning (Fig.2.1).

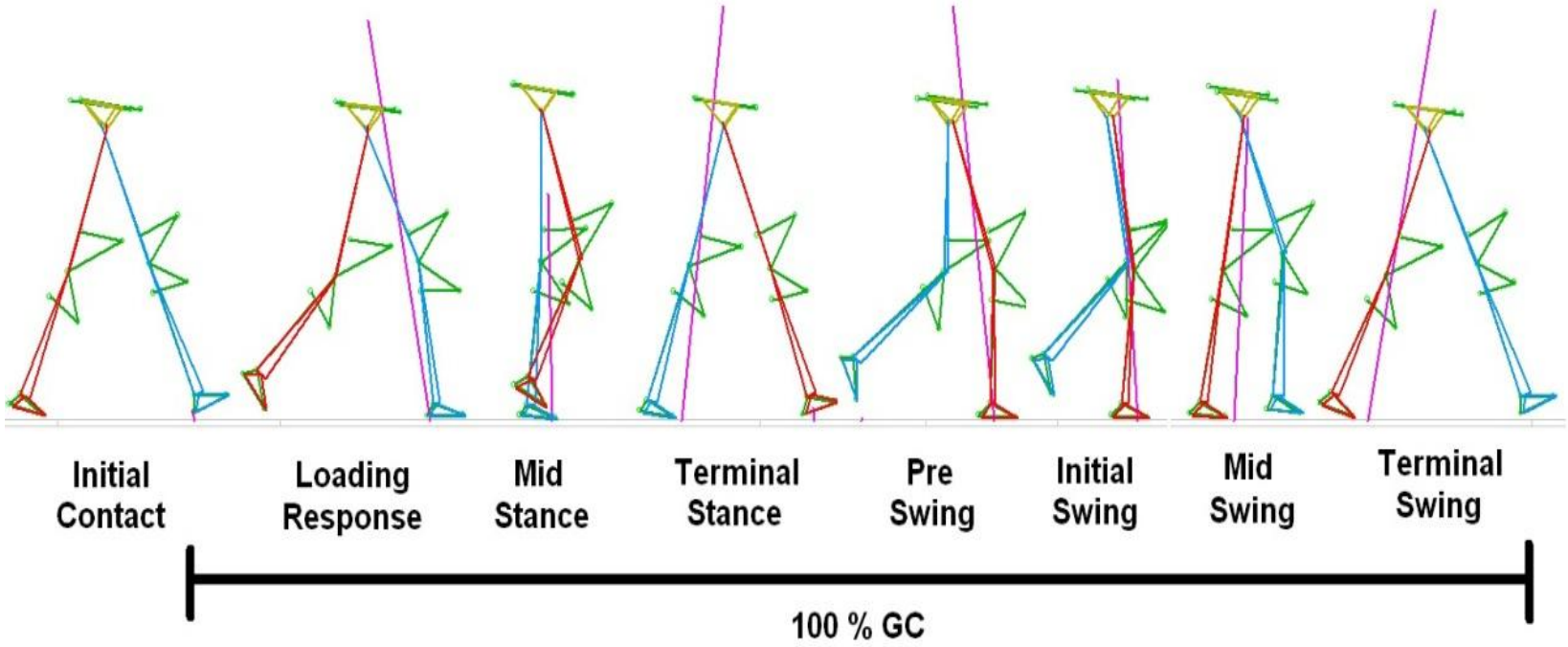

Figure 2.1: The normal gait cycle. This stick figure gives a clear demonstration of the gait pattern and it is best understood in the sagittal plane. The blue leg is used here to demonstrate each gait cycle event.

Terminal Swing: Terminal swing marks the eighth and final stage of the gait cycle and occurs between 90 – 100%. This marks the transition phase between swing and stance. Limb advancement is completed, achieving maximum step length, and the foot is positioned for initial contact. Hamstring muscle contraction firstly slows down, stops and then reverses flexion at the hip. The knee becomes extended due to the contraction of the quadriceps muscle. Hamstring contraction at this stage prevents hyperextension at the knee joint (Fig.2.1).

2.4.3 Gait Patterns associated with Cerebral Palsy

CP affects movement and often influences ambulation and while the condition is non progressive in relation to the neurological injury, the clinical manifestations are not static and change as the child develops (Kuban and Leviton, 1994, Essex, 2003). Many studies have examined and described the various patterns associated with CP with the aim of providing a better understanding of the underlying pathologies. In the context of this study, it is hypothesised that the various patterns associated with CP may influence trunk movement and spinal loading during gait. With this in mind, the aim of this section is to provide a brief description of some of the main abnormalities associated with CP gait.

A number of studies have attempted to define specific patterns in CP gait. Winters and colleagues described four patterns in spastic hemiplegic CP population: (1) equinus, (2) recurvatum (knee hyperextension during stance), (3) stiff knee in swing and (4) excessive hip flexion (Winters et al., 1987). Similar grouping have been described by O'Byrne and colleagues, where CP subjects were clustered into 8 groups: (1) Mobile crouch, (2) Stiff crouch with toe walking, (3) Drop foot pattern, (4) Ankle double bump pattern, (5) Proximally flexed ankle walkers, (6) Mild recurvatum, (7) Severe recurvatum and (8) Severe crouch (O'Byrne et al., 1998)(Fig.2.2). In a recent comprehensive review of specific gait abnormalities in CP, stiff knee in swing was the most common feature (Wren et al., 2005). That study examined CP subtypes

(hemiplegic, diplegic and quadriplegic) and split the group into two sub-groups, namely with and without previous surgery (Fig.2.5). The most common abnormalities in the group as a whole were stiff knee in swing (80%), crouch gait (69%) (Fig.2.2), excessive hip flexion (65%), in toeing (64%)(Fig.2.3) and equinus (61%)(Fig.2.3) (Wren et al., 2005).

Figure 2.2: An example of severe crouch during CP gait looking from the coronal and sagittal planes.

A similar pattern was present for the diplegic subgroup with stiff knee in swing presenting in 88% of cases. In the quadriplegic subgroup, there was a greater likelihood of having crouch, scissoring, excessive hip adduction and valgus compared to diplegics (Wren et al., 2005). The most common abnormalities in hemiplegic subjects were equinus (64%), stiff knee (56%), intoeing (54%), excessive hip flexion (48%) and crouch (47%) (Wren et al., 2005). A definition of gait abnormalities is provided in Table 2.1.

Figure 2.3: A child with CP demonstrating bilateral fixed equinus, in toeing of the left foot and hyperextension of the left knee during stance.

Figure 2.4: An example of drop foot in a child with CP. The foot contacts the floor with a forefoot position instead of with a heel contact. The child may circumduct the hip to aid ground clearance in this case.

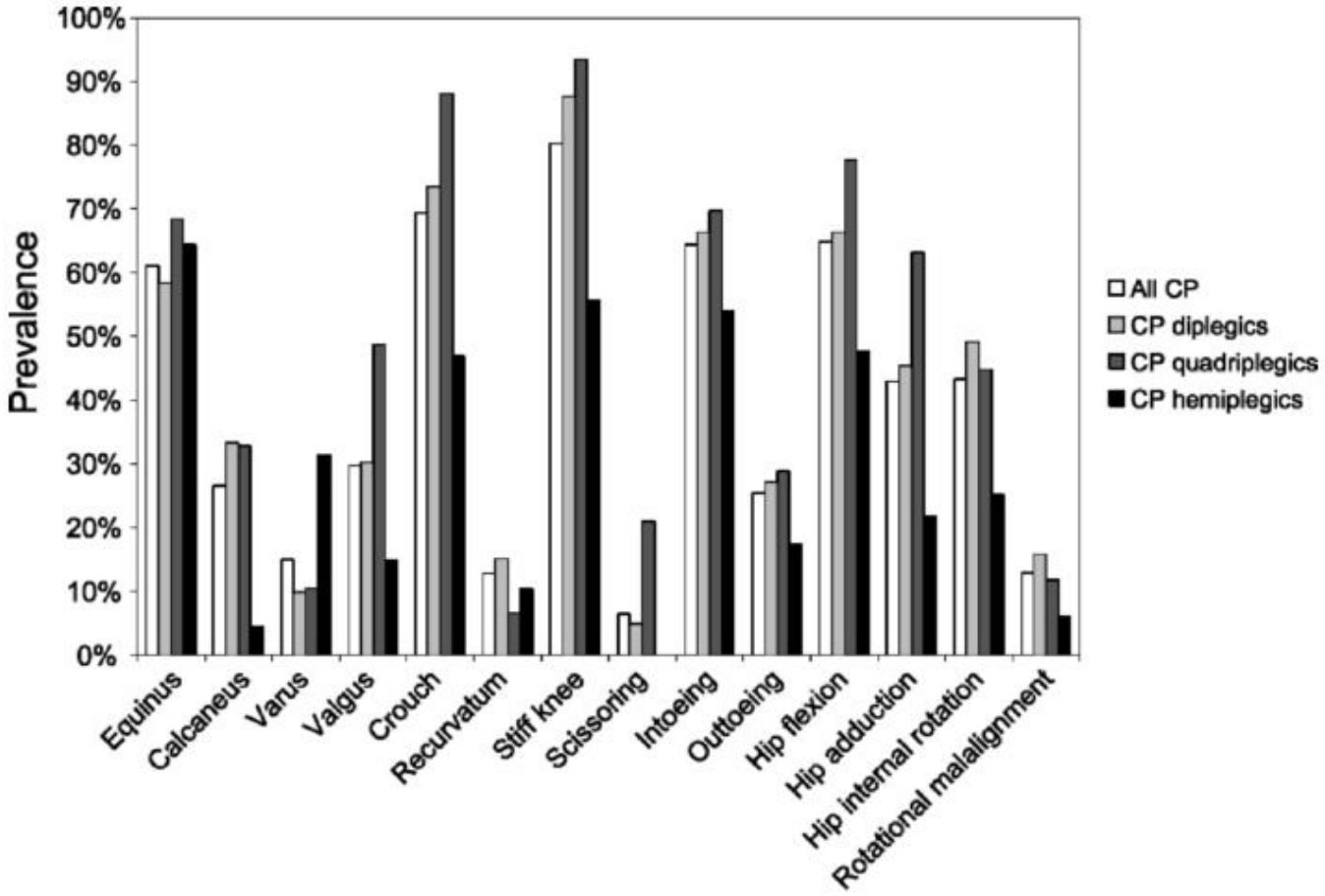

Figure 2.5: A breakdown of gait abnormalities common to CP across subgroups (diplegia, hemiplegia and quadriplegia). Adapted from (Wren et al., 2005).

Table 2.1: A description of abnormalities commonly found in CP gait. Adapted from (Wren et al., 2005). Note: The most common abnormalities in hemiplegic subjects were equinus (64%), stiff knee (56%), intoeing (54%), excessive hip flexion (48%) and crouch (47%) (Wren et al., 2005).

Gait Abnormality	Definition
Equinus	Ankle plantarflexion >1 standard deviation (SD) below the mean for normal during stance phase, with or without hindfoot and/or forefoot varus or valgus
Calcaneus	Dorsiflexion >1 SD above the mean for normal for a significant portion of stance phase (>50% of stance)
Ankle varus	Hindfoot and/or forefoot varus/supination in stance or swing, with or without equinus
Ankle valgus	Hindfoot and/or forefoot valgus/pronation or midfoot break in stance or swing, with or without equinus
Crouch	Knee flexion >1 SD above the mean for normal in a significant portion of stance phase
Recurvatum	Knee extension in stance beyond 0°
Stiff knee	Decreased arc of knee motion from maximum knee extension in stance to peak knee flexion in swing, and/or delay in peak swing knee flexion to mid- or terminal swing, hindering foot clearance
Scissoring	Leg crossing in swing causing problems with foot clearance
Intoeing	Internal foot progression >1 SD more than mean for normal
Out-toeing	External foot progression >1 SD more than mean for normal
Excessive hip flexion	Hip flexed >0° in terminal stance
Excessive hip adduction	Hip adducted >1 SD above normal for significant portion of stance
Excessive internal hip rotation	Internal hip rotation >1 SD more than mean for normal for significant portion of stance
Rotational malalighment	Excessive internal hip rotation with excessive external foot progression (>1 SD more than mean for normal, regardless of cause, tibial torsion versus foot deformity)

2.4.4 Gait Indices

Gait indices can be useful as an additional tool in the assessment of gait and have become increasingly popular in recent years. A gait index can be used to calculate the amount by which a subject's gait deviates from normal and is usually presented by means of a single number (Schutte et al., 2000). A number of indices are available in the literature. In general, a gait index will require the use of certain features (patterns) of a subject's kinematic pattern with the distance between these features and the features of a normal control group scaled to provide a single measure of overall gait pathology (Schwartz and Rozumalski, 2008, Baker et al., 2009). The majority of indices relate to kinematic data such as the Gait Deviation Index (GDI) (Schwartz and Rozumalski, 2008) and the Gait Profile Score (GPS) (Baker et al., 2009) with the validity of these indices well documented in the literature (Molloy et al., 2010). More recently, an index was proposed to measure overall pathology with respect to kinetic data, namely the GDI-Kinetic (Rozumalski and Schwartz, 2011). Gait indices can be useful in identifying clinically significant differences, also referred to as clinically meaningful important differences (CMID), in a subject's gait pathology. The CMID is an important consideration when interpreting results of clinical research. Gait indices will be used throughout this thesis as measures of CMID.

2.4.5 Trunk modelling during gait

The human trunk is defined as the area of the body between the neck and pelvic region excluding the head and limbs. The trunk has previously been termed a "passenger unit" where movement is suggested to be entirely as a consequence of the way the lower limbs move (Perry, 1992). Contrary to this, the trunk has also been termed an "active segment" where it is considered to play a role in locomotion (Armand et al., 2014, Leardini et al., 2009). Heyrman and colleagues suggested that movements observed during gait in children with CP may not be solely compensatory due to lower limb deficits but instead due to an underlying

trunk control deficit (Heyrman et al., 2014). Regardless of the terms used to define the trunk, the heavy mass of the trunk will have a major effect on the dynamics of walking (Baker, 2013). This is particularly obvious during certain pathological gait patterns. In particular, children with CP will often lean the trunk laterally over the hip joint to reduce the moment arm about the hip and reduce the demand on weak hip abductors (Krautwurst et al., 2013, Õunpuu et al., 1996).

Movement of the trunk can occur at many levels and this can pose problems when it comes to the most suitable method for analysis. The trunk is made up of many joints with generally small movements at each joint. In contrast, the lower limbs present for a more straightforward analysis as there are a small number of joints with generally large movements. With this in mind, simplifications are often made when it comes to modelling the trunk during movement. Methods for modelling the trunk during human movement range in complexity (Gutierrez et al., 2003, Houck et al., 2006, Krebs et al., 1992, Nguyen and Baker, 2004, Romkes et al., 2007). While many methods have been proposed, a consensus has not been reached as to the most suitable method (Baker, 2013). Some studies have considered the trunk as one segment (Fig. 2.6) (Bartonek et al., 2002).

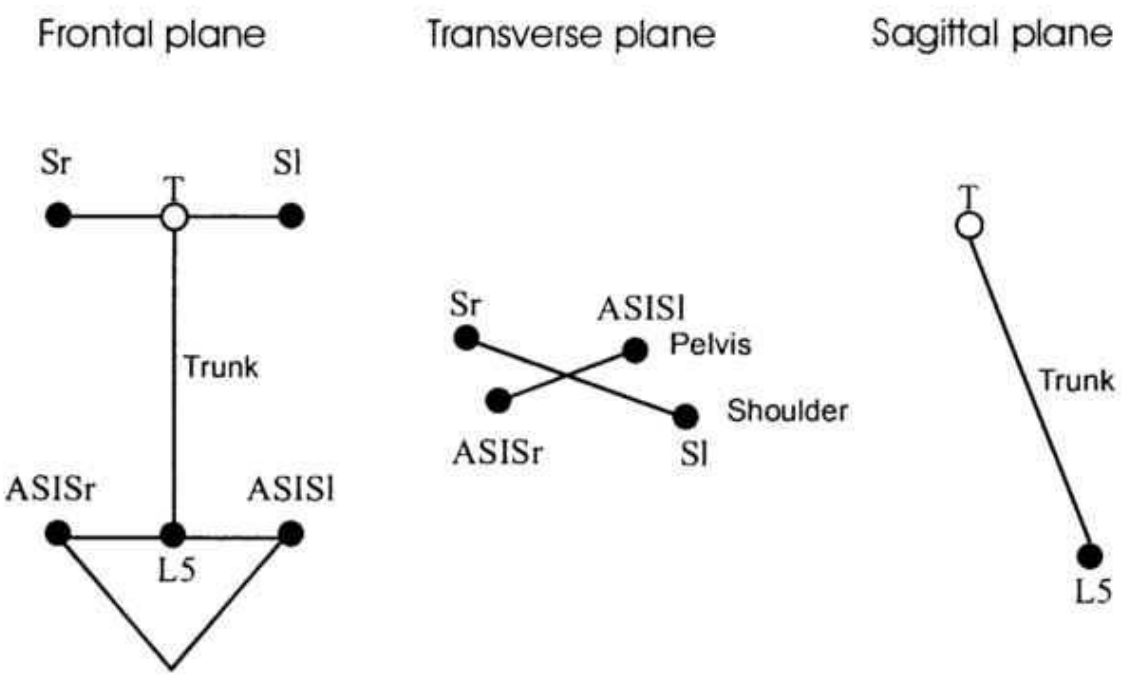

Figure 2.6: A single segment trunk model used to measure trunk kinematics in children with lumbo-sacral myelomeningocele (adapted from Bartonek et al., 2002). (Sr – shoulder right; Sl – shoulder left; ASIS – Anterior Superior Iliac Spine).

However, in the case of where the trunk is treated as a single segment, vital information may be lost due to deformation within the trunk itself (Baker, 2013). To gain a better appreciation of movement within the trunk, some studies have measured movement of thorax with respect to the pelvis (Armand et al., 2014, Attias et al., 2015). The thorax is generally treated as one segment and has been tracked by means of skin surface markers or rigid cluster mounts (Armand et al., 2014, Attias et al., 2015, Krebs et al., 1992). However, differences have arisen in the specific technical definitions of the thorax which can lead to varying results between protocols. The International Society of Biomechanics (ISB) recommend tracking the anatomical landmarks of the 7th cervical vertebra (C7), 8th thoracic vertebra (T8), IncisuraJugularis (IJ) and Xypoid Process (XP) (Wu et al., 2005) (Fig 2.7). The technical axes system is then defined using the mid-points of C7 and IJ (M1) and T8 and XP (M2) (Fig 2.7). In a recent study by Armand and colleagues, an "optical and minimal" marker set was recommended whereby markers were placed directly at IJ, 2nd thoracic vertebra (T2) and T8 and used to define the axes system

(Armand et al., 2014) (Fig 2.7). Immediately, the difference in technical axes system is obvious (Fig 2.7). Other studies have also attempted to expand the assessment further and include movement of the lumbar spine in conjunction with movement of the thorax (Heyrman et al., 2013b, Leardini et al., 2011, Seay et al., 2008). However, similar problem can present when determining technical axes definition (Fig 2.8).

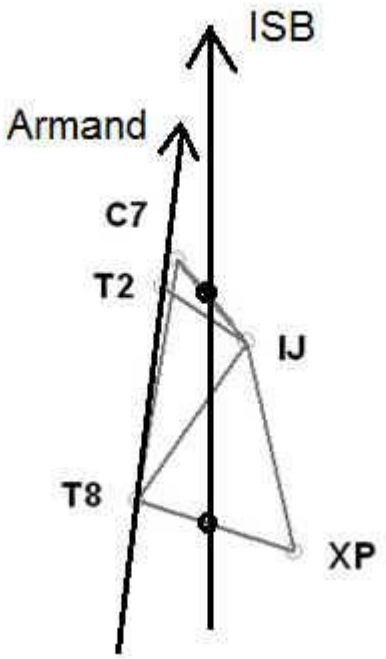

Figure 2.7: The technical axes systems defined by ISB and Armand for the thorax. The offset between axes systems is immediately obvious with the Armand protocol demonstrating a slight forward tilt compared to ISB demonstrating clearly the issues that can occur when choosing different kinematic protocols for the thorax.

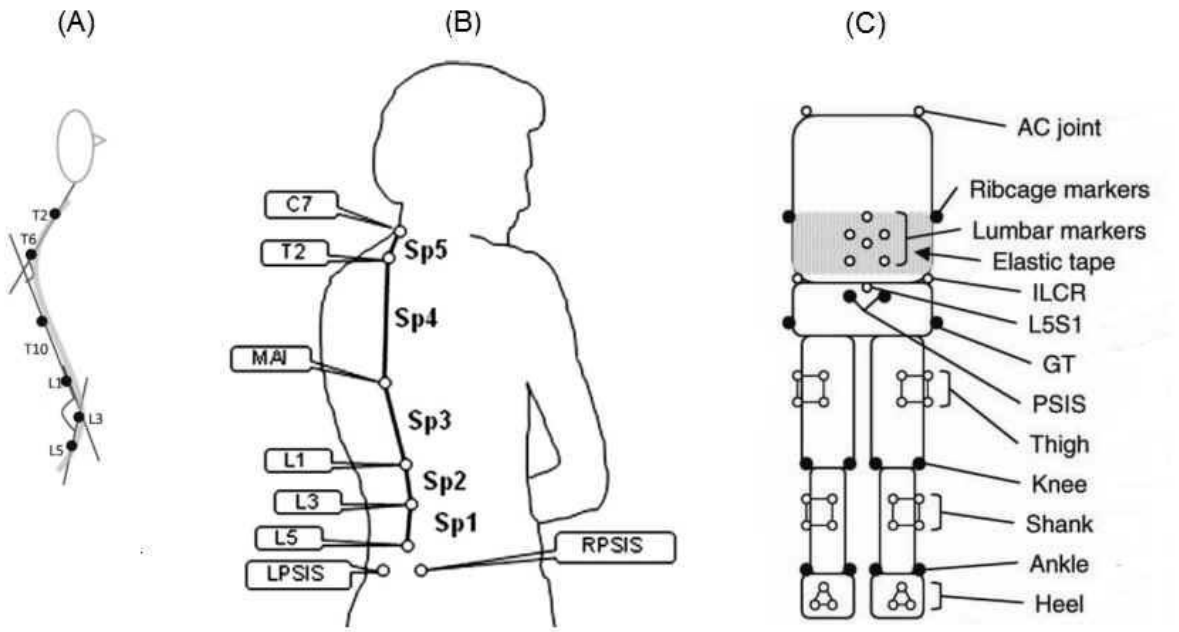

Figure 2.8: Examples of different marker protocols and technical axes definitions that exist to define the lumbar spine. (A – adapted from Heyrman et al., 2013; B – adapted from Leardini et al., 2011; C – adapted from Seay et al., 2008).

One advantage of assessing movement at the trunk is that the trunk is one region (unlike the lower limbs where there is a left and right). Consequently, one would expect a symmetrical movement of the trunk during normal gait as the subject progresses through the left and right gait cycle (Note: the gait cycles overlap and as a consequence there is a period of trunk movement common to both during double support). This symmetry can be a useful tool and can provide clinical insight into pathological movement where symmetry may not be present. For example, a child with hemiplegic CP may present excessive trunk lean during gait towards the affected side while the trunk may stay within normal limits on the unaffected side. The measure of symmetry in normal graphs may also provide a useful tool for quality assurance and data checking.

2.4.6 Normal Trunk Kinematic Patterns – An Overview

During gait analysis, it is common practice to calculate trunk kinematic angles as (1) the rotation between the trunk axes system and the pelvic axes system and (2) the rotation between the trunk axes system and the global or lab axes system, with the lab axes system defined during system calibration (Fig. 2.9).

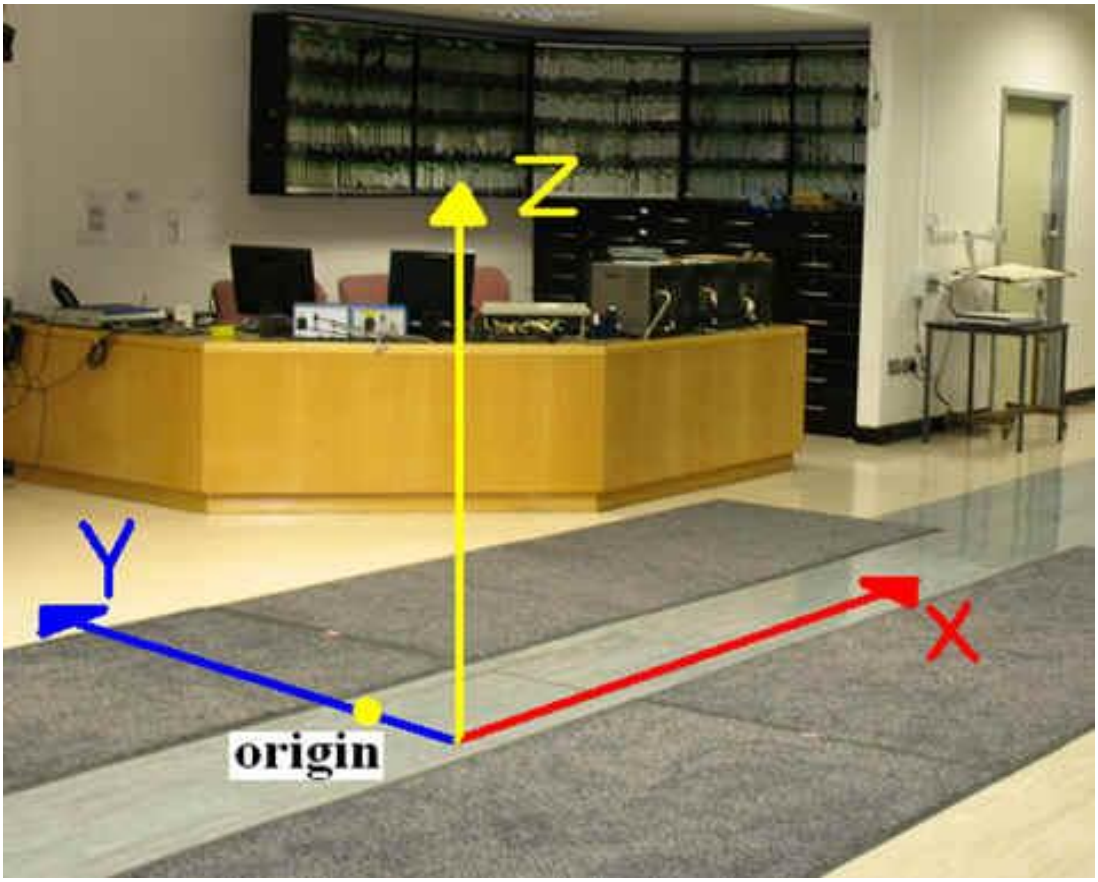

Figure 2.9: The global or Lab axes system defined during system calibration. This reference system provides a neutral reference frame for segment orientation.

In the sagittal plane, normal trunk movement during gait demonstrates only a small angular displacement (flexion / extension). When the trunk is referenced to the laboratory, approximately 15^{o} of flexion is maintained throughout with two distinct periods of extension after initial contact and at the start of the swing phase (Fig.2.10). When compared to the

pelvis, the trunk maintains an approximate neutral position. This is directly related to the anterior tilting of the pelvis.

In the coronal plane (lateral bending), the trunk demonstrates a range of motion of approximately 10^{o} with respect to the laboratory and an increased range of 15^{o} to 20^{o} with respect to the pelvis (Fig.2.10). At initial contact, the trunk demonstrates a neutral position (w.r.t pelvis) followed by a lateral flexion towards the supporting limb leading into loading response phase. Throughout stance, the trunk gradually flexes towards the opposite limb where peak flexion of the trunk occurs at toe off. This is followed by a gradual flexion back towards neutral as the limb progresses through swing. A similar but less pronounced pattern is evident when the trunk is compared to the laboratory.

In the transverse plane (rotation), the trunk demonstrates a range of motion of approximately 18^{o} when compared to the pelvis (Fig.2.10). The trunk begins at an initial position of backwards rotation towards the supporting leg. As the gait cycle progress, the trunk rotates forwards towards the opposite limb where it peaks and then gradually rotates backwards towards the ipsilateral leg.

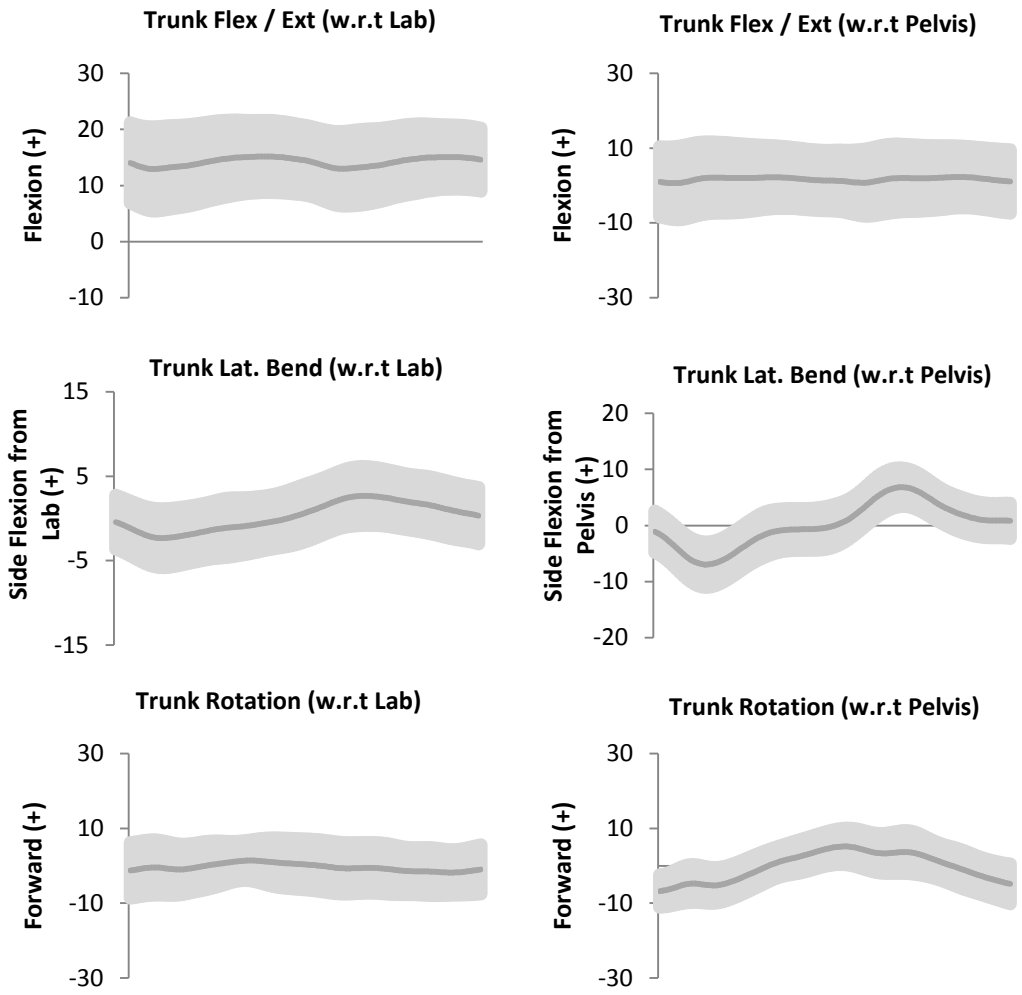

Figure 2.10: Trunk normal kinematic graphs (Mean ± 1SD) for trunk w.r.t the Lab or global frame (left column) and for trunk w.r.t the pelvis (right column).

2.4.7 Patterns of Trunk movement associated with Cerebral Palsy

Studies reporting trunk kinematics in children with CP are limited (Romkes et al., 2007, Pratt et al., 2012, Heyrman et al., 2013a). Romkes *et al* reported greater range of motion (RoM) of the thorax and spine in the sagittal and frontal planes in children with CP when compared to typically developed controls (Romkes et al., 2007). An increased tilting of the thorax was also reported. It was suggested that this was as a result of increased pelvic tilt. However, motion of the spine was considered as only the relative motion of the thorax with respect to the pelvis and as a result it is not clear what input lumbar spinal motion had with respect to thorax tilting. Heyrman *et al* reported a pattern of ipsilateral bending of the trunk during stance followed by a contralateral bending during swing in children with CP (Heyrman et al., 2013a). In contrast, typically developing children maintained a neutral position throughout the gait cycle. Pratt *et al* reported similar findings (Pratt et al., 2012). In this case, the authors made reference to aberrant thorax movements in the frontal plane acting as compensatory mechanisms to (1) account for hip abductor weakness and (2) to facilitate unloading of the contralateral limb during pre-swing secondary to Plantarflexor weakness (Pratt et al., 2012). The study by Heyrman and colleagues also discussed spinal movement between CP and typically developing groups. Reference was made to differences between groups. However, sensors were placed along the spine allowing only a 2-dimensional assessment of movement (Heyrman et al., 2013a). A limited number of studies have reported deformities of the lumbar spine in CP (Harada et al., 1993, McCarthy and Betz, 2000). However, these were limited only to radiographic review. A 3-dimensional kinematic assessment of lumbar spinal movement in a CP group has not been reported in the literature.

In the case of where abnormal trunk kinematic patterns exist, the potential exists for abnormal loading of the lumbar spine. Reference has been made to the importance of the role of the trunk in lower limb net joint kinetics (Õunpuu et al., 1996). As discussed, the trunk may

demonstrate an increased lateral lean to compensate for weak hip abductors (Pratt et al., 2012). The purpose of this is to reduce the hip abductor moment during stance (Õunpuu et al., 1996). A forward trunk lean will increase the hip extensor moment arm in amplitude or also may compensate for increased knee extensor moment arm during crouch by moving the ground reaction force closer to the joint (Õunpuu et al., 1996). Due to the role of the trunk in manipulating lower limb kinetics during pathological gait, the potential exists for compensatory trunk kinematic patterns to adversely affect lower lumbar spinal loading. Lower lumbar spinal kinetic profiles have not been reported in the literature for a CP group.

2.5 Evaluating Kinetics at the Lower Lumbar Spine

It is not common practice to report lower lumbar spinal reactive forces and moments during gait. Most clinical gait laboratories have a combination of one or two force platforms integrated with the 3-dimensional kinematic measurement system and as a result it is not always possible to measure the ground reaction force through a complete gait cycle. To achieve this at least 3 force platforms would be required where the ground reaction from the contralateral limb during the period of double support can be measured. As a compromise, some studies have reported lower lumbar spinal forces and moments throughout the stance phase of gait only (Leteneur et al., 2009). Alternatively, some studies have estimated reactive forces and moments of the contralateral limb based on an assumption of symmetry and time shifting data of the ipsilateral limb (Callaghan et al., 1999). While the assumption of symmetry is reasonable for normal gait, this will not hold true for pathological gait such as in CP. While a number of studies have reported lower lumbar spine kinetics during normal gait, no studies exist for CP subjects. Loading at the lower lumbar spine during normal gait, and the need for assessment during CP gait, will now be discussed.

2.5.1 Lower Lumbar Spine Kinetics during Normal Gait

A limited number of studies have reported 3-dimensional lower lumbar spine kinetics during normal gait (Fig.2.11) (Callaghan et al., 1999, Hendershot and Wolf, 2014, Fernandes et al., 2016). In relation to reactive forces, a consistent compression force is present during gait with peaks occurring at between 5 – 15% and 55 – 65% coinciding with toe off of the contralateral limb and ipsilateral limbs respectively (Fig.2.11) (Callaghan et al., 1999, Hendershot and Wolf, 2014). In the anterior / posterior direction, the reaction force is distributed about the zero line with a posterior force at heel contact followed by a sharp anterior force during loading response returning slowly from anterior to posterior as the leg approaches terminal stance/ pre-swing. At the point of toe-off, the force is once again a posterior force with the same pattern of a quick return to anterior as the contralateral leg contacts and loads (Fig.2.11) (Callaghan et al., 1999, Hendershot and Wolf, 2014). The lateral force component also crosses the zero line with the force directed towards the supporting leg (Fig.2.11) (Callaghan et al., 1999, Hendershot and Wolf, 2014).

When lower lumbar spine reaction moments are considered, reasonable agreement exists in the literature. However, different model estimates of the point at which the reactive moments are realised ultimately affects data between studies. In general, the lateral bending moment follows a similar but opposite pattern to the medial/lateral reactive force (Fig.2.11). At initial contact, there is a lateral bending moment towards the contralateral side. During loading response and into mid-stance the moment switches towards the swinging limb and gradually returns towards a neutral position. During the double support phase the moment alternates slightly between sides and, as the opposite limb undergoes loading, the moment switches back rapidly towards the ipsilateral limb where the pattern repeats (Fig.2.11) (Callaghan et al., 1999). The flexion / extension moment demonstrates a bimodal shape with two peak values occurring during loading response and then during toe off (corresponding to loading response of the contralateral limb) (Fig.2.11) (Callaghan et al., 1999). A more recent

study demonstrated a similar (but offset into extension) profile (Hendershot and Wolf, 2014), highlighting the effect of using different kinematic and kinetic protocols. Axial twist moments are low overall and demonstrate an axial moment towards the swing leg during initial contact and loading response. This is followed by a neutral moment during stance returning to an axial moment back towards the contralateral side during swing (Fig.2.11) (Callaghan et al., 1999, Hendershot and Wolf, 2014).

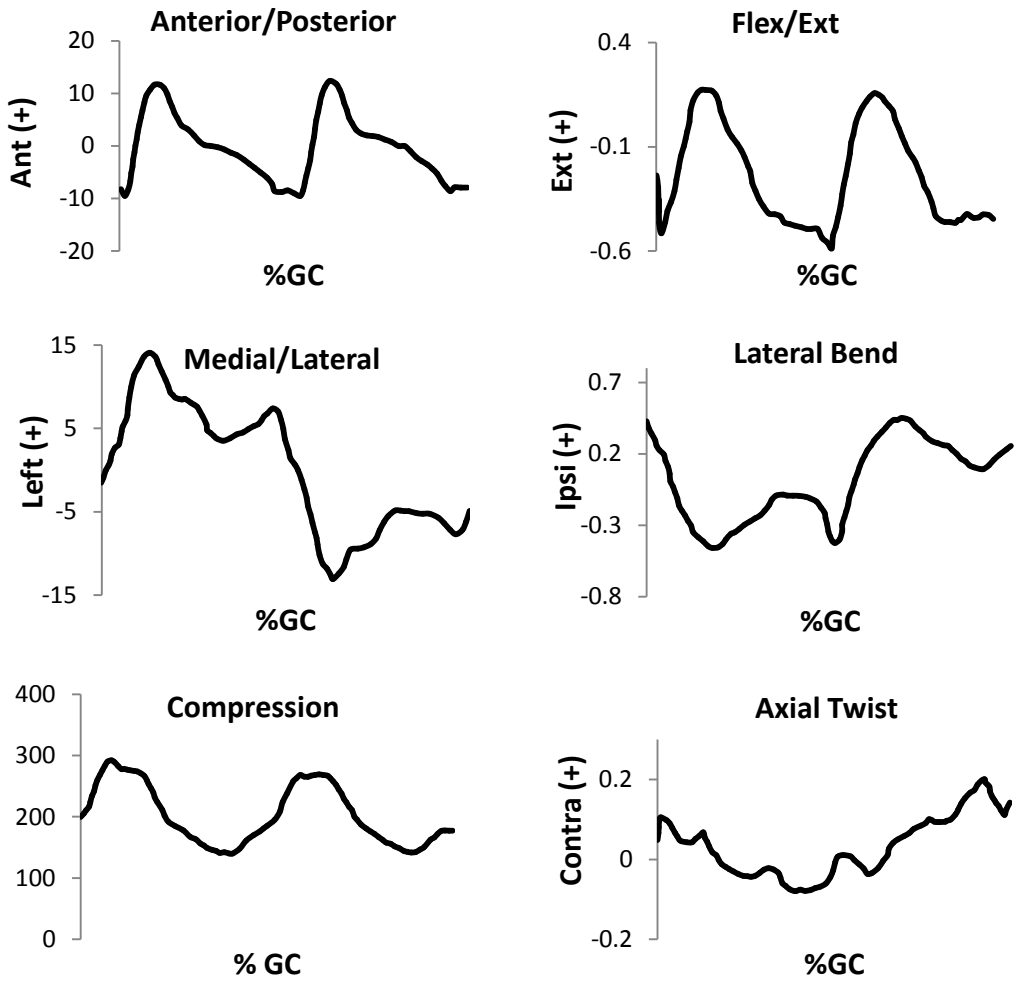

Figure 2.11: Normative reactive forces at the lower lumbar spine (left Column – normalised to % bodyweight) and normative reactive moments at the lower lumbar spine (right Column – normalised to % bodyweight by height). The black line represents data recorded at normal walking speed. Produced using WebPlotDigitizer v3.10 (http://arohatgi.info/WebPlotDigitizer/) - Adapted from (Callaghan et al., 1999)

2.5.2 Lower Lumbar Spine Kinetics in Cerebral Palsy Gait

Lower lumbar spine kinetic data during CP gait has not been reported in the literature. Reference has been made in Section 2.4.6 to how altered trunk and pelvic motion may affect lower lumbar spinal loading. Hip abductor weakness is a classic example of one such pathology that results in compensatory movement of the trunk and it is commonly seen in patients with CP (Gage and Novacheck, 2001, Krautwurst et al., 2013). As previously discussed, a consequence of hip abductor weakness is pelvic obliquity and this can be compensated for by leaning of the trunk to the ipsilateral side to maintain gait stability (Krautwurst et al., 2013). Small changes in trunk inclination during lifting have been shown to increase muscle demands and spinal loading (Mitnitski et al., 1998). Consequently, the question presents as to whether compensatory trunk kinematic patterns during gait in this pathological group could result in increased reactive forces and moments at the lower lumbar spine? In many cases a compensatory trunk pattern may be considered acceptable if the child demonstrates good levels of ambulation. However, increased forces could cause mechanical changes to the structural tissue over time resulting in negative effects at the spine. For example, higher incidences of low back pain have been reported in CP (Jahnsen et al., 2004). Consequently, a clinical need exists to measure and report characteristic trunk kinematic and kinetic patterns during CP gait. Data such as this could highlight another risk factor for potential future problems and will provide an additional tool when planning treatment in CP. Typically developed trunk kinematic and kinetic patterns are also required and will help identify possible deviations from normal in the CP group. Therefore, an investigation into movement of the trunk, assessed at both the thoracic and lumbar level, and kinetic profiles at the lower lumbar spine will be presented as a chapter in this thesis. This investigation is reported in Chapter 10.

2.6 Trendelenburg and Duchenne walking during Cerebral Palsy gait

To demonstrate a specific clinical application of L5/S1 loading during CP gait, the impact of Trendelenburg and Duchenne type gait will be considered. As previously discussed, excessive movement of the trunk and pelvis are often demonstrated during CP gait (Attias et al., 2015, Heyrman et al., 2013a, Romkes et al., 2007, O'Sullivan et al., 2007, Salazar-Torres et al., 2011). In particular, Trendelenburg and Duchenne type gait patterns often present in this group (Metaxiotis et al., 2000). A Trendelenburg gait is characterised by a drop of the pelvis in the coronal plane on the unloaded side during stance with a trunk lean in relation to the pelvis towards the stance limb (Metaxiotis et al., 2000, Westhoff et al., 2006) (Fig.2.12). In the original paper by Trendelenburg, he described a rising and sinking motion of the pelvis in a direction opposite to the direction of the upper body in the child with bilateral congenital dislocation of the hip (Trendelenburg, 1895). It was previously thought that this upper body movement was a consequence of an upwards sliding of the femoral head on the pelvis. However, Trendelenburg highlighted that in order for this to be true then the pelvis would need to move in a similar motion to the upper body towards the supporting limb and it did not (Trendelenburg, 1895). During normal gait the pelvis remains in a horizontal position due to the action of the abductors and Trendelenburg highlighted that, where the action of the abductors was limited or absent, the pelvis would drop during gait in the described manner (Trendelenburg, 1895). Abnormal shortness of the abductor muscles, abnormal direction of the fibres, a reduced or missing femoral neck resulting in a shorter lever arm or general muscle weakness could all limit the ability of the abductors (Trendelenburg, 1895). A Duchenne type gait pattern is characterised by a trunk lean towards the supporting limb with the pelvis level or elevated on the unloaded side (Metaxiotis et al., 2000, Westhoff et al., 2006) (Fig.2.12). The original description of a Duchenne type movement is not as clear as that of Trendelenburg. Both patterns are thought to be as a consequence of weak hip abductors. However, the question presents as to how to both patterns, which are quite distinct from each other, can

arise from the same pathology? It would seem a logical assumption that for a Trendelenburg movement, action of the hip abductors would be present but reduced or inefficient. In Duchenne, due to the excessive lean of the trunk well outside normal limits, one would expect a complete absence of any hip abductor function causing the trunk to compensate in order to maintain the CoM within the base of support. However, regardless of the level of input of the hip abductors, the general consensus is that the hip abductors are the prime contributor to these types of movement patterns (Krautwurst et al., 2013, Metaxiotis et al., 2000, Trendelenburg, 1895, Westhoff et al., 2006).

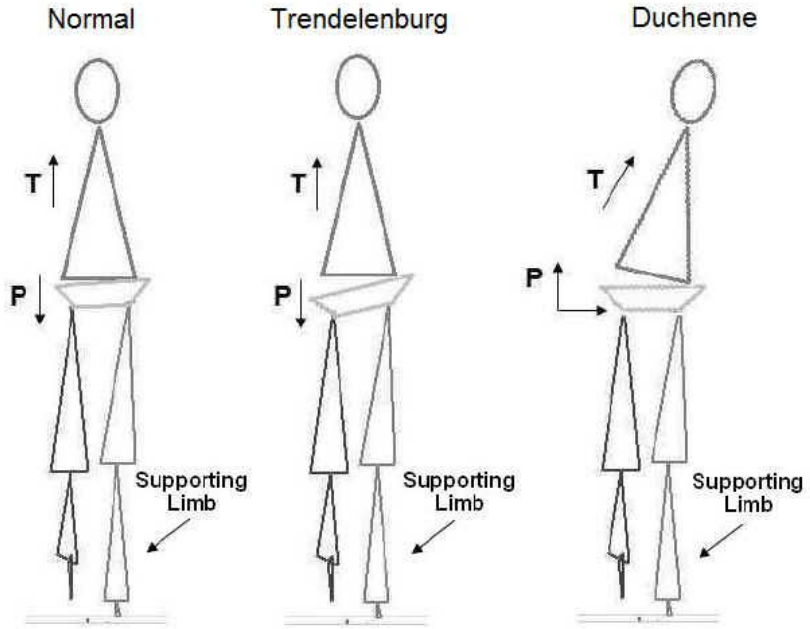

Figure 2.12: A simple stick figure diagram representing trunk and pelvic positions during normal, Trendelenburg and Duchenne type gait (T – Trunk; P – Pelvis).

While excessive movement of the thorax has been reported during CP gait, very few studies have examined movement related directly to those children demonstrating a definite Trendelenburg or Duchenne type movement pattern (Krautwurst et al., 2013, Metaxiotis et al., 2000). A Duchenne type pattern has been reported to have negative effects at the knee due to an increased lever arm around the knee (Stief et al., 2014). A Trendelenburg is thought to be harmful to the hip (Metaxiotis et al., 2000). However, as both Trendelenburg and Duchenne are most pronounced in the coronal plane, it is possible that reactive forces and moments

further up the kinematic chain at the lower lumbar spine might be affected in children presenting with these patterns. In the original work of Trendelenburg, reference was made to the impact of opposing movements of the pelvis and trunk at the lumbar spine. The case was presented of how changes were found at the lumbar spine in older subjects (assessed by means of autopsy) presenting with these types of movements (Trendelenburg, 1895). However, the effects of this movement on lower lumbar spinal loading are unclear and warrant further investigation. With this in mind, an investigation into the affects of Trendelenburg and Duchenne type movement on loading at the lower lumbar spine during CP gait will form a chapter in this thesis. This investigation is reported in Chapter 11.

2.7 Conclusions and Implications

It is clear that movement analysis has a role to play in the management and treatment of children with CP. While the knowledge base relating to movement pathologies in the lower limbs has been well established, movement pathologies of the upper body, specifically the trunk, are less well defined. The limited studies examining trunk movement in CP have identified substantial pathological movement during gait. However, there still exist a number of gaps in the current knowledge base relating to the impact of this pathological movement further up the kinematic chain. Consequently, the following areas have been highlighted as in need of further investigation:

(1) An analysis of thoracic movement during CP gait.

(2) An analysis of lumbar segment movement during CP gait.

(3) An assessment of loading at the lower lumbar spine during CP gait.

(4) An investigation into the effects of Trendelenburg and Duchenne type movement patterns on loading at the lower lumbar spine during CP gait.

The next chapter will explore the role of gait analysis in measuring movement of the trunk, both the thorax and lumbar region, in addition to the estimation of forces at the lower lumbar spine. Challenges faced with the associated kinematic and kinetic models will also be discussed. Chapter 4 will then describe overall goals and specific objectives associated with this thesis.

Chapter 3: Literature Review: Assessment of thoracic and lumbar movement during gait and estimation of forces and moments at the lower lumbar spine

3.1 Introduction

The previous chapter has demonstrated that gait analysis can be a useful tool in management and treatment of CP. While the role of the lower limbs has been well established, investigations into movements of the upper body are relatively new and, as a result, significant gaps remain in current knowledge. While movements of the trunk during CP gait have been examined in the literature, focus has remained primarily at the level of the thorax. Little is known about the contribution of the lumbar region. Furthermore, no data exist regarding the impact of excessive trunk movement on kinetics at the spine in CP, in particular the effects of Trendelenburg and Duchenne type movements. The purpose of this chapter is to examine some of the challenges faced with the associated models needed to measure the kinematics and kinetics of interest. The potential of gait analysis to assess thoracic and lumbar kinematics and to provide estimates of reactive forces and moments at the level of L5/S1 will be discussed. The development of aims and specific objectives for the current study will then follow. These will be outlined in Chapter 4.

3.2 Kinematic models used to measure lower limb movement

Various lower limb kinematic models exist in the literature that have been used both for clinical and research purposes. This has led to the existence of many models, primarily designed based on clinical experience. They often involve the use of different marker configurations and anatomical and technical frame definitions. One common approach to lower limb kinematic analysis is the use of skin surface and wand based marker sets where wands, containing markers, are based on each segment and skin surface markers are shared between segments. This gives at least 3 markers per segment required for segment definition. One of the original wand based models is the Helen Hayes marker set (Sutherland, 2002). The

Coda lower limb model used in the CRC gait laboratory, and used for the purposes of this study, is referred to as a modified Helen Hayes marker set. Femoral and tibial wands define the anatomical axes of each joint and are used in combination with skin surface markers to define the joint centres and the segment coordinate systems needed to measure segment kinematics. The advantage to this type of model is that it is relatively straightforward to use and is applicable to analysis of gait in children (Sutherland, 2002). However, like all kinematic models, there exist limitations that need to be considered when interpreting clinical output.

3.3 Uncertainties in lower limb kinematic models

There are a number of potential sources of uncertainty in movement analysis that can have major implications on the final kinematic and kinetic output. These range from errors associated with the optoelectronic system, such as poor system calibration or errors associated with electronic noise, to problems associated with inaccurate palpation of landmarks for marker placement. Various solutions have been proposed to compensate for the different inaccuracies associated with movement analysis. However, in many cases, there are no conclusive solutions to many of the problems. Some of the main problems and proposed solutions will now be discussed.

3.3.1 Kinematic Crosstalk

Varus / Valgus crosstalk is a common problem in lower limb gait analysis and occurs when axial rotations about one axis are misinterpreted as occurring around another axis (Baker et al., 1999). An incorrect alignment of the thigh wand (either too internal or external) will lead to errors in the measured position of the knee joint centre (Baker et al., 1999). In the case of the Coda model, an internal misalignment of the thigh wand will pull the measured knee joint position into a more posterior and lateral position resulting in a varus wave. This will affect calculation of knee flexion/ extension data and will have further effects at the hip and ankle. If the thigh wand is misaligned too externally the position of the knee joint centre will be

incorrectly measured as too anterior and lateral, resulting in a valgus wave. An incorrect position of the knee joint centre will ultimately affect calculation of kinetics at the knee. As the model is a link segment model, errors will propagate further up the kinematic chain. This will have consequences for the estimation of kinetics at the position of L5/S1. With this in mind, it is important that error is minimised when aligning lower limb wands. For the purposes of this study, and for what is current practice in the CRC gait laboratory, a dynamic walking trail belonging to the subject was produced while the subject underwent the gait assessment. A number of trials were recorded and the subject was then instructed to rest. The data were checked for sign of varus / valgus crosstalk and wands realigned if necessary. This approach provided data more consistent with clinical observation and helped ensure a more accurate wand placement. While some software packages offer the option to mathematically correct for varus / valgus crosstalk, it has been suggested that a better solution would be to ensure for more accurate placement (Baker et al., 1999). For the purposes of this thesis, no further assessment or processing of varus / valgus crosstalk was conducted.

3.3.2 Skin Movement Artefact (SMA)

Skin movement artefact (SMA) is an important consideration when conducting movement analysis. Rigidity of segments is assumed in the kinematic calculations. However, movement analysis deals with soft tissues that are deformable and thus there is relative movement between sensors and the underlying bone (Leardini et al., 2005). Patterns and magnitudes of SMA have been well defined in the literature (Akbarshahi et al., 2010, Benoit et al., 2006, Holden et al., 1997), with different levels of SMA present depending on marker location, segment and task (Peters et al., 2010). By means of a systematic review of the literature, Peters and colleagues reported SMA of approximately 40mm for some areas of the thigh while markers placed over particular anatomical landmarks of the thigh, such as the lateral epicondyle, can exhibit >10mm SMA (Peters et al., 2010). Many ways have been proposed to compensate for SMA such as dynamic calibration (Lucchetti et al., 1998), point

cluster technique (Alexander and Andriacchi, 2001), multi-body or global optimisation (Lu and O'Connor, 1999), subject specific multi-body optimisation (Clement et al., 2015) or double anatomical landmark calibration (Cappello et al., 2005). However, none of these methods has become universally accepted (Clement et al., 2015). Multi-body optimisation has been suggested to have advantages over other techniques (Clement et al., 2015, Lu and O'Connor, 1999). This approach uses an optimal pose of a multi-link model for each data frame such that the overall distance between the measured and model-determined marker coordinates are minimized in a least squares sense, throughout all the body segments. Unlike most other SMA reduction techniques, global optimisation does not treat each segment separately. Further advancement of this technique, using subject specific models of the knee, has shown that results of the multi-body optimisation approach can be improved (Clement et al., 2015). For the purposes of this thesis, the approach of multi-body optimisation, as described by Lu and O'Connor (Lu and O'Connor, 1999), will be used to compensate for the effects of SMA. This approach is automatically implemented in the Visual 3D software used in this study. Many of the current methods described to improve or compensate for SMA were not suitable to implement for the purposes of this study. With this in mind, further investigation regarding the effects of SMA on kinematics and kinetics was not performed.

3.3.3 Anatomical Landmark Identification

Palpation of anatomical landmarks and accurate placement of sensors with respect to those landmarks is a major issue in movement analysis (Della Croce et al., 2005). The majority of anatomical landmarks are subcutaneous and can be palpated. Others are internal, such as the knee or hip joint centres, and their positions need to be estimated (problems associated with hip joint centre identification will be discussed in the following paragraph). Three main issues result in the misidentification of anatomical landmarks; (1) anatomical landmarks are not points but instead can be large uneven surfaces; (2) the thickness of the soft tissue layer over the landmark can vary; (3) interpretation of the method of palpation can vary between

clinicians (Della Croce et al., 2005). Misinterpretation of anatomical landmarks can affect the resultant kinematic and kinetic output. It has been suggested that the problem of landmark misidentification should be addressed by either reducing the uncertainty in determination of specific points or by reducing the effects of uncertainty on kinematic output (Della Croce et al., 2005). For the purposes of this study, an approach of ensuring a more accurate placement of markers was used. The CRC gait laboratory maintains a standard protocol for landmark identification with all clinicians trained to this protocol. Regular in-service training is conducted to maintain levels of competency to these standards. Furthermore, an annual inspection of repeatability of lower limb gait data is conducted among clinicians in the laboratory in accordance with CMAS standards. Finally, prior to the initiation of this study, an assessment of repeatability was performed by the laboratory engineer to demonstrate repeatability of laboratory gait data (Kiernan et al., 2014b). No further investigation was considered necessary regarding the effects of landmark identification for the purposes of this thesis.

3.3.4 Location of the Hip Joint Centre

The position of the hip joint centre (HJC) during gait analysis has been extensively investigated in the literature (Andersen et al., 2013, Hara et al., 2016, Peters et al., 2012, Sangeux et al., 2011, Sangeux et al., 2014, Sangeux, 2015). The location of the HJC is needed to define the thigh coordinate frame for kinematic analysis and it is the point at which inverse dynamics at the hip are realised. Error in locating the HJC can propagate kinematic errors to the knee and ankle and, in addition, errors in the inverse dynamic calculation will propagate up the kinematic chain towards L5/S1. For these reasons, accurate identification of the HJC is essential. For the purposes of clinical gait analysis, two methods, functional calibration and regression equations based on anatomical measurements, are primarily used to determine the position of the HJC. Both approaches have pros and cons related to their use. Functional calibration relies on the relative movement of segments during a number of calibration trials

which can be difficult for subjects with pathology, such as CP, to perform (Sangeux et al., 2014). However, functional calibration is recommended as more accurate than regression equations (Sangeux et al., 2011). Regression equations, based primarily on anatomy of the pelvis or on leg length, are the most widely used in clinical gait analysis and are straightforward to implement. However, many rely on accurate identification of bony landmarks and the populations on which they are based are often different to the populations on which they are used. Furthermore, the choice of regression equation set can also introduce error with some sets shown to be more accurate than others (Harrington et al., 2007). For the purposes of this thesis, a regression equation set will be used for the purpose of HJC location as the population of interest is CP and functional calibration would be difficult to implement. Consequently, it will be necessary to select an appropriate regression equation set. Peters and colleagues suggest that, in the case of where functional calibration is not an option, the regression equations of Harrington et al (Harrington et al., 2007) should be used (Peters et al., 2012). These equations were compared to the best performing functional calibration set and performed well (Harrington et al., 2007). However, during the analysis, only one other widely used regression equation set of Davis et al was compared and the associated impact on kinematics and kinetics were not investigated. The current lower limb model used in the CRC gait laboratory utilises the regression equations set described by Bell et al (Bell et al., 1989). This set had previously been recommended for use when functional calibration was not an option (Stagni et al., 2000). While the evidence supports the use of the equations of Harrington, differences arising from the use of other sets must be considered, both statistically and clinically, as the use of other commonly used sets could be dismissed while in fact the overall effects are small or even negligible. With this in mind, further investigation is warranted as to the selection of HJC regression equation for this study. This investigation will form a chapter of this thesis and is reported in Chapter 7.

3.4 Kinematic Measurements of the Upper Body

Movement analysis of the upper body is still developing. However, as discussed in Section 2.4.6, the ability to assess movement of the upper body, in particular the trunk, can provide further insight into the pathological movements of the child with CP. The trunk acts as an active segment rather that a passive unit during gait and it has been suggested that trunk kinematics should be considered an important part of the pathological gait assessment (Gutierrez et al., 2003, Lamoth et al., 2002). However, methods for modelling the trunk range in complexity. Some studies have focused specifically on movement of the thorax (Armand et al., 2014, Attias et al., 2015), while others have incorporated movement of the lumbar region and spine (Heyrman et al., 2013a, Seay et al., 2008). For the purposes of this thesis, it was decided to assess both movement of the thorax and the lumbar region as the potential exists for aberrant pelvic and thorax motion, both characteristic of CP gait (Attias et al., 2015, Heyrman et al., 2013a, Metaxiotis et al., 2000, O'Sullivan et al., 2007, Romkes et al., 2007), to affect motion of the lumbar spine due to the direct relationship of the pelvis, lumbar spine and thorax along the kinematic chain. However, similar to lower limb analysis, a number of practical challenges exist when assessing movement of the upper body. These will now be discussed.

3.4.1 Thorax kinematic assessment

Three dimensional thoracic movements have been assessed by a number of different protocols in the literature. The International Society of Biomechanics (ISB) report anatomical landmarks required to define the thorax (Wu et al., 2005). If researchers choose to use these guidelines it is then a matter for those researchers to relate tracking sensors to these points. Alternatively, other researchers have proposed their own protocols (Armand et al., 2014). In many cases, skin surface sensors will be used. However, a number of drawbacks exist to using the skin surface approach. As previously discussed, SMA and anatomical landmark

identification are important considerations. Additionally, for pathological groups such as CP, cooperation during sensor application may be an issue when applying multiple sensor sets. Furthermore, the requirement of a Xypoid Process sensor can raise a number of practical and potentially embarrassing issues for assessment on females (Armand et al., 2014). As an alternative to the skin surface approach, rigid clusters placed at specific points on the thorax have been used to measure movement (Houck et al., 2006, Krebs et al., 1992). However, these studies are few in numbers and often it is not clear how well they perform compared to the reference standard. Consequently, there is a clinical need for the development of an alternative protocol to measure thorax movement during gait that helps overcome the day-to-day practical issues of other commonly used protocols. The development of a new thoracic cluster protocol will be considered as part of this study and will form a chapter in this thesis. This study is reported in Chapter 8.

3.4.2 Lumbar Spine kinematic assessment

Motion of the lumbar region during gait can be measured by means of a 2-dimensional assessment with sensors placed along the spine or by means of a 3-dimensional assessment treating the lumbar region as a rigid segment. The lumbar region is of course not one rigid segment and is made up of a number of individual vertebrae. Measuring the movement of each vertebra in 3 dimensions using skin mounted optoelectronic sensors is not possible. Instead, sensors placed along the spine have been used to provide assessment of movement in 2 planes (Heyrman et al., 2013a). Treating the lumbar region as rigid acts as a compromise between clinical utility and clinically useful information and has been achieved by means of sensors placed at specific points around the lumbar region (Crosbie et al., 1997, O'Sullivan et al., 2010a, Seay et al., 2008), and by the use of rigid cluster mounts (Konz et al., 2006, Needham et al., 2014, Schache et al., 2002). However, no reference standard exists for assessing rigid motion of the lumbar region. As a result, protocols have been developed based primarily on clinical experience. Preferably, before a protocol is used, a preliminary validation

of the protocol would be to compare it, during use, against a reference standard. Similarly, when choosing a protocol for use in a particular study, it is important to know how the protocol performs and whether it is suitable for the study of interest. No study has examined the use of different protocols for the 3-dimensional assessment of the lumbar region during gait. Before one is chosen for the purposes of this study, it will be necessary to compare a number of protocols from the literature so that differences between protocols can be fully understood. A comparison of a number of lumbar segment protocols will be conducted as part of this study and will form a chapter in this thesis. This study is reported in Chapter 9.

3.5 The Role of Inverse Dynamics during Gait

Inverse dynamics are used to estimate the forces and moments that cause the movements recorded by the kinematic model. Inverse dynamics are performed by means of link-segment modelling. The inputs required for this procedure are detailed in Figure 3.1.

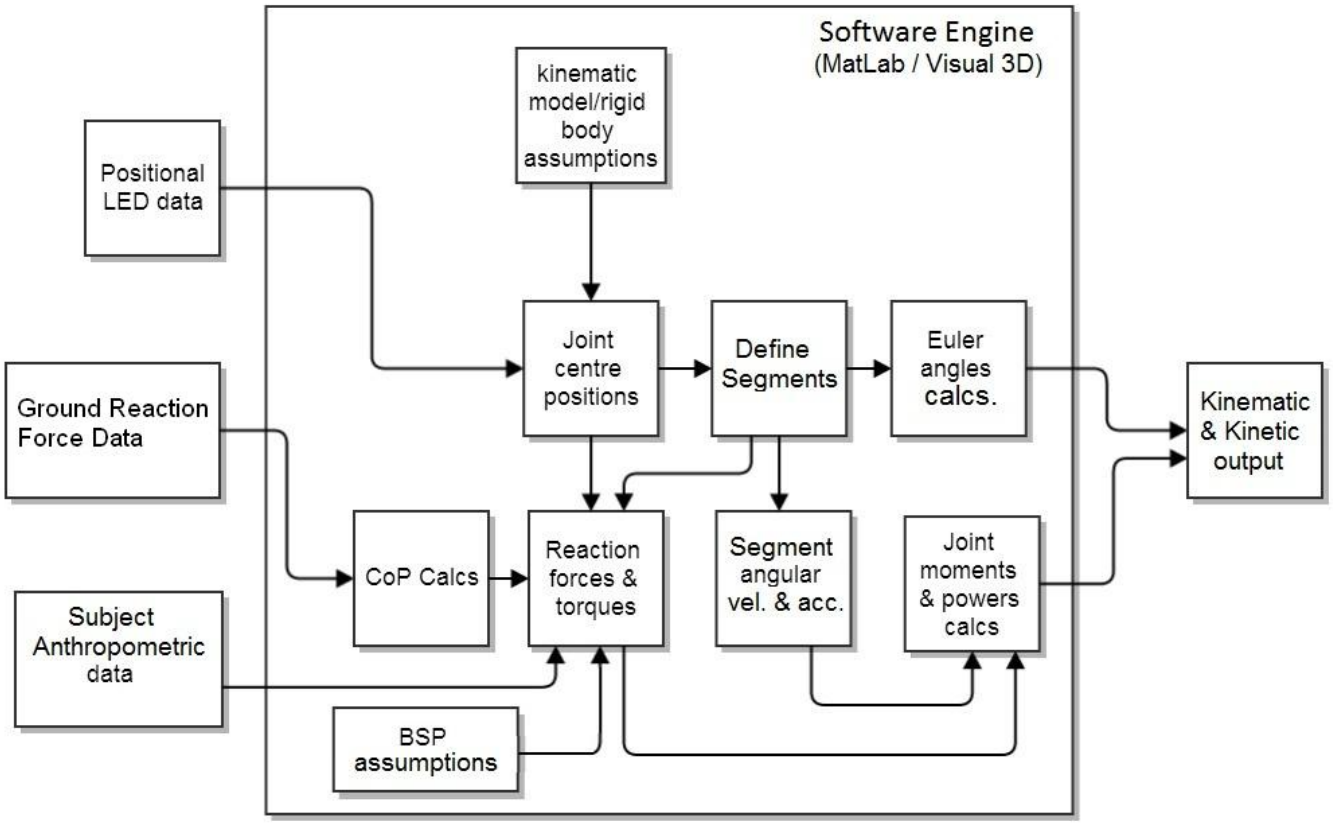

Figure 3.1: A flow chart describing the constituents of the Inverse Dynamic Model. Positional marker data, ground reaction force data and subject anthropometric data are all fed into the inverse dynamic mode to calculate reactive forces and moments at each joint.

Positional marker data, ground reaction force data recorded by means of external force platforms embedded in the laboratory floor and subject anthropometric measures (e.g. height, weight) recorded during the clinical assessment are input into the model and used to calculate the joint reaction forces and moments at each time point during the gait cycle. Similar to the kinematic model, there exist a number of limitations to the inverse dynamic approach. Some of the main problems will now be discussed.

3.6 Uncertainties in the Inverse dynamic approach

Segment orientation, joint centre position, segment mass, centre of mass (CoM) and moment of inertia (MoI) are all required for the inverse dynamic analysis. A link segment model is needed to provide joint centre positions and segment orientations. Estimates are made for mass, CoM and MoI using body segment parameter sets from the literature. A measure of the ground reaction force (GRF) is needed if inverse dynamics are realised using the "bottom up" approach. Additionally, the following assumptions are made (Winter, 2009):

- Each segment has a fixed mass (located at CoM).
- The length of each segment remains constant.
- The CoM remains fixed.
- The MoI about the CoM remains constant
- The joints are assumed to be ball and socket or hinged

In reality, due to the soft tissue makeup of individual segments and errors associated with link segment modelling discussed earlier, these assumptions do not necessarily hold true. In addition to the previously discussed uncertainties related to the kinematic model, a number of uncertainties present when using the inverse dynamic approach.

3.6.1 Centre of Pressure Alignment

Inaccurate alignment of the centre of pressure (CoP) with segment endpoint coordinates is a potential source of error during the movement analysis procedure (McCaw and DeVita, 1995, Riemer et al., 2008, Silva and Ambrósio, 2004). Inaccuracies in the spatial alignment of the CoP and the foot segment arise primarily due to the fact that two independent systems, usually sampling at different rates, are used to measure kinematic and kinetic data (McCaw and DeVita, 1995). Alignment errors of well over 10mm have been reported (Camargo-Junior et al., 2013, McCaw and DeVita, 1995), while some authors suggest 12mm as an acceptable error (Lewis et al., 2007). It has been reported that the effect of such error on the resultant torques can be as much as 14% of maximum value (McCaw and DeVita, 1995). However, from and end user point of view, improving the alignment of the CoP can be difficult. In relation to the force platform, piezoelectric force plates have been demonstrated as being sensitive to the construction of the plate, in particular bending moments of the measurement posts (Schmiedmayer and Kastner, 1999). Correction parameters have been devised and used to improve the calculation of the centre of pressure (Schmiedmayer and Kastner, 1999). However, there is no standard automated correction technique (Lewis et al., 2007). For the purposes of this thesis, and for what is routine practice in the CRC gait laboratory, correction parameters have been applied to the Kistler platforms. Improvement of the synchronisation between the kinematic and kinetic systems has also been suggested as a consideration for improving the quality of the inverse dynamic results (Silva and Ambrósio, 2004). However, performance of the systems can be difficult to improve as alignment and calibration procedures are mainly implemented by the manufacturers. However, on-going calibration checks can help maintain confidence in system performance. A basic requirement of a clinical gait laboratory is implementation of both spot checks and more in-depth calibration tests on an on-going basis (Lewis et al., 2007). This allows for an assessment of system performance and the identification of system failure. Various calibration checks and

spot checks have been presented in the literature to assess performance of both 3-dimensional and force plate systems (Baker, 1997, Holden et al., 2003, Lewis et al., 2007). For the purposes of this thesis, a measure of consistency of system performance was performed by means of an instrumented pole test before data acquisition for all subjects (Holden et al., 2003). This is a mandatory requirement of the Clinical Movement Analysis Society UK and Ireland (CMAS) accreditation process. System performance was found to fall within set thresholds and, as a result of this, no further investigation into the effect of CoP misalignment was conducted for the purposes of this thesis.

3.6.2 Body Segment Parameter Estimates

Estimated body segment parameters (BSP), such as segment mass, COM and MoI, are required for the inverse dynamic calculations. However, concerns associated with the use of BSP sets have been reported in the literature, in particular where subject age and gender fall outside the population originally used to formulate the BSPs (Damavandi et al., 2009, Kingma et al., 1996). Reduction in errors in BSP by the use of subject specific geometric models that integrate shape and density information has been suggested as an approach to improve the inverse dynamic results (Riemer et al., 2008). However, this approach would be difficult to implement in the clinical setting. As an acceptable compromise, BSP sets from the literature are routinely used and, for the purposes of this thesis, BSP estimates from the literature will be used in the inverse dynamic model. However, no consensus has been reached as to the most suitable set for use during gait. Some authors have reported the inverse dynamic calculations to be sensitive to the underlying BSP set (Chen et al., 2011, Rao et al., 2006). Others have reported the effects to be minimal (Ganley and Powers, 2004). As the population of interest for this study are children with CP, additional concerns present relating to asymmetries, such as leg length or reduced muscle volume, which may further impact on the inverse dynamic results. However, no study has investigated the effect of using different BSP sets on the kinetic profiles of children with CP. Before a BSP set can be chosen for the

purposes of this study, further investigation is warranted, from both a statistical and clinical point of view, into the effects of using different BSP sets on inverse dynamic calculations during gait. An investigation into the use of different BSP sets will be conducted as part of this research and will form a chapter in this thesis. This investigation is reported in Chapter 6.

3.7 Models for evaluating forces at the lower lumbar spine

The need for an investigation into levels of loading at the lower lumbar spine during CP gait has been highlighted in Chapter 1. However, in general, very few studies have examined loading at the lower lumbar spine during gait. For the few that have, the kinematic and inverse dynamic procedures often differ making direct comparisons difficult. Reed and colleagues presented the use of regression equations as an approach to estimating the position of the L5/S1 joint that was based on pelvic anatomy and pelvic and leg length measures (Reed et al., 1999). However, this approach was primarily for use during assessment of automobile occupant posture and may not be as suitable for assessment during gait (Reed et al., 1999). Lariviere and colleagues estimated the L5/S1 joint as the position of a tracking marker placed on the skin over the L5/S1 joint space (Lariviere and Gagnon, 1999). However, while this could be considered a close approximation, some error in position of the L5/S1 would be expected due to marker size and skin surface to joint space distance. Khoo and colleagues estimated the position of L5/S1 as a point 5% along the length of the line from the L5/S1 skin surface marker to the mid-point of the ASISs. This approximate position of the L5/S1 joint was based on CT scans using mean subject position (Khoo et al., 1995). This approach has since been used in a number of studies examining both running and walking (Mason et al., 2014, Seay et al., 2008, Fernandes et al., 2016). Ideally, subject specific measurements of the lower lumbar spine would be used to identify the L5/S1 joint space. However, for the purposes of this study, it was not feasible to access the types of imaging techniques required to achieve this. The next best approach would be to compare the resultant L5/S1 kinetic output using a

number of different methods of locating L5/S1 from the literature. However, this was not conducted as part of this study as the regression equations of Reed and colleagues were not considered suitable based on their estimation using a seated posture and the approach of using a skin surface marker as the L5/S1 joint was considered a simplified approach that may add unnecessary error. As few other methods of L5/S1 identification have been reported in the literature, the approach described by Khoo and colleagues was used for the purposes of this study. Consequently, no further examination of the affects of L5/S1 position was considered as part of this thesis.

3.8 Conclusions and Implications:

The purpose of this chapter has been to highlight the main uncertainties associated with 3-dimensional movement analysis and to highlight some of the issues associated with assessing thoracic and lumbar movement and kinetics at the lower lumbar spine during gait. The following issues were highlighted as in need of further investigation:

(1) Selection of BSP set.

(2) Selection of HJC regression equation set.

(3) Selection of a protocol for assessment of lumbar segment movement during gait.

(4) Development of a new thoracic kinematic protocol.

This preparatory work on the kinematic and kinetic models will form a number of chapters in this thesis. This preparatory work will be used to develop the final kinematic and kinetic models required to assess movement of the thorax and lumbar region and to assess loading at the lower lumbar spine during CP gait. Overall gaols and specific objectives of this thesis will now be discussed in Chapter 4.

Chapter 4: Thesis Objectives

4.1 Introduction

The overall goal of this study was to investigate levels of loading at the lower lumbar spine during gait in children with CP, with a view to determine whether a relationship existed between pathological movement of the upper and lower trunk and kinetic profiles at the lower lumbar spine, and to investigate whether children with CP presenting with Trendelenburg and Duchenne type gait patterns demonstrated altered patterns of lower spinal loading compared to TD controls. A secondary goal was to assess particular aspects of the kinematic and kinetic models before implementation in this study. The specific objectives of this thesis were as follows:

4.1.1 Objective 1: Body Segment Parameter set - Sensitivity Analysis

To perform a sensitivity analysis and assess the clinical impact of using different body segment parameter sets from the literature, with the purpose of selecting a suitable set for use in the inverse dynamic model (Chapter 6).

4.1.2 Objective 2: Hip Joint Centre regression equation set - Sensitivity Analysis

To perform a sensitivity analysis and assess the clinical impact of using different hip joint centre regression equation sets from the literature, with the purpose of selecting a suitable set for use in the kinematic model (Chapter 7).

4.1.3 Objective 3: Thorax protocol development

To develop a thorax kinematic protocol, that will provide practical advantages for use during the gait assessment, to be used to measure thorax kinematics (Chapter 8).

4.1.4 Objective 4: Lumbar segment protocol assessment

To determine a suitable kinematic protocol to measure 3-dimensional lumbar segment movement during gait (Chapter 9).

4.1.5 Objective 5: Thoracic, Lumbar and L5/S1 kinetics pattern assessment

To investigate 3-dimensional thorax movement, lumbar segment movement and 3-dimensional reactive forces and moments at the lower lumbar spine in paediatric CP subjects compared to TD during gait and to determine whether a relationship exists between thorax kinematics and lower lumbar spinal kinetics (Chapter 10).

4.1.6 Objective 6: Biomechanical assessment of Trendelenburg / Duchenne type gait

To investigate the effects of Trendelenburg and Duchenne type movements on L5/S1 kinetics in paediatric CP subjects compared to TD children during gait (Chapter 11).

Chapter 5: General Methodology

5.1 Introduction

This chapter details the general methodology associated with this research. Ethical considerations, participant identification and recruitment, constituents of the lower limb kinematic and kinetic model and the procedure for gait analysis, including data collection and data processing, are described.

5.2 Ethical considerations

Ethical approval for this study was obtained from the Central Remedial Clinic's Ethical committee. The subject information leaflet and consent form were considered appropriate and no ethical issues were raised. The letter of ethical approval is provided in Appendix 5.1. The participant information leaflet and consent forms are provided in Appendix 5.2 and Appendix 5.3 respectively.

5.3 Participants

5.3.1 Source of recruitment

The Gait Laboratory at the Central Remedial Clinic is the national referral centre for adults and children with complex walking disabilities in the Republic of Ireland and served as the source of recruitment for this study.

5.3.2 Identification of participants

Potential participants with a diagnosis of hemiplegic or dipelgic cerebral palsy were identified based on referral to the gait laboratory of the Central Remedial Clinic.

5.3.3 Inclusion and exclusion criteria

Inclusion Criteria for CP subjects:

- Subjects with a diagnosis of hemiplegic or dipelgic cerebral palsy
- Subjects aged between 6 and 18 at time of assessment
- Subject or Parents/Guardians who were willing to give written and informed consent.
- Subject who were able to walk 10m either independently or with assistance of a mobility aid.

Exclusion Criteria for CP subjects:

- Subjects who had surgery within 1-year of presenting to the gait laboratory.
- Subjects who presented for a repeat assessment during the course of the study – the repeat assessment was not included in the study.

Typically developed children with any previous history of neurological, musculoskeletal or orthopaedic problems were excluded from the study.

5.3.4 Recruitment

Participants who fitted the inclusion criteria were identified prior to their assessment in the gait laboratory. Potential participants were then asked to participate in the study. An information leaflet on the study was made available to all participants. Each subject or parent /guardian was then asked to sign a consent form if they agreed to participate in the study. Typically developed children were sourced through employees of the clinic. Employees were asked whether their children would like to participate in the research project. On presentation to the gait laboratory, an information leaflet on the study was made available to all participants. Each subject or parent /guardian was asked to sign a consent form if they agreed to participate in the study.

5.4 Constituents of a Kinematic Model

The study of kinematics refers to mechanics of movement of a body without concern for the mass or the forces acting on it. In relation to human movement, it is the study of the relative positions of limb segments. That is, the angles and displacements between adjacent segments. Kinematic analysis with respect to human movement is performed by means of link segment modelling. The inputs required for this procedure are outlined in Figure 5.1.

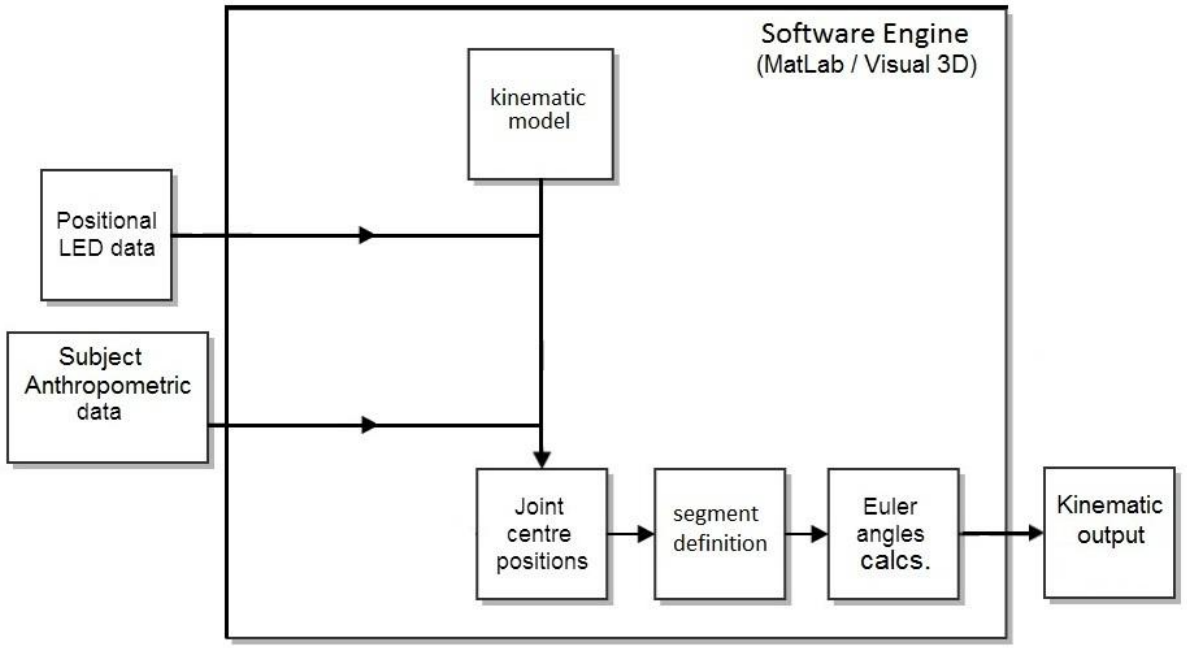

Figure 5.1: A simple flow diagram demonstrating the constituents of a kinematic model. Positional marker data is captured by the Coda active marker system. This data, combined with subject specific anthropometric data, is fed into the system. Joint centre positions (hip, knee and ankle) are calculated and the corresponding lower limb segments are defined. Euler mathematics are then used to determine angular movement in all 3 planes.

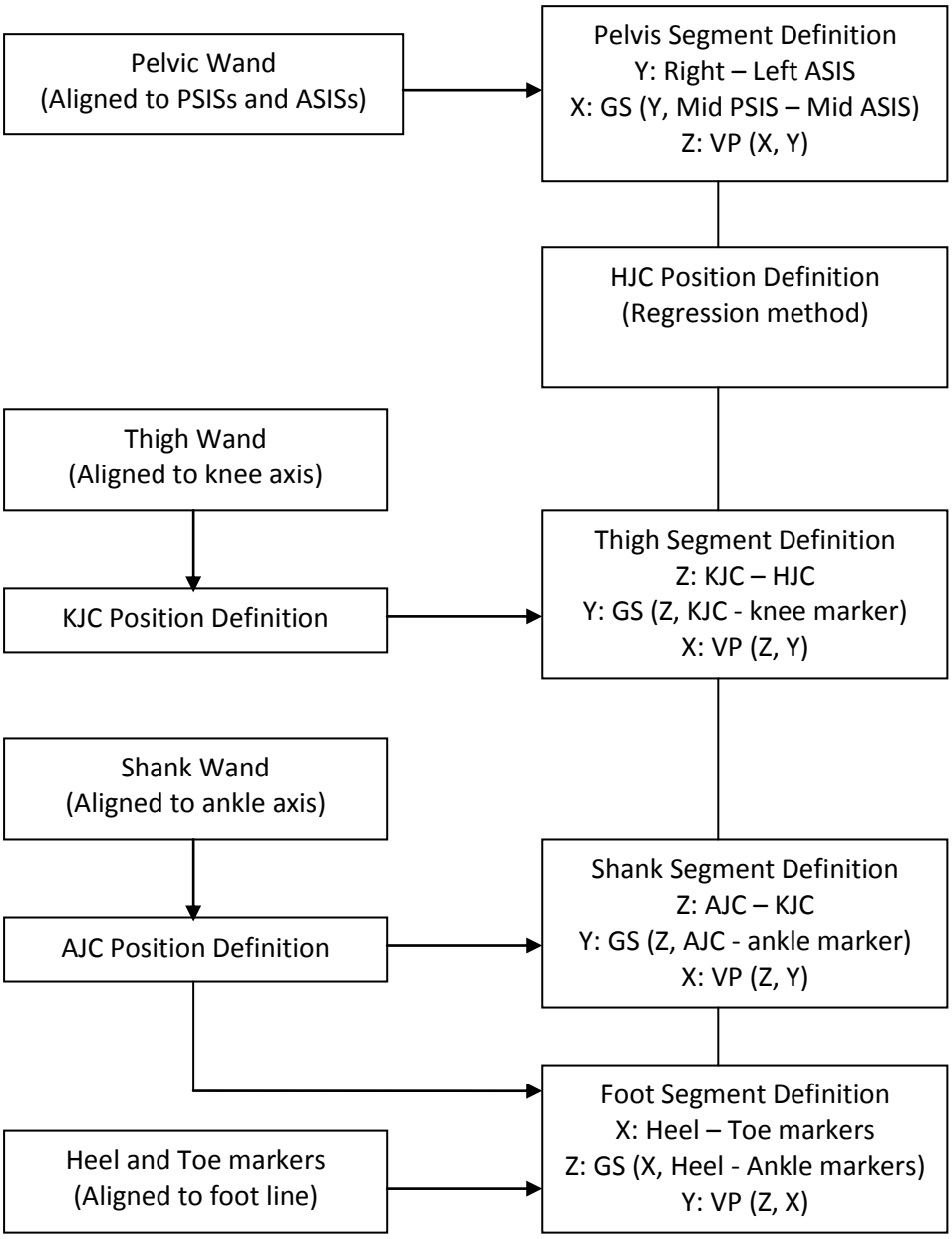

Figure 5.2: A simple flow diagram describing the kinematic model used in this study. The model was a top-down link segment model with 3 degrees of freedom at each joint. Joint centre positions were calculated based on marker position. Joint centre position combined with marker data were then used to define each lower limb segment (GS- Gram Schmidt mathematical procedure for generating orthogonal axes, VP – vector product, PSIS – Posterior Superior Iliac Spines, ASIS – Anterior Superior Iliac Spines, HJC – Hip Joint Centre, KJC – Knee Joint Centre, AJC – Ankle Joint Centre).

5.5 Lower Limb Kinematic Model

The lower limb model used in this research was a top-down link segment model with 3 degrees of freedom at each joint. The model worked from the pelvis down and consisted of 7 segments. The segments were the pelvis, left and right thigh, left and right shank and left and right foot (Fig.5.2). The local co-ordinate system (LCS) for each segment was determined from 3 or more non co-linear points using a right-hand axis system. The model is that used in clinical practice on a day-to-day basis in the CRC gait laboratory. This model has previously shown good overall reliability, comparing well to other models (Kiernan et al., 2014b).

5.5.1 Motion Analysis System

The motion analysis system was a 4 camera CODA cx1 active marker system (Charnwood Dynamics Ltd., Leicestershire). The system depends on accurate placement of active markers on specific bony landmarks. Two cx1 cameras were located on each side of a central walkway, parallel to the walkway. Each cx1 camera tracked markers in 3-dimensions. Three 1-dimensional linear sensors measured the angle to a marker by means of cross-correlation of a shadow mask pattern. Two sensors measured the X and Y coordinates by means of triangulation and the third sensor measured the Z coordinate. Each marker was connected to a drive battery box that received an infra-red signal from the cx1 camera. The drive battery box provided an identity to the marker allowing for straightforward identification during post processing. Kinematic data were captured at 100Hz using Codamotion v.6.78.1 software (Chapters 6-9) and Codamotion ODIN software (v1.06 Build 01 09) (Chapters 10-11).

5.5.2 Marker Placement Protocol

Markers were placed both directly on the skin and on segment mounted wands (Fig.5.3). To track the foot, markers were attached to the lateral head of the fifth metatarsal, the posterolateral aspect of the calcaneous and the anteroinferior tip of the lateral malleolus. The marker for the knee was attached at a point just superior to the palpable knee joint space

and anterior to the fibular head. Two wands were needed per lower limb, one at the distal femur and one on the tibia. The tibial wand was comprised of a rigid horizontal wand and a rigid vertical frame which was placed on the anterior-lateral aspect of the shank and held in place by two straps. Two markers were positioned on the anterior and posterior aspects of the horizontal wand. The femoral wand was similar to the tibial wand, except it had a smaller frame. It was placed at the distal end of the femoral shaft on the lateral aspect. To track the pelvic segment, 4 markers were mounted on a pelvic brace, which in turn was attached to the subject by means of a pelvic belt. The belt was aligned with its superior margins aligned with the Anterior Superior Iliac Spine (ASISs) and the Posterior Superior Iliac Spines (PSISs).

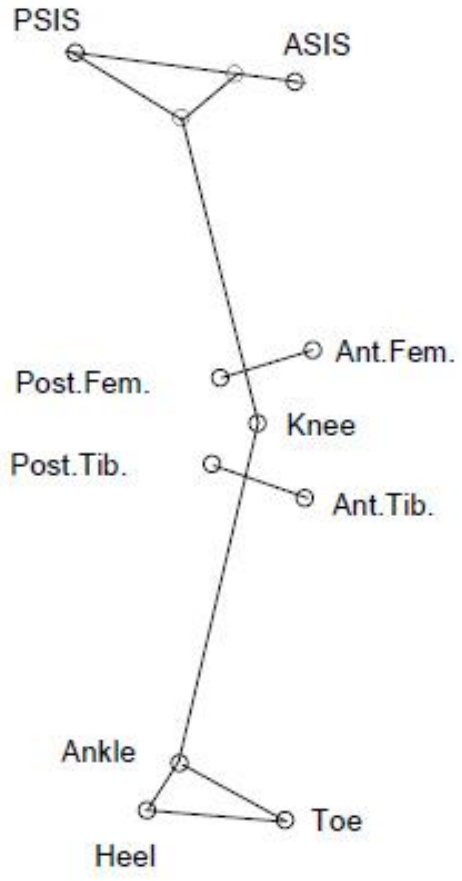

Figure 5.3: Schematic showing marker position for lower limb kinematic analysis. markers were attached using double sided sticky tape to the heel, toe, ankle and knee. Segment mounted wands were used in the definition of the thigh and shank segment. A pelvic brace, aligned to the PSISs and ASISs, was attached to the pelvis using a pelvic band.

A number of subject specific anthropometric measures were needed for the lower limb kinematic model. These were used in the regression equations in order to estimate segment variables such as approximate mass, centre of mass (CoM) and moment of inertia (MoI). These variables are listed in Table 5.1.

Table 5.1: Subject specific anthropometric measures required for the lower limb kinematic model. All variables were measured before application of the kinematic set

Anthropometric Measure	*Description*
Height (m)	Recorded barefoot with back against fixed wall scale
Weight (kg)	Body weight recorded using Seca Electronic Weight Scale.
Pelvic Width (mm)	ASIS to ASIS measure using standard measuring tape
Pelvic Depth (mm)	ASIS to PSIS measure using standard measuring tape
Knee Width (mm)	Medial to lateral femoral epicondyle
Ankle Width (mm)	Medial to lateral malleolus

5.5.3 Pelvis Segment Definition

The pelvic LCS was calculated from markers located on a pelvic frame. The pelvic frame was fitted to the subject and aligned with the ASISs and PSISs (Fig.5.4). The y-axis was obtained from the medio-lateral line between the ASIS markers. The x-axis was calculated using a Gram-Schmidt orthogonal procedure of the line passing through the mid-points of the ASIS and PSIS markers and the y-axis. The Gram-Schmidt procedure constructs an orthogonal basis from a set of non-orthogonal functions. Once the x-axis was known, the resulting z-axis was the vector product of the x-axis and y-axis. The origin of the pelvic LCS was the mid-point of the PSIS markers.

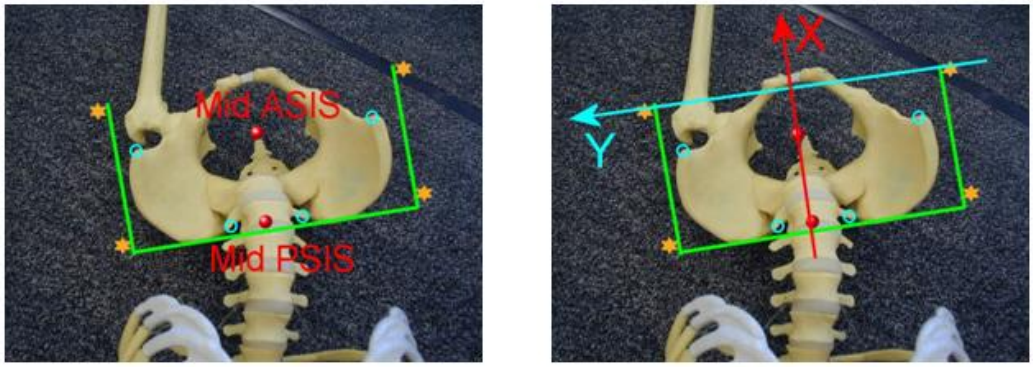

Figure 5.4: Skeletal representation of the pelvic LCS. Yellow stars represent actual marker positions. White circles represent segment reference points (ASIS and PSIS). X and Y indicate axes direction. The Z axis was determined as the vector product of the X and Y axes.

5.5.4 Thigh Segment Definition

The hip joint centre (HJC) was required for calculation of the thigh LCS along with the knee joint centre (KJC). HJCs were positioned relative to pelvic bony landmarks and were determined by offsets described using regression equation sets from the literature. The LCS of the pelvis determined the direction of the offsets. The rationale for selecting the regression equation set for HJC estimates is documented in detail in Chapter 7. For the calculation of the KJCs, a virtual HJC point was required (Fig.5.5). The virtual HJC (VirHJC) was determined by offsetting the HJC by half the knee width in a direction perpendicular to the plane formed by the actual HJC and the femoral wand markers. The purpose of this was to align the axis closer to the line of the femur and provide a better medio-lateral knee axis. The KJC was then offset medially by half the knee joint width from the knee marker (lateral femoral epicondyle). This offset occurred in a direction mutually perpendicular to the plane defined by the VirHJC and the knee marker and the vector defined by the femoral wand markers (Fig.5.5).

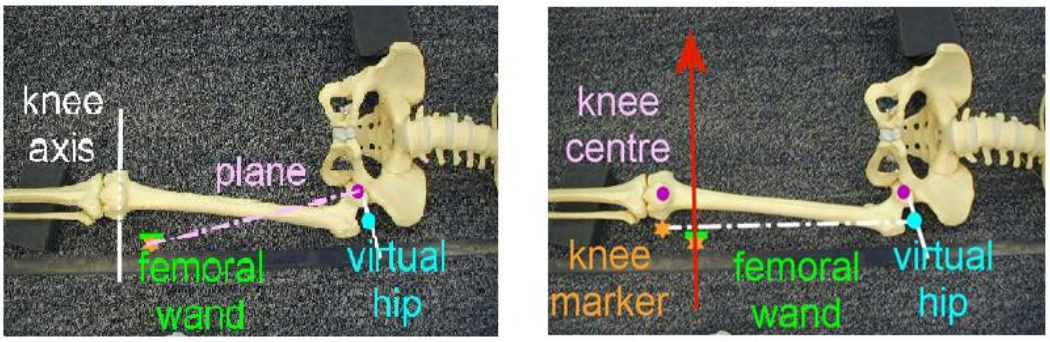

Figure 5.5: Definition of the KJC required for thigh segment definition. The KJC was offset by half the knee width in a direction perpendicular to the plane formed by the VirHJC, knee marker and femoral wand.

The LCS for the thigh was then calculated. The z-axis was the principle femoral axis defined between the HJC and KJC. The x-axis was calculated using the Gram-Schmidt procedure of the line passing through the femoral wand markers and the z-axis. The resulting y-axis was the vector product of the z-axis and x-axis.

5.5.5 Shank (Lower Leg) Segment Definition

The ankle joint centre (AJC) was required along with the previously described KJC for the definition of the Shank LCS. The AJC was offset medially from the ankle joint marker (lateral malleolus) by half the ankle width along the ankle axis. The ankle axis was mutually perpendicular to the vector defined by the knee and ankle marker and the vector defined by the tibial wand markers (Fig.5.6). The LCS for the shank was then calculated. The z-axis was the principle tibial axis defined between the KJC and AJC. The x-axis was calculated using the Gram-Schmidt procedure of the line passing through the tibial wand markers and the z-axis. The resulting y-axis was the vector product of the z-axis and x-axis (Fig.5.6).

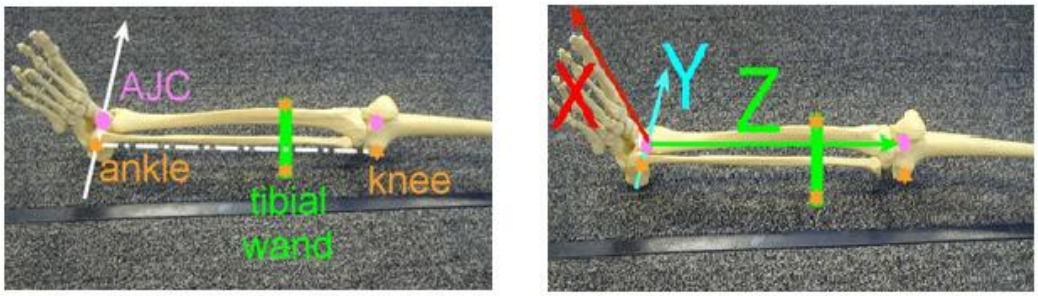

Figure 5.6: Skeletal representation of the Shank LCS. Blue dots represent knee and ankle joint centres (X, Y & Z denote axes system). The Z-axis was the principle tibial axis defined between the KJC and AJC. The X-axis was calculated using the Gram-Schmidt procedure of the line passing through the tibial wand markers and the Z-axis. The resulting Y-axis was the vector product of the Z-axis and X-axis.

5.5.6 Foot Segment Definition

The foot segment was calculated from the AJC and the heel and toe markers (Fig.5.7). The heel and toe markers were offset medially by half the ankle width. The principle axis of the foot, the x-axis, was parallel to the line between the heel and toe markers. The z-axis was calculated using the Gram-Schmidt procedure of the line defined by the ankle and heel markers and the x-axis. The resulting y-axis was the vector product of the x-axis and z-axis.

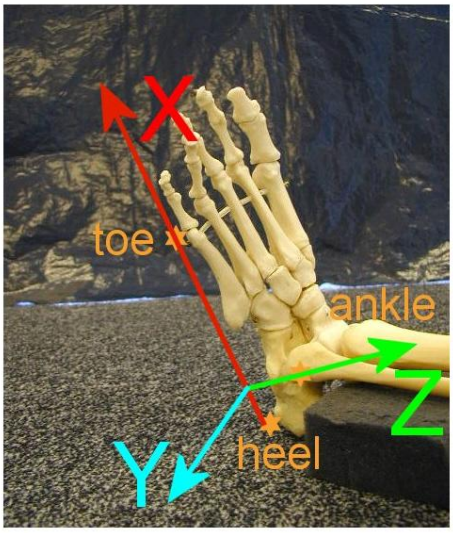

Figure 5.7: Skeletal representation of the Foot LCS. Yellow stars represent actual heel and toe marker positions. The X-axis describes the principle axis of the foot. The Z-axis was defined using the GS procedure while the Y-axis was the resultant vector product of the X and Z axes.

5.5.7 Segment Rotations – Euler Mathematics

In clinical gait analysis a body is represented by a minimum of three strategically placed non-collinear markers. This allows definition of an embedded axes system. As described previously in this section, the local axes system for each segment was aligned in such a way as to be anatomically meaningful. Euler mathematics dictates that the orientation of a rigid body can be described by the succession of three rotation angles about a particular set of axes. For the link segment model used in this study, the distal segment was considered relative to the proximal segment. If, for example, the distal segment was initially in a neutral position with respect to the proximal segment, the Euler angles would be zero. If the distal segment was moved, an alternative set of Euler angles would be needed to describe the rotations that result in this new segment position. A single rotation about a proximal axis can be represented by a rotation matrix. The corresponding rotation matrices are presented in Figure 5.8.

$$X\_rotation(\alpha) = \begin{pmatrix} 1 & 0 & 0 \\ 0 & \cos(\alpha) & -\sin(\alpha) \\ 0 & \sin(\alpha) & \cos(\alpha) \end{pmatrix}$$

$$Y\_rotation(\beta) = \begin{pmatrix} \cos(\beta) & 0 & \sin(\beta) \\ 0 & 1 & 0 \\ -\sin(\beta) & 0 & \cos(\beta) \end{pmatrix}$$

$$Z\_rotation(\gamma) = \begin{pmatrix} \cos(\gamma) & -\sin(\gamma) & 0 \\ \sin(\gamma) & \cos(\gamma) & 0 \\ 0 & 0 & 1 \end{pmatrix}$$

Figure 5.8: Single rotation matrix definitions about the X, Y and Z axes. Euler mathematics dictates that the orientation of a rigid body can be described by the succession of three rotation angles about a particular set of axes.

The meaning of the derived clinical angles is a product of the order of rotation of the three individual axes. From a mathematical point of view, all rotations are valid. However, in order for derived angles to make sense from a clinical point of view, some rotation sequences are more suitable than others. A sequence order of rotation, obliquity, tilt was used to define all lower limb angles in this study. A rotation order of tilt, obliquity, rotation was used to define thorax, lumbar segment and pelvic angles. As an example, the compound rotation matrix relating to tilt, obliquity, rotation is presented in Figure 5.9.

$$YXZ = \begin{pmatrix} \cos(\beta)\cos(\gamma)+\sin(\beta)\sin(\alpha)\sin(\gamma) & -\cos(\beta)\sin(\gamma)+\sin(\beta)\sin(\alpha)\cos(\gamma) & \sin(\beta)\cos(\alpha) \\ \cos(\alpha)\sin(\gamma) & \cos(\alpha)\cos(\gamma) & -\sin(\alpha) \\ -\sin(\beta)\cos(\gamma)+\cos(\beta)\sin(\alpha)\sin(\gamma) & \sin(\beta)\sin(\gamma)+\cos(\beta)\sin(\alpha)\cos(\gamma) & \cos(\beta)\cos(\alpha) \end{pmatrix}$$

Figure 5.9: Compound rotation matrix corresponding to the sequence order: tilt, obliquity, rotation. This sequence order has been recommended, in particular for pelvic angles providing for a more clinically meaningful interpretation of data

Using standard matrix manipulation, each term (α, β, and ϒ) can then be solved providing angle definitions in all 3 planes. It is worth noting that α and β would remain undefined if cos α = 0. This is referred to as "gimbal-lock". This would happen when $\alpha = \pm 90^{o}$. In lower limb analysis this is unlikely. This is more common during upper limb analysis. However, in this case an alternative sequence order of rotation may be chosen to avoid gimbal-lock.

5.6 Constituents of an Inverse Dynamic Model

As discussed in Section 3.5, the study of inverse dynamics refers to the forces that cause the movements recorded by the kinematic model. Inverse dynamics are performed by means of link-segment modelling. The inputs required for this procedure are detailed in Figure 3.1. Positional marker data recorded from the optoelectric system, ground reaction force data recorded by means of external force platforms embedded in the laboratory floor and subject anthropometric measures (e.g. height, weight), recorded during the clinical assessment, are

fed into the model and used to calculate the joint reaction forces and moments at each time point during the gait cycle.

5.7 Force Platform Configuration

Two Kistler 9281B force platforms (Kistler UK, Kistler Instruments Ltd., 13 Murrel Green Business Park, Hampshire, UK) and two AMTI Accugait force platforms (Advanced Medical Technology, Inc., 176 Waltham Street, Watertown, MA, USA) were used to measure ground reaction force data for the purposes of this study. The gait laboratory in the CRC has two Kistler force platforms embedded in the laboratory floor. In order to measure forces and moments at the lower spine using a "bottom up" approach, it is necessary that ground reaction force data is recorded containing both left and right feet completely inside the boundary of two consecutive force platforms during successive initial contacts of the same foot. To achieve this, at least 3 force platforms need to be in situ in the laboratory walkway. With this in mind, it was necessary to incorporate additional force platforms into the laboratory walkway for the purposes of this study. In order to incorporate the additional AMTI force platforms in series with the Kistler platforms, a fibreglass walkway was used to accommodate all plates (Fig.5.11). This walkway is used on gait laboratory outreach clinics based in CRC satellite centres and can accommodate two AMTI force platforms. The Kistler force platforms were raised to the level of the walkway and the walkway was modified to fit around these plates (Fig.5.11). For purposes where both AMTI and Kistler plates were used in the one configuration (Chapters 10 and 11), kinetic data were captured for both AMTI and Kistler platforms at a rate of 200Hz. For purposes where Kistler plates only were used (Chapters 6 and 7), kinetic data were captured at 400Hz.

Figure 5.11: Fibreglass walkway configuration to incorporate additional AMTI force platforms in the current CRC gait laboratory setup.

5.8 Link Segment Model and Inverse Dynamic Assumptions

As previously discussed in Section 3.6, segment orientation, joint centre positions, segment mass, centre of mass (CoM) and moment of inertia (MoI) are all required for the inverse dynamic analysis. There are also a number of assumptions that are made (e.g. fixed segment mass) that do not necessarily hold true (Section 3.6). However, the inverse dynamic analysis can be a useful tool in predicting forces and moments at specific joints. The ability to identify specific joint kinematic and kinetic patterns, while relating this to clinical measurements, has been reported as an important component in the understanding of the mechanisms of gait (Õunpuu et al., 1996).

5.9 Segmental Free Body Diagrams

Inverse dynamic analysis involves analysis of one segment at a time. For the purposes of this study, a “bottom up” approach was used with the inverse dynamic analysis starting at the foot. For the purposes of inverse dynamic analysis, the link segment model was broken up into individual segments using the joint centres as the breaks. Using the segmental free body

diagram, all *known* forces and moments of force were drawn at their points of application. Additionally, all *unknown* variables were drawn at their points of application. Using the associated equations of motion, unknown variables were solved. This allowed the reactive forces acting at each joint to be estimated. The process then moved onto the next segment in the kinematic chain where reactive forces and moments at the distal end were the reverse direction of those at the proximal end of the lower kinematic segment. Each segment was taken in turn and all the unknown reactive forces and moments were calculated. Figure 5.12 demonstrates a 2-dimensional free body diagram of the pelvis. Reactive forces and moments at the hip joint centres were the reverse direction of the reactive forces and moments estimated from the thigh free body diagram using Newton's 3rd law. The mass, CoM and MoI of the segment were calculated using estimates from the anthropometric data set. Components of acceleration of the CoM, segment angular velocity and acceleration and joint positional data were measured using the kinematic model. Unknowns at the proximal joint (reactive forces and moments at L5/S1) were then calculated (Fig.5.12).

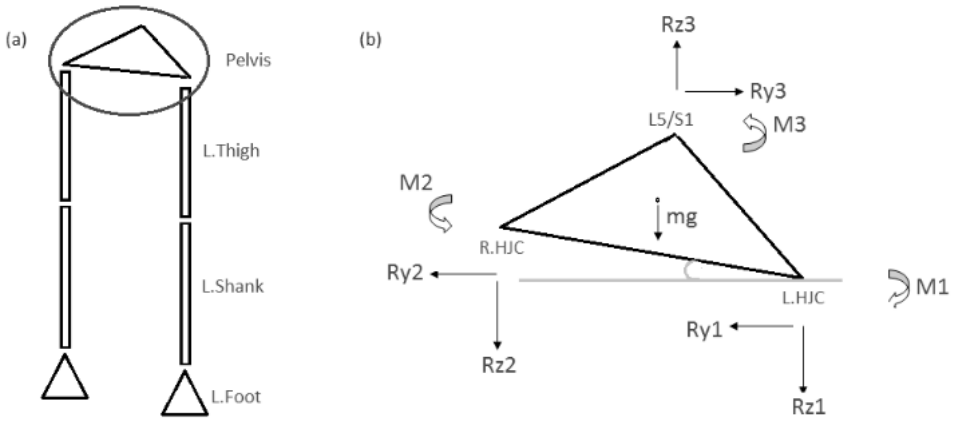

Figure 5.12: (a) Coronal Plane Link Segment Model of the lower limbs consisting of the pelvis, left and right thigh, left and right shank and left and right feet. (b) Free Body Diagram of the Pelvis (Rz, Ry – Joint reactive forces, M1, M2 &M3 – Joint Reactive Moments).

5.10 Ground Reaction Force and Centre of Pressure

As the foot makes contact with the ground during walking, an equal but opposite force is applied to the foot by the ground according to Newton's 3rd law. This force is referred to as the ground reaction force (GRF). The GRF is 3-dimensional vector consisting of a vertical component and two shear components and is the most common force acting on the body during gait (Winter, 2009). Two types of force platforms, Kistler 9281B and AMTI AccuGait, were used to measure GRF in this study. The Kistler force platforms were piezo-electric force platforms supported by 4 triaxial transducers. The 12 resulting signals were combined into 8 channels with the raw signal converted to a force by conversion factors in the force platform calibration files supplied by the manufacturer. Each channel represented the force in the orthogonal direction for a given leg (Table 5.2).

Table 5.2 Channel representations of force components for each force platform. Some components were inverted to correspond to the Coda cx1 direction

Channel	Signal
1	-(Fy1+Fy2)
2	-(Fy3+Fy4)
3	-(Fx1+Fx4)
4	-(Fx2+Fx4)
5	Fz1
6	Fz2
7	Fz3
8	Fz4

The resultant force components were then solved according to the following equations: Fx = -(ch1+ch2), Fy = - (ch3+ch4) and Fz = ch5+ch6+ch7+ch8. The centre of pressure, relative to the centre of the platform was found by:

- Px = 1/Fz((FxT) + L/2(Fz1 + Fz2 – Fz3 – Fz4))
- Py = 1/Fz((FyT) + W/2(Fz1 - Fz2 - Fz3 + Fz4))

Where L was the length along the X axis between transducers, W was the width along the Y-axis between transducers and T was the effective thickness of the plate (Fig.5.13).

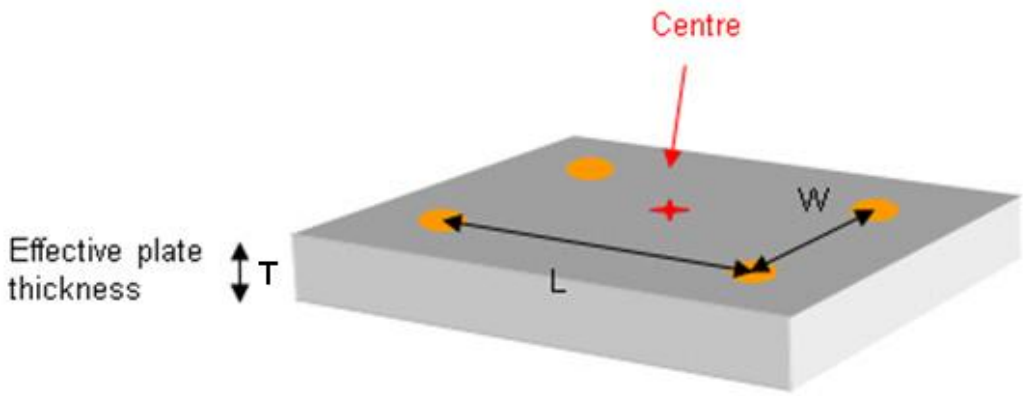

Figure 5.13: Schematic of a Kistler force platform. L is the length along the X-axis between the transducers. W is the width along the Y-axis between the transducers. T is the effective thickness of the platform.

The AMTI AccuGait force platforms used in this study were based on a Hall Effect sensor design with one centrally located sensor. The AccuGait system was connected to the Coda Hub by means of an RS-232 serial port. The RS-232 serial output allowed up to 200Hz capture rate.

5.11 Reaction Forces and Moments

As the first segment in the chain was the foot, this provided the most suitable starting point at which to describe the inverse dynamic procedure. The foot was treated as a free body and was subject to a number of forces such as weight acting at the CoM, the GRF acting at the CoP and the ankle moment reaction. A free body diagram, as discussed in Section 5.9, was required (Fig.5.14) (Table 5.3).

Reactive forces at the ankle were estimated using Newton's 2nd law where the sum of the external forces was a product of mass and acceleration:

$$Fg + F_A + W_F = (M_F)(CoM_{acc})$$

This was expanded further to determine individual components of force:

$$F_{AX} = (M_F)(CoM_{acc\_X}) - Fgx;\ F_{AY} = (M_F)(CoM_{acc\_Y}) - Fgy;\ F_{AZ} = (M_F)(CoM_{acc\_Z}) - Fgz - M_Fg$$

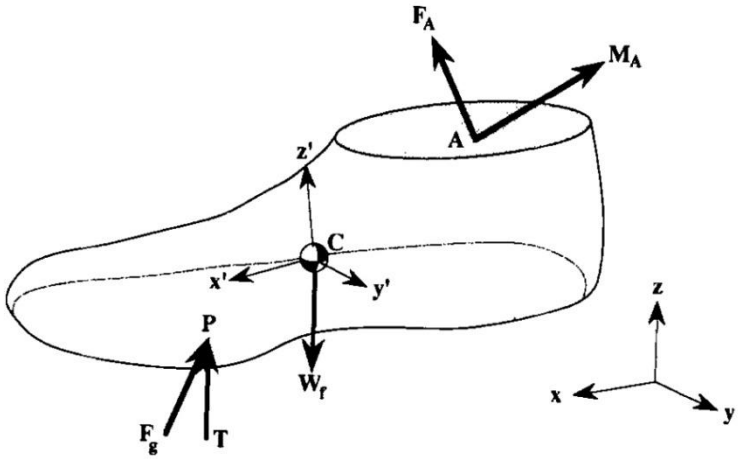

Figure 5.14: Free body diagram of the foot highlighting points of application of known and unknown variables. Wf denotes the weight of the foot. Fg denotes the ground reaction force vector. T denotes the torque vector. P is the point of application. C is the Centre of Mass of the foot. Unknowns at the proximal joint (Ankle – A) can then be estimated (adapted from (Õunpuu et al., 1996)).

Table 5.3: Variables required for the inverse dynamic procedure for the foot segment (Õunpuu et al., 1996). The same variables were then required for each segment along the kinematic chain.

Variable	*Description*
M_F	Mass of foot
W_F	Weight of foot (M_F x g)
P	CoP (as described in Section 5.6)
Fg	GRF vector (as described in Section 5.6)
T	Ground torque (vertical reaction vector)
A	3-d ankle joint centre (AJC)
C	CoM foot (anthropometric estimate)
CoM_{acc}	Linear acceleration of CoM foot
F_A and M_A	Reactive force and moment (unknown)

Treating the foot as a free body, the applied torques were calculated and summed.

$Q_P = Fg \times d_P$, where dp is distance between CoM and CoP

$Q_R = F_A \times d_A$, where d_A is the distance between CoM and AJC

$^{foot}Q = Q_p + Q_R$ where ^{foot}Q equals total torque

The torque vector was then transformed into a torque vector localised into the co-ordinate system defined by the principle axes system of the foot. This was achieved by means of a transformation using the embedded vector base (local coordinate frame) of the foot, as described in Section 5.5.6. The applied torque was combined with inertial aspects and the corresponding moments were calculated using Euler's equations of motion:

$$M_{A0} = I_0 \alpha_0 + (I_2 - I_1)\, \omega_2\, \omega_1 + Q_0$$

$$M_{A1} = I_1 \alpha_1 + (I_0 - I_2)\, \omega_0\, \omega_2 + Q_1$$

$$M_{A2} = I_2 \alpha_2 + (I_1 - I_0)\, \omega_1\, \omega_0 + Q_2$$

where

I_0, I_1 and I_2, → principle moments of inertia.

α_0, $\alpha_{1 \text{ and }} \alpha_2$, → angular acceleration of the segment.

ω_0, ω_1 and ω_2, → angular velocity of segment.

Q_0, Q_1 and Q_2 → individual components of the torque vector

(Subscripts 0, 1, 2 denote components corresponding to the principal axes of the segment, the zeroth axis being the longitudinal or main segmental axis whereas the second axis is in the local lateral direction and axis 1 is perpendicular to 0 and 2).

The analysis for the knee moments on the shank, the hip moments on the thigh and the lumbar moments on the pelvis followed the same procedure with the ground reaction vector replaced by the distal joint reaction.

5.12 Limitations of the Inverse Dynamic approach

The reactive forces produced by the inverse dynamic approach employed in this study were the net inter-segmental reactive forces between the foot and the shank, the shank and

the thigh, the thigh and the pelvis and the pelvis and the trunk. The net inter-segmental force at each joint reflected the effects of external loads such as segmental weights, accelerations and ground reaction forces. Muscle and soft tissue forces that acted across the joints were not represented in this inverse dynamic approach and can produce additional compressive and shear forces across the joint surface (Winter, 2009). When these additional forces are considered, the total "bone-on-bone" force has been shown to be generally larger than the net inter-segmental force (Paul, 1966). In this instance, it would be necessary to add the additional muscle and ligamentous induced forces to the free body diagram. However, this can be difficult due to the dynamic nature of the line of action and the associated moment arm of the muscles as they continuously change with time. There are also many muscles in the lower limbs and trunk that need to be considered. An explicit solution to this situation is generally not possible due to uncertainty as to what muscles are acting at any one instance (Paul, 1966). Electromyography (EMG) can be used to guide the clinician as to what muscles are active. However, this approach has its own difficulties. Activity from surrounding muscles can be misinterpreted as being from a specific muscle (EMG cross-talk) and the accurate placement of electrodes on many muscles in close proximity to each other can be difficult. For the purposes of this study, EMG activity was not considered. The addition of many electrodes on the child with CP was considered too invasive and impractical. A primary problem in CP is that activity can be present in both agonist and antagonist muscles acting across a joint. A limitation of the analysis of this research was that the contribution of individual muscles across each joint was not considered. Any spasticity or stiffness that may have been present across the joint was essentially grouped into this net summation. The same limitations applied to the reactive moments at each joint. While these limitations are acknowledged, the inverse dynamic approach used in this study can provide a close prediction of the net inter-segmental reactive forces and moments at each joint. As the purpose of this study was an investigation into the effects of excessive trunk movements during CP gait on lower limb and lumbar spine kinetics,

the approach of considering net inter-segmental forces and moments was deemed an acceptable compromise. Net inter-segmental forces and moments will provide an estimate of the effects of external loads as a result of excessive trunk movement.

5.13 Procedure for gait analysis

5.13.1 Equipment Overview

The 3-dimensional system used in this study was a 4 camera CODA cx1 active marker system (Charnwood Dynamics Ltd., Leicestershire), 2 x Kistler 9281B force platforms and 2 x AMTI AccuGait force platforms. The Coda system was that described in Section 5.5.1. The force platform configuration was that described in Section 5.8. A description of the principles of operation of the force platforms was provided in Section 5.11.

5.13.2 Data Collection

On presentation to the gait laboratory, the researcher (clinical engineer) met the subject and/or parent/guardian to discuss the study. If the subject agreed to participate, the lead physiotherapist and clinical engineer conducted the gait assessment as per normal protocol with additional markers on the trunk and spine. The subject was asked to walk along a 10m walkway where at least 4 clean data trials were captured at a self selected speed. A clean data trial was described as having no gaps in marker trajectory according to standard laboratory protocol. A final static standing trial of the subject located on one force platform was recorded. Depending on the clinical situation, kinetic data were captured if possible. After all required information was collected the subject returned to the clinical examination area and was seated. After all data were checked for quality assurance according to standard laboratory protocol, the researcher (clinical engineer) removed all markers from the spine and trunk. The data capture procedure was then complete. The marker placement protocol was that described in full in Section 5.5.2.

5.13.3 Data Processing

The raw marker and analogue data was automatically stored in a file format specific to the Coda system. The raw Coda data file was then exported in a format suitable for further analysis in Matlab v8.1.0.604 (The MathWorks, Natick, MA, USA), Visual 3D v4.96.0 (C-Motion Inc., Germantown, MD, USA) or Microsoft Excel software depending on individual study requirements.

5.13.3.1 Computerised processing of gait trials in Visual 3D

The Coda file was imported into Visual 3D using the "Import_Codamotion_Files" command from the Pipeline Workshop. All dynamic walking trials were then associated with the static standing trial that provided an average location of all markers used in the analysis. marker positions were then averaged over all frames to compensate for noise in the data. A pre-defined model template was then applied to all files. This model template defined in full the link segment model needed for the kinematic and kinetic analysis. The link-segment model was that described in detail in Section 5.5. Individual gait trials were then processed in the "Signals and Events" tab of the Visual 3D software. At this point, initial contact and toe off points were set for each limb. Visual 3D pipeline script is presented in Appendix 5.4. Visual 3D segment definitions are presented in Appendix 5.5.

5.13.3.2 Kinematic and Kinetic calculations

In order to calculate the required kinematic and kinetic variables, a pre-defined report template was loaded that contained all model based calculations. The report was then automatically populated with the required kinematic and kinetic curves zoomed to the individual gait cycles. Data were then extracted to Matlab, Microsoft Excel and SPSS for statistical processing. This was done using the "File /Save Export" command in the visual 3D software. Statistical processing software is listed in each chapter.

5.13.4 Data filtering parameters

Once all trials had gait cycle events set, data were then filtered. Small gaps in marker trajectories were inspected and filled using a least-squares fit of a 3rd order polynomial, with 3 frames before and after the gap used to calculate the coefficients of the polynomial. The maximum gap that could be replaced with interpolation values was set at 10 frames. Data with larger gaps were discarded at the data collection stage. All kinematic raw data were filtered using a 4th order Butterworth low-pass filter with a cut-off frequency of 8Hz. Kinetic data were filtered using a 4th order Butterworth filters of 8Hz (Chapters 6,7) and 20Hz (Chapters 10 and 11) respectively. Filtering parameters are listed in individual chapters.

5.13.5 System Calibration

The coda cx1 active marker system is a pre-calibrated collection of units. It is essential that each unit is aligned to the same global co-ordinate frame. This was done as part of gait lab protocol on the morning of an assessment. The alignment procedure required 3 markers. The markers were set on a plastic rig at 90^{o}. The rig was designed to fit with the geometry of the force platform. The first marker determined the origin. This was set at the corner of the force platform. The second marker defined the X-axis and was set along the length of the force platform. The third, located approximately at right angles to the other two markers, completed the definition of the floor plane. An instrumented pole test was carried out daily as part of the quality assurance procedure (Holden et al., 2003). This test examined the difference in the point of application of an instrumented pole and the resultant ground reaction force. The angle between the ground reaction force, as measured by the force platforms, and the pole, as measured by the Coda cx1 system, was calculated for each plane and compared to a pre-defined threshold value.

5.14 Conclusions

The purpose of this chapter has been to describe the general methods of recruitment, data collection, model definition and data processing used in this study. Chapters 6 – 9 will describe development of specific elements of both the kinematic and inverse dynamic models.

Chapter 6: Selection of a Body Segment Parameter set

This chapter has been published as follows:

Kiernan, D., Walsh, M., O'Sullivan, R., O'Brien, T. & Simms, C. K. 2014. *The influence of estimated body segment parameters on predicted joint kinetics during diplegic cerebral palsy gait*. J Biomech*,* 47**,** 284-288.

Chapter Highlights

- An assessment of BSP sets from the literature was considered necessary for the inverse dynamic model of this thesis.
- Kinetic data of 14 CP and 14 TD children, derived using three parameter sets from the literature, were compared from a statistical and clinical perspective.
- Statistically significant differences were recorded for BSP estimates.
- No clinically meaningful differences were recorded for kinetic profile between sets.
- The effects of using different BSP sets were considered clinically insignificant and the BSP set of Jensen et al was used for the purposes of this thesis.

6.1 Introduction

Inverse Dynamic analysis is routinely used in gait laboratories where measured kinematic and ground reaction data are combined with estimated Body Segment Parameters (BSP), such as Mass, Centre of Mass and Moments of Inertia (MoI), to determine inter-segmental forces and net joint moments during gait. The various concerns associated with the use of estimated BSPs have been widely discussed throughout the literature, in particular when subject age and sex fall outside the population originally used to estimate the BSPs (Damavandi et al., 2009, Kingma et al., 1996, Pearsall and Costigan, 1999, Rao et al., 2006). Some authors have shown inverse dynamic calculations to be sensitive to the BSP set used (Chen et al., 2011, Jensen., 1989, Rao et al., 2006), while others report the effect to be negligible (Ganley and Powers, 2004). Concerns have also been raised for pathological groups where limb asymmetry is common such as Cerebral Palsy (CP) (Chen et al., 2011, Damavandi et al., 2009, Niiler and Riad, 2012). Asymmetries that may exist within CP, such as limb length discrepancy or reduced muscle volume (Lampe et al., 2006, Moreau et al., 2009, Shortland,

2009), could result in significantly altered reactive forces and moments during gait when different BSPs are applied. However, no study has examined the effects of different BSP sets on the kinetic profiles of a CP population. Ideally, when dealing with a pathological group such as CP, the BSPs specific to the subject would be directly measured. However, it is not always feasible for most gait laboratories to access the types of imaging techniques required to achieve this. For this reason, the use of published BSP sets acts as an acceptable compromise. However, the choice of BSP set may introduce unnecessary error in the resultant kinetic calculations. Following from this, the aim of this chapter was to determine whether any clinically meaningful difference existed in the predicted kinetic profiles of a cohort of CP subjects when different published BSP sets were used in the reactive force and moment calculations during gait. The purpose was to identify a BSP set suitable for use in the inverse dynamic model of this thesis (Chapters 7, 10 and 11).

6.2 Materials and Methods

6.2.1 Subjects

Fourteen children (n = 28 limbs) presenting for routine gait analysis with a diagnosis of diplegic CP and fourteen TD children (n = 28 limbs) participated in the study (Table 6.1). Ethical approval was obtained as described in Section 5.2. Informed written consent was obtained from all participants and from their parents when legally minor as described in Section 5.3.4.

Table 6.1: Mean Anthropometric data for CP and TD groups. Note that only walking speed was significantly different (p<0.01).

	CP Mean (SD) *N = 14*	TD Mean (SD) *N=14*	p-value
Age	9.43 (1.91)	8.29 (1.20)	0.069
Male/Female	10/4	10/4	
Height (m)	1.34 (0.15)	1.33 (0.10)	0.832
Weight (kg)	29.41 (7.44)	28.38 (5.81)	0.685
Left Thigh (mm)	345.36 (37.9)	344.32 (32.73)	0.939
Left Shank (mm)	316.07 (43.02)	322.43 (33.33)	0.666
Left Foot (mm)	195.71 (25.26)	192.50 (19.88)	0.711
Right Thigh (mm)	348.21 (33.26)	340.71 (34.47)	0.563
Right Shank (mm)	316.79 (43.17)	326.43 (31.71)	0.507
Right Foot (mm)	196.79 (26.50)	193.21 (20.25)	0.692
Walking speed (m/s)	1.11 (0.13)	1.33 (0.14)	<0.01*

6.2.2 Data Collection

A full barefoot 3-dimensional kinematic analysis was performed using the CODA cx1 active marker system (Charnwood Dynamics Ltd., Leicestershire). The marker placement protocol and underlying mathematical model followed implementation as previously described in Section 5.5. Two Kistler 9281B force platforms were used to collect GRF data at a capture frequency of 400Hz. Subjects walked unassisted at a self-selected pace. One representative walking trial containing a clean strike of the left and right force plate was analysed for each subject. Subject specific clinical examination data required for the kinematic model were recorded for each subject (Table 6.1). Additionally, subject specific segment lengths required for the kinetic model were recorded for each subject (Table 6.1). Segment lengths were measured using a measuring tape. Thigh length was measured from a mark representing the hip joint centre (adjacent to the greater trochanter) to a mark representing the knee joint centre (adjacent to the lateral epicondyle). Shank length was measured from the knee joint centre mark to the ankle joint centre mark (adjacent to the lateral malleolus). Foot length was measured from the mid-point of the posterior plantar aspect of the foot to the tip of the third toe. For each representative trial, three separate sets of proportional BSPs

from the literature were applied and the corresponding joint moments calculated. Kinetic data were filtered using a 4th order Butterworth filter of 8Hz. All kinetic calculations were performed using Codamotion v6.78.1 software. For the purposes of this chapter only sagittal plane kinetic data were reported. Summary tables of the proportional BSP sets are reported (Table 6.2). Walking speed was calculated using kinematic data.

6.2.3 Anthropometric Models

Three proportional anthropometric sets, Set 1 – Jensen (Jensen., 1989), Set 2- Ganley and Powers (Ganley and Powers, 2004) and Set 3- Cadaveric (Dempster, 1955) (adapted from (Winter, 2009)) were used (Table 6.2).

Table 6.2 : Proportional Body Segment Parameter data used in the reactive force and moment calculations. (Mass is calculated as a % of Body Mass while CoM Radius and Radius Gyration are calculated as a % of segment length).

		Ganley & Power			Jensen							Cadaver
age		**7 -8**	**9-10**	**11-13**	**7**	**8**	**9**	**10**	**11**	**12**	**13**	**N/A**
Mass	Thigh	0.11	0.114	0.117	0.0919	0.0967	0.1009	0.1046	0.1077	0.1103	0.1124	0.1
	Shank	0.0462	0.0473	0.0483	0.0464	0.0484	0.0500	0.0512	0.0521	0.0526	0.0527	0.0465
	Foot	0.0137	0.0149	0.0149	0.0195	0.0201	0.0205	0.0207	0.0209	0.0208	0.0207	0.0145
CoM	Thigh	0.463	0.465	0.468	0.4609	0.4609	0.4609	0.4609	0.4609	0.4609	0.4609	0.433
Rad.	Shank	0.415	0.416	0.415	0.4295	0.4274	0.4253	0.4232	0.4211	0.4190	0.4169	0.433
	Foot	0.482	0.488	0.483	0.4161	0.4161	0.4161	0.4161	0.4161	0.4161	0.4161	0.5
Rad.	Thigh	0.256	0.252	0.256	0.2909	0.2909	0.2909	0.2909	0.2909	0.2909	0.2909	0.323
Gyr	Shank	0.274	0.274	0.276	0.2880	0.2873	0.2866	0.286	0.2853	0.2846	0.2839	0.302
	Foot	0.259	0.259	0.259	0.2437	0.2437	0.2437	0.2437	0.2437	0.2437	0.2437	0.47

6.2.4 Data Analysis

The Mean Absolute Variability (MAV) was calculated as a measure of the variability of each set (Ferrari et al., 2008). The MAV was calculated as the maximum minus the minimum, at each point in the gait cycle, across all subjects. This was carried out for each set. The MAV was calculated for each joint moment in the sagittal plane. An ensemble average of lower limb joint moments was calculated and visually analyzed for deviations across BSP sets.

The Gait Deviation Index Kinetic (GDI-Kinetic) score, as discussed in Section 2.3.4, was calculated for each leg (Rozumalski and Schwartz, 2011). The GDI-kinetic was used to determine whether a clinically meaningful important difference (CMID) existed in the kinetic profiles between sets. The GDI-kinetic is an index which scales the difference in pathological gait to normal gait and it is used to quantify the pathology present in the kinetic profiles of subjects. The GDI-kinetic CMID was calculated as the mean difference plus one standard deviation between each set and the reference. A threshold of clinical significance of 3.6 points (CMID) was calculated for this study. The relationship of the GDI-Kinetic has only been examined with respect to the Gilette Functional Assessment Questionnaire (FAQ) (Rozumalski and Schwartz, 2011). The authors report the mean decrement from FAQ levels 10 to 7 as 2.4 points (Standard Deviation of 1.2 points). For the purpose of this chapter, the mean change in FAQ level plus one standard deviation was considered clinically meaningful (CMID = 3.6 points). Recalling that the GDI-Kinetic is measured in ten-fold standard deviation units implies that BSP sets can differ by 0.36 standard deviations before being deemed clinically significant.

Subject anthropometric values were compared between the CP and TD groups using a Student's *t*-test with significance level set at $p<0.05$. GDI-Kinetic scores were statistically compared using a one-way repeated measures analysis of variance (ANOVA). Mean BSP estimates were calculated for each BSP set for both groups and visually analyzed. A one-way repeated measures ANOVA was used to determine whether any statistical difference existed between BSP estimates. MAV scores were calculated in Microsoft Excel while GDI-kinetic

scores and all statistical calculations were performed in MATLAB 8.1.0.604 (The MathWorks, Natick, Massachusetts, U.S.A).

6.3 Results

6.3.1 Subject Anthropometric Data

Subject anthropometric data were examined and no statistically significant difference existed between the CP and TD groups (Table 6.1). Walking speed demonstrated a significant difference between groups with the TD group on average 0.22 m/s faster ($p<0.01$) than the CP group (Table 6.1).

6.3.2 Body Segment Parameter Estimates

Statistically significant differences were found for each variable (Mass, CoM Radius and MoI) for each segment for both the CP and TD groups using the 3 BSP sets as determined by a one-way repeated measures ANOVA (Table 6.3). While statistically significant, mean BSP estimates were similar (Fig.6.1).

Table 6.3: Results of a One-Way Repeated Measures ANOVA of BSP estimates for all 3 sets for TD and CP groups. Statistically significant differences were found for each variable for each group (*statistically significant at p<0.01).

Measure	Segment	TD	CP
Mass	**Thigh**	F (2,54) =87.93, p < 0.01*	F (2,54) =99.36, p < 0.01*
	Shank	F (2,54) =58.85, p < 0.01*	F (2,54) =53.04, p < 0.01*
	Foot	F (2,54) = 683.8, p<0.01*	F (2,54) = 351.42, p<0.01*
CoM Radius	**Thigh**	F (2,54) =199.39, p < 0.01*	F (2,54)=208.97, p < 0.01*
	Shank	F (2,54) =34.54, p < 0.01*	F (2,54) =114.02, p < 0.01*
	Foot	F (2,54) = 122.18, p<0.01*	F (2,54) = 182.87, p<0.01*
MoI	**Thigh**	F (2,54) =29.07, p < 0.01*	F (2,54) =57.42, p < 0.01*
	Shank	F (2,54) =16.52, p < 0.01*	F (2,54) =111.1, p < 0.01*
	Foot	F (2, 54) = 178.9, p< 0.01*	F (2,54) = 137.77, p<0.01*

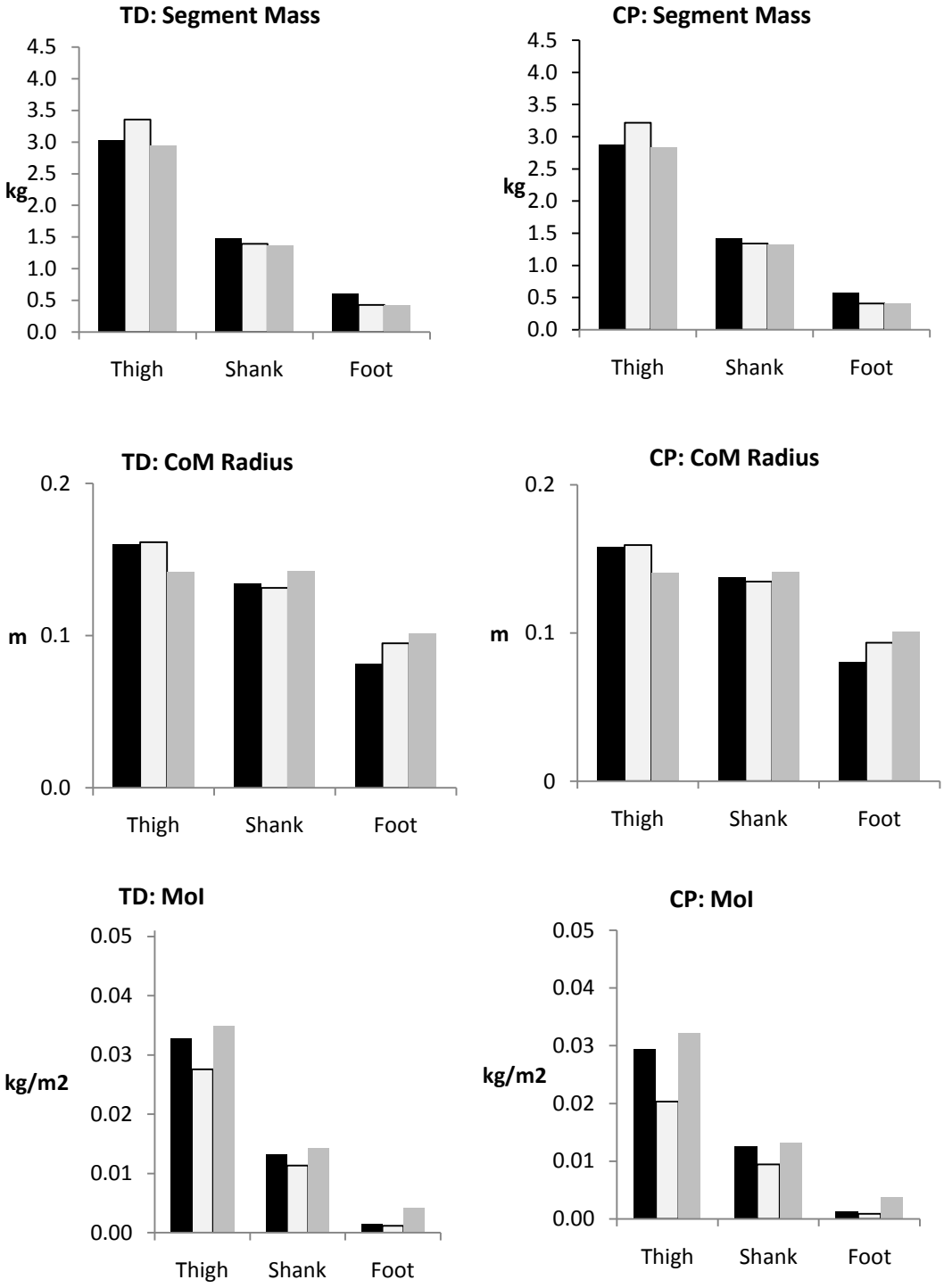

Figure 6.1: Mean Anthropometric estimates for CP and TD groups (CoM – Centre of Mass; MoI – Moment of Inertia). Bar graphs are represented as follows: Black – Jensen; White – Ganley and Power; Gray – Cadaver. Note: Statistically significant differences were found for each variable for each group.

6.3.3 GDI-Kinetic Scores

A statistically significant difference was present between the GDI-kinetic scores for the three BSP sets in both the TD group ($F(2, 54) = 12.36$, $p < 0.01$) and CP group ($F(2, 54) = 11.39$, $p < 0.01$) as determined by a one-way repeated measures ANOVA. For the TD group, the Jensen set (set 1) demonstrated the lowest mean score of 100 points. This was followed with almost equal scores for the remaining 2 sets (Ganley (set 2) and Cadaveric (set 3)) at 101.7 and 101.6 points respectively. A similar trend was present for the CP group. The Jensen set (set 1) demonstrated the lowest mean score of 72.5 points. This was followed by similar scores for the remaining 2 sets (Ganley (set 2) and Cadaveric (set 3)) at 74.5 and 74.2 points respectively.

There was no clinically meaningful difference between GDI-kinetic scores for the different BSP sets in either group as determined by the threshold of clinical significance (3.6 points). The maximum difference between BSP sets was 2.4 and 2.8 points for TD and CP groups respectively.

6.3.4 Kinetic Profiles MAV

MAV between BSP sets was low at all levels of the hip, knee and ankle measuring 0.07, 0.04 and 0.01Nm/kg respectively for the TD group and 0.04, 0.02 and 0.01Nm/kg respectively for the CP group (Table 6.4).

Table 6.4: Mean Absolute Variability (MAV) of moment calculations between Anthropometric sets. MAV between sets was low at all 3 levels of the hip, knee and ankle.

Moments (Nm/kg)	**MAV Variability**	
	TD	**CP**
	MAV	**MAV**
Hip Flex/Ext	0.07	0.04
Knee Flex/Ext	0.04	0.02
Ankle Dorsi/ Plantarflexion	0.01	0.01

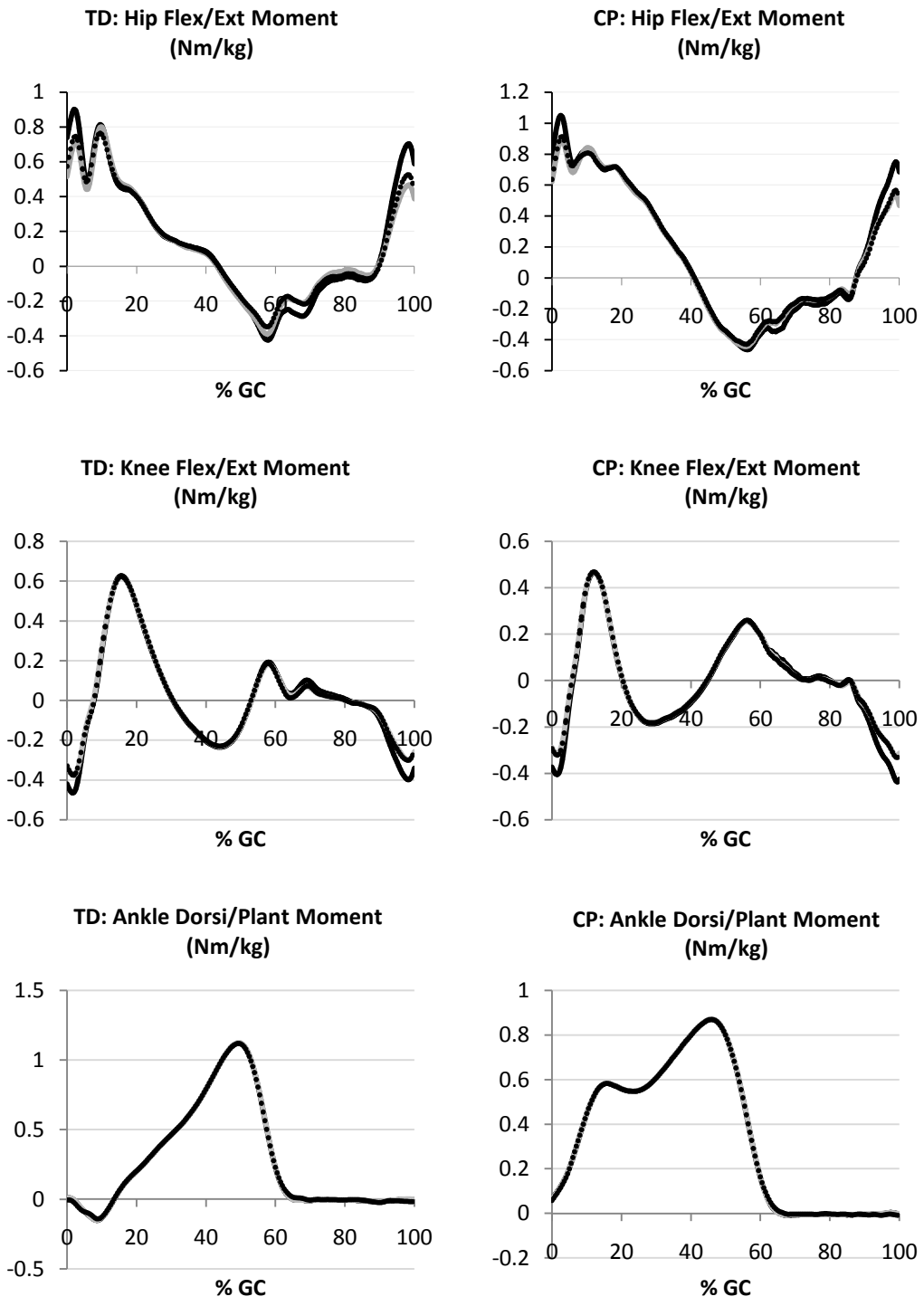

Figure 6.2: Ensemble average moment profiles for each anthropometric set for CP and TD groups (Dashed – Jensen; Gray – Ganley and Powers; Dotted – Cadaver). Note that peak differences are confined mainly to early stance, pre-swing and terminal swing for the knee and hip (GC – Gait Cycle).

6.4 Discussion

The use of BSP sets from the literature is common practice in inverse dynamic calculations. If BSP sets are used interchangeably, the potential exists for changes in kinetic profiles to be mistaken as clinically meaningful. The aim of this chapter was to examine the effects of using different BSP sets on the kinetic profiles of TD children and children with CP. The purpose of this was to identify an anthropometric data set suitable for use in the inverse dynamic model of this thesis. Significant differences were present between BSP estimates. When further investigated, variability of predicted kinetic profiles between sets was low. Despite a statistically significant difference in GDI-Kinetic score between BSP sets, the GDI-Kinetic demonstrated no clinically meaningful difference across all 3 BSP sets.

No significant differences were found between the CP and the TD group with respect to anthropometric data (Table 6.1). It has been well documented in the literature that CP muscle architecture differs to normal and reduced muscle volume is common (Lampe et al., 2006, Moreau et al., 2009, Shortland, 2009). This potential for error, due to differences in body morphology, formed part of the rationale for this chapter. Statistically significant differences were present for some variables. The one-way repeated measures ANOVA (Table 6.3) demonstrated significant differences between the three BSP estimates for Mass, CoM Radius and Moment of Inertia (MOI) for both groups (Fig.6.1). The resulting MAV ranged from 0.01 – 0.04 Nm/kg for the CP group and 0.01 – 0.07 Nm/kg for the TD group. In percentage terms, a 0.04Nm/kg and 0.07Nm/kg difference at the hip for the CP and the TD group equates to approximately 3% and 6% of the range of the hip respectively (Note: normal hip moment graph range approximately 1.2Nm/kg (Fig.6.2)). A visual inspection of the ensemble average profiles showed peak differences confined mainly to initial contact, pre-swing and terminal swing for the knee and hip in both groups (Fig.6.2). The significantly slower walking speed in the CP group would suggest lower segment velocities and accelerations when compared to the

TD group. This would somewhat reduce the impact of the inertial characteristics in the CP group, a finding evident in the lower levels of variability at the hip and knee (Table 6.4).

To understand the differences from a clinically meaningful point of view, the GDI-Kinetic score was calculated to determine if the levels of variability previously discussed could be classed as clinically significant. The GDI-kinetic is a direct analogue of the GDI, but based on kinetics rather than kinematics (Rozumalski and Schwartz, 2011). As the validity of the GDI has been well established (Molloy et al., 2010), the use of the GDI-kinetic was deemed suitable for this investigation. The mean GDI-kinetic ranged from 72.5 to 74.5 points for the CP group and 100 to 101.7 points for the TD group depending on the BSP set used. For both groups, the maximum difference between the 3 BSP sets was 2.8 points (CP) and 2.4 points (TD). As these scores are below the threshold of 3.6 points, it can be concluded that no clinically meaningful difference exists when the three different BSP sets are used.

6.5 Conclusion

It was concluded that the predicted kinetic profiles for TD children and children with CP were not particularly sensitive to changes in the underlying anthropometric data set used in the inverse dynamics calculations. As a consequence of this, the anthropometric set reported by Jensen will be used in the inverse dynamic model of this thesis. The Jensen set is that currently used in the CRC lower limb model and provides an in-depth estimation of body segment parameters.

Chapter 7: Selection of a Hip Joint Centre regression equation set

This chapter has been published as follows:

Kiernan, D., Malone, A., O'Brien, T. & Simms, C. K. 2015. *The clinical impact of hip joint centre regression equation error on kinematics and kinetics during paediatric gait*. Gait & Posture, 41, 175-179.

Chapter Highlights

- An assessment of HJC regression equations was considered necessary for the biomechanical model of this thesis.
- Kinematics and kinetics, derived using three equation sets from the literature, were compared to those derived using a reference standard on 18TD children.
- Bell et al. predictive equations performed closest to the reference standard set.
- Errors in inverse dynamics associated with Davis et al set could be misinterpreted as clinically meaningful.
- Equations of Bell et al. as valid as Harrington et al. for HJC estimation during gait analysis and to be used for the purpose of this thesis.

7.1 Introduction

In lower limb gait analysis the location of the hip joint centre (HJC) is needed to define the thigh coordinate frame for kinematic analysis and it is the point at which inverse dynamics at the hip are calculated. As a result, accurate definition of this point is essential if inverse dynamic calculations are to be carried out further up the kinematic chain. Ideally the HJC location specific to the subject would be directly measured. However, the imaging techniques required to achieve this would not be available to most gait laboratories. As the HJC cannot be directly palpated, its position is usually estimated using one of two approaches. The first, referred to as functional calibration, relies on relative movement of the segments usually during a number of calibration trials (Camomilla et al., 2006, Leardini et al., 1999, Piazza et al., 2001). However, while this approach has been shown to yield the best results, it may be difficult to implement when dealing with pathological groups such as CP where function is impaired (Sangeux et al., 2014). As a result, implementation in the clinical setting has been limited. The second approach is the use of regression equations based primarily on the

anatomy of the pelvis (Bell et al., 1989, Davis et al., 1991, Harrington et al., 2007). Regression equations work on the basis of estimating the HJC using the anatomy of the pelvis and "regressing" from a set point on the pelvis (e.g. mid-ASISs) using offsets based on percentages of pelvic width, depth and sometimes leg length (Fig. 7.1). These regression equations will usually have been derived from cadaveric samples or using various imaging techniques.

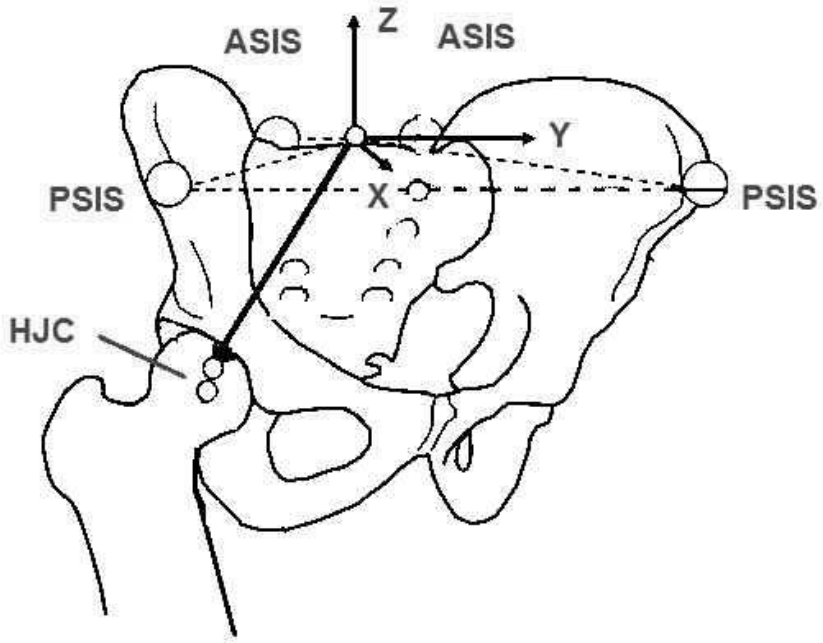

Figure 7.1: The use of regression equations based on pelvic anatomy to estimate the position of the HJC during gait. The ASIS and PSIS markers define the pelvic frame (X, Y and Z axes). The HJCs are then estimated from the mid-point of the PSIS markers using direction based on pelvic frame definition. Offset distances are taken as a percentage of pelvic width and height and subject leg length. The HJC is then an estimate based on geometry of the pelvis.

These types of regression equations will usually have been derived from radiographic or cadaveric measurements and are by far the most widely used in clinical gait analysis (Peters et al., 2012, Sangeux et al., 2011, Sangeux et al., 2014). However, while their use is considered an acceptable compromise, regression equations have their limitations. Most rely on accurate identification and measurement of pelvic bony landmarks and the subject populations on which they were originally based may be quite different to subject populations on which they are used. Errors up to 31mm have been reported between true and estimated HJC position (Stagni et al., 2000, Harrington et al., 2007). Recent studies have reported that the regression

equations reported by Harrington and colleagues (Harrington et al., 2007) should be used during gait analysis (Peters et al., 2012, Sangeux et al., 2011, Sangeux et al., 2014). These equations performed very closely to the best performing functional calibration method while the older and widely used regression equations performed with less agreement. However, these studies only examined two sets of regression equations (Davis et al., 1991, Harrington et al., 2007), with only the Davis et al set widely used in clinical gait analysis. Also, the effects on kinematics and kinetics were not considered. Few studies in the literature have examined the effect of regression equation error on kinematic and kinetic output (Kirkwood et al., 1999, Stagni et al., 2000). While the Harrington set has been recommended as the most accurate for gait analysis (Sangeux et al., 2011, Sangeux et al., 2014, Peters et al., 2012), differences resulting from the use of other commonly used sets must be considered, not only from a statistical perspective but also from a clinical perspective. Otherwise, these older commonly used sets could be incorrectly dismissed as not suitably accurate when in fact the overall effect on clinical data is small or even negligible. Following from this, the aim of this chapter was to determine whether any clinically meaningful difference existed in both kinematic and kinetic data when a number of widely used regression equation sets from the literature were used to determine HJC location during paediatric gait. The purpose of this will be to identify a suitable HJC regression equation set for use in the kinematic and kinetic model of this thesis.

7.2 Materials and Methods

7.2.1 Subjects

Eighteen healthy children (n = 36 limbs) were recruited: 7 male and 11 female (Table 7.1). Ethical approval was obtained as described in Section 5.2. Informed written consent was obtained from all participants and from their parents when legally minor as described in Section 5.3.4.

Table 7.1: Mean subject anthropometric data including pelvic width, depth and leg length required for HJC regression equation offset calculations.

Parameters	***Mean (SD) (N=18)***
Age	10.83 (2.45)
Male/Female	7/11
Height (m)	1.45 (0.14)
Weight (kg)	40.17 (12.65)
Pelvic Width	216.67 (30.05)
Pelvic Depth	128.22 (20.45)
Left Leg Length (mm)	727.78 (80.24)
Right Leg Length (mm)	731.39 (79.87)

7.2.2 Data Collection

A full barefoot 3-dimensional analysis was performed using the CODA cx1 active marker system (Charnwood Dynamics Ltd., Leicestershire). The marker placement protocol and underlying mathematical model followed implementation as previously described in Section 5.5. Subjects walked unassisted at a self-selected pace. Two Kistler 9281B force platforms, embedded into the laboratory walkway, were used to measure ground reaction force data at a frequency rate of 400Hz. One representative walking trial containing a clean strike of the left and right force plate was analysed for each subject. Subject specific clinical examination data, required for the kinematic and kinetic models, were recorded for each subject (Table 7.1). Leg lengths were measured using a measuring tape. Pelvic width (PW) was taken as the distance between the ASISs while pelvic depth (PD) was taken as the distance between the ASISs and PSISs. The corresponding kinematics and kinetics were calculated for each representative trial using Codamotion 6.78.1 software.

7.2.3 HJC Regression Equations

Four regression equation sets were used in this chapter. The first was based on measures of pelvic width (PW), pelvic depth (PD) and leg length (LL) (Harrington et al., 2007). It has been suggested that this set performs very closely to the best functional calibration

technique and should be used during gait analysis when the functional calibration technique is not an option (Peters et al., 2012, Sangeux et al., 2011, Sangeux et al., 2014). For this reason, the equations described by Harrington (Har) were used as the reference standard against which the three other commonly used sets were compared. The second set (Bell) was based on measures of PW (Bell et al., 1989). This set is widely used in clinical gait analysis and has been incorporated into the standard gait model as implemented in Codamotion Analysis software (Charnwood Dynamics Ltd., Leicestershire). The third set (Davis) was that which is most widely used in clinical gait analysis as part of the Conventional Gait Model implemented in Vicon Plug-in-Gait software (Sangeux et al., 2011), and was based on measures of LL and PW (Davis et al., 1991, Harrington et al., 2007). The final set (Ortho), based on software recommendations for Orthotrak Motion Analysis Corp., has widespread use in clinical gait analysis and was based on measures of PW (Harrington et al., 2007).

7.2.4 Data Analysis

The co-ordinate distance for the HJC position between the reference standard (Har – baseline zero) and the Bell, Davis and Ortho regression equation sets was calculated for Anterior/Posterior (x-axis), Medial/Lateral (y-axis) and Superior/Inferior (z-axis) directions and all expressed in the same pelvic co-ordinate system frame. Ensemble average kinematic and kinetic profiles were visually analyzed for deviations for each of the three sets when compared to the Har reference.

The Gait Profile Score (GPS), as discussed in Section 2.4.4, was calculated for each subject (Baker et al., 2009). The GPS is a single measure of the quality of a subject's gait pattern. It was used to assess whether any Clinically Meaningful Important Difference (CMID) existed in the kinematic profiles derived from the different sets (Bell, Davis and Ortho) compared to the kinematic profiles derived from the Har (reference) set. The GPS CMID was calculated as the mean difference plus one standard deviation between each set and the

reference. The minimal clinically important difference of the GPS has been shown to be 1.6^{o} (Baker et al., 2012). For the purposes of this study, this value of 1.6^{o} was used as the threshold of clinical significance (CMID).

The Gait Deviation Index Kinetic (GDI-Kinetic) score (Rozumalski and Schwartz, 2011), as discussed in Section 2.4.4, was calculated for each leg. The GDI-kinetic was used as an additional tool to determine whether any CMID existed in the kinetic profiles between groups. The GDI-kinetic CMID (3.6 points) was calculated as described in Section 6.2.4.

A Dunnett's test was used for comparison of each set (Bell, Davis and Ortho) with the Har reference for HJC co-ordinate difference, GPS and GDI-Kinetic scores. Significance level was set at $p < 0.05$. A test of normality was conducted using the Shapiro–Wilk normality test with all variables found to follow a normal distribution. All statistical analyses were performed using IBM SPSS Statistics (v23.0.0.2).

7.3 Results

7.3.1 Hip Joint Centre (HJC) location estimates

When anterior/posterior direction was considered, no statistically significant difference was present for Bell (Mean Difference (MD) = -0.28mm, p = .99) while significant differences were found for both Davis (MD = 16.2mm, p = .00) and Ortho (MD = -7.0mm, p = .00) sets when compared to the Har reference (Table 7.2) (Fig.7.2). In the medial/lateral direction, no significant differences were present for the Bell set (MD = 0.47mm, p = 0.99) or the Davis set (MD = 3.26mm, p = 0.70). However, a statistically significant difference was present for the Ortho set compared to the Har reference (MD = 9.14mm, p = 0.04) (Table 7.2) (Fig.7.2). In contrast, for the superior/ inferior direction, no statistically significant differences were found for Bell (MD = 5.95mm, p = 0.15), Davis (MD = -0.17mm, p = 0.99) or Ortho sets (MD = -2.7mm, p = 0.72) when compared to the Har reference (Table 7.2) (Fig.7.2).

Table 7.2: Statistical relationship of the GPS, GDI-Kinetic and the HJC position in the pelvic coordinate frame for Bell, Davis and Orthotrak regression equation sets, compared using a Dunnett's test, to the Harrington reference set. Mean difference (Mean Diff.), 95% Confidence Intervals [95% CI] and concurrent p-values are reported for each variable. (HJCx – anterior/posterior; HJCy – medial/lateral; HJCz – superior/inferior) (* Statistically significant at p < 0.05).

Parameters	**Mean Diff. Har – Bell**	**95% CI**	***P***	**Mean Diff. Har – Davis**	**95% CI**	***P***	**Mean Diff. Har – Ortho**	**95% CI**	***P***
GPS (deg)	-0.2	-0.9,0.87	.99	0.03	-0.86,0.92	.99	-0.15	-1.04,0.74	.96
GDI-Kinetic	0.07	-5.6,5.8	.99	1.21	-4.5,6.9	.92	0.02	-5.7,5.7	.99
HJCx (mm)	-0.28	-5.23,4.68	.99	16.2*	11.2,21.1	.00	-7.0*	-12.0,-2.03	.00
HJCy (mm)	0.47	-8.3,9.2	.99	3.26	-5.5,12.0	.70	9.14*	0.40,17.9	.04
HJCz (mm)	5.95	-1.6,13.5	.15	-0.17	-7.7,7.4	.99	-2.7	-10.3,4.8	.72

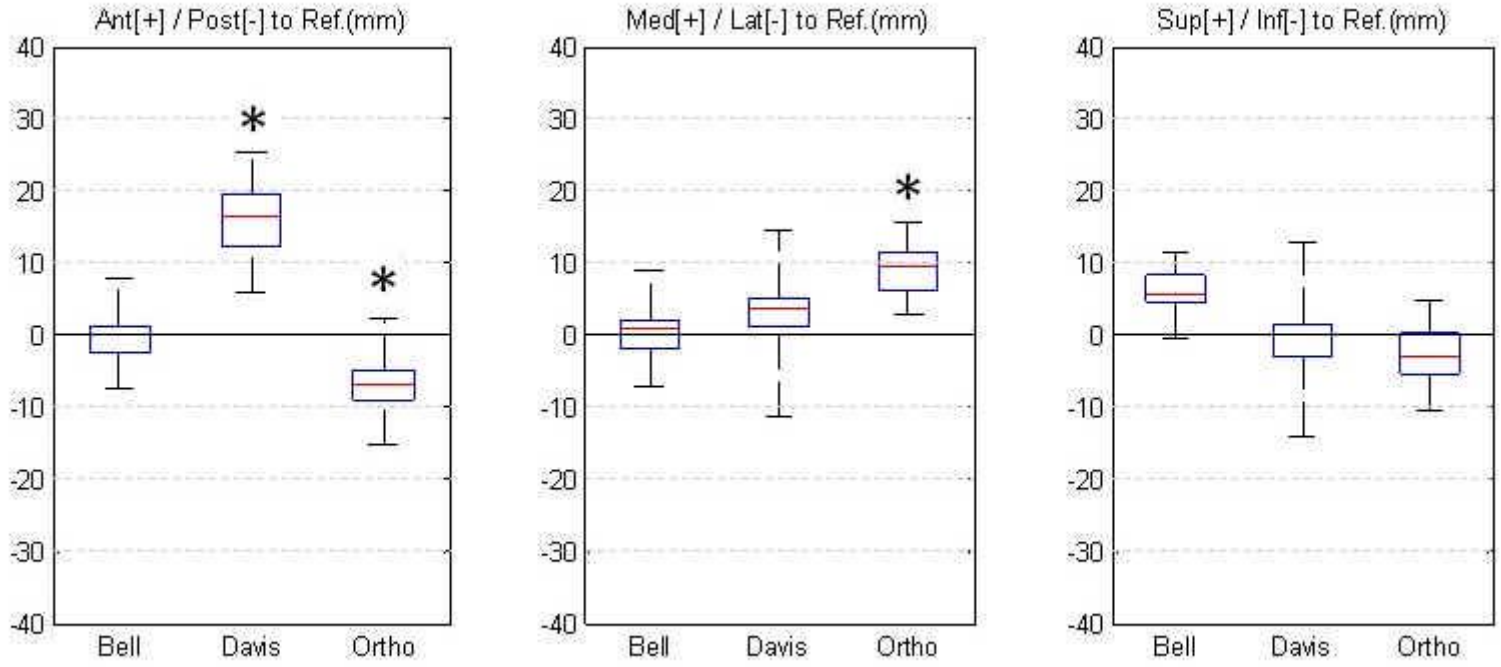

Figure 7.2: Box and Whisker plots of co-ordinate distance between the reference standard (Harrington – baseline zero) and the Bell, Davis and Orthotrak regression equation sets. Anteiror/Posterior – X axis, Medial/Lateral – Y axis and Superior/Inferior – Z axis. (* Statistically Significant at p< 0.05).

7.3.2 GPS Scores

No statistically significant differences were present for GPS scores for Bell, Davis or Ortho regression equation sets when compared to the Har reference as determined using Dunnett's test (Table 7.2). The Davis set demonstrated the lowest GPS score at 5.8^{o} followed by Bell at 5.8^{o} and Ortho at 6.0^{o}. There was no clinically meaningful difference in GPS score (Mean difference + 1 SD) for Bell (0.1^{o}), Davis (0.6^{o}) or Ortho (0.3^{o}) when compared to the Har reference as determined by the threshold of clinical significance (1.6^{o}).

7.3.3 GDI-Kinetic Scores

No statistically significant differences were recorded in GDI kinetic score for any set compared to the Har reference as determined using the Dunnett's test (Table 7.2). The Har set demonstrated a mean score of 100 points. This was expected due to the use of the Har set as the control set required for GDI-Kinetic measurements. This was followed closely by Ortho at 99.9 points and Bell at 99.9 points respectively, with the Davis set recording a mean of 98.8 points. A clinically meaningful difference was present for the Davis set when compared to the Har reference (4.4 points) as determined by the threshold of clinical significance (3.6 points). No clinically meaningful difference was recorded for Bell (0.8 points) or Ortho (2.3 points).

7.3.4 Ensemble Averages

Kinematic ensemble average graphs displayed almost identical curve displacement for the hip in all 3 planes for Bell, Davis and Ortho sets when compared to the Har reference (Fig.7.3). The most obvious deviation was for the Davis set for hip flexion/extension where the hip was marginally offset into increased extension in the sagittal plane (Fig.7.3).

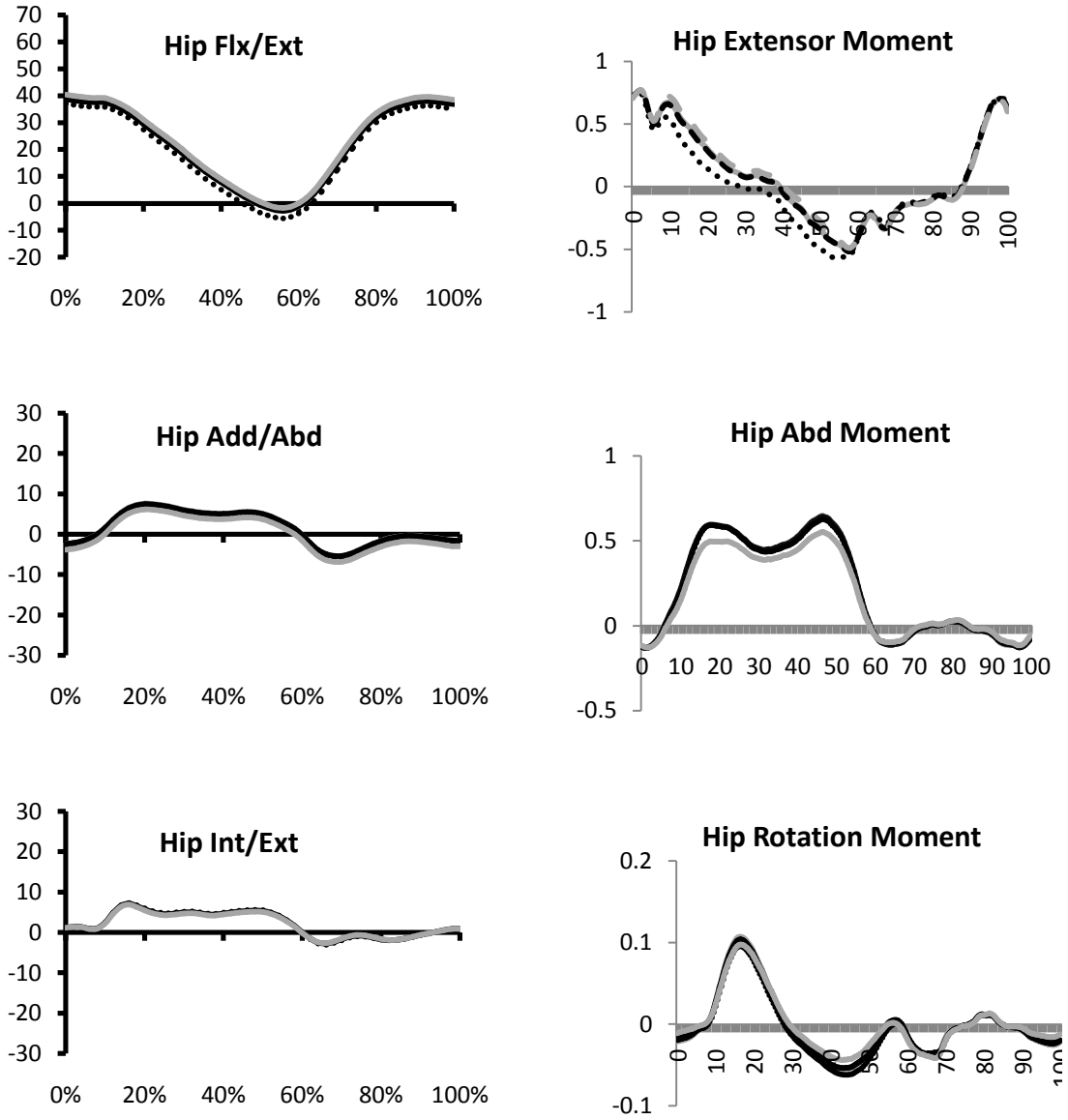

Figure 7.3: Ensemble average kinematic and kinetic profiles for the hip in all 3 planes for Bell, Davis and Orthotrak sets compared to the Harrington reference set. Note: Almost identical kinematic curve displacement for all sets (left column). Kinetic profiles display a reduced hip extensor moment for the Davis set and a reduced hip abduction moment for the Orthotrak set (right column). Key: Gray Dotted– Harrington; Black Dashed – Bell; Dotted – Davis; Gray - Orthotrak.

A noticeable reduction in hip extensor moment (approximately 0.1Nm/kg) was present for the Davis set when compared to the Har reference during the stance phase of gait (Fig.7.3). The Ortho set had a marginally increased hip extensor moment (approximately 0.02Nm/kg) during stance while the Bell set displayed almost identical curve displacement (Fig.7.3). Hip abduction moment was reduced for the Ortho set (approximately 0.1 Nm/kg during stance) while Bell and Davis closely followed the Har reference. There were no obvious deviations from the Har reference for Bell, Davis or Ortho for hip rotation moment (Fig.7.3).

7.4 Discussion

The use of regression equations from the literature to estimate HJC location is common practice during clinical gait analysis. However, regression equations are not without their limitations and the errors associated with such sets have been well documented. Recently, the Harrington set (Harrington et al., 2007) has been recommended over other sets for use in gait analysis, based on a comparison between functional calibration methods, 3-dimensional ultrasound and medical imaging identification of the HJC as the reference standard (Sangeux et al., 2011, Sangeux et al., 2014, Peters et al., 2012). However, differences resulting from the use of other commonly used sets were not considered, particularly from a clinical point of view. No study has investigated the clinical impact of regression equation error on kinematic and kinetic output. The aim of this chapter was to examine whether any clinically meaningful difference existed for both kinematic and kinetic profiles when different commonly used regression equations were applied during paediatric gait. It is worth noting that while a straightforward manipulation of the position of HJC could be used to assess the impact of altered HJC position, assessing the impact during gait as in this chapter allows for further assessment of the clinical impact (by means of GPS and GDI-Kinetic) of using different HJC regression equation sets.

When the Davis set was considered, the largest difference can be seen in the anterior/posterior direction (MD = 16.2mm). While no differences were recorded for GPS (statistical or clinical) and the effects on kinematics were small (Fig.7.3), a large deviation can be seen in the hip extensor/flexor moment for the Davis set (Fig.7.3). Particular reference has been made to the sensitivity of the hip extensor/flexor moment to error in this direction (Stagni et al., 2000), and this is evident in our findings. While not statistically significant, the GDI-Kinetic score for the Davis set demonstrated a clinically significant difference (4.4 points). With this in mind it must be concluded that error associated with the use of the Davis set for inverse dynamic calculations could be considered clinically meaningful. Kinematic output was only mildly affected and no statistically significant or clinically meaningful difference was recorded with GPS. Consequently, the use of this set for kinematic analysis would be clinically acceptable. However, care must be taken when this set is used in the inverse dynamic analysis. Concerns about the performance of this set, albeit only with respect to absolute HJC location, have been previously reported (Peters et al., 2012, Sangeux et al., 2011, Sangeux et al., 2014).

The Orthotrak set demonstrated statistically significant differences in the anterior/posterior and medial/lateral directions for HJC coordinate distance compared to the Harrington reference (Fig.7.2) (Table 7.2). The magnitude of the difference in the anterior/posterior plane was smaller than that seen for the Davis set (MD = -7.0mm, $p = .00$). Consequently, the hip extensor/flexor moment graph followed the Harrington reference graph quite closely, with the negative difference resulting in slightly increased extensor moment (Fig.7.3). The largest difference for the Orthotrak set was in the medial/lateral direction (MD = 9.14mm, $p < 0.04$). The consequence of this was reduced hip abduction moment when compared to the Harrington reference (Fig.7.3). Hip abduction moment has been shown to be the second most sensitive measure, after hip extensor/flexor moment, to HJC location error and it is particularly sensitive to error in the medial/lateral direction (Stagni et al., 2000). No significant deviations were present in the hip rotation moment graph for the Orthotrak set

(Fig.7.3). When the GDI-Kinetic was considered, no statistically significant (p = 0.99) or clinically significant (2.3 points) differences were present. A similar trend was demonstrated for GPS score with very little deviation in the kinematic graphs (Fig.7.3). It has been suggested that HJC estimation methods with minimal anterior/posterior error should be preferred (Stagni et al., 2000). Taking this into consideration, along with the findings of no statistical or clinical differences in GDI-Kinetic or GPS, it was concluded that the Orthotrak set could be used confidently in the clinical setting as an alternative to the Harrington set. Results suggested that the associated errors would not be incorrectly mistaken as a clinically meaningful difference.

The Bell regression equation set was the best performing set compared to the Harrington reference across all measured variables. No statistically significant differences were present for HJC coordinate distance in any direction. The ensemble average moment graphs were almost identical to the Harrington reference graphs for all three measures at the hip (Fig.7.3). When the GDI-Kinetic and GPS were considered, no statistically significant (p = 0.99 and p = 0.99 respectively for GDI-Kinetic and GPS) or clinically significant (0.8 points and 0.1^{o} respectively for GDI-Kinetic and GPS) were present. Kinematic graphs were identical for Bell when compared to the Harrington reference (Fig.7.3). Consequently, it was concluded that the Bell regression equation set could also be used confidently in the clinical setting as an alternative to the Harrington set.

7.5 Conclusion

The current findings suggested that the use of the Bell regression equation set (Bell et al., 1989) was equally as valid as using the Harrington regression equation set (Harrington et al., 2007) for HJC location during paediatric gait analysis. While differences in HJC location were statistically significant in two of the three axes for the Orthotrak set, there were no clinically significant differences and it is unlikely any error would be incorrectly considered

clinically meaningful. However, when using the Orthotrak set, clinicians must be aware of the increased error in the medial/lateral direction and the consequences on the hip abduction moment. The Davis set performed poorly compared to the Harrington set with respect to the kinetic output and the potential exists for error to be incorrectly considered clinically meaningful. Therefore it should be used with caution, particularly when comparing data derived using other regression equation sets. Consequently, it is proposed that the Harrington or Bell regression equation sets are used during paediatric gait analysis especially where inverse dynamic data are calculated. While not tested in this study, it is not expected that results would significantly differ for CP or adult subjects. In a recent study assessing actual HJC position, measured using MRI scans in adults, healthy children and children with CP, absolute measurement errors were shown to be comparable across groups (Harrington et al., 2007). The authors infer that in relative terms the errors would in fact be less significant for adults due to larger pelvises. For the purposes of this thesis, the Bell regression equation set will be used in the kinematic model to determine HJC position (Bell et al., 1989).

Chapter 8: Development of the Thorax Kinematic Protocol

This chapter has been published as follows:

Kiernan, D., Malone, A., O'Brien, T. & Simms, C. K. 2014. *A 3-dimensional rigid cluster thorax model for kinematic measurements during gait.* J Biomech, 47, 1499-1505.

Chapter Highlights

- The development of a new thoracic kinematic protocol was highlighted as necessary for the purposes of this thesis.
- A protocol was proposed and preliminary validated against other reference protocols based on the analysis of 15 TD subjects during gait.
- The proposed protocol demonstrated excellent waveform similarity and agreement with the reference protocols.
- Results suggested the proposed protocol can be confidently used in the clinical setting.

8.1 Introduction

The trunk acts as an active segment rather than a passive unit during gait (Armand et al., 2014, Leardini et al., 2009). Plantarflexor weakness, hip abductor weakness and hip extensor weakness can all result in compensatory trunk patterns and, consequently, it has been suggested that trunk kinematics should be considered an important part of the pathological gait assessment (Gutierrez et al., 2003, Lamoth et al., 2002). Methods for modelling the trunk range in complexity, depending on the movement of interest, with trunk kinematics often described by tracking a combination of skin surface markers placed directly on the thorax segment (Gutierrez et al., 2003, Nguyen and Baker, 2004, Romkes et al., 2007, Su et al., 1998). A number of drawbacks exist when using this approach. Skin surface markers require experienced clinicians for palpation and localisation of anatomical landmarks, although there is still room for error regardless of the experience of the clinician (Armand et al., 2014). For pathological groups such as CP this can be made all the more difficult as cooperation may be an issue when applying multiple marker sets. Many thorax protocols require a marker on the Xypoid Process (XP). Issues regarding the practicality and invasiveness of accurately

applying this marker in females have been previously highlighted (Armand et al., 2014). Skin surface markers are also susceptible to Skin Movement Artefact (SMA), where soft tissue moves over the underlying bone. As an alternative to the skin surface marker approach, a rigid marker cluster model that attaches to a single point on the thorax is proposed in this chapter. Few studies have used rigid marker clusters for measuring thorax movement during gait and where they have been used the specific point of attachment is often not reported (Houck et al., 2006, Krebs et al., 1992, Wu et al., 2004). When placed at the appropriate point, a rigid cluster has the potential to address many of the limitations of the skin surface marker approach and provide a better fit for the clinical assessment. Consequently, there is a clinical need for such a protocol. Following from this, the aim of this chapter was to describe and validate a rigid cluster protocol for thorax movement during gait that better fits with the clinical assessment. This thorax protocol will then be used to address the primary aims of this thesis regarding thorax motion in Chapters 10 and 11.

8.2 Materials and Methods

8.2.1 Subjects

Fifteen healthy subjects were recruited: 9 male, 6 female, aged 6 to 18 years. Ethical approval was obtained as described in Section 5.2. Informed written consent was obtained from all participants and from their parents when legally minor as described in Section 5.3.4.

8.2.2 Thorax Protocol

The thorax protocol of this research (that will be referred to as the Central Remedial Clinic Thorax Model - CRCTM) was developed using custom scripts in Matlab 8.1.0.604 (The MathWorks, Natick, Massachusetts, USA). The CRCTM is further development of a protocol used previously in our laboratory for measuring functional movements at the low back (Rice et al., 2004). Markers were placed on a rigid mount attached to the thorax at the level of T3 (3rd Thoracic Vertebra). T3 has been previously highlighted to lie within the area of least skin

movement artefact during active movement of the trunk (Rice et al., 2002). The mount was made of lightweight plastic with a small rectangular base that attached to the skin using double sided sticky tape (Fig.8.1).

Figure 8.1: Position of the CRCTM on a normal subject. The rigid cluster was made of lightweight plastic with a small rectangular base that attached to the skin using double sided sticky tape. The mount sat proud of the back so markers were not obscured by shoulder or arm movement.

The mount was placed proud of the back so markers were not obscured by shoulder or arm movement. Three active markers were attached to the mount. The centre lines of the mount's longitudinal axis was marked and aligned with the vertical axis of the spine and the centre of T3. The Z-axis of the protocol was defined using two markers along the base of the mount. Positive Z-axis was defined as m2 to m1 (Fig.8.2).

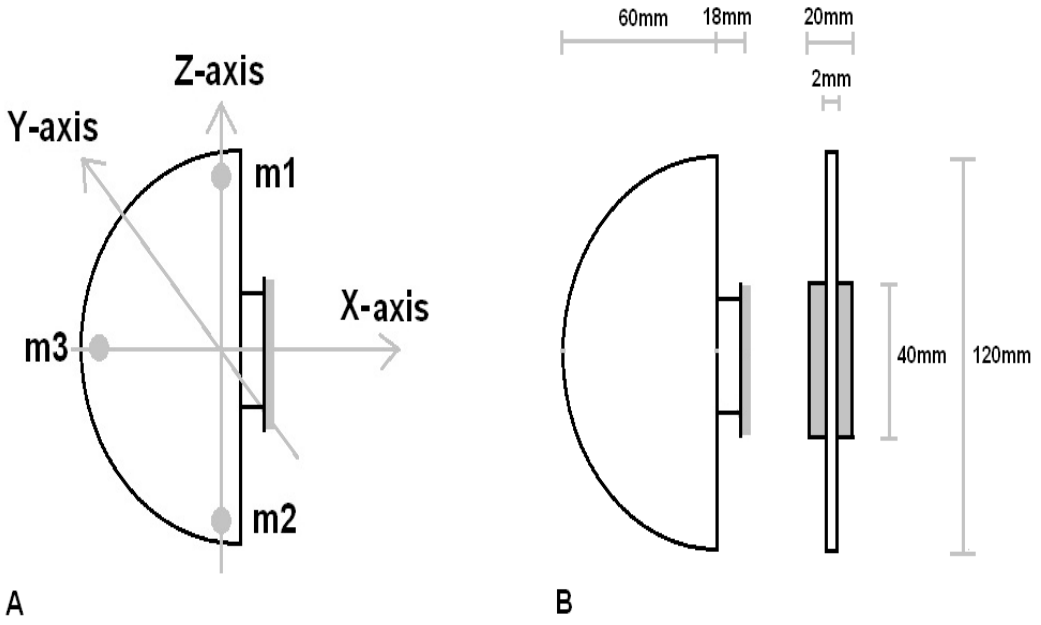

Figure 8.2: Schematic and dimensions of the thorax mount and the corresponding axes of the mathematical model. The Z-axis was defined by the vector between marker 2 (M2) and marker 1 (M1). The X-axis was defined as the vector between marker 3 (M3) and the mid-point of M2 and M3. A Gram-Schmidt orthogonal procedure was used to define the Y-axis.

The X-axis was defined using a Gram-Schmidt procedure incorporating m3 and the Z-axis with positive X-direction forward through the body (Fig.8.2). The Y-axis was defined as the vector product of the X-axis and Z-axis.

The CRCTM angles were calculated according to International Society of Biomechanics (ISB) recommendations as the rotation between (1) the thorax axes system and the pelvic axes system and (2) the thorax axes system and the laboratory. The pelvic axes system was as previously described in Section 5.5.3. The laboratory coordinate system was defined with the x-axis pointing forward along the laboratory walkway, the y-axis pointing in a medio-lateral direction and the z-axis in a vertical direction. Subjects walked along the x-axis of the laboratory. The sequence for angular decomposition was Y-X-Z.

8.2.3 Validation of the Protocol

For validation purposes, the CRCTM was compared with two reference thorax protocols from the literature. Protocol 1 (ISB) was defined according to anatomical landmarks as reported by the ISB to define the thorax segment (Wu et al., 2005). The anatomical landmarks were the 7th cervical vertebra (C7), 8th thoracic vertebra (T8), Incisura Jugularis (IJ) and XP (Fig.8.3). It is the role of individual researchers to relate tracking markers to these points. For the purposes of this study, skin surface markers were attached directly to these points. Protocol 2 (Armand) was defined using an "optical and minimal" skin marker set (Armand et al., 2014). Markers were placed directly at IJ, 2nd thoracic vertebra (T2), and T8. Thorax rotations for both protocols were defined according to ISB recommendations (Fig.8.3). For comparison purposes, the relationship between ISB and Armand protocols was also reported.

8.2.4 Data Collection

The 3-dimensional kinematic analysis was performed using the CODA cx1 active marker system (Charnwood Dynamics Ltd., Leicestershire). Data for all three protocols were captured simultaneously (Fig.8.3). Due to the rigid nature of the thorax and the duplication of data during the double support phase of gait, only one side of data (left) was reported for the purposes of this study. Subjects were asked to walk at a self selected pace with two representative files recorded and averaged per subject. A static standing trial was also recorded for each subject. Final parameters were calculated as the thorax angle (at each point in the gait cycle) minus the mean of the static standing angle for each model. The purpose of this was to perform a "zeroing effect" and account for the offset due to different definitions of anatomical axes (Collins et al., 2009).

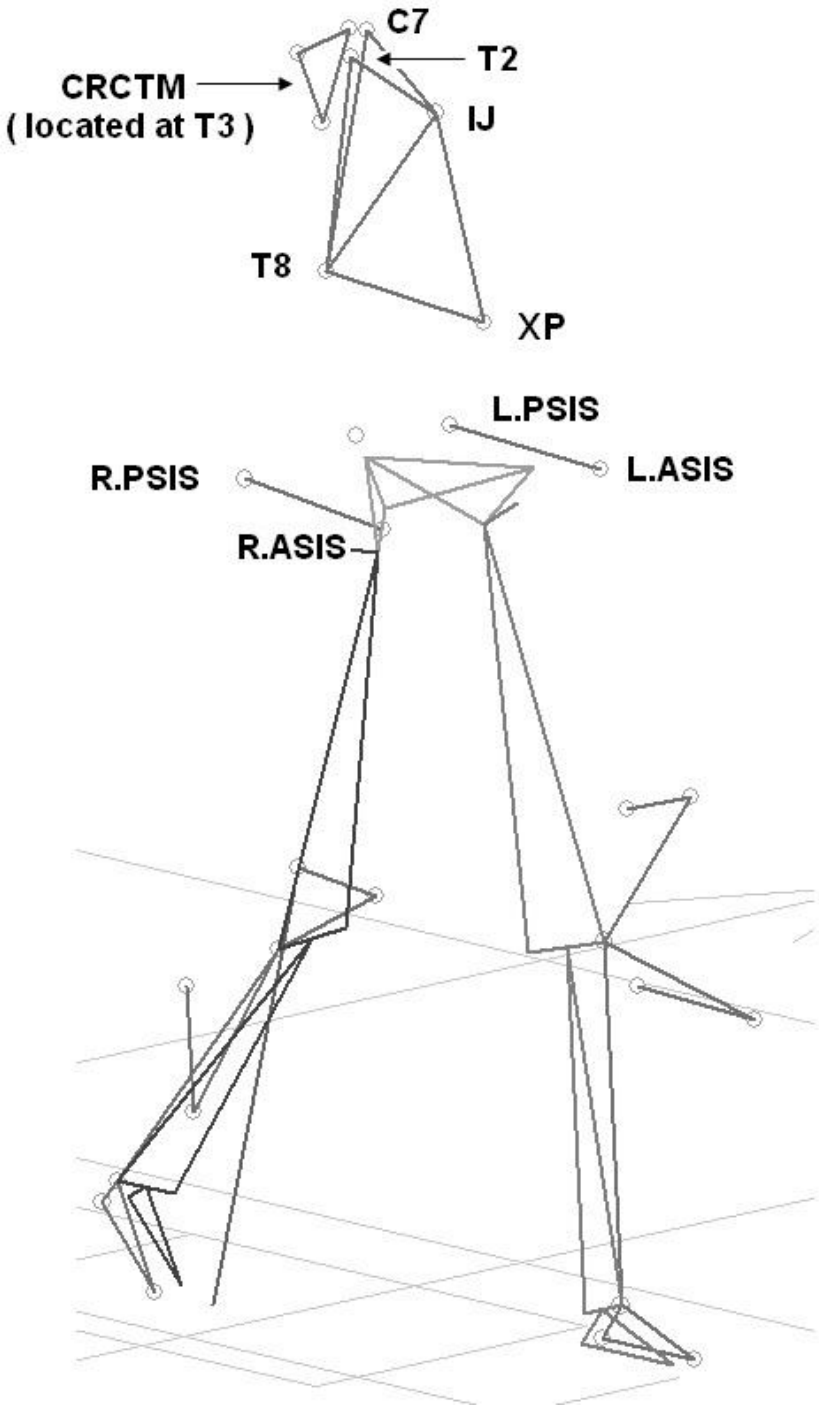

Figure 8.3: A stick figure diagram of all three thorax protocols in situ. Protocol 1 (ISB) defined using ISB recommendations, with markers placed directly at C7, T8, IJ and XP. Protocol 2 (Armand) defined using an "optical and minimal" skin marker set (Armand et al., 2014), with markers placed directly at IJ, T2 and T8. Protocol 3 (CRCTM) with mount placed directly at T3 and aligned with the vertical axis of the spine.

8.2.5 Data Analysis

An alternative formulation of the coefficient of multiple correlation (CMC) was used to assess waveform similarity across the gait cycle (Ferrari et al., 2010). This approach is recommended for the calculation of CMCs of waveforms measured simultaneously by different protocols (Roislien et al., 2012b). A CMC > 0.9 was chosen as the minimum acceptable value to demonstrate high similarity. Bland and Altman 95% Limits of Agreement (LoA) were calculated for peak and range parameters of each angle to assess agreement between models. Ensemble average profiles of thorax angles were visually analysed for deviations across the three thorax protocols. CMC values were calculated in Matlab 8.1.0.604 (The MathWorks, Natick, Massachusetts, USA), while Bland and Altman results and ensemble average graphs were calculated in Microsoft Excel.

8.3 Results

8.3.1 Waveform Similarity

Excellent waveform similarity as measured by the CMC was present between all 3 protocols in all 3 planes for calculations both with respect to the lab and pelvic co-ordinate frames (Table 8.1). CMC values ranged from 0.96 to 0.99. The highest level of similarity between CRCTM and Armand was for thorax flexion (w.r.t pelvis) (CMC = 0.99). The lowest waveform similarity values were recorded between CRCTM and ISB for thorax rotation (w.r.t lab) (CMC = 0.97), and between CRCTM and ISB for thorax flexion (w.r.t lab) (CMC = 0.96).

Table 8.1: Alternative CMC values averaged over 15 subjects. Due to the simultaneous measurement of all 3 protocols and assumptions with respect to the rigid nature of the thorax segment, a CMC > 0.90 was chosen as the minimum acceptable value to demonstrate high similarity between waveforms.

CMC	CRCTM – Armand		CRCTM - ISB		ISB - Armand	
	Mean	SD	Mean	SD	Mean	SD
Thorax Flex (w.r.t Lab)	0.96	0.11	0.99	0.02	0.99	0.02
Thorax Side Flex (w.r.t Lab)	0.98	0.02	0.98	0.03	0.99	0.01
Thorax Rotation (w.r.t Lab)	0.99	0.01	0.97	0.11	0.96	0.04
Thorax Flex (w.r.t Pelvis)	0.99	0.00	0.99	0.01	0.99	0.00
Thorax Side Flex (w.r.t Pelvis)	0.98	0.04	0.98	0.04	0.99	0.00
Thorax Rotation (w.r.t Pelvis)	0.99	0.02	0.99	0.02	0.99	0.00

8.3.2 Limits of Agreement (LoA)

LoA for peak kinematic parameters were high overall with similar agreement demonstrated between CRCTM and Armand and CRCTM and ISB (Table 8.2). LoA ranged from -3^{o} to 3^{o} for thorax side flexion (w.r.t pelvis) to -5^{o} to 6^{o} for thorax flexion (w.r.t lab) between CRCTM and Armand. When CRCTM was compared to ISB, LoA ranged from -4^{o} to 4^{o} for thorax side flexion (w.r.t lab) to -4^{o} to 7^{o} for thorax rotation (w.r.t pelvis) (Table 8.2). LoA for range kinematic parameters were high and similar both between CRCTM and Armand and CRCTM and ISB (Table 8.3).

Table 8.2: Bland and Altman 95% Limits of Agreement (LoA) for peak kinematic parameters between CRCTM and Armand, CRCTM and ISB and ISB and Armand protocols (degrees).Note: LoA for peak kinematic parameters were high overall.

Parameter	CRCTM - Armand			CRCTM - ISB			ISB - Armand		
	Bland- Altman 95% LoA			Bland- Altman 95% LoA			Bland- Altman 95% LoA		
	D	SD(D)	95% LoA	D	SD(D)	95% LoA	D	SD(D)	95% LoA
Thorax Flex (w.r.t Lab)	1	3	-5 to 6	-0	2	-4 to 4	1	1	-2 to 3
Thorax Side Flex (w.r.t Lab)	0	2	-3 to 3	-0	2	-3 to 4	0	1	-2 to 2
Thorax Rotation (w.r.t Lab)	1	2	-4 to 6	1	2	-4 to 6	0	1	-1 to 1
Thorax Flex (w.r.t Pelvis)	1	3	-5 to 6	0	2	-4 to 4	1	1	-2 to 3
Thorax Side Flex (w.r.t Pelvis)	0	2	-3 to 4	1	2	-3 to 4	-0	1	-2 to 2
Thorax Rotation (w.r.t Pelvis)	2	3	-4 to 7	2	3	-4 to 7	0	1	-1 to 2

Table 8.3: Bland and Altman 95% Limits of Agreement (LoA) for range (Max – Min) kinematic parameters between CRCTM and Armand, CRCTM and ISB and ISB and Armand protocols (degrees). LoA for range kinematic parameters were high and similar between CRCTM and Armand and CRCTM and ISB.

Parameter	CRCTM - Armand			CRCTM - ISB			ISB - Armand		
	Bland- Altman 95% LoA			Bland- Altman 95% LoA			Bland- Altman 95% LoA		
	D	SD(D)	95% LoA	D	SD(D)	95% LoA	D	SD(D)	95% LoA
Thorax Flex (w.r.t Lab)	-1	1	-2 to 1	-1	1	-2 to 1	0	0	-1 to 1
Thorax Side Flex (w.r.t Lab)	-3	1	-3 to 2	-1	1	-2 to 1	0	1	-1 to 2
Thorax Rotation (w.r.t Lab)	-1	2	-5 to 3	-2	2	-6 to 3	0	1	-1 to 2
Thorax Flex (w.r.t Pel)	-1	1	-2 to 1	-1	1	-2 to 1	0	0	-1 to 1
Thorax Side Flex (w.r.t Pel)	-1	1	-3 to 1	0	1	-2 to 2	-1	1	-2 to 1
Thorax Rotation (w.r.t Pel)	1	2	-3 to 5	1	2	-3 to 5	0	1	-1 to 1

A high level of agreement was present between ISB and Armand models for both peak and range parameters. Bland and Altman plots corresponding to data in Tables 8.2 and 8.3 are provided in Appendix 8.1.

8.3.3 Ensemble Averages

Ensemble average profiles showed almost identical curve displacement for each angle when comparing CRCTM and Armand (Fig.8.4) and CRCTM and ISB (Fig.8.5). Thorax rotation (w.r.t lab and pelvis) demonstrated a slightly higher standard deviation band for the CRCTM when compared to both reference protocols, with a small deviation from reference protocol mean value evident during the swing phase of gait. Ensemble average graphs comparing Armand and ISB are also presented (Fig.8.6).

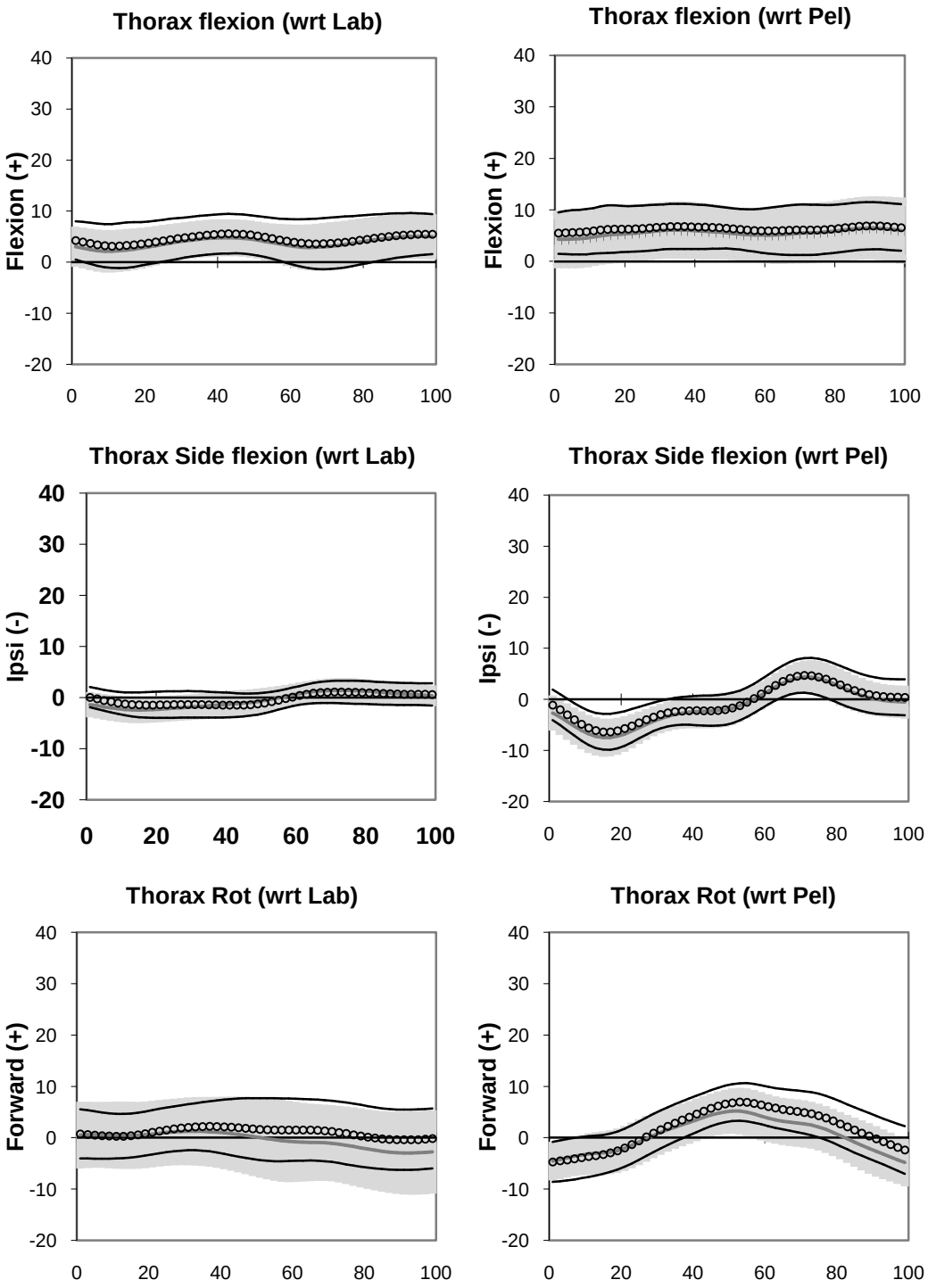

Figure 8.4: CRCTM compared to Armand. Thorax kinematic curves (degrees) for one gait cycle averaged over 15 normal subjects. Mean static standing angle deducted from walking trials to account for the offset due to different definitions of anatomical axes. CRCTM - grey dashed line (mean), grey band (± 1 SD). Armand- black line of circles (mean), solid black lines (± 1SD).

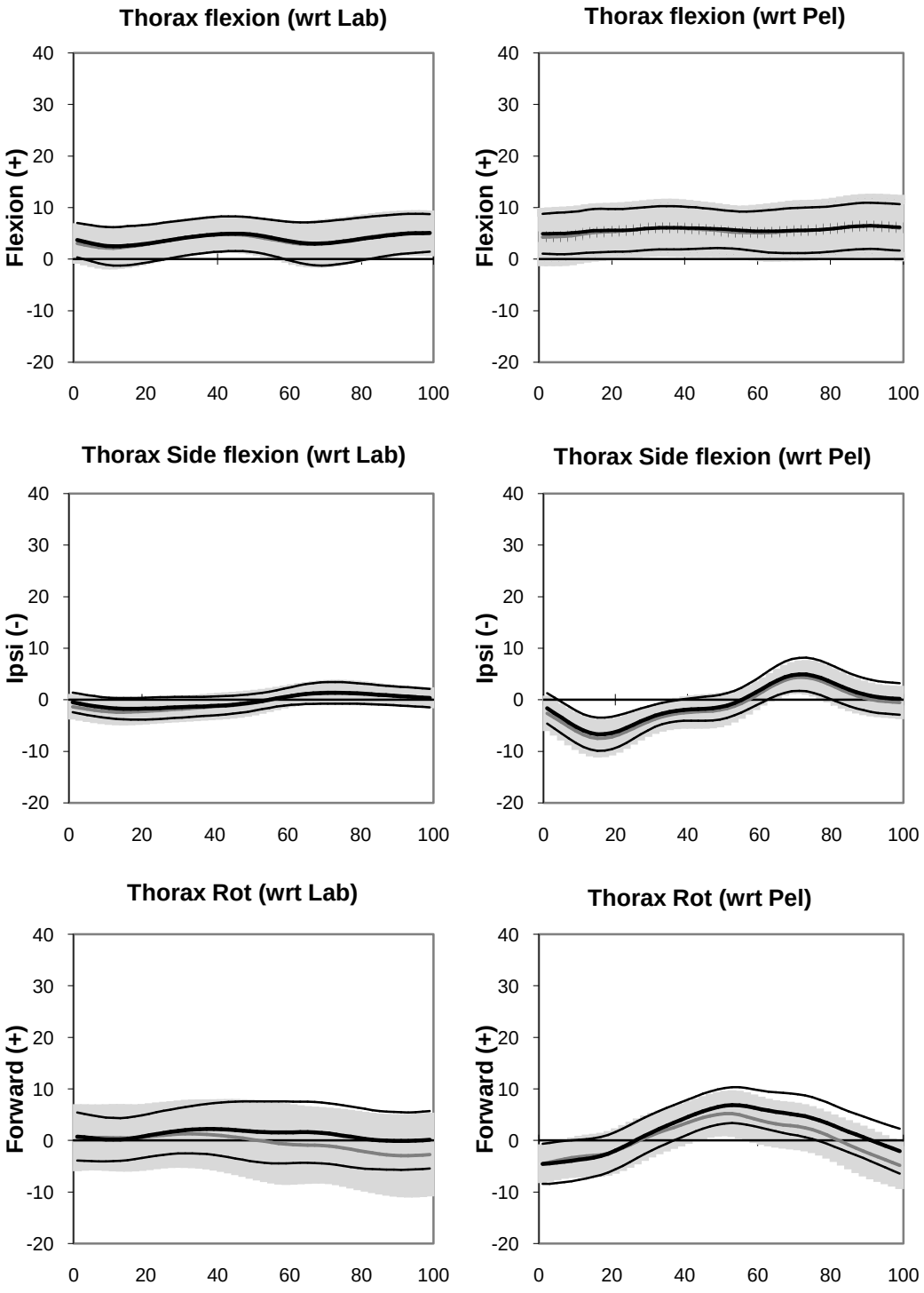

Figure 8.5: CRCTM compared to ISB. Thorax kinematic curves (degrees) for one gait cycle averaged over 15 normal subjects. Mean static standing angle deducted from walking trials to account for the offset due to different definitions of anatomical axes. CRCTM - grey dashed line (mean), grey band (± 1 SD). ISB- heavy solid black line (mean), light solid black lines (± 1SD).

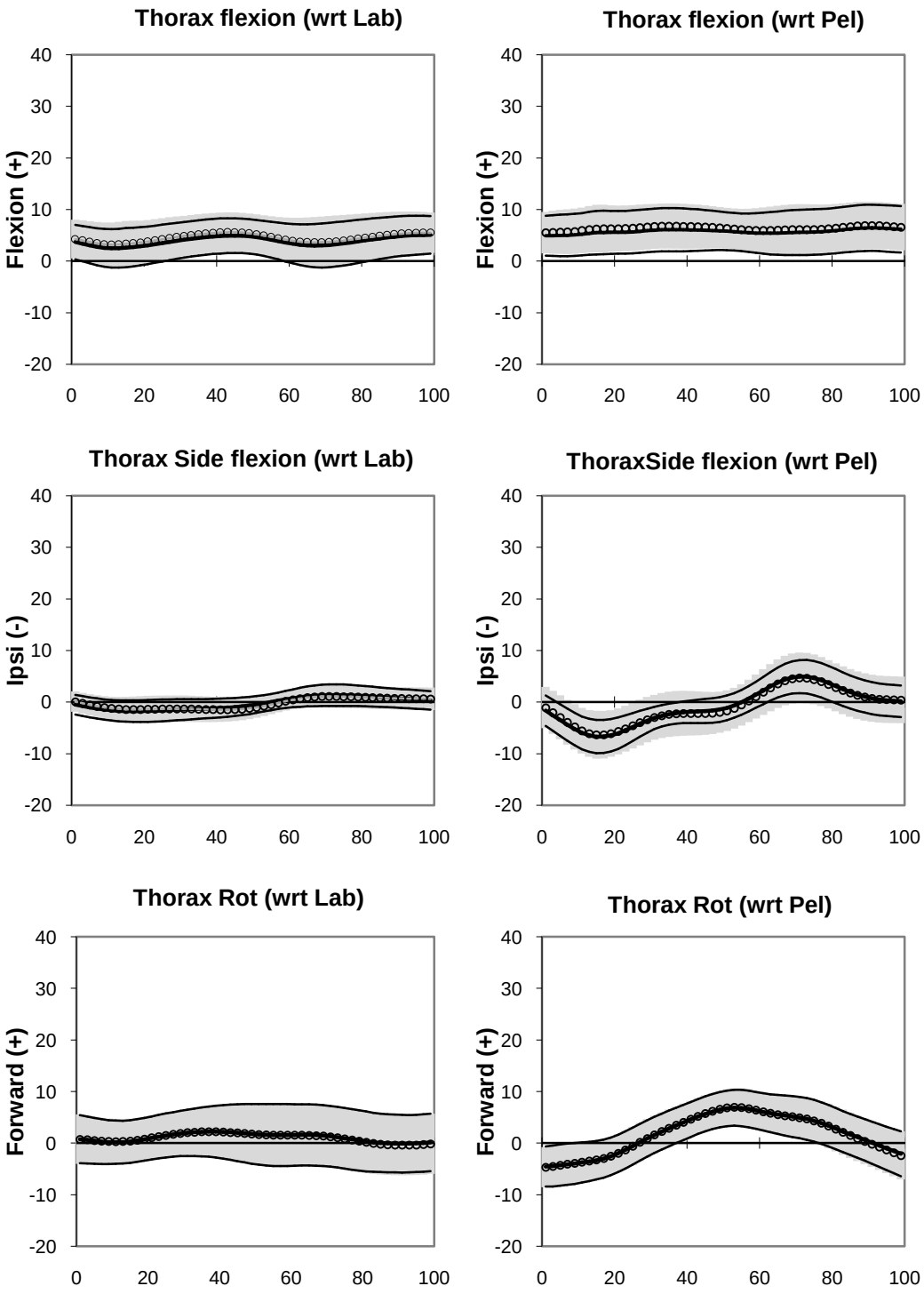

Figure 8.6: ISB compared to Armand. Thorax kinematic curves (degrees) for one gait cycle averaged over 15 normal subjects. Mean static standing angle deducted from walking trials to account for the offset due to different definitions of anatomical axes. ISB - heavy solid black line (mean), light solid black lines (± 1SD). Armand - black circles (mean), grey band (± 1 SD).

8.4 Discussion

The CRCTM had a number of advantages over other thorax protocols. While a reliability analysis was not part of this study, the position of T3 was easily identifiable in the majority of subjects thus potentially reducing the error associated with the palpation of landmarks. The rigid cluster was easily attached which can be particularly useful when patient cooperation is an issue. The rigid mount stood proud of the thorax so as not to be obscured by arm movements thus improving marker visibility. There was no need for the XP marker thus avoiding any practical and potentially embarrassing issues for assessment on females and, although not tested in this study, the proposed protocol has the potential to be less susceptible to SMA error as it is positioned on an area of least skin movement on the trunk (Rice et al., 2002). In relation to validation of the CRCTM, excellent waveform similarity was demonstrated when compared to both reference protocols, with CMC values all greater than 0.97 (Table 8.1). This suggested that the CRCTM measures almost identical movements to both reference protocols.

When considering LoA, it has been suggested that acceptable LoA are matter of clinical judgement (Bland and Altman, 1986). For the purposes of this study, the LoA and ensemble average graphs were assessed in conjunction with each other. LoA for peak kinematic parameters were closest between the two reference models (ISB – Armand) (Table 8.2). This was evident in the ensemble average graphs where mean and standard deviation bands were practically identical (Fig.8.6). When CRCTM was compared to Armand, the mean difference between models was low in all 3 planes (0^o – 2^o) with wider LoA most evident for thorax rotation w.r.t the lab (range 10^o) and pelvis (range 11^o). Similar findings were present between CRCTM and ISB. LoA for range kinematic parameters demonstrated a similar trend to peak parameters (Table 8.3).

As the technical axes system of the CRCTM was not based on the anatomical axes system of the thorax, the potential exists for kinematic crosstalk where axial rotations around

one axis are misinterpreted as occurring around another axis (Baker et al., 1999, Rivest, 2005). The reported differences between the CRCTM and reference models might be as a consequence of this. It is also possible that wobble error, due to oscillations of the mount during periods of higher accelerations of the thorax, may contribute somewhat to the reported differences, most evident for CRCTM thorax rotation compared to both reference models during the swing phase of gait (Figs.8.4 & 8.5). Future studies are necessary to test the CRCTM in activities where larger accelerations of the thorax occur, such a cutting manoeuvres or running.

A limitation of the "zeroing process", used to account for different axes systems of the CRCTM and reference models, was the potential to mask alignment issues such as kyphosis. For the purposes of this chapter, data were collected on normal subjects with no obvious spinal deformities. However, on subjects where kyphosis may be an issue, the axes systems of CRCTM and the reference protocols may be altered depending on the vertebral levels at which the kyphosis occurs. This alignment issue is a limitation of all protocols, including the current reference standard. The validity of 3-dimensional trunk kinematics in people with spinal deformities has not been tested with any of the existing protocols, and is an important area for future study.

8.5 Conclusion

When considering the CRCTM for use during gait, the question presented whether the differences measured by the CRCTM were small enough to be considered insignificant from a clinical point of view. The mean differences between CRCTM and reference protocols were all below 3^{o} (absolute difference) for peak and range parameters (Tables 8.2 and 8.3). Waveform similarity was excellent for all angles and while LoA for thorax rotation were wide, the mean CRCTM angle remained close to both reference protocol mean values and well within the ± 1 SD band. With this in mind, and in the absence of a single measure to define an acceptable

clinically meaningful difference between protocols, it was concluded that the recorded differences were not large enough to be considered clinically meaningful. Consequently, it was concluded that the proposed model can be confidently used as an alternative to other thorax protocols in the clinical setting. For the purposes of this thesis, the proposed thorax protocol will be used to address the primary aims of this thesis in Chapters 10 and 11.

Chapter 9: Selection of a Protocol to Assess Lumbar Segment Motion during Gait

This chapter has been published as follows:

Kiernan, D., Malone, A., O'Brien, T. & Simms, C. K. 2015. *A quantitative comparison of two kinematic protocols for lumbar segment motion during gait.* Gait & Posture, 41, 699-705.

Chapter Highlights

- A protocol for the assessment of lumbar segment movement was required for the purpose of this thesis.
- Two lumbar kinematic protocols from the literature were selected and kinematic output, recorded simultaneously during gait, were compared between protocols.
- Large differences in kinematic output were measured between protocols.
- Functional Limits of Agreement demonstrated only a poor to moderate agreement between protocols
- The skin surface marker protocol was considered more suited to studies of axial rotation and was chosen for the purposes of this thesis.

9.1 Introduction

Deformities of the lumbar spine have been reported in people with CP (Harada et al., 1993, Johnson et al., 2004). Consequently, when assessing trunk motion during gait in CP, an assessment of the lumbar spine may provide useful information. Some studies report spinal movement as the relative movement of the thorax with the pelvis (Romkes et al., 2007). However, it has been suggested that in order to measure motion of the lumbar spine more accurately, markers are needed on the spine (Romkes et al., 2007). However, this can add to model complexity and increase the time needed for data collection. Some trunk models described in the literature extend to the lumbar spine (Heyrman et al., 2013a, Leardini et al., 2011, Needham et al., 2014, Seay et al., 2008). However, the use of skin surface markers placed along the lumbar spine allows only a 2-dimensional representation of movement. In many cases, as a compromise between clinical utility and clinically useful information, the lumbar spine has been treated as a rigid segment thus allowing for the analysis of movement

in 3-dimensional space (Mason et al., 2014, Seay et al., 2008, Schache et al., 2002). In relation to CP gait, 3-dimensional movement of the lumbar region has not been reported and could provide useful insight into the overall movement and compensatory patterns of the trunk.

Kinematic modelling of the spine as a rigid segment could involve the placement of a set of skin surface markers placed over the lumbar region at specifically defined points (Seay et al., 2008, O'Sullivan et al., 2010a, Crosbie et al., 1997), or alternatively as a rigid cluster mount placed at a specific anatomical location on the lumbar spine (Konz et al., 2006, Needham et al., 2014, Schache et al., 2002, Whittle and Levine, 1999). However, when rigid cluster mounts have been used, the specific point of application of the mount can vary between studies (Needham et al., 2014, Schache et al., 2002, Konz et al., 2006, Whittle and Levine, 1999). Ideally, before a kinematic model or protocol is used, a preliminary validation would be a comparison to a reference standard. However, for spinal motion, the International Society of Biomechanics (ISB) only report standards concerning intervertebral motion between adjacent vertebra (Wu et al., 2002). The ISB suggest that the principles can be extended to regional spinal movement. However, no specific reference standard for rigid lumbar segment kinematics has been described. In the absence of a reference standard, most protocols are designed based on clinical experience. This can lead to the existence of many protocols essentially designed to measure motion of the same segment. In many cases these are designed specific to a clinical problem and often involve different marker sets and technical and anatomical frame definitions (Leardini et al., 2009). Consequently, differences may exist in the resulting kinematic output when these protocols are used. However, it is not unusual for kinematic data to be shared and interpreted irrespective of the protocol (Leardini et al., 2009). When choosing a protocol from the literature, at the very least a structured comparison with other available protocols should be considered to assess the pros and cons of each. In relation to the lumbar region, no study has examined the effects of using different protocols for 3-dimensional kinematic measurements during gait. It is possible that differences in kinematic

output could be considered clinically meaningful and it is vital that these differences are fully understood before clinical judgment is made (Leardini et al., 2009, Hashish et al., 2014, Kiernan et al., 2014c). Following from this, the aim of this chapter was to determine the influence of using two 3-dimensional lumbar segment protocols, available in the literature, on the resultant kinematic output during gait. The purpose of this was to assess the most suitable kinematic protocol for lumbar segment motion during gait that will then be used to measure lumbar segment motion for the purposes of this thesis. The first protocol was a skin surface marker protocol (Seay et al., 2008). The protocol was chosen due to the wide spread of markers across the lumbar region and for its availability in the literature having recently been used in a number of studies (Seay et al., 2008, Mason et al., 2014). The second protocol was a rigid cluster protocol with the cluster placed on the third lumbar vertebrae (L3). This protocol has also recently been used in a number of studies (Konz et al., 2006, Needham et al., 2014) and it was felt it would provide an appropriate measure of lumbar segment motion.

9.2 Materials and Methods

9.2.1 Subjects

Ten healthy subjects were recruited: 7 male and 3 female, aged 17 to 37 years (Mean age of 24.8 years). Ethical approval was obtained as described in Section 5.2. Informed written consent was obtained from all participants and from their parents when legally minor as described in Section 5.3.4.

9.2.2 Skin Surface marker Protocol

The skin surface (SS) marker protocol involved placement of active markers directly on the skin at the level of the T12-L1 joint space and 4 markers placed on the lumbar region either side of the mid-line markers with a distance of 4cm between all markers (Seay et al., 2008) (Fig.9.1C & Fig.9.1D). Two virtual points were created as the mid-point between the T12-L1 and M1 markers (V1) and the mid-point between T12-L1 and M2 markers (V2) (Fig.9.1C). A least squares plane was then fit to both virtual points and markers M3 and M4, thus defining the segment frontal plane (Fig.9.1C). The least squares fit was applied so that the sum of the squares distance between the markers and the frontal plane was minimized (Soderkvist and Wedin, 1993). The proximal and distal endpoints of the segment were defined as the midpoint of V1 and V2 and M4 and M3 respectively (Fig.9.1C). The segment Z-axis was defined as the unit vector between distal endpoint to the proximal endpoint. The Y-axis was defined as the unit vector perpendicular to the frontal plane and Z-axis. The X-axis was defined using the right hand rule. Angles were calculated according to ISB recommendations as the rotation between (1) the lumbar axes system and the pelvic axes system and (2) the lumbar axes system and the laboratory. The pelvic axes system was as previously described in Section 5.5.3. An order of rotation of tilt, obliquity and rotation, similar to the conventional sequence traditionally applied to the pelvis, was chosen for this protocol (Baker, 2001).

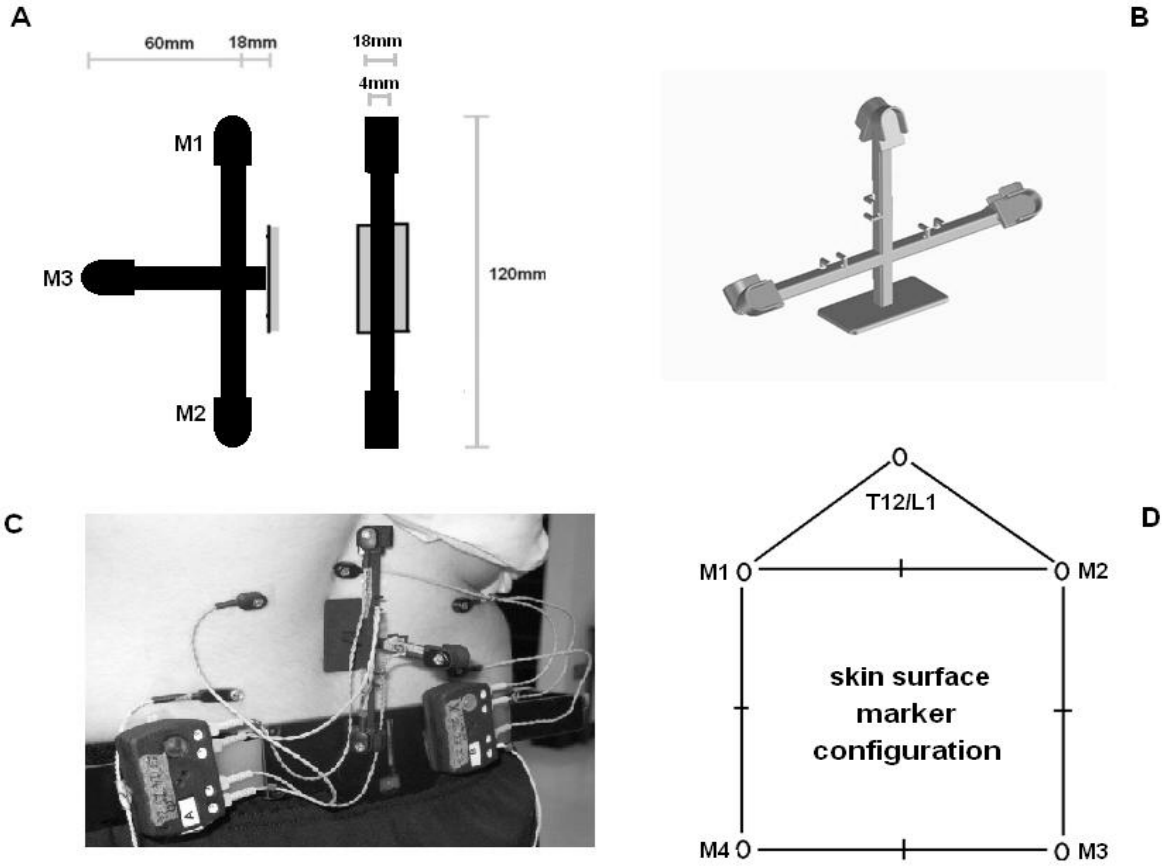

Figure 9.1: (A) Schematic of the rigid cluster mount used in this study. (B) The mount was made of lightweight plastic with a small rectangular base that attached directly to the skin using double sided sticky tape. (C) The rigid cluster and skin surface protocols in-situ. (D) The skin surface protocol configuration.

9.2.3 Rigid Cluster Protocol

The rigid cluster (RC) protocol and technical axes definitions were similar to that described in Section 8.2.2. In short, markers were placed on a rigid mount attached to the lumbar spine at the level of the 3rd lumbar vertebra (L3) (Konz et al., 2006, Needham et al., 2014). The mount was made of lightweight plastic with a small rectangular base that attached directly to the skin using double sided sticky tape (Figs.9.1A and Figs.9.1B). Three active markers were attached to the mount. The 3 markers were used to define a plane from which a virtual lateral marker was projected. This virtual marker and markers M1 and M2 were then used to define the segment frontal plane with M1 and M2 defining the proximal and distal endpoints (Fig.9.1A & Fig.9.1C). The segment axes, angle definitions and order of rotation were defined as per the skin surface protocol.

9.2.4 Data Acquisition and Analysis

The 3-dimensional kinematic analysis was performed using the CODA cx1 active marker system (Charnwood Dynamics Ltd., Leicestershire). Data for both models were captured simultaneously at a frame capture rate of 100Hz. Due to the assumption of rigidity of the lumbar segment and the duplication of data during the double support phase of gait, only one side of data (left) was reported for the purposes of this study. Subjects were asked to walk at a self selected pace with three files recorded per subject. One representative file was then chosen. A static standing trial was also recorded for each subject. Final parameters were calculated as the lumbar angle (at each point in the gait cycle) minus the mean of the static standing angle for each model. The purpose of this was to perform a "zeroing effect" and account for the offset due to different definitions of technical axes (Collins et al., 2009, Kiernan et al., 2014a). Ensemble average graphs prior to the "zeroing effect" are also reported and discussed. Data were filtered with a 4th order Butterworth low-pass filter with a cut-off

frequency of 8Hz. All kinematic analysis and data filtering were carried out using Visual 3D v4.96.0 software (C-Motion Inc., Germantown, MD, USA).

9.2.5 Statistical Analysis

An alternative formulation of the coefficient of multiple correlation (CMC) was used to assess waveform similarity across the gait cycle (Ferrari et al., 2010). The CMC is a single measure between 0 and 1 providing a measure of similarity of waveforms. This alternative approach is recommended for the calculation of CMCs of waveforms measured simultaneously by different protocols (Roislien et al., 2012b).

Functional Limits of Agreement (FLoA) were calculated to assess agreement between gait curves recorded by each model (Roislien et al., 2012a). This approach expands on the Limits of Agreement described by Bland and Altman (Bland and Altman, 1986) and allows the functional data structure for the entire stride to be examined (Olsen et al., 2013). In the case of where the mean difference follows the zero line closely and the width of the FLoA are relatively small, this would indicate good agreement between protocols. Where the mean difference moves away from the zero line and the FLoA are wider, this would indicate poorer agreement (Roislien et al., 2012a).

The Mean Absolute Variability (MAV) was calculated as a measure of the variability of each protocol (Ferrari et al., 2008). The MAV was calculated as the maximum minus the minimum, at each point in the gait cycle, across all subjects. This was carried out for both protocols. Ensemble averages were also visually analysed for deviations across both lumbar protocols.

CMC values were calculated in Matlab 8.1.0.604 (The MathWorks, Natick, Massachusetts, USA), while FLoA, ensemble average graphs and MAV scores were calculated in Microsoft Excel.

9.3 Results

9.3.1 Ensemble Averages

Ensemble average graphs demonstrated similar mean kinematic profiles between protocols (Figs.9.2 & 9.3). Before the "zeroing effect" was applied, the largest offset between protocols was in the sagittal plane (lumbar flexion) with the SS protocol demonstrating an increased lumbar extension of approximately 5^{o} compared to the RC protocol (w.r.t lab and pelvis) (Fig.9.2). No other ensemble average plots demonstrated a large mean offset between protocols (Fig.9.2). When model technical definitions were taken into account, mean curve displacement was similar between protocols for all planes (w.r.t lab and pelvis) (Fig.9.3). Marginally wider standard deviation bands were present for the RC protocol for lumbar side flexion during mid to late stance and for lumbar rotation during mid-stance through to terminal swing (w.r.t pelvis) (Fig.9.3).

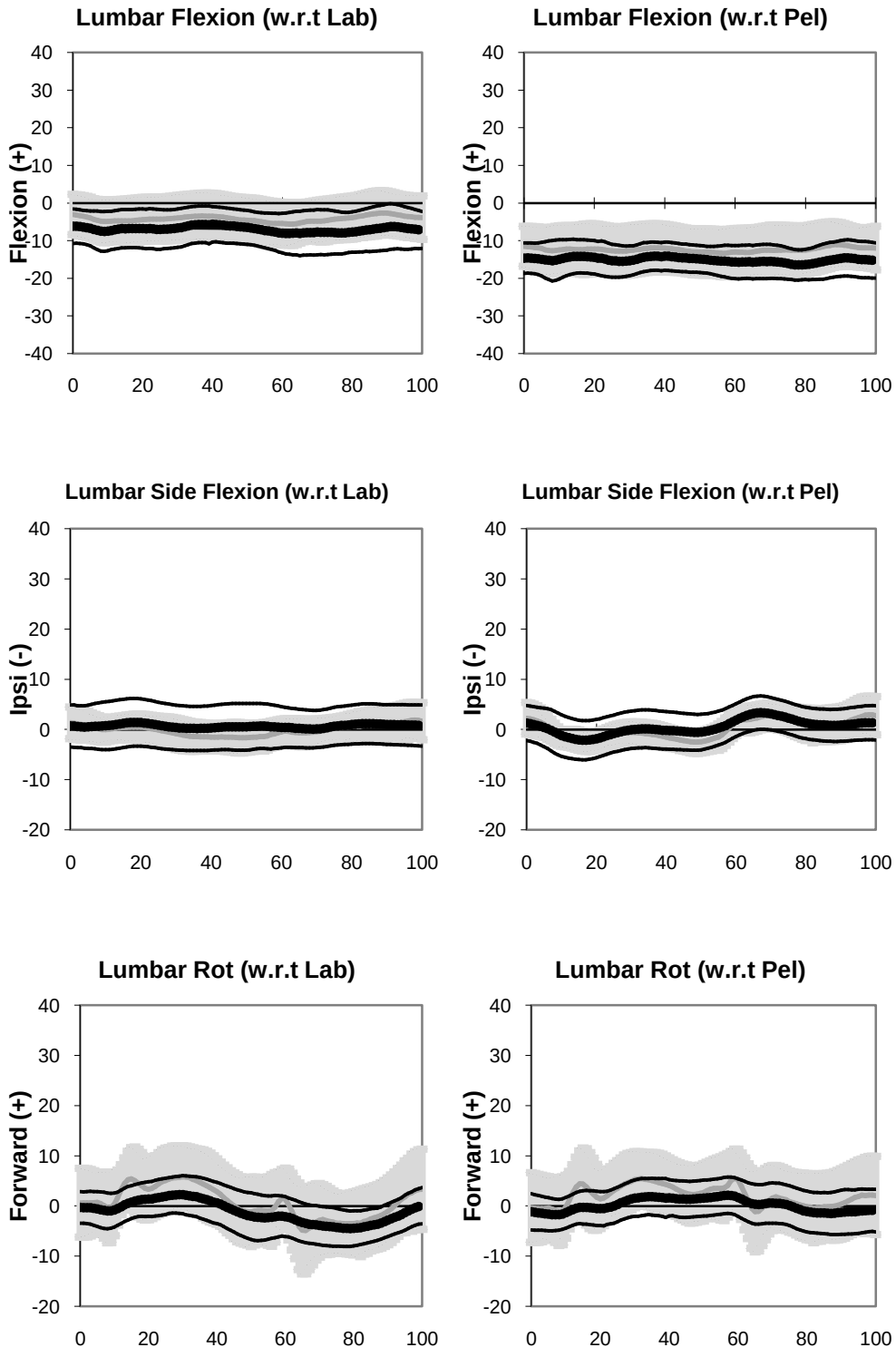

Figure 9.2: Ensemble average graphs (degrees) prior to the "zeroing effect" for lumbar segment kinematics for one gait cycle averaged over 10 normal subjects. Rigid Cluster model – grey dashed line (mean) and grey band (± 1 SD). Skin Surface model – heavy black line (mean) and light solid black lines (±1 SD).

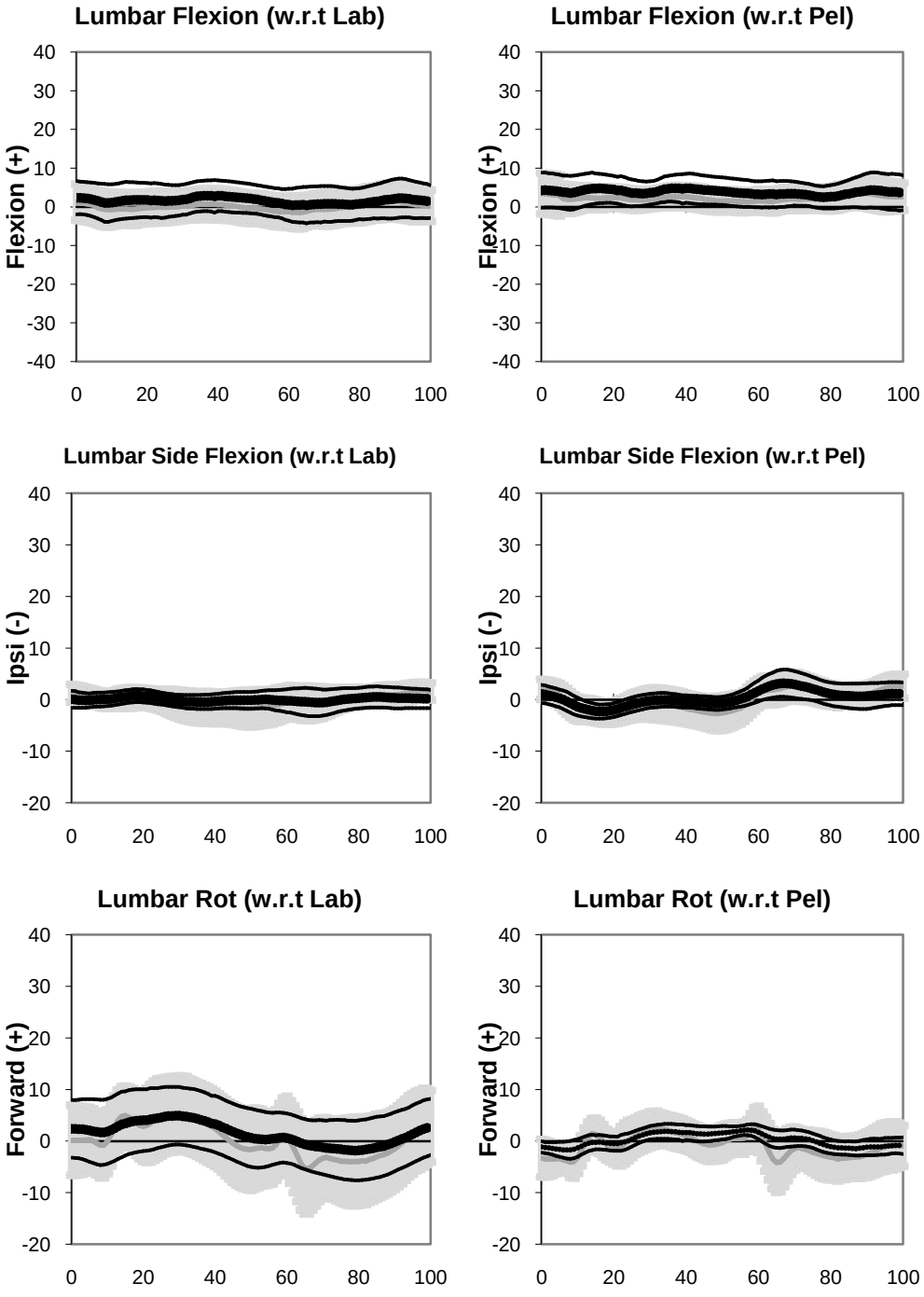

Figure 9.3: Ensemble average graphs (degrees) post the "zeroing effect" for lumbar segment kinematics for one gait cycle averaged over 10 normal subjects. Mean static standing angle deducted from walking trials to account for the offset due to different definitions of anatomical axes. Rigid Cluster model – grey dashed line (mean) and grey band (± 1 SD). Skin Surface model – heavy black line (mean) and light solid black lines (±1 SD).

9.3.2 Functional Limits of Agreement (FLoA):

FLoA demonstrated a moderate agreement between protocols overall (Fig.9.4). For lumbar flexion (w.r.t lab and pelvis), the mean difference followed the zero line reasonably closely (approximately -3^{o}) with FLoA of approximately +6^{o} to -8^{o} indicating a moderate agreement between protocols during the full gait cycle (Fig.9.4). For lumbar side flexion (w.r.t lab and pelvis), an initial mean difference of approximately 1^{o} dropping close to 0^{o} (FLoA of approximately ±4^{o}) suggested good agreement in early stance. Late stance demonstrated a poorer agreement between protocols with a slight deviation away from the zero line and wider FLoA (approximately ±6^{o}). The mean difference returned to follow the zero line closely during swing with FLoA of approximately ±4^{o} demonstrating good agreement during this phase of gait. For lumbar rotation (w.r.t lab and pelvis), a mean difference of approximately -3^{o} and FLoA of approximately +4^{o} to -7^{o} suggested only moderate agreement at initial contact (Fig.9.4). Fluctuations of the mean difference close to the zero line during early to mid-stance (FLoA of approximately ±5^{o}) suggested only a moderate agreement during this period of the gait cycle. At initial swing, the mean difference reached approximately -5^{o} with FLoA of approximately +6^{o} to -15^{o}. The mean difference returned closely to the zero line for the remainder of the swing phase with FLoA of +5^{o} to -10^{o}.

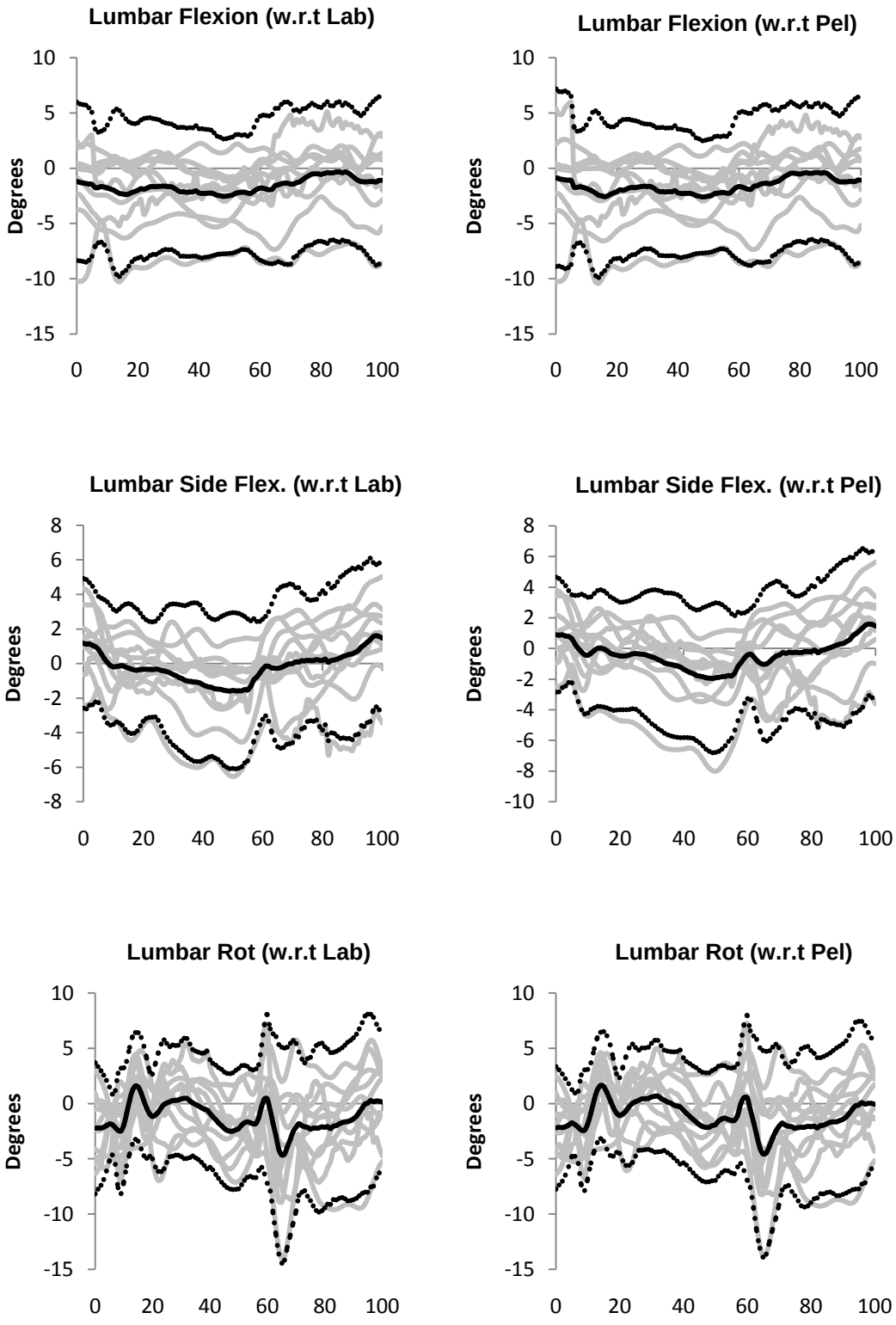

Figure 9.4: Time continuous differences for each individual (grey solid lines), mean difference (black solid line), and functional limits of agreement (FLoA) (black dotted lines) for one gait cycle averaged over 10 normal subjects.

9.3.3 CMC Waveform Similarity

A poor to moderate waveform similarity was demonstrated between the SS and RC protocols as determined by the CMC in all 3 planes (w.r.t lab and pelvis) (Table 9.1). CMC values ranged from 0.29 to 0.71. The highest levels of similarity were recorded for lumbar rotation (w.r.t lab) (CMC = 0.71) followed by lumbar side flexion (w.r.t pelvis) (CMC = 0.69). The lowest levels of similarity were recorded for lumbar flexion (w.r.t lab and pelvis) with CMC values of 0.31 and 0.29 respectively. Poor to moderate waveform similarity was present for lumbar side flexion (w.r.t lab) and lumbar rotation (w.r.t pelvis) of 0.33 and 0.48 respectively (Table 9.1).

Table 9.1: Alternative CMC values and Mean Absolute Variability (MAV) between protocols. CMC demonstrated only a poor to moderate waveform similarity while MAV was moderate overall with higher variability in general for the rigid cluster model. RC – Rigid Cluster, SS – Skin Surface.

Measure	CMC	(SD)	RC MAV	SS MAV
Flexion (w.r.t lab)	0.31	(0.35)	13^{o}	15^{o}
Side Flexion (w.r.t lab)	0.33	(0.43)	8^{o}	6^{o}
Rotation (w.r.t lab)	0.71	(0.18)	23^{o}	17^{o}
Flexion (w.r.t pelvis)	0.29	(0.36)	9^{o}	12^{o}
Side Flexion (w.r.t pelvis)	0.69	(0.28)	8^{o}	5^{o}
Rotation (w.r.t pelvis)	0.48	(0.26)	11^{o}	4^{o}

9.3.4 Kinematic profiles MAV

MAV was higher in 4 of the 6 measures for the RC protocol compared to the SS protocol. MAV for the SS protocol was higher for lumbar flexion but lower for lumbar side flexion and rotation (w.r.t lab and pelvis) when compared to the RC protocol (Table 9.1). The

largest difference in MAV between protocols was for lumbar rotation (w.r.t lab and pelvis) with higher MAV values of 23^{o} and 11^{o} for the RC protocol compared to MAV values of 17^{o} and 4^{o} for the SS protocol (w.r.t. lab and pelvis). A smaller difference was present for lumbar side flexion between protocols (w.r.t lab and pelvis). For this measure the SS protocol demonstrated MAV values of 6^{o} and 5^{o} compared to MAV values of 8^{o} and 8^{o} for the RC protocol. The opposite trend was present for lumbar flexion where MAV values were lower for the RC protocol compared to the SS protocol (Table 9.1). The RC protocol demonstrated MAV values of 13^{o} and 9^{o} compared to MAV values of 15^{o} and 12^{o} for the SS protocol (w.r.t lab and pelvis) (Table 9.1).

9.4 Discussion

A number of protocols exist in the literature to describe rigid lumbar segment kinematics during gait. As no reference standard exists, these protocols are primarily based on clinical experience and involve different marker configurations. Consequently, the potential exists for large differences in kinematic output when these protocols are used. The aim of this chapter was to quantify the differences in kinematic output when two recently reported protocols were used during gait. Results showed moderate to large differences between protocols.

When ensemble average graphs were considered, a definite offset of approximately 5^{o} can be seen in the lumbar flexion graphs between protocols before the “zeroing effect” was applied. This was not surprising as the protocol marker configurations were different. When the static angle between protocols was taken into account, the largest correction was for the lumbar flexion graph. Lumbar side flexion and lumbar rotation displayed similar mean curves in both cases. While a visual inspection of ensemble average graphs suggested similar curve displacement between protocols, the larger standard deviation bands for the RC model for lumbar side flexion and lumbar rotation could not be ignored. MAV values confirmed greater levels of variability primarily for the RC protocol. Only lumbar flexion demonstrated lower

differences in MAV values for the RC protocol. CMC values demonstrated only poor waveform similarity for lumbar flexion and lumbar side flexion and moderate to good waveform similarity for lumbar rotation (w.r.t lab and pelvis). The overall poor to moderate agreement between protocols was confirmed by FLoA. Lumbar side flexion demonstrated the closest FloA showing it to be the most agreeable measure between protocols. Lumbar flexion and rotation demonstrated considerably wider FLoA demonstrating only a poor agreement between protocols.

While results demonstrated large differences between protocols, the extent to which these differences were due to different marker set up or skin movement artefact (SMA) is unknown. A limitation of both protocols is that the lumbar region was considered a rigid segment. This of course was not the case. Due to the spread of markers across the lumbar segment, the SS protocol in particular would be highly susceptible to a combination of SMA and non-rigid body motion of the lumbar segment. Calculating the motion of the lumbar region by fitting all the skin surface markers in a least squares sense would ultimately have improved kinematic output and was applied in this case (Soderkvist and Wedin, 1993). However, depending on the phase of gait, movement of the underlying musculature on both sides of the spine would still be expected to impact on marker movement.

The ensemble average graphs demonstrated a side flexion towards the supporting limb during swing. As the lumbar segment side-flexed, the skin and marker would have been expected to move. A similar but opposite movement would then occur during stance as the contralateral limb progressed through swing. As the SS protocol was constructed according to the plane defined by the skin surface markers, SMA and subsequent deviation of this plane would affect axes definitions. In the original study describing the skin surface protocol (Seay et al., 2008), Elastikon elastic wrap was used to potentially minimize the effects of SMA. However, it was not reported whether SMA was in fact reduced or whether kinematics were affected. Consequently, it was decided not to use it in this study at the risk of altering

kinematic output. Due to the position of the cluster mount on the 3rd lumbar vertebra, the RC protocol would be less susceptible to this type of movement. However, the RC protocol would be susceptible to SMA caused by rotation of the spine itself. Axial rotation of the lumbar spine involves twisting of the intervertebral discs (Bogduk and Twomey, 1991). As the spine rotates, the underlying vertebra will move with respect to the skin on which the mount was attached. This would help explain somewhat the greater levels of variability recorded by the MAV for the RC protocol for lumbar rotation (w.r.t lab and pelvis).

The RC protocol has a number of practical advantages over the SS protocol. While not tested in this study, the position of L3 is readably identifiable in the majority of subjects potentially reducing error associated with palpation of landmarks. The RC protocol does not require multiple marker configurations thus providing straightforward attachment when patient cooperation is an issue. However, the cluster mount may be susceptible to wobble error. Care is needed if the RC protocol is used in activities such as cutting manoeuvres or running due to oscillations of the mount during periods of higher accelerations. At the very least, the mount should be well anchored to the subject using both double sided sticking tape and a hypoallergenic paper tape across the base.

9.5 Conclusion

Due to the clear differences in kinematic output reported in this study, it was concluded that the SS and RC protocols could not be used interchangeably. Choice of protocol will for the most part depend on the functional task and clinical population. However, while similar levels of variability were present for lumbar flexion and side flexion between protocols, the greater variability recorded by the RC protocol during lumbar rotation suggested that the SS protocol may be more suited to studies where axial rotation is a consideration. Consequently, for the purposes of this thesis, the SS protocol will be used to measure lumbar segment motion during the gait cycle (Chapter 10).

Chapter 10: Assessment of levels of loading at the low back during gait in paediatric cerebral palsy subjects compared to typically developed controls

This chapter has been published as follows:

Kiernan, D., A. Malone, T. O'Brien, and C.K. Simms. 2016. *Children with cerebral palsy experience greater levels of loading at the low back during gait compared to healthy controls.* Gait & Posture, 48: p. 249-255.

Kiernan, D., A. Malone, T. O'Brien, and C.K. Simms. 2017. *Three-dimensional lumbar segment movement characteristics during paediatric cerebral palsy gait.* Gait & Posture, 53: p. 41-47.

Chapter Highlights

- Thoracic and lumbar segment movements and lower lumbar spinal loading during paediatric CP gait were measured and compared to TD.
- CP children demonstrated increased movement of the thorax and lumbar segment in addition to increased reactive forces and moments at the lower lumbar spine.
- Loading at the lower lumbar spine and excessive thorax movement were related.
- Moderate links existed between loading at the lower lumbar spine and lumbar segment movement.
- Greater demands were placed on the lower lumbar spine as GMFCS level increased.

10.1 Introduction

The trunk makes up a large proportion of body mass and has been shown to be dominant in the production of external forces during gait (Gillet et al., 2003). Reference has been made to how an increased trunk lean, known to be characteristic of CP gait (Heyrman et al., 2013a, Romkes et al., 2007), can reduce the hip abductor moment during stance and aid stabilization of the pelvis (Krautwurst et al., 2013, Õunpuu et al., 1996). Kinematic analysis of the trunk during gait has been described by various different protocols throughout the literature (Armand et al., 2014, Attias et al., 2015, Heyrman et al., 2013a, Leardini et al., 2011, Kiernan et al., 2014a). When referring to the trunk, some studies have focused specifically on movement of the thorax (Armand et al., 2014, Attias et al., 2015, Kiernan et al., 2014a), while others have

expanded their protocols to include movement of the whole spine (Heyrman et al., 2013a, Leardini et al., 2011). However, in general, measurements of the lumbar spine are ignored, most likely due to the intricate nature of the spine and the requirement for complex spinal marker sets (Leardini et al., 2011). As discussed in Section 2.4.6, markers placed along the line of the spine at individual vertebra will only allow for a 2-dimensional assessment of movement of the lumbar region (Heyrman et al., 2013a). As an alternative to the 2-dimensional approach, and as a compromise between practicality of use and clinically useful information, the lumbar region has also been modelled as one rigid segment (Mason et al., 2014, Schache et al., 2002, Seay et al., 2008). As movement of the lower limbs has been shown to have a direct relationship with movement at the spine (Konz et al., 2006), the ability to perform a 3-dimensional assessment of movement of the lumbar spine during gait may be beneficial. However, while the potential exists for aberrant lumbar segment movement during CP gait, a 3-dimensional assessment of movement of the lumbar region has not been reported in this population.

Mechanical loads at the spine and the surrounding areas are influenced by gravity, inertia and externally applied loads. Consequently, as discussed in Section 2.4.6, excessive trunk movement may increase lower lumbar spinal loading. In a recent study examining the effects of amputee gait on lower lumbar spinal loading, positive correlations were found between increased trunk movements and increased reactive forces and moments at the lower lumbar spine (Hendershot and Wolf, 2014). Section 2.5.1 discussed the types of reactive forces and moments that are present at the lower spine during gait in normal subjects. However, no data exists for people with CP (Section 2.5.2). Prolonged exposure to pathological changes in the mechanics of motion of the trunk during CP gait may result in changes to the structural tissue within and surrounding the lower lumbar spine (Bogduk and Twomey, 1991, Harada et al., 1993). Additionally, while the link between excessive trunk movement and low back pain in any population group is difficult to establish, it is worth noting that the incidence of low back

pain has been reported to be higher in CP (Jahnsen et al., 2004). With this in mind, there is a need to better understand the impact of pathological gait, in particular the role of the trunk at thoracic and lumbar level, on loading at the lower lumbar spine in this population.

Levels of functional impairment in CP are also a consideration. Excessive movements have been shown to increase with increasing levels of gross motor function classification system (GMFCS) score (Attias et al., 2015). Consequently, the potential exists for increased lower lumbar spine loading as functional impairment increases. At the very least, reactive forces and moments at the lower lumbar spine during CP gait, and the relationship with excessive trunk movement and functional level of impairment, need to be better understood to be given consideration in the clinical decision making process. Following from this, the aims of this chapter were:

(1) To investigate 3-dimensional reactive forces and moments at L5/S1 in children with CP compared to TD children.

(2) To investigate the relationship between 3-dimensional reactive forces and moments at L5/S1 and level of functional impairment, expressed using the GMFCS levels I & II (Palisano et al., 1997);

(3) To investigate 3-dimensional thorax and lumbar segment movement characteristics during paediatric CP gait compared to TD children.

The relationship between reactive forces and moments at L5/S1 and principal diagnosis (hemiplegic and diplegic) is also reported in Appendices 10.1 to 10.5.

10.2 Materials and methods

10.2.1 Subjects

Ethical approval was obtained as described in Section 5.2. Informed written consent was obtained from all participants and from their parents when legally minor as described in Section 5.3.4.

Fifty-two children with CP were recruited from a cohort attending the gait analysis laboratory over a period of 9 months (GMFCS I: n = 26, 15M, 11F, mean age 11.65 (2.91) yrs; GMFCS II: n = 26, 18M, 8F, mean age 10.38 (3.02) yrs). Inclusion criteria for children with CP and TD are outlined in Section 5.3.3. Full participant data can be found in Table 10.1.

10.2.2 Data Collection

A full barefoot 3-dimensional analysis was performed using the CODA cx1 active marker system (Charnwood Dynamics Ltd., Leicestershire). The lower limb marker placement protocol and underlying mathematical model followed implementation as previously described in Section 5.5. Trunk kinematic data were recorded using the single cluster described in Chapter 8. The anthropometric estimates of Jensen et al (Jensen., 1989) were used in the model as described in Chapter 6. The hip joint centre regression equations of Bell et al (Bell et al., 1989) were used in the kinematic model as described in Chapter 7. The L5/S1 joint was implemented as described in Section 3.7. In short, a skin surface marker was placed at the L5/S1 joint space. A virtual point was then created, corresponding to 5% of the length of the line from the L5/S1 marker to the mid-point of ASISs, at which L5/S1 reactive forces and moments were calculated (Seay et al., 2008). The lumbar spine was treated as a single segment with active markers placed directly on the skin at T12-L1 joint space and 4 markers placed on the lumbar region either side of the mid-line markers (Seay et al., 2008). This protocol was assessed in Chapter 9 and demonstrated suitability for studies where axial rotation is a consideration.

Subjects walked unassisted at a self-selected pace. Two Kistler 9281B and two AMTI Accugait force platforms, as described in Section 5.8, were used to measure ground reaction force data. One representative walking trial, containing both left and right feet completely inside the boundary of two consecutive force platforms during successive initials contacts of the same foot, was analysed for each subject. Due to the replication of data at the L5/S1 joint during the double support phase, data were analysed for one limb only, namely the involved limb of the children with hemiplegia and a random limb (selected by coin toss) for TD and children with diplegia.

Data were collected using Codamotion ODIN software (v1.06 Build 01 09) at capture rates of 100Hz (kinematic) and 200Hz (kinetic) respectively. Kinematic and kinetic data were filtered with a 4^{th} order Butterworth filter with a cut-off frequency of 8Hz and 20Hz respectively. All kinematic and kinetic analysis and data filtering were performed in Visual 3D v4.96.0 software (C-Motion Inc., Germantown, MD, USA).

10.2.3 Sample Size Calculation

A sample size calculation was conducted based on a pilot study of coronal plane trunk flexion in TD subjects that demonstrated a mean RoM of 11.7^{o} and a standard deviation of 4.8^{o}. Assuming a mean difference of 1 standard deviation (4.8^{o}) between TD and CP groups, a power of 0.95 and significance of 0.05, a sample size of 26 was calculated (Stata 11.2, StataCorp LP, USA). For the purposes of this study, 26 participants were recruited to both GMFCS I and GMFCS II groups giving 52 CP subjects in total. Twenty-six subjects were recruited to the TD group.

10.2.4 Data Analysis

For the purposes of this study, “flexion”, “ipsilateral” and “forward” refer to positive direction while “extension”, “contralateral” and “backwards” refer to negative direction for sagittal, coronal and transverse planes respectively (Fig.10.1).

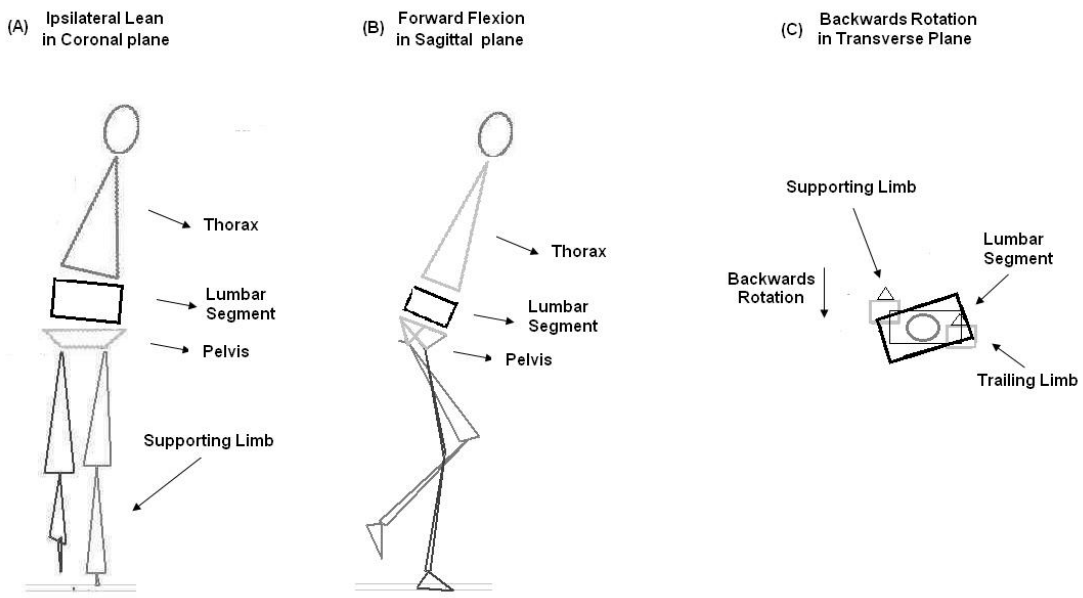

Figure 10.1: Movement patterns in the coronal, sagittal and transverse planes. (A) an ipsilateral lean of the thorax and lumbar segment, displayed on ensemble average profiles as positive direction; (B) a forward flexion of the thorax and lumbar segment, displayed on ensemble average profiles as positive direction; (C) backwards rotation of the lumbar segment, displayed on ensemble average profiles as negative direction.

Thorax movement (w.r.t pelvis and laboratory), lumbar segment movement (w.r.t pelvis and laboratory) and L5/S1 reactive forces and moments were the measures of interest. Children with CP were assessed according to level of functional impairment (GMFCS level). Additionally, children with CP were regrouped and assessed according to diagnosis (hemiplegia and diplegia). This additional data corresponding to diagnosis are reported in Appendices 10.1 to 10.5.

Walking speed (m/s) and a number of discrete kinematic and kinetic parameters were assessed between groups. Discrete parameters were: value at initial contact (IC), root mean square (RMS), peak value (Peak), time to peak (TTP) and range of movement (RoM / Range). Data were checked for distribution using the Shipiro-Wilk normality test. For data that followed a normal distribution, differences between groups were assessed using a one-way analysis of variance (ANOVA) with Bonferroni post-hoc tests for comparisons between groups. Dunnett's tests were also used to compare each group with the TD group. For data that did

not follow a normal distribution, differences were assessed using a Kruskal-Wallis test and post hoc Mann-Whitney U-tests. Median and range data were reported for non-normally distributed data. A Pearson correlation coefficient was used to assess the relationship between thorax and lumbar segment kinematic patterns and L5/S1 reactive forces and moments. The level of significance was set at 0.05. All statistical analyses were performed using IBM SPSS Statistics (v23.0.0.2). Additionally, ensemble average kinematic and kinetic profiles were visually analyzed for deviations between groups. Ensemble average profiles and corresponding discrete parameters for the pelvis are provided in Appendix 10.6.

10.3 Results:

10.3.1 Assessment according to groups

Children with CP were grouped according to functional level of impairment and regrouped according to diagnosis. Very similar results were demonstrated according to these groups. This was likely due to many of the children with CP GMFCS I presenting as hemiplegia and many of the children with CP GMFCS II presenting as diplegia. When regrouped, the hemiplegia group consisted of 21 subjects (18 GMFCS I and 3 GMFCS II) while the diplegia group consisted of 31 subjects (8 GMFCS I and 23 GMFCS II) (Appendix 10.1). As a result, it was decided that only data according to functional level of impairment were reported and discussed in the main body of this chapter. Participant data and results according to diagnosis are presented in Appendices 10.1 to 10.5.

10.3.2 Subject Data

Walking speed was significantly reduced for both GMFCS I and GMFCS II groups compared to TD children (-0.12 m/s, p = 0.004). No significant differences were recorded for mean walking speed between GMFCS I (1.07 m/s) and GMFCS II groups (1.07 m/s). Additionally, no significant differences were present for age, height or weight between groups (Table 10.1).

Table 10.1: Mean (SD) participant data for typically developed (TD), GMFCS level 1 (GMFCS I) and GMFCS level 2 (GMFCS II) groups. Significant differences were present for walking speed between groups as determined by one-way analysis of variance (ANOVA). *Post hoc comparisons demonstrated significantly slower walking speed between GMFCS I and TD and GMFCS II and TD (Dunnett's test).

Parameter	**TD (*n = 26*)**	**GMFCS I (*n = 26*)**	**GMFCS II (*n = 26*)**	***p*-Value**
Age (years)	10.15 (3.17)	11.65 (2.91)	10.38 (3.02)	0.166
Male / Female	15 / 11	15 / 11	18 / 8	------
Height (m)	1.40 (0.18)	1.49 (0.15)	1.42 (0.18)	0.085
Weight (kg)	35.31 (12.85)	42.96 (14.12)	36.69 (14.67)	0.115
Walking Speed (m/s)	1.19 (0.13)	1.07 (0.16)	1.07 (0.14)	0.004*

10.3.3 Thorax Kinematics (w.r.t Pelvis)

In the sagittal plane, the thorax demonstrated a slight forward flexion for TD and GMFCS I groups while the GMFCS II group demonstrated excessive movement throughout the gait cycle (Fig.10.2). For discrete parameters, only RoM was statistically significant between all 3 groups ($p < 0.001$). Both GMFCS I and II demonstrated higher RoM compared to TD ($\approx 2^{o}$ and 6^{o} respectively) (Table 10.2). No significant differences were recorded between groups for RMS or peak flexion values.

In the coronal plane, ipsilateral peak was significantly increased for GMFCS II children compared to GMFCS I and TD children ($\approx 7^{o}$). Contralateral peak, occurring during swing, demonstrated no significant differences between groups. Timings to peak values were similar across groups. RMS and RoM parameters were statistically significant for both GMFCS I and II compared to TD (increased by 1^{o} and 4^{o} for RMS and 2^{o} and 9^{o} for RoM) (Table 10.2).

In the transverse plane, similar kinematic patterns were present for the thorax for all 3 groups (Fig.10.2). The thorax started in a backwards position moving forwards until late stance where direction was reversed backwards throughout swing (Fig.10.2). GMFCS II demonstrated

significantly increased RoM (≈ 6^{o}) compared to TD (Table 10.2). No other parameters were significantly different between groups.

Table 10.2: Mean (SD) thorax kinematic values (w.r.t Pelvis) for TD, GMFCS I and GMFCS II groups with concurrent p-values. Distribution of data was assessed using a Shipiro-Wilk normality test (*Median and Range for non-normally distributed data).

Results of post-hoc tests are indicated as follows: statistically significant differences between (a) GMFCS I and TD; (b) GMFCS II and TD; (c) GMFCS I and GMFCS II. (GC- Gait Cycle)

Parameters	**TD Mean (SD)**	**GMFCS I Mean (SD)**	**GMFCS II Mean (SD)**	**ANOVA *p*-Value**
Tnk Flex / Ext (Sag. Plane) (deg)				
Value at Initial Contact (IC)	3 (8)	4 (13)	3 (11)	0.951
RMS*	6 (15)	10 (17)	10 (20)	0.058
Peak value (Flexion)*	6 (27)	3 (36)	7 (39)	0.759
Time To Peak Flexion (%GC)*	48 (98)	56 (98)	52 (98)	0.894
Peak value (Extension)	-2 (8)	-4 (11)	-8 (13)	0.190
Time to Peak Extension (%GC)*	61 (48)	56 (48)	39 (49)	0.226
RoM*	8 (12)	10 (12)	14 (8)	<0.001(a)(b)(c)
Tnk Side Flex (Cor. Plane) (deg)				
Value at Initial Contact (IC)	-1 (4)	1 (8)	2 (7)	0.250
RMS*	6 (11)	7 (13)	9 (13)	0.001(a)(b)
Peak Value (Ipsi)	6 (5)	8 (7)	14 (7)	<0.001(b)(c)
Time To Peak Ipsi (%GC)*	18 (86)	20 (98)	20 (12)	0.298
Peak Value (Contra)	-9 (5)	-10 (8)	-10 (9)	0.932
Time To Peak Contra (%GC)*	68 (42)	68 (22)	70 (16)	0.192
RoM	16 (5)	18 (5)	24 (10)	<0.001(b)(c)
Tnk Rot (Trans. Plane) (deg)				
Value at Initial Contact (IC)	-6 (8)	-8 (10)	-10 (8)	0.245
RMS*	8 (11)	10 (14)	10 (19)	0.184
Peak value	9 (7)	12 (8)	12 (10)	0.395
Time To Peak (%GC)*	54 (26)	52 (52)	53 (46)	0.934
RoM*	19 (19)	21 (34)	24 (66)	0.017(b)

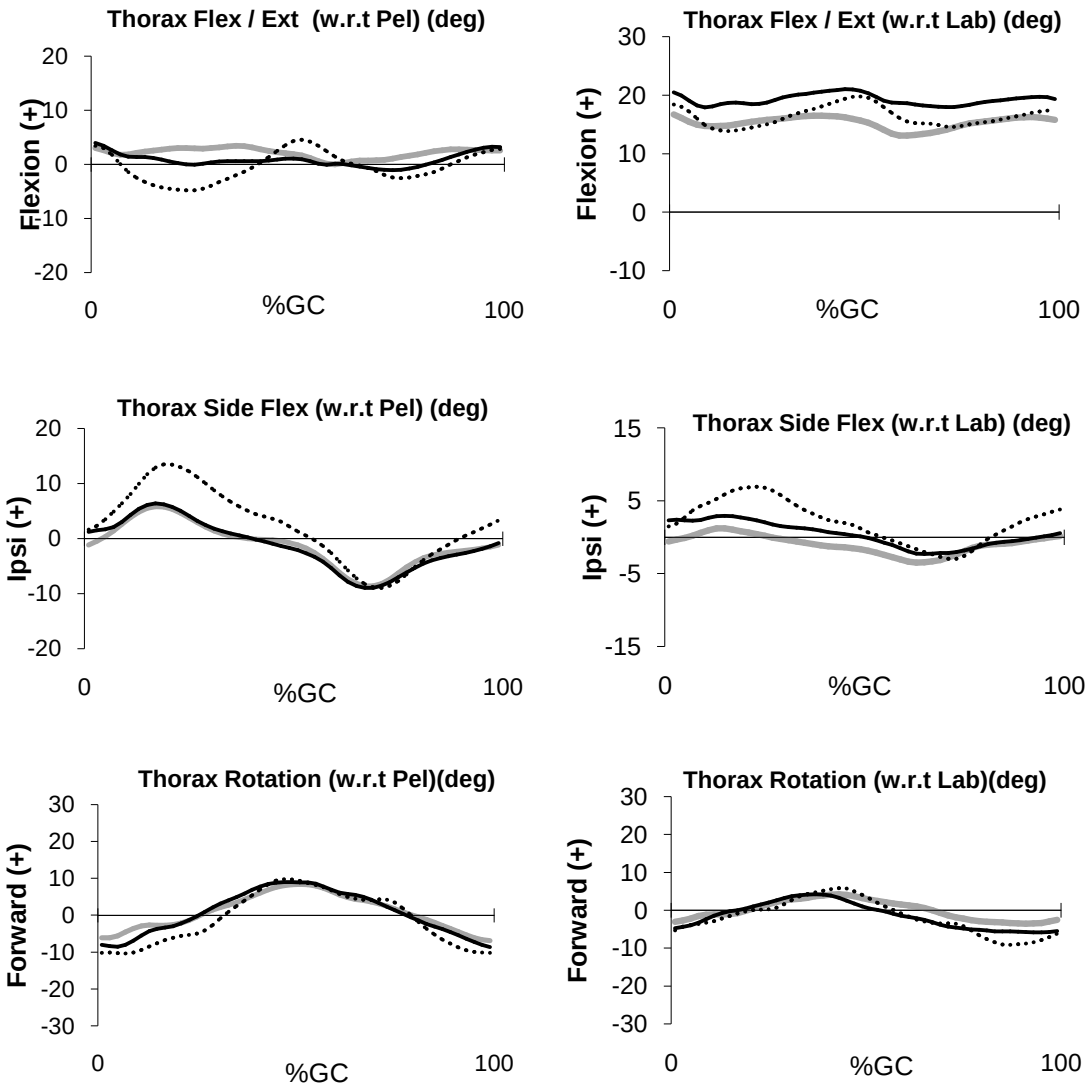

Figure 10.2: Ensemble average profiles for the thorax in all 3 planes (w.r.t Pelvis) (left column) and (w.r.t Lab) (right column). (Gray – Typically Developed, Black – GMFCS I, Dotted – GMFCS II) (%GC –% Gait Cycle). Note: Mean and SD profiles for all GMFCS I and II groups are presented in Appendix 10.7.

10.3.4 Thorax Kinematics (w.r.t Lab)

In the sagittal plane, ensemble average profiles demonstrated a more flexed position of the thorax for GMFCS I children compared to GMFCS II (increased by 3^{o}) and TD (increased by 4^{o}) (Fig.10.2, Table 10.3). However, these increases were not statistically significant (Table 10.3). Movement became more excessive as functional level of impairment increased and this was evident in RoM values with statistically significant differences for both GMFCS I and GMFCS II groups compared to TD (Table 10.3).

In the coronal plane, ipsilateral peak was significantly increased for GMFCS II children compared to TD only (increase of 6^{o}). This increased peak was evident in ensemble average profiles (Fig.10.2). No statistically significant difference existed between GMFCS groups for ipsilateral peak value (Table 10.3). RMS and RoM values were statistically significant for GMFCS I and II children compared to TD with both sets of values increasing according to functional level of impairment (Table 10.3).

In the transverse plane, similar kinematic profiles were demonstrated between all groups (Fig.10.2). However, RoM was increased for both GMFCS groups compared to TD (increase of 4^{o} and 10^{o} for GMFCS I and GMFCS II respectively) (Table 10.3). No other parameters were statistically significant in the transverse plane between groups.

10.3.5 Lumbar Kinematics (w.r.t Pelvis)

In the sagittal plane, GMFCS II children showed significantly more flexion compared to both GMFCS I and TD (increased flexion of 6^{o} and 8^{o} respectively) (Table 10.4, Fig.10.3). GMFCS I children were similar to TD. RoM was also statistically significantly increased for GMFCS II (Table 10.4).

Table 10.3: Mean (SD) thorax kinematic values (w.r.t Lab) for TD, GMFCS I and GMFCS II groups with concurrent p-values. Distribution of data was assessed using a Shipiro-Wilk normality test (*Median and Range for non-normally distributed data).

Results of post-hoc tests are indicated as follows: statistically significant differences between (a) GMFCS I and TD; (b) GMFCS II and TD; (c) GMFCS I and GMFCS II. (GC- Gait Cycle)

Parameters	**TD Mean (SD)**	**GMFCS I Mean (SD)**	**GMFCS II Mean (SD)**	**ANOVA *p*-Value**
Tnk Flex / Ext (Sag. Plane) (deg)				
Value at Initial Contact	17 (6)	20 (7)	18 (7)	0.151
RMS*	16 (6)	19 (7)	17 (7)	0.161
Peak value*	19 (6)	23 (7)	22 (8)	0.083
Time To Peak (%GC)*	46 (35)	39 (27)	39 (30)	0.943
RoM*	7 (3)	9 (3)	12 (6)	<0.001(a)(b)(c)
Tnk Side Flex (Cor. Plane) (deg)				
Value at Initial Contact	-1 (4)	2 (6)	1 (6)	0.152
RMS*	4 (2)	6 (4)	6 (3)	0.001(a)(b)
Peak value (Ipsi)	2 (4)	5 (7)	8 (9)	0.001(b)
Time To Peak Ipsi (%GC)*	36 (35)	33 (35)	37 (31)	0.122
Peak value (Contra)*	-4 (5)	-4 (7)	-5 (7)	0.985
Time To Peak Contra (%GC)*	60 (17)	64 (20)	62 (23)	0.396
RoM*	7 (3)	9 (4)	13 (8)	<0.001(a)(b)
Tnk Rot (Trans. Plane) (deg)				
Value at Initial Contact	-3 (8)	-5 (12)	-5 (10)	0.702
RMS*	8 (4)	9 (6)	10 (6)	0.865
Peak value	6 (9)	7 (10)	12 (10)	0.456
Time To Peak (%GC)*	43 (20)	38 (18)	43 (19)	0.221
RoM*	12 (6)	16 (5)	22 (15)	0.001(a)(b)

Table 10.4: Mean (SD) lumbar segment kinematic values (degrees) (w.r.t Pelvis) for TD, GMFCS I and GMFCS II groups with concurrent p-values. Distribution of data was assessed using a Shipiro-Wilk normality test (*Median and Range for non-normally distributed data) (ES – Early Stance; LS – Late Stance).

Results of post-hoc tests are indicated as follows: statistically significant differences between (a) GMFCS I and TD (b) GMFCS II and TD and (c) GMFCS I and GMFCS II.

Parameters (deg)	**TD Mean (SD)**	**GMFCS I Mean (SD)**	**GMFCS II Mean (SD)**	**ANOVA *p*-Value**
Lumbar Flex / Ext (w.r.t Pel)				
Value at Initial Contact	-18 (8)	-14 (9)	-7 (9)	<0.001(b)(c)
RMS*	16 (29)	14 (31)	8 (18)	0.001(b)(c)
RoM	7 (2)	7 (4)	11 (5)	<0.001(b)(c)
Lumbar Side Flex (w.r.t Pel)				
Value at Initial Contact	-1 (5)	0 (5)	-1 (4)	0.611
RMS*	4 (9)	4 (9)	3 (8)	0.314
Peak Value Early Stance (ES)	3 (5)	3 (5)	2 (5)	0.613
Time To Peak ES (%GC)*	18 (20)	20 (28)	18 (28)	0.755
Peak Value Late Stance (LS)	3 (5)	3 (4)	1 (5)	0.321
Time To Peak LS (%GC)*	50 (26)	42 (30)	32 (30)	0.076
Peak Contralateral Value	-2 (5)	-2 (5)	-3 (4)	0.656
Time to Peak Contra (%GC)	65 (38)	54 (33)	55 (29)	0.123
RoM	6 (2)	5 (2)	5 (2)	0.123
Lumbar Rotation (w.r.t Pel)				
Value at Initial Contact	-2 (3)	-1 (4)	-2 (3)	0.355
RMS*	3 (5)	3 (8.)	3 (6)	0.923
RoM*	7 (9)	6 (11)	7 (9)	0.352

In the coronal plane, no statistically significant differences were present for lumbar side flexion between groups (Table 10.4, Fig.10.3). GMFCS I and TD children demonstrated two distinct ipsilateral peaks during early and late stance followed by a consistent neutral position during swing (Fig.10.3). The second peak at late stance was slightly reduced for GMFCS II children.

In the transverse plane, no statistically significant differences were present for lumbar rotation between groups (Table 10.4, Fig.10.3). The lumbar segment moved from a backwards

position during early stance into a forward position during mid-stance to early swing followed by a return to a backwards position during mid to late swing.

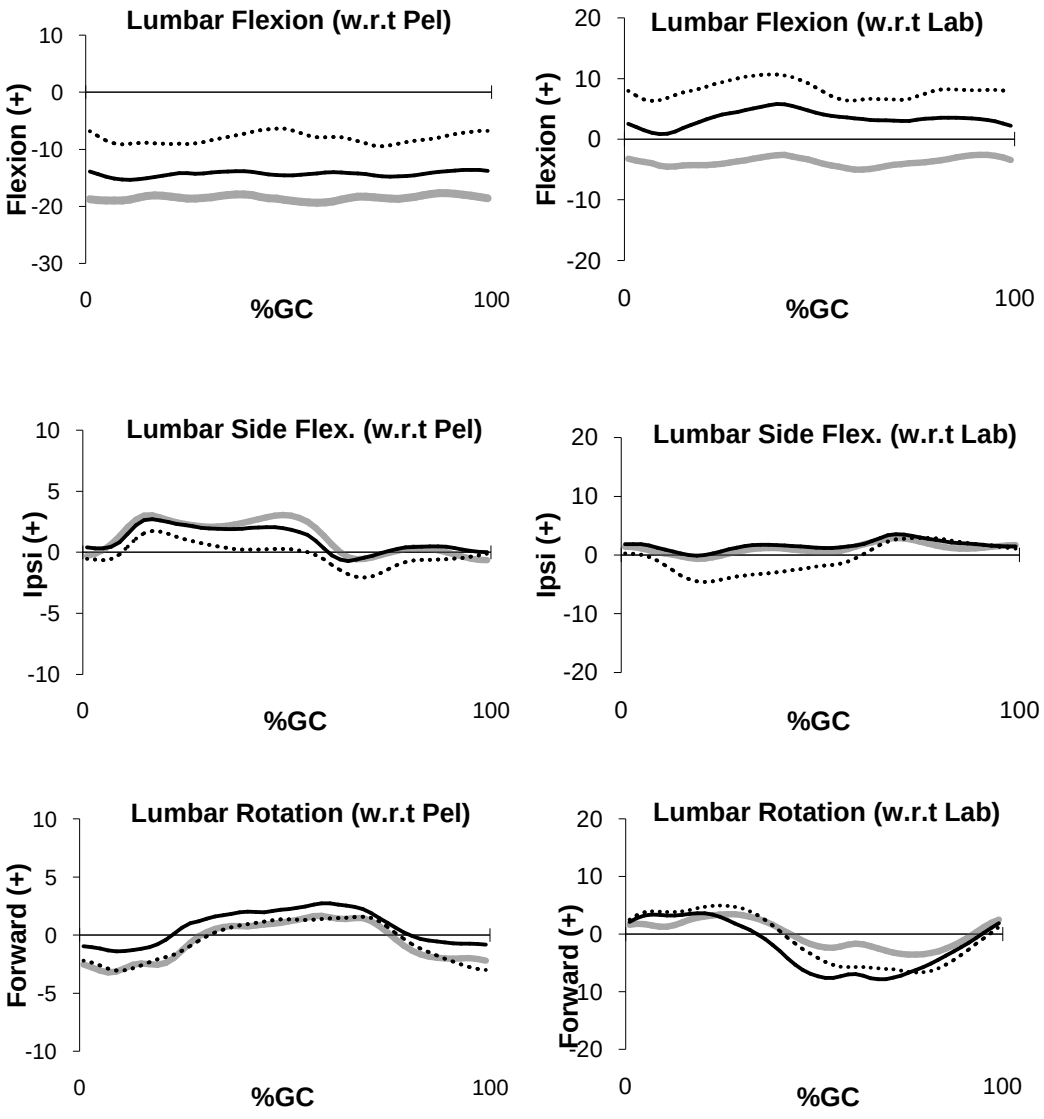

Figure 10.3: Ensemble average profiles for the lumbar segment in all 3 planes. Left column are movements with respect to the pelvic reference frame while the right column are movements with respect to the global reference frame (Gray – Typically Developed, Black – GMFCS I, Dotted – GMFCS II).

10.3.6 Lumbar Kinematics (w.r.t Lab)

In the sagittal plane, ensemble average profiles for both GMFCS I and II groups demonstrated a flexed lumbar segment position compared to an extended position for TD (increased flexion of 2^{o} and 5^{o} respectively) (Fig.10.3, Table 10.5). However, only GMFCS II position was statistically significant compared to TD (Table 10.5). RoM was increased for GMFCS II children compared to both GMFCS I children and TD (increased RoM of 3^{o} and 5^{o} respectively) (Table 10.5). This more pronounced movement was evident for GMFCS II children in ensemble average profiles (Fig.10.3).

In the coronal plane, peak lumbar side flexion directed towards the contralateral side demonstrated a statistically significant increase for GMFCS II children compared to GMFCS I children and TD (increased peaks of 4^{o} respectively). RoM was also increased for GMFCS II children for lumbar side flexion compared to GMFCS I children and TD (increased RoM of 3^{o} and 5^{o} respectively) (Table 10.5).

In the transverse plane, statistically significant differences were present for RMS and RoM for both GMFCS I and II groups compared to TD (increased by 3^{o} and 4^{o} for RMS and 6^{o} and 7^{o} for RoM) (Table 10.5). When ensemble average profiles were considered, the lumbar region demonstrated a forward position during early stance followed by a move backwards during late stance into early swing with a reversal in direction towards a forward position during late swing (Fig.10.3).

Table 10.5: Mean (SD) lumbar segment kinematic values (degrees) (w.r.t Lab) for TD, GMFCS I and GMFCS II groups with concurrent p-values. Distribution of data was assessed using a Shipiro-Wilk normality test (*Median and Range for non-normally distributed data). (Ipsi – towards ipsilateral side; Contra – towards contralateral side)

Results of post-hoc tests are indicated as follows: statistically significant differences between (a) GMFCS I and TD (b) GMFCS II and TD and (c) GMFCS I and GMFCS II.

Parameters	**TD Mean (SD)**	**GMFCS I Mean (SD)**	**GMFCS II Mean (SD)**	**ANOVA *p*-Value**
Lumbar Flex / Ext (w.r.t Lab)				
Value at Initial Contact	-4 (8)	3 (9)	8 (11)	<0.001(a)(b)
RMS*	5 (20)	8 (14)	10 (27)	0.020(b)
RoM	7 (3)	9 (3)	12 (6)	0.001(b)(c)
Lumbar Side Flex (w.r.t Lab)				
Value at Initial Contact	1 (5)	2 (5)	0 (6)	0.553
RMS*	4 (12)	4 (9)	6 (11)	0.164
Peak Value (Ipsi)	3 (5)	5 (5)	4 (6)	0.436
Time To Peak Ipsi (%GC)*	69 (98)	68 (92)	72 (96)	0.268
Peak Value (Contra)	-2 (6)	-2 (5)	-6 (6)	0.013(b)(c)
Time To Peak Contra (%GC)*	24 (84)	23 (94)	22 (94)	0.448
RoM*	5 (10)	7 (11)	9 (20)	0.001(b)(c)
Lumbar Rotation (w.r.t Lab)				
Value at Initial Contact	1 (5)	2 (7)	3 (10)	0.841
RMS*	5 (7)	8 (10)	8 (25)	<0.001(a)(b)
RoM*	9 (13)	15 (31)	16 (30)	<0.001(a)(b)

10.3.7 L5/S1 Reactive Forces

Anterior / posterior forces demonstrated a number of significant differences between groups. Posterior force at initial contact was reduced for GMFCS II compared to GMFCS I (difference ≈ 0.4 N/kg or ≈69%) (Table 10.6). Significant differences were present in magnitude (+0.397 N/kg or ≈36%) and timing (+3.3%) of peak anterior force in stance for GMFCS II compared to TD (Fig.10.4, Table 10.6). Both GMFCS I and II showed significantly reduced peak posterior force values compared to TD (≈ 0.5 N/kg or ≈65%). However, no significant differences were present in the timings of these peaks between groups (p = 0.473). During

double support, a second anterior peak force occurred at ipsilateral toe off (Fig.10.4). No significant differences were present between GMFCS I, GMFCS II and TD groups in magnitude (p = 0.092) or timing (p = 0.383) of this peak. Additionally, Range was significantly higher for children with GMFCS II compared to TD. RMS did not differ between groups (Table 10.6).

Medial / lateral forces were, for the most part, directed towards the supporting limb with peaks occurring at contralateral and ipsilateral toe off (Fig.10.4). GMFCS II showed significantly increased ipsilateral peak (difference of 0.27N/kg or ≈55%) compared to TD with no differences in timing (p = 0.137). Both GMFCS I and II showed significantly increased contralateral peaks (difference of 0.4 N/kg or ≈63%) compared to TD with no difference in timing (Table 10.6). GMFCS I and II children both demonstrated significantly increased RMS and Range compared to TD.

Vertical force remained compressive for the duration of the gait cycle as expected (Fig.10.4). Significant differences were present for Range for GMFCS II compared to both GMFCS I and TD. Peak value was also marginally raised for GMFCS II compared to GMFCS I (≈ 0.1N/kg) (Table 10.6).

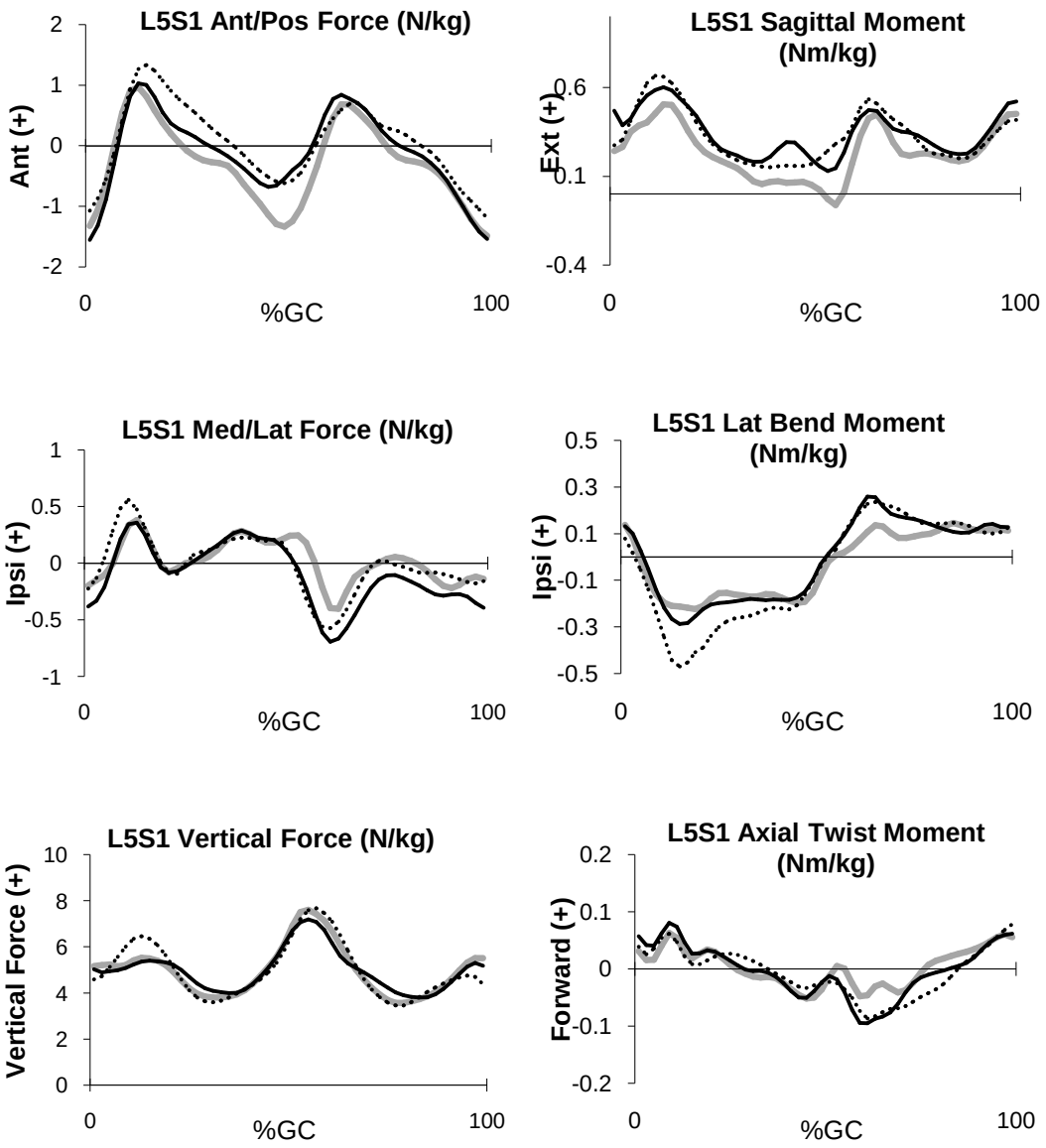

Figure 10.4: Ensemble average profiles for L5/S1 reactive forces in all 3 directions (left column) and L5/S1 moments in all 3 planes (right column). (Gray – Typically Developed, Black – GMFCS I, Dotted – GMFCS II). Note: Mean and SD profiles for all GMFCS I and II groups are presented in Appendix 10.7.

Table 10.6: Mean (SD) L5/S1 reactive force values for TD, GMFCS I and GMFCS II groups with concurrent p-values. Distribution of data was assessed using a Shipiro-Wilk normality test (*Median and Range for non-normally distributed data).

Results of post-hoc tests are indicated as follows: statistically significant differences between (a) GMFCS I and TD (b) GMFCS II and TD; (c) GMFCS I and GMFCS II.

Parameters	TD Mean (SD)	GMFCS I Mean (SD)	GMFCS II Mean (SD)	ANOVA *p*-Value
L5/S1 Ant/Pos Force (N/kg)				
Value at Initial Contact (IC)	-1.31 (0.46)	-1.55 (0.63)	-1.07 (0.66)	0.017 (c)
RMS	0.83 (0.14)	0.84 (0.19)	0.91 (0.199)	0.246
Peak Anterior value (stance)	1.11 (0.51)	1.16 (0.57)	1.49 (0.61)	0.038(b)
Time To Peak (stance) (%GC)*	12.0 (8.0)	14.0 (14.0)	15.00 (14.0)	<0.001(b)
Peak Posterior value	-1.45 (0.39)	-0.95 (0.56)	-1.04 (0.68)	0.004(a)(b)
Time To Peak Posterior (%GC)	52.2 (2.94)	50.5 (4.97)	51.8 (6.91)	0.473
Peak anterior value (swing)	0.85 (0.47)	1.12 (0.60)	1.20 (0.72)	0.092
Time To Peak (swing) (%GC)*	68.0 (10.0)	66.0 (18.0)	69.0 (34.0)	0.383
Range	2.83 (0.49)	3.16 (0.67)	3.26 (0.74)	0.047(b)
L5/S1 Med/Lat Force (N/kg)				
Value at Initial Contact (IC)	-0.199 (0.35)	-0.38 (0.40)	-0.23 (0.41)	0.185
RMS*	0.33 (0.496)	0.48 (0.55)	0.52 (0.71)	0.002(a)(b)
Peak Ipsilateral value	0.50 (0.34)	0.53 (0.34)	0.77 (0.45)	0.023(b)
Time To Peak Ipsilateral (%GC)*	14.0 (30.0)	14.0 (32.0)	12.0 (38.0)	0.137
Peak Contralateral value	-0.63 (0.35)	-0.99 (0.41)	-1.03 (0.47)	0.001(a)(b)
Time To Peak Contralat (%GC)*	62.0 (98.0)	62.0 (98.0)	62.0 (98.0)	0.989
Range	1.23 (0.33)	1.599 (0.39)	1.89 (0.595)	<0.001(a)(b)
L5/S1 Vertical Force (N/kg)				
Value at Initial Contact (IC)	5.16 (1.24)	5.02 (0.90)	4.59 (1.28)	0.184
RMS*	5.01 (3.82)	5.03 (1.42)	5.16 (3.08)	0.667
Peak value	8.05 (1.29)	7.80 (0.899)	8.76 (1.77)	0.036(c)
Time To Peak (%GC)*	56.0 (98.0)	56.0 (36.0)	56.0 (58.0)	0.407
Range*	4.83 (4.48)	4.35 (5.20)	5.51 (11.4)	0.009(b)(c)

10.3.8 L5/S1 Moments

Similar patterns were present for L5/S1 sagittal moments for all groups (Fig.10.4). Children with CP GMFCS I and II demonstrated significantly increased RMS compared to TD (≈ 0.09Nm/kg or ≈27%) (Table 10.7). Peak values in both stance and swing were significantly increased for GMFCS I and II children compared to TD. However, the timings of these peaks were similar. No significant differences were present between groups for any of the remaining parameters (Table 10.7).

L5/S1 lateral bend moments demonstrated the greatest number of significant differences for discrete parameters between groups (Table 10.7). GMFCS II children showed a significantly increased contralateral peak compared to GMFCS I (difference of 0.06Nm/kg or ≈20%) and TD (difference of 0.26 Nm/kg or ≈90%) (Fig.10.4). Peak contralateral timings were not different between groups (p = 0.226). Both GMFCS I and II children showed significantly increased ipsilateral peak values compared to TD (≈ 0.1Nm/kg (46%) and ≈ 0.15Nm/kg (67%) increases respectively) (Fig.10.4). However, no statistically significant difference was present between GMFCS level for ipsilateral peak. RMS and Range were statistically significantly increased for both GMFCS I and II compared to TD. Comparison of GMFCS level demonstrated significantly higher RMS and Range in GMFCS II compared to GMFCS I (Table 10.7).

L5/S1 axial twist moments also demonstrated a number of significant differences between groups (Fig.10.4, Table 10.7). Range parameters for both GMFCS levels were statistically significantly increased compared to TD (difference ≈ 0.09 Nm/kg or ≈50%). Both GMFCS I and II demonstrated increased RMS compared to TD (difference ≈ 0.02 Nm/kg or ≈44%). However, comparisons between GMFCS level for RMS showed no statistically significant difference. Peak backwards value was also increased for both GMFCS I and II compared to TD (difference ≈ 0.05 Nm/kg or ≈55%).

Table 10.7: Mean (SD) L5/S1 moment values for TD, GMFCS I and GMFCS II groups with concurrent p-values. Distribution of data was assessed using a Shipiro-Wilk normality test (*Median and Range for non-normally distributed data).

Results of post-hoc tests are indicated as follows: statistically significant differences between (a) GMFCS I and TD (b) GMFCS II and TD; (c) GMFCS I and GMFCS II.

Parameters	**TD Mean (SD)**	**GMFCS I Mean (SD)**	**GMFCS II Mean (SD)**	**ANOVA *p*-Value**
L5/S1 Sagittal Mom (Nm/kg)				
Value at Initial Contact (IC)	0.24 (0.49)	0.47 (0.48)	0.27 (0.38)	0.146
RMS	0.33 (0.13)	0.42 (0.10)	0.42 (0.12)	0.007(a)(b)
Peak value (stance)*	0.57 (1.02)	0.81 (1.63)	0.71 (1.3)	0.029(a)(b)
Time To Peak (stance) (%GC)*	12.0 (16.0)	10.0 (20.0)	10.0 (18.0)	0.840
Peak value (swing)*	0.38 (1.33)	0.54 (0.71)	0.61 (0.82)	0.006(a)(b)
Time To Peak (swing) (%GC)*	68.0 (16.0)	66.0 (26.0)	66.0 (26.0)	0.156
Range*	0.87 (0.97)	0.91 (1.80)	0.93 (2.31)	0.519
L5/S1 Lat. Bend Mom (Nm/kg)				
Value at Initial Contact (IC)	0.14 (0.12)	0.13 (0.09)	0.08 (0.166)	0.211
RMS*	0.17 (0.16)	0.20 (0.32)	0.27 (0.295)	<0.001(a)(b)(c)
Peak Ipsilateral value*	0.23 (0.47)	0.33 (0.68)	0.38 (0.699)	0.001(a)(b)
Time To Peak Ipsilat (%GC)*	66.0 (36.0)	64.0 (38.0)	66.0 (38.0)	0.674
Peak Contralateral value	-0.29 (0.09)	-0.35 (0.10)	-0.55 (0.21)	<0.001(b)(c)
Time to Peak Contralat (%GC)	26.7 (14.1)	25.0 (18.6)	22.31 (12.7)	0.226
Range*	0.56 (0.57)	0.68 (0.57)	0.87 (0.95)	<0.001(a)(b)(c)
L5/S1 Axial Tw. Mom (Nm/kg)				
Value at Initial Contact (IC)	0.03 (0.05)	0.06 (0.063)	0.04 (0.07)	0.277
RMS*	0.045 (0.08)	0.06 (0.09)	0.07 (0.09)	<0.001(a)(b)
Peak Forward Value*	0.089 (0.23)	0.11 (0.21)	0.13 (0.22)	<0.001(a)(b)
Time To Peak Forward (%GC)*	16.0 (98.0)	14.0 (98.0)	40.0 (98.0)	0.558
Peak Backward Value	-0.09 (0.03)	-0.14 (0.04)	-0.13 (0.04)	<0.001(a)(b)
Time to Peak Backward (%GC)	55.2 (13.8)	58.0 (11.3)	54.2 (18.0)	0.682
Range*	0.16 (0.33)	0.25 (0.32)	0.26 (0.31)	<0.001(a)(b)(c)

10.3.9 Correlations between Kinematic Measures and L5/S1 Reactive Forces and Moments

A number of statistically significant correlations were present between thorax kinematics and L5/S1 reactive forces and moments (Table 10.8). Of note, for RMS parameters, thorax side flexion demonstrated a moderate to strong correlation with L5/S1 lateral bend moment ($r = 0.519$, $p < 0.01$) and medial/lateral force ($r = 0.352$, $p < 0.01$) (Table 10.8). Similarly, for RoM parameters, moderate to strong correlations were present between thorax side flexion and L5/S1 lateral bend moment ($r = 0.388$, $p < 0.01$) and thorax side flexion and L5/S1 medial/lateral force ($r = 0.517$, $p < 0.01$) (Table 10.8). Thorax rotation and L5/S1 axial twist moment demonstrated a moderate correlation for RoM ($r = 0.326$, $p < 0.01$), while no significant correlations were present for peak parameters (Table 10.8).

Lumbar segment kinematic data and L5/S1 reactive force and moment data demonstrated a number of significant correlations (Table 10.8). Of note, in the sagittal plane, moderate to strong correlations were present for RMS parameters for lumbar flexion/extension and L5/S1 sagittal moments ($r = 0.427$, $p <0.01$ and $r = 0.448$, $p < 0.01$ with respect to lab and pelvis respectively). In the coronal plane, no significant correlations existed for RMS parameters for lumbar side flexion (Table 10.8). A low to moderate correlation was present for lumbar side flexion with L5/S1 lateral bend moment and L5/S1 medial/lateral force for RoM parameters ($r = 0.348$, $p <0.01$ and $r = 0.241$, $p < 0.05$ for moment and force respectively). In the transverse plane, the only significant correlation was for lumbar rotation (w.r.t lab) and L5/S1 axial twist moment for RoM parameters ($r = 0.441$, $p < 0.01$) (Table 10.8). No other significant correlations were present for lumbar rotation (w.r.t lab or pelvis) for either RMS or RoM parameters.

Table 10.8: Correlation (r) between kinematic measurements and L5/S1 reactive force and moments for RMS and RoM parameters.

Correlation (*r*):	L5/S1 Sag Mom	L5/S1 Ant/ Pos Force		L5/S1 Lat Bend Mom	L5/S1 Med/ Lat Force		L5/S1 Axial Twist Mom	L5/S1 Vertical Force
RMS								
Tnk Flex / Ext (w.r.t Pel)	0.021	0.104	Tnk Side Flex (w.r.t Pel)	0.519**	0.352**	Tnk Rotation (w.r.t Pel)	0.326**	-0.138
Lumbar Flex / Ext (w.r.t Pel)	0.448**	0.159	Lumbar Side Flex (w.r.t Pel)	-0.006	-0.221	Lumbar Rotation (w.r.t Pel)	-0.031	0.112
Lumbar Flex / Ext (w.r.t Lab)	0.427**	0.100	Lumbar Side Flex (w.r.t Lab)	-0.014	-0.181	Lumbar Rotation (w.r.t Lab)	-0.110	-0.083
RoM								
Tnk Flex / Ext (w.r.t Pel)	0.018	0.378**	Tnk Side Flex (w.r.t Pel)	0.388**	0.517**	Tnk Rotation (w.r.t Pel)	0.575**	0.253*
Lumbar Flex / Ext (w.r.t Pel)	0.039	0.250*	Lumbar Side Flex (w.r.t Pel)	-0.026	-0.072	Lumbar Rotation (w.r.t Pel)	0.091	0.147
Lumbar Flex / Ext (w.r.t Lab)	0.052	0.309**	Lumbar Side Flex (w.r.t Lab)	0.348**	0.241*	Lumbar Rotation (w.r.t Lab)	0.441**	0.170

* Significant correlation at $p < 0.05$

** Significant correlation at $p < 0.01$

10.4 Discussion

10.4.1 Coronal Plane Kinematics

Thorax movement in the coronal plane demonstrated increased medial/lateral bending for children with CP compared to TD children that was shown to increase with level of functional impairment (Fig. 10.5). This was not surprising and was consistent with the literature (Attias et al., 2015, Heyrman et al., 2013a, Romkes et al., 2007).

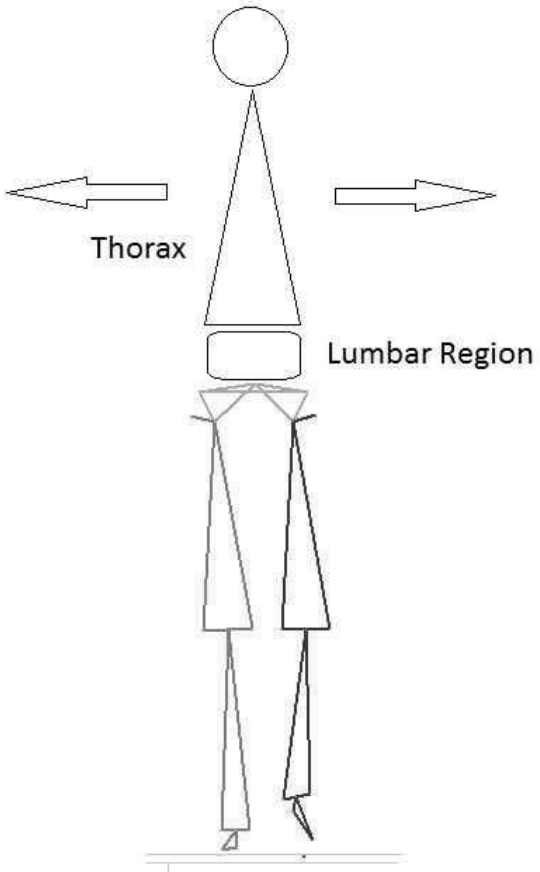

Figure 10.5: Children with CP demonstrated increased medio/lateral lean of the thorax as level of functional impairment increased. The lumbar region in the coronal plane demonstrated only small deviations for children with CP compared to TD.

Children with CP often present with weak hip abductors that result in a contralateral pelvic drop where a compensatory movement of the trunk is required to help stabilize the pelvis (Krautwurst et al., 2013). The impact of this increased lateral lean was directly evident in the kinetic data, particularly for GMFCS II children. As the thorax moved towards excessive ipsilateral bending for the GMFCS II group, a significantly increased ipsilateral peak force and

contralateral peak moment were measured. Interestingly, the timings of each of these peaks were not different between groups suggesting thorax coordination may be unaffected for children with CP (Romkes et al., 2007). During swing, the thorax side flexed towards the contralateral side with similar peak flexion between groups, a finding previously reported for thorax side flexion relative to the pelvis (Heyrman et al., 2013a). Increased RMS and RoM for GMFCS I and II for both L5/S1 reactive forces and moments (and between GMFCS level for L5/S1 moments) highlighted the additional demand on trunk musculature for CP subjects as they moved the thorax into a suitably compensatory position during the gait cycle, with demand increasing according to level of functional impairment. The strong positive correlation of thorax movement with L5/S1 medio/lateral force and lateral bend moment help support this theory. It is worth noting that due to the nature of the thorax as one segment, one would expect symmetry in movement during stance and swing (as the thorax side flexes from one side to the other). For GMFCS II children, this symmetry is not present unlike for GMFCS I and TD. This is most likely due to the grouping of subjects where hemiplegic and diplegic children were part of each group. It is possible that some more severe hemiplegia subjects dampened the effect of movement during swing due to less (or normal) involvement of the non-pathological side. In the graphs presented in Appendix 10.2, the data are presented according to hemiplegia and diplegia diagnosis. A more symmetrical movement is demonstrated when are regrouped according to principle diagnosis.

For lumbar segment movement, the most obvious deviation in the coronal plane was for GMFCS II children with respect to the lab, as evidenced in the ensemble average profiles. As the contralateral leg lifted off during early stance, GMFCS II children tended to tilt the lumbar region towards that side, in contrast to TD children where a neutral position was maintained. However, lumbar side flexion with respect to the pelvis demonstrated similar patterns of motion for all groups. This suggested that GMFCS II children experienced a small drop of the pelvis at contralateral toe off and, as an associated movement, the lumbar region

tilted towards that side. It has been well reported that children with CP undergo a compensatory movement of increased lateral lean of the trunk towards the ipsilateral leg to counteract weak hip abductors and aid stabilization of the pelvis (Krautwurst et al., 2013). Our findings suggest that this ipsilateral trunk lean occurs primarily above the level of the lumbar region. The low to moderate correlation of lumbar side flexion, in the global frame, and L5/S1 lateral bend moment fit with the findings of raised contralateral peak and RoM for GMFCS II children. The mechanical effect of this excessive movement, albeit during early stance, partially contributed to an increased L5/S1 loading. However, when taken into account with the previously reported strong correlation of L5S1 loading with thorax movement, it appears that movement of the lumbar segment was not a dominant factor in lateral L5/S1 loading in this plane. Similar to the thorax, the lumbar segment is one segment and so symmetry of movement would be expected during stance and swing. However, in Figure 10.3, lumbar side flexion is absent in swing for the TD group suggesting an unexpected asymmetry. It is possible that the skin surface protocol, while demonstrating the ability to differentiate between pathological and normal movement, may be susceptible to SMA to the point where it is a limitation of the protocol. This may especially be the case where small movements are recorded. With this in mind, it needs to be stated that this should be considered a limitation of the protocol.

10.4.2 Sagittal Plane Kinematics

In the sagittal plane, larger motions of the thorax were evident for children with CP in general. The effect of level of functional impairment was immediately obvious with a substantially greater level of RoM for GMFCS II compared to GMFCS I children (Fig. 10.6). This was suggested to be as a result of reduced anterior / posterior stability as functional impairment increases (Heyrman et al., 2013a).

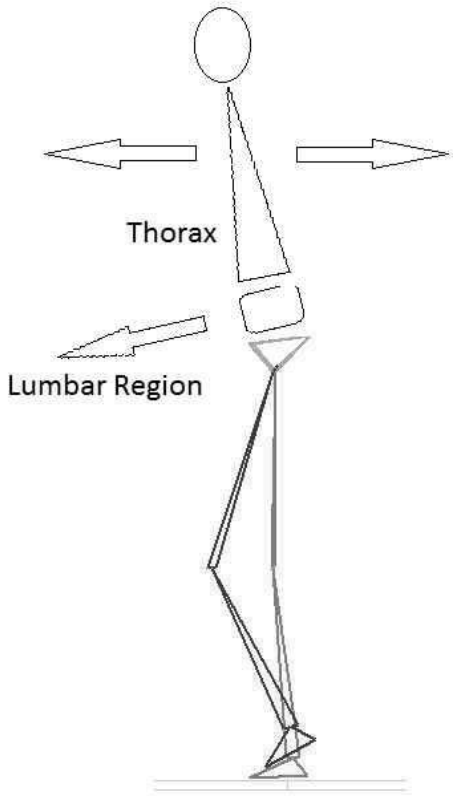

Figure 10.6: Larger motions of the thorax were evident in the sagittal plane for children with CP (shown to increase with functional level of impairment). In addition, children with CP demonstrated a more flexed lumbar segment position.

The associated impact on L5/S1 force was an increased anterior force during stance for GMFCS II children followed by a significantly reduced posterior force for both GMFCS I and II at contralateral heel strike. Additionally, L5/S1 moments were raised for both GMFCS I and II compared to TD. However, the effect of functional level on L5/S1 kinetics was not significant in the sagittal plane. It seems that for both GMFCS groups to maintain a suitable thorax-pelvic alignment, increased demands are placed on the corresponding musculature as evidenced by an increased L5/S1 extensor moment throughout the gait cycle.

TD children maintained an extended lumbar segment position in the sagittal plane throughout the gait cycle, a finding consistent with the literature for normal gait (Fernandes et al., 2016). In contrast, children with CP demonstrated a more flexed lumbar segment position (Fig. 10.6). Functional level of impairment was also an important factor with flexion becoming more excessive as GMFCS level increased. Increased lumbar lordosis and, in particular,

increased pelvic tilt are most likely the main contributors to this excessive forward flexion. Both of these conditions have previously been reported to be characteristic of CP gait (Heyrman et al., 2013a, Salazar-Torres et al., 2011). Lumbar lordosis, defined as an anterior convexity of the lumbar spine (Bogduk and Twomey, 1991), undergoes changes generally associated with changes in pelvic tilt (Levine and Whittle, 1996). In essence, lordosis becomes more pronounced as the pelvis tilts forwards (Kapandji, 1974, Levine and Whittle, 1996). As evidenced by the results of this study, the net effect of this can be an increased forward flexion of the lumbar region. Interestingly, it has been suggested that increased pelvic tilt forces the thorax into a more extended position during CP gait (Heyrman et al., 2013a). This was reported as a compensatory mechanism in order to dynamically counterbalance pelvic movement (Heyrman et al., 2013a). The results of this study suggested that increased flexion of the lumbar segment must also be given due consideration when considering thorax position. Increased lumbar flexion, particularly with respect to the pelvis, demonstrated that it is not just the lumbar segment moving forward on a tilting pelvis and that, in fact, there was an additional forward flexion of the lumbar region itself. Failure of the abdominal muscles to control the lumbar region may be a factor. Additionally, increased lumbar flexion may also allow children with CP to better accommodate changes in thorax-pelvic alignment. Interestingly, a moderate correlation was present between lumbar segment flexion and L5/S1 sagittal plane moments (Table 10.7). The thorax, however, demonstrated no such correlation. This suggests that, contrary to the coronal plane, in the sagittal plane the lumbar segment may play more of a role in the contribution of L5/S1 loading than the position of the thorax.

10.4.3 Transverse Plane Kinematics

In the transverse plane, RoM was increased for GMFCS II compared to TD for thorax rotation while GMFCS I and TD were similar. This was in agreement with the literature (Heyrman et al., 2013a). This increased thorax RoM for GMFCS II was reflected in both vertical force and axial twist moment. Interestingly, while no differences were present in thorax

rotation for GMFCS I compared to TD, peak values, RMS and RoM and were all increased. Excessive pelvic retraction/protraction, shown to be present for children with CP in this study (ensemble average profiles available in Appendix 10.6) and documented to be characteristic of CP gait (O'Sullivan et al., 2007, Salazar-Torres et al., 2011), may mask any obvious contribution of the thorax to increases in these variables for this group. Dynamic tightness of the gastro-soleus and internal rotation of the hip may play a role in this case (O'Sullivan et al., 2007). However, when correlations between thorax rotation and axial twist moment were considered, a moderate to strong relationship was demonstrated for RMS and RoM respectively. This suggested that increased thorax rotation does, to some extent, affect low back axial twist moments during CP gait. One point to note with respect to the L5/S1 vertical force is that a level of symmetry would be expected in the TD data where peak value at early stance would be expected to be similar to peak value during early swing. In relation to the data presented in Figure 10.4, the initial peak is reduced compared to the later peak. The reason for this is unclear. It is suspected that due to the integration of two different types of force platform (designed and constructed using different sensor technology as discussed in Section 5.10), there may be a difference in how GRF was measured between plates. Due to the layout of the plates during data acquisition, the first and second plate would always be a combination of Kistler and AMTI. This may have resulted in some small error primarily in vertical force measurement.

Transverse motion of the lumbar region with respect to the pelvis was similar for all groups. However, this was not the case for lumbar segment rotation with respect to the lab. During late stance and into early swing, both GMFCS I and GMFCS II children demonstrated increased backwards rotation compared to TD. Pelvic retraction, a common pathological feature of CP gait (O'Sullivan et al., 2007), most likely masked this backwards lumbar rotation when movement was considered with respect to the pelvis. Dynamic tightness of the gastro-soleus and dynamic flexion and internal rotation of the hip have been suggested as the most

significant features associated with pelvic retraction in hemiplegic and diplegic CP (O'Sullivan et al., 2007). It appears that backwards rotation of the lumbar region, occurring in unison with retraction of the pelvis, may be linked to some of these previously reported findings relating to pelvic retraction. Lumbar segment rotation, in the global frame, and axial twist moment demonstrated the only statistically significant correlation. The increased backward rotation from late stance into early swing for both groups appeared to be a contributor as it occurred at a similar time point in the gait cycle as previously reported increased backward axial twist moment.

10.5 Conclusions

Children with CP demonstrated increased reactive forces and moments during gait at the lower lumbar spine compared to TD children. These increased reactive forces and moments were strongly linked to excessive thorax motion, particularly in the coronal plane. In the sagittal plane, L5/S1 loading was linked more so with movement of the lumbar region. Furthermore, children with GMFCS II showed significantly more involvement, particularly for thorax kinematics and L5/S1 moments. Similar findings were present when children with CP were divided according to diagnosis, primarily due to many of the children with CP GMFCS I presenting as hemiplegia and many of the children with CP GMFCS II presenting as diplegia. It is important that intervention for these children is aimed at reducing trunk motion, specifically in the coronal plane, in order to reduce abnormal loading which could, in turn, impact the health of the spine in this population. In addition, our results highlight the importance of considering lumbar segment movement in tandem with thorax movement when assessing overall trunk motion during CP gait. The ability to understand lumbar segment movement during walking in CP, considered in unison with movement of the thorax, may provide an additional basis for examination and treatment in this population.

Chapter 11: An investigation into the influence of Trendelenburg and Duchenne movement patterns on lower lumbar spinal loading during paediatric cerebral palsy gait

This chapter has been accepted for publication as follows:

Kiernan, D.,O'Sullivan, R., Malone,A., O'Brien,T., and Simms, C.K.2017.*Pathological movements of the Pelvis and Trunk during gait in children with Cerebral Palsy: A cross-sectional study with 3-dimensional kinematics and lower lumbar spinal loading. Physical Therapy.* Accepted for publication.

Chapter Highlights

- Trendelenburg and Duchenne type movements often present during CP gait and affect movement of the thorax and pelvis, thus increasing the potential for altered loading at the lower lumbar spine.
- Thoracic movement and lower lumbar spinal loading were assessed in CP children who demonstrated Trendelenburg or Duchenne type movements during gait.
- Three distinct patterns were observed – Trendelenburg, Duchenne and a mix of Trendelenburg / Duchenne.
- Lateral bending moments were increased for the Duchenne group while mixed Trendelenburg / Duchenne demonstrated the greatest deviations compared to TD.
- Altered loading was present at the lower lumbar spine where a Duchenne type movement was demonstrated.

11.1 Introduction

Excessive movement of the trunk and pelvis have been shown to be characteristic of walking in children with CP (Attias et al., 2015, Heyrman et al., 2013a, Romkes et al., 2007, O'Sullivan et al., 2007, Salazar-Torres et al., 2011). In particular, Trendelenburg and Duchenne type gait patterns are often seen in this population (Metaxiotis et al., 2000). A Trendelenburg gait is characterised by a drop of the pelvis in the coronal plane on the unloaded side during stance (Metaxiotis et al., 2000, Westhoff et al., 2006). The trunk is tilted towards the supporting limb with respect to the pelvis while maintaining a neutral position with respect to the global reference frame (Westhoff et al., 2006). Hip adduction of the supporting limb is also increased (Westhoff et al., 2006). A Duchenne type gait pattern is characterised by a trunk

lean towards the supporting limb with the pelvis level or elevated on the unloaded side (Metaxiotis et al., 2000, Westhoff et al., 2006). This type of compensatory movement of the trunk moves body weight towards the centre of the hip resulting in a reduced hip abductor moment (Metaxiotis et al., 2000, Stief et al., 2014). Both movement patterns are often a compensatory mechanism for hip abductor weakness or hip dysfunction on the supporting limb (Metaxiotis et al., 2000, Krautwurst et al., 2013, Stief et al., 2014). However, as previously mentioned in Section 2.6, the question presents as to how to both patterns, which are quite distinct from each other, can arise from the same pathology? In the work by Metaxiotis and colleagues (Metaxiotis et al., 2000), reference was made to how a contralateral pelvic drop and an ipsilateral trunk lean were evident in 17 out of 19 of their subjects. However, by strict definition this finding does not fit either description of Trendelenburg or Duchenne. The authors in that case suggested that the contralateral drop may be caused by abductor insufficiency, adductor contracture or abductor contracture on the opposite side. However, the authors also suggested this to be the cause of the excessive trunk lean and no reasoning was given as to how the same pathology can result in what are essentially two different types of movement (Metaxiotis et al., 2000). In a later paper by Westhoff and colleagues (Westhoff et al., 2006), the authors do discriminate between Trendelenburg and Duchenne and make reference to how Trendelenburg type gait does not reduce loading at the hip while Duchenne does (due to the position of the trunk). However, the suggestion remains that both patterns are a consequence of hip abductor dysfunction. In the original paper by Trendelenburg, abnormal shortness of the abductor muscles, abnormal direction of the fibres, a reduced or missing femoral neck resulting in a shorter lever arm or general muscle weakness are all suggested as confounding factors in the Trendelenburg type movement (Trendelenburg, 1895). As previously mentioned in Section 2.6, it would seem a logical assumption that for a Trendelenburg movement, action of the hip abductors would be present but reduced or inefficient. In Duchenne, due to the excessive lean of the trunk well outside normal limits, one

would expect a complete absence of any hip abductor function causing the trunk to compensate in order to maintain the CoM within the base of support. However, while Trendelenburg and Duchenne movements during gait have been examined in the literature, little more than hip abductor weakness has been suggested as the cause. In relation to the impact of these types of movements on the lower limbs, a Duchenne type pattern is thought to have negative effects on the knee joint by increasing the lever arm around the knee leading to increased lateral tibio-femoral compartment loads (Stief et al., 2014). Additionally, it has been suggested that a Duchenne type gait may result in spinal problems (Metaxiotis et al., 2000). Likewise, a Trendelenburg type pattern is thought to be harmful to the hip (Metaxiotis et al., 2000). However, while the effects of Trendelenburg and Duchenne type walking patterns on kinetics at the knee and hip have been considered (Metaxiotis et al., 2000, Westhoff et al., 2006, Stief et al., 2014), the effects of this movement further up the kinematic chain, particularly at the lower lumbar spine, are unknown.

Increased reactive forces and moments at the lower lumbar spine have been demonstrated in children with CP during gait, as discussed in Chapter 10. As thorax coronal plane movement became more excessive, children with CP demonstrated increased peak L5/S1 reactive forces and moments of up to 63% and 90% respectively (Chapter 10). Consequently, as Trendelenburg and Duchenne type gait patterns are most significant in the coronal plane, the question presented as to whether loading at the lower lumbar spine would be adversely affected in children with CP when walking with these types of movement patterns. As the position of the trunk changes with respect to the pelvis during Trendelenburg and Duchenne type gait, mechanical loads at the spine must change. However, the extent to which this occurs is unclear. A thorough understanding of any potential negative effects at the spine is important as Duchenne type patterns have previously been reported as protective to the hip joint by covering the femoral head (Metaxiotis et al., 2000). In addition, this type of walking pattern has also been recommended as a non-invasive intervention for hip pain in

adults and as a conservative treatment in children with Legg-Calvé-Perthes disease (Schröter et al., 1999, Svehlik et al., 2012). However, while it is not clear whether these recommendations are followed routinely in clinical practice, the potential for increased demands at the spine may make such recommendations counterproductive. Therefore, it is important that clinicians are fully aware of any adverse effects that may occur further up the kinematic chain at the lower lumbar spine when presented with Trendelenburg or Duchenne type gait patterns. Following from this, the aim of this chapter was to assess trunk and pelvic kinematics and three-dimensional reactive forces and moments at the lower lumbar spine in children with CP who appeared on clinical presentation to have Trendelenburg or Duchenne type patterns of movement during gait.

11.2 Materials and Methods

11.2.1 Subjects

Ethical approval was obtained as described in Section 5.2. Informed written consent was obtained from all participants and from their parents when legally minor as described in Section 5.3.4.

The subjects of this study were the same cohort as described in Chapter 10. In short, 52 children with CP (Hemiplegia: n = 21, 11M, 10F, mean age 11.81 (3.12) yrs; Diplegia: n = 31, 22M, 9F, mean age 10.49 (2.86) yrs) and 26 TD children were recruited. Inclusion criteria for children with CP and TD are outlined in Section 5.3.3. Full participant data are provided in Chapter 10, Table 10.1 and in Appendix 10.1.

11.2.2 Data Collection

The data collection procedure was implemented as described in Chapter 10. In short, a full barefoot 3-dimensional analysis was performed using the CODA cx1 active marker system (Charnwood Dynamics Ltd., Leicestershire). The lower limb marker placement protocol and

underlying mathematical model followed implementation as previously described in Section 5.5. Trunk kinematic data were recorded using the single cluster described in Chapter 8. The L5/S1 joint was implemented as described in Section 3.7. In short, a skin surface marker was placed at the L5/S1 joint space. A virtual point was then created, corresponding to 5% of the length of the line from the L5/S1 marker to the mid-point of the ASISs, at which L5/S1 reactive forces and moments were calculated (Seay et al., 2008).

Subjects walked unassisted at a self-selected pace. Two Kistler 9281B and two AMTI Accugait force platforms as described in Section 5.8 were used to measure ground reaction force data. Data were collected using Codamotion ODIN software (v1.06 Build 01 09) at capture rates of 100Hz (kinematic) and 200Hz (kinetic) respectively. Kinematic and kinetic data were filtered with a 4^{th} order Butterworth filter with a cut-off frequency of 8Hz and 20Hz respectively. All kinematic and kinetic analysis and data filtering were performed in Visual 3D v4.96.0 software (C-Motion Inc., Germantown, MD, USA).

11.2.3 Coronal Plane Pattern Assessment

In order to determine pattern type, coronal plane kinematic data of all subjects were visually analyzed and compared to TD data. For the purposes of this study, normal data were defined as ± 1 standard deviation (± 1 SD) about average. Values outside this range were considered abnormal. Trendelenburg gait pattern (Type 1) was defined by a pelvic drop on the unloaded side during stance phase outside the ± 1SD band with a laterally flexed trunk position towards the supporting limb in relation to the pelvis and an upright trunk position in relation to the global reference frame (Westhoff et al., 2006, Svehlik et al., 2012) (Fig.11.1b). Duchenne gait pattern (Type 2) was defined by a stable or elevated pelvis on the unloaded side in conjunction with a trunk lean towards the supporting limb outside the ± 1SD band (Westhoff et al., 2006, Svehlik et al., 2012) (Fig.11.1c). Additionally, a third pattern of movement was observed. This pattern demonstrated a distinctive pelvic drop on the unloaded side during stance in conjunction with an excessive lean of the trunk outside TD limits towards

the supporting limb with respect to both the pelvis and global reference frames (Fig.11.1d). This pattern (Type 3) was best described as a combination of Trendelenburg and Duchenne and for the purposes of this study this pattern was termed “complex Trendelenburg–Duchenne”. Subjects were then divided according to pattern Types 1-3.

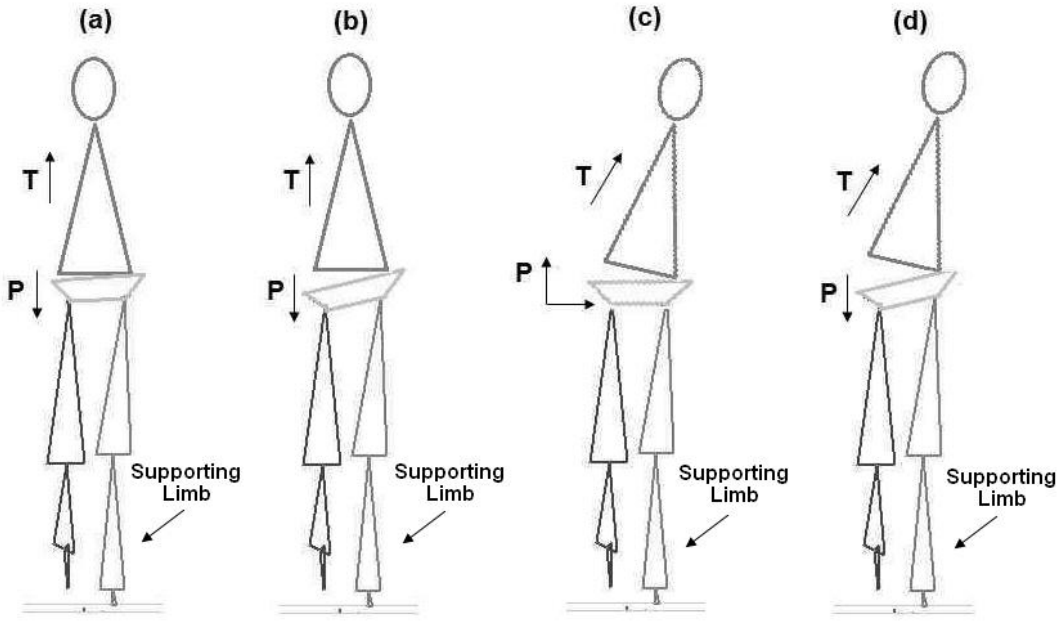

Figure 11.1: Movement patterns in the coronal plane. (A) Demonstrates a TD trunk and pelvic position. Note the straight position of the trunk in the global frame and the mild drop of the pelvis on the contralateral side. (B) Demonstrates a Trendelenburg type pattern. Note the straight position of the trunk in the global frame and the significant drop of the pelvis on the contralateral side. (C) Demonstrates a Duchenne type pattern. Note the lateral lean of the trunk in the global frame and the level (or slightly raised on the contralateral side) position of the pelvis. (D) Demonstrates a complex Trendelenburg – Duchenne pattern. Note the lateral lean of the trunk in the global frame combined with a drop of the pelvis on the contralateral side

11.2.4 Data Analysis

A number of discrete kinematic and kinetic parameters were assessed between groups (Table 11.1). Data were checked for distribution using the Shapiro-Wilk normality test. For data that followed a normal distribution, differences between movement types and TD children were assessed using a one-way analysis of variance (ANOVA) with Bonferroni post-hoc tests for comparisons between groups. Dunnett’s tests were also used to compare each

movement type with the TD control group. For data that did not follow a normal distribution, differences were assessed using a Kruskal-Wallis test and post hoc Mann-Whitney U-tests. All statistical analyses were performed using IBM SPSS Statistics (v23.0.0.2). The level of significance was set at 0.05. Additionally, ensemble average kinematic and kinetic profiles were visually analyzed for deviations between groups.

Table 11.1: Kinematic and Kinetic variables of interest (Ipsi – Ipsilateral; Contra – Contralateral)

Kinematic Parameters	**Kinetic Parameters**
Max Pelvic Obliquity Stance (^{o})	Hip Abductor Moment Peak 1 (Nm/kg)
Max Tnk Side Flex. Stance (w.r.t Lab) (^{o})	Hip Abductor Moment Peak 2 (Nm/kg))
Max Tnk Side Flex. Stance (w.r.t Pelvis) (^{o})	Peak L5S1 Med / Lat Force Towards Ipsi. Side (N/kg)
Max Hip Adduction in stance (^{o})	Peak L5S1 Med / Lat Force Towards Contra. Side (N/kg)
----------	Peak L5S1 Lat. Bend Moment Towards Ipsi. Side (Nm/kg)
----------	Peak L5S1 Lat. Bend Moment Towards Contra. Side (Nm/kg)

11.3. Results

11.3.1 Subject kinematic classification

Coronal plane kinematics demonstrated 3 distinctive patterns of movement in children with CP (Fig.11.1). According to the defined criteria (Section 11.2.3), 8 of 52 subjects (15.4%, 6 diplegia, 2 hemiplegia) demonstrated a Trendelenburg gait pattern (Type 1). Four subjects (7.7%, 3 diplegia, 1 hemiplegia) demonstrated a Duchenne gait pattern (Type 2). Twenty-two subjects (42.3%, 21 diplegia, 1 hemiplegia) demonstrated the complex Trendelenburg–Duchenne pattern (Type 3). Fourteen of the remaining subjects (26.9%, 14 hemiplegia) demonstrated patterns not consistent with Trendelenburg or Duchenne type gait

and were excluded from further evaluation. Four subjects (7.7%, 1 diplegia, 3 hemiplegia) demonstrated pelvic and trunk kinematic patterns within normal ranges. These 4 subjects were also excluded from further evaluation.

11.3.2 Trendelenburg gait pattern – Type 1

For children with CP with a Trendelenburg gait pattern, peak pelvic obliquity in stance was increased by 5^{o} compared to TD (Fig.11.2). Peak trunk side flexion (w.r.t pelvis) was increased by 8^{o}, while peak trunk side flexion (w.r.t Lab) remained within normal limits throughout the gait cycle. Peak hip adduction in stance was increased by 5^{o} compared to TD. Hip abductor moment remained close to TD with no statistically significant differences present (Table 11.2).

L5/S1 ensemble average kinetic profiles were similar for CP Type 1 children compared to TD (Fig.11.2). However, CP Type 1 children demonstrated an increased peak L5/S1 force directed towards the contralateral limb at initial swing phase (increase of 0.35N/kg or ≈66%). No other statistically significant differences were present for L5/S1 medial/lateral force. Lateral bend moment for CP Type 1 children compared to TD was not statistically significantly different (Table 11.2). However, during early swing, the ensemble average profiles demonstrated a distinct increased moment towards the ipsilateral side just outside normal limits (Fig 11.2). This coincided with the increased force towards the contralateral limb.

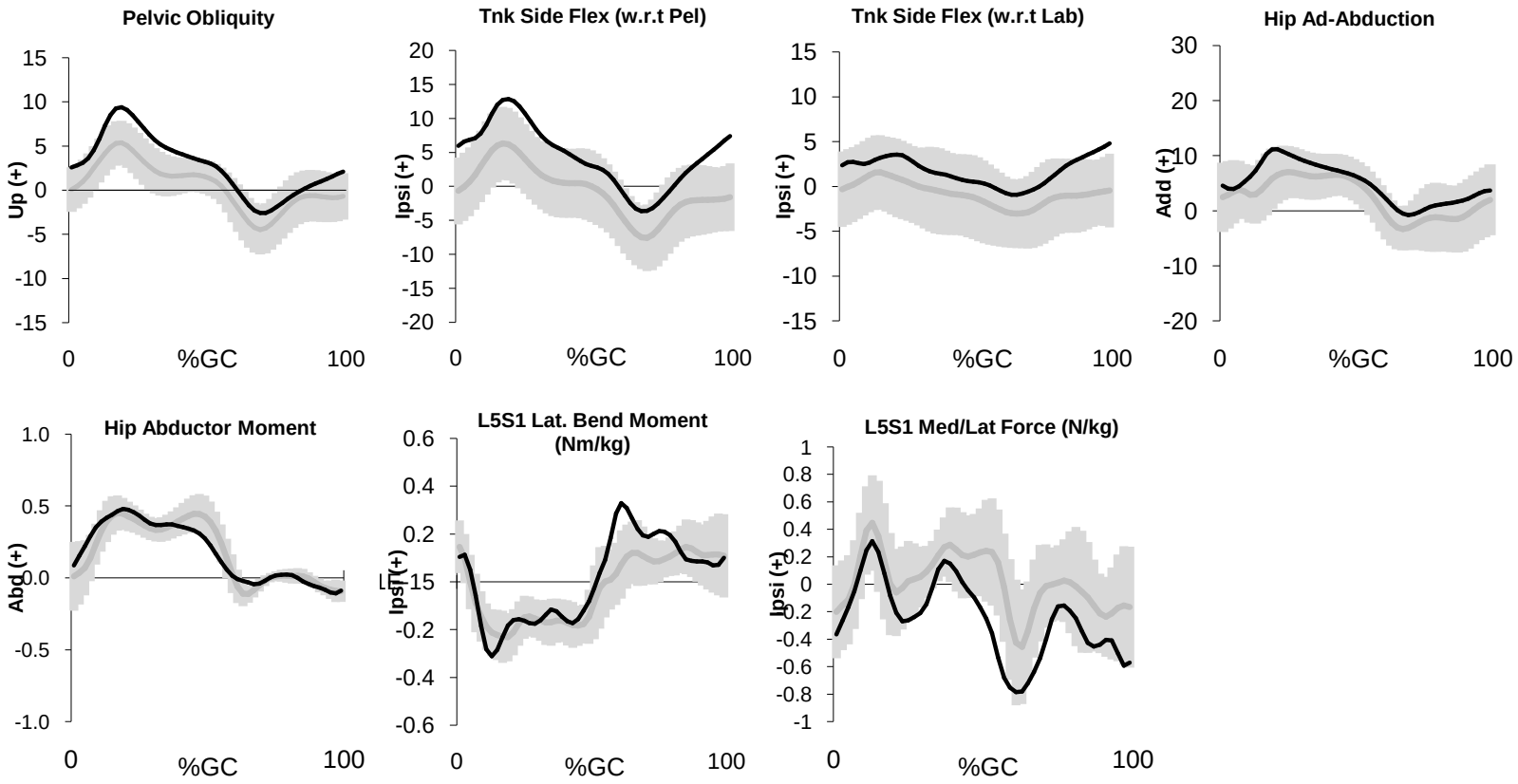

Figure 11.2: Kinematic and kinetic ensemble average profiles for Trendelenburg (Type 1) gait pattern. The black line indicates the analysed side and the gray band indicates ± 1 standard deviation about average for TD.

Table 11.2: Mean (SD) (*Median and Range for non-normally distributed data with distribution of all data assessed using a Shipiro-Wilk normality test) values for TD children and CP children according to movement Type 1 (Trendelenburg only) and Type 3 (Trendelenburg – Duchenne) with concurrent p-values. Descriptive statistics are reported for Type 2 (Duchenne only). Results of post-hoc tests are indicated as follows:

(A) Type 1 - TD; (B) Type 3 - TD; (C) Type 1 - Type 3;

Parameters	**TD**	**Type 1 (n = 8)**	**Type 2 (n = 4)**	**Type 3 (n = 22)**	**ANOVA *p*-Value**	**Post-hoc Comparison**
Peak Pelvic Obliquity stance	5 (2)	10 (3)	2 (1)	10 (3)	$p < 0.001$	A; B
Peak Hip Adduction in stance*	7 (20)	12 (10)	6 (7)	10 (24)	$p = 0.019$	A; B
Peak Tnk Side Flex (w.r.t Lab)	2 (4)	4 (2)	9 (2)	11 (4)	$p < 0.001$	B; C
Peak Tnk Side Flex (w.r.t Pel)	6 (5)	14 (4)	12 (3)	19 (6)	$p < 0.001$	A; B
Peak L5S1 Moment Towards Contra*	-0.29 (0.41)	-0.37 (0.41)	-0.47 (0.7)	-0.49 (0.8)	$p < 0.001$	B
Peak L5S1 Moment Towards Ipsi*	0.24 (0.56)	0.33 (0.33)	0.32 (0.35)	0.37 (1.12)	$p = 0.012$	B
Hip Abductor Moment Peak 1	0.53 (0.14)	0.56 (0.14)	0.58 (0.64)	0.41 (0.17)	$p = 0.113$	---
Hip Abductor Moment Peak 2	0.46 (0.14)	0.34 (0.24)	0.50 (0.26)	0.25 (0.23)	$p = 0.003$	B
Peak L5S1 Force Towards Contra*	-0.53 (1.42)	-0.88 (0.92)	-0.79(0.44)	-1.1 (2.03)	$p = 0.003$	A; B
Peak L5S1 Force Towards Ipsi*	0.55 (1.48)	0.32 (0.88)	0.70 (0.29)	0.61 (1.65)	$p = 0.546$	---

11.3.3 Duchenne gait pattern – Type 2

The number of Duchenne only (Type 2) subjects were too small for statistical analysis (n = 4). As an alternative, descriptive statistics are provided and ensemble average profiles commented on. For children with CP with a Duchenne gait pattern, pelvic obliquity remained relatively flat and close to a neutral position throughout the gait cycle (Fig.11.3). Peak pelvic obliquity was reduced compared to TD (reduction of 3^{o}) (Table 11.2). Peak trunk side flexion (w.r.t pelvis) demonstrated an increase of 6^{o} compared to TD. In addition, peak trunk side flexion (w.r.t lab) was also increased compared to TD by 7^{o} (Table 11.2).

Ensemble average profiles demonstrated an increased L5/S1 lateral bend moment towards the contralateral side outside normal limits during stance for CP Type 2 children compared to TD (Fig.11.3). Peak L5/S1 moment towards the contralateral side during stance was up to 62% greater compared to TD (Table 11.2). L5/S1 lateral bend moment towards the ipsilateral side during swing remained within normal limits (Fig.11.3). While medial/lateral force remained within normal limits throughout the gait cycle, there was a distinct increased position compared to TD during mid to late stance (Fig.11.3).

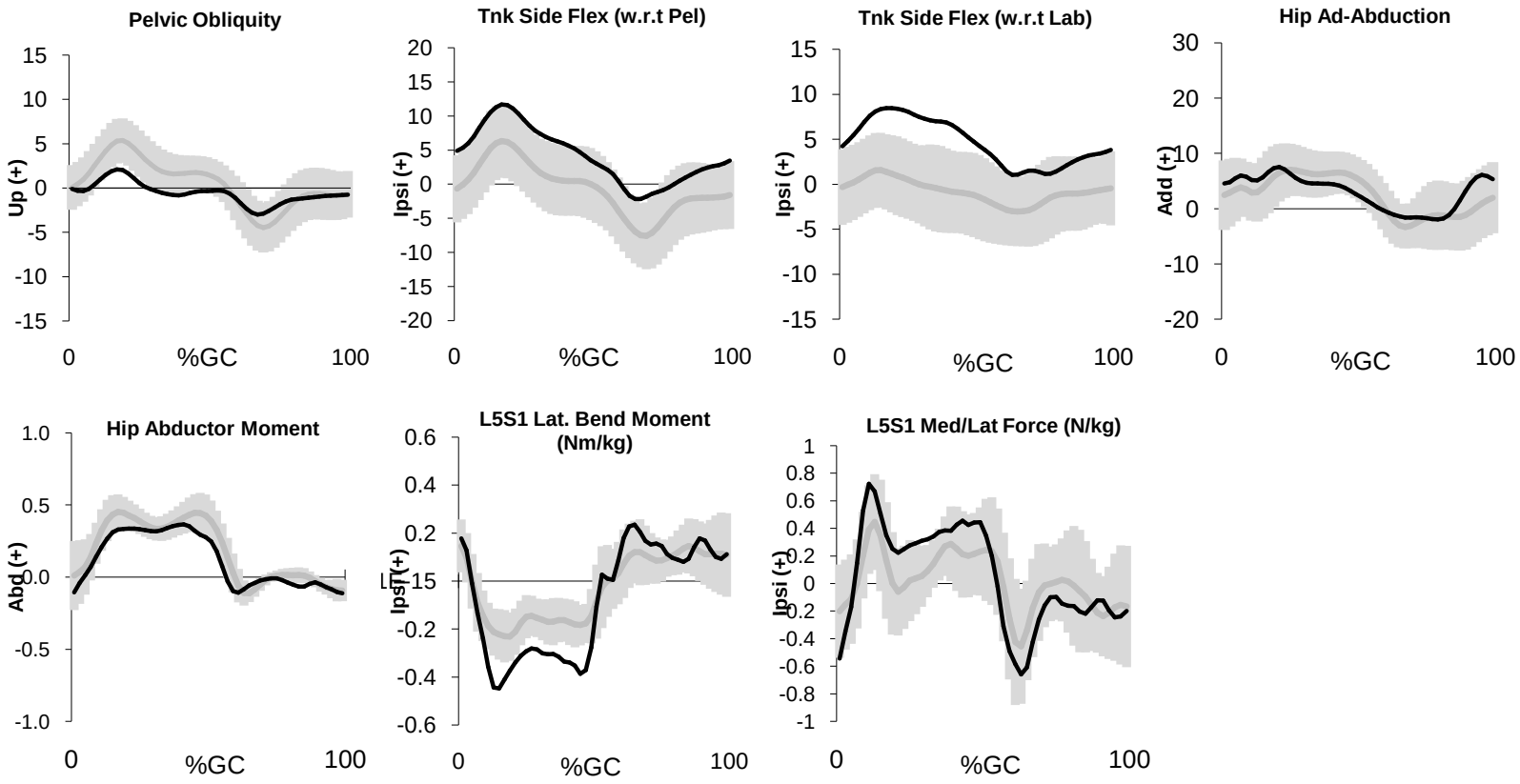

Figure 11.3: Kinematic and kinetic ensemble average profiles for Duchenne (Type 2) gait pattern. The black line indicates the analysed side and the gray band indicates ± 1 standard deviation about average for TD.

11.3.4 Combined Trendelenburg-Duchenne gait pattern – Type 3

For children with CP with a complex Trendelenburg–Duchenne gait pattern, peak pelvic obliquity was significantly increased by 5^{o} compared to TD (Table 11.2, Fig.11.4). A similar increase was demonstrated when compared to Duchenne only gait pattern (Table 11.2). Peak trunk side flexion, w.r.t both pelvis and Lab, were significantly increased by 13^{o} and 9^{o} respectively (Table 11.2). Peak hip adduction in stance demonstrated a statistically significant increase of 3^{o}. Hip abductor moment peak 1 remained within normal limits. However, hip abductor peak 2 was significantly reduced for CP Type 3 children compared to TD (reduction of 0.21 Nm/kg or ≈54%) (Table 11.2).

A number of significant deviations were evident in the kinetic ensemble average profiles for CP Type 3 compared to TD (Fig.11.4). Similar to those children with Trendelenburg only (Type 1) gait pattern, CP Type 3 children demonstrated an increased peak L5/S1 force directed towards the contralateral limb at initial swing phase. However, in this case, peak force was approximately double that of TD (increase of 0.57N/kg or ≈107%) (Table 11.2). Both peak L5/S1 ipsilateral and contralateral directed moments were also increased for CP compared to TD (increased by 69% and 54% respectively).

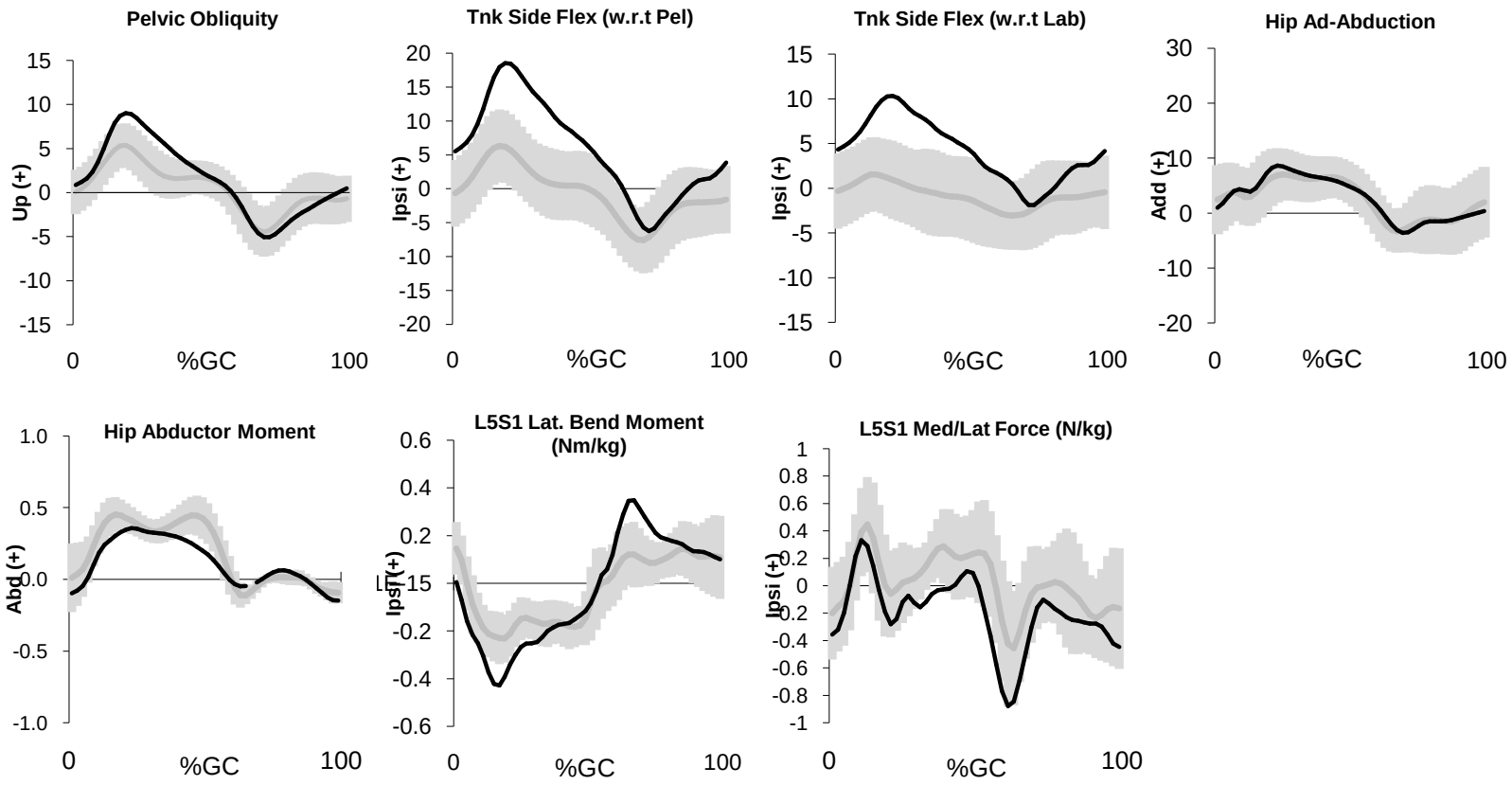

Figure 11.4: Kinematic and kinetic ensemble average profiles for combined Trendelenburg - Duchenne (Type 3) gait pattern. The black line indicates the analysed side and the gray band indicates ± 1 standard deviation about average for TD.

11.4. Discussion

This chapter investigated the effect of Trendelenburg, Duchenne and complex Trendelenburg-Duchenne type gait patterns on lower lumbar spinal loading during paediatric CP gait. Trendelenburg and Duchenne type movements were not always distinct of each other and a third type of movement, the complex Trendelenburg-Duchenne, was most common in the cohort of this study. Small increases were found for L5/S1 reactive forces and moments for Trendelenburg only pattern compared to normal. Additionally, L5/S1 moments were increased outside normal limits for Duchenne only pattern compared to TD. However, for those children with a complex Trendelenburg–Duchenne gait pattern, significant increases in loading were present with peak reactive forces and moments increased by up to 107% and 69% respectively.

11.4.1 Trendelenburg gait pattern (Type 1)

Pelvic, trunk and hip kinematics during Trendelenburg gait in this study were consistent with the literature when describing this type of movement pattern (Westhoff et al., 2006). Hip abductor moment remained within normal limits. Consequently, as hip abductor moment represents the predominant factor in hip joint loading (Brinckmann et al., 1981, Westhoff et al., 2006), loading at the hip was judged to be close to normal. The resulting effects at the lower lumbar spine were small. Only mild differences were present between CP and TD groups. Most notably, at the point of ipsilateral toe off, medial/lateral force directed towards the contralateral side was increased. At this point, the pelvis was raised on the contralateral side, the trunk leaned towards the contralateral pelvis and a resultant increased force was demonstrated. When ensemble average profiles were considered, an increased lateral bend moment was evident at this point (Fig.11.2). However, this increased moment was not statistically significant and remained just within normal limits suggesting the impact on the spine and corresponding trunk musculature was small or even negligible. Consequently,

it would be unlikely that a Trendelenburg gait pattern would negatively impact the health of the spine over time.

11.4.2 Duchenne gait pattern (Type 2)

The number of children with CP presenting with a Duchenne only type pattern was low and as a result statistical analysis could not be performed. Previous studies report higher incidence of Duchenne type gait pattern in CP, with Metaxiotis and colleagues reporting a positive Duchenne pattern in 17 out of 19 subjects in their study (Metaxiotis et al., 2000). However, the majority of those subjects had a positive Trendelenburg sign also. For the purposes of this study, Duchenne only gait pattern was a pattern of interest and so descriptive statistics and ensemble average profiles are discussed.

During Duchenne type gait, the pelvis maintained an almost neutral position while the trunk leaned towards the supporting limb, well outside normal limits. Again, this was consistent with the literature for this type of movement pattern (Westhoff et al., 2006). One reported feature of a Duchenne type pattern is a reduction in loading at the hip (Westhoff et al., 2006). It has been suggested that, as a compensatory mechanism for weak hip abductors, the trunk tilts over the supporting limb moving body weight closer to the hip joint (Metaxiotis et al., 2000, Stief et al., 2014). Demands at the hip are then reduced, evident by means of a decreased hip abductor moment (Westhoff et al., 2006). However, a reduced hip abductor moment was not evident in our results with values remaining close to normal limits. As previously mentioned, the hip abductor moment has been suggested to represent the predominant factor in hip joint loading (Brinckmann et al., 1981, Westhoff et al., 2006), and while strength data were not collected, no evidence of a reduced hip abductor moment suggested that hip abductor weakness may not be the primary deficit in this case. It is difficult to ascertain why hip abductor moment patterns were not as expected. Small numbers in this group may be a factor. Alternatively, a Duchenne type pattern has also been reported as a compensatory mechanism to aid foot clearance where hip or knee flexion or ankle dorsiflexion

are inadequate (Bohm et al., 2013). Consequently, this may help account for normal hip abductor moment values in this group.

Reactive forces at the lower lumbar spine were slightly raised though remained within normal limits. However, an increased L5/S1 lateral bend moment during stance, with two distinct peaks occurring at contralateral toe off and heel strike, was evident. This increased moment towards the contralateral side was not altogether surprising. L5/S1 lateral bend moments during CP gait have been shown to increase with excessive trunk movement in the coronal plane, as discussed in Chapter 10. This would suggest that a Duchenne type pattern, while it may have the potential to reduce demands at the hip for some subjects, can result in greater loading on the lower lumbar spine as the trunk moves into a suitably compensatory position. This type of movement pattern has been previously reported as a therapy for unloading the hip joint during gait (Schröter et al., 1999, Svehlik et al., 2012). However, our results suggest that a consequence of this could be a negative impact on loading at the lower lumbar spine. While it is not clear whether this recommended therapy has been used routinely in clinical practice, the promotion of this type of movement pattern as a form of therapy may have to be considered with caution.

11.4.3 Complex Trendelenburg–Duchenne gait pattern (Type 3)

A complex Trendelenburg–Duchenne pattern involving both contralateral pelvic drop and excessive trunk lean was the most common pattern amongst the cohort in this study with just over 40% of subjects in this category. It was felt that describing this pattern as a combination of Trendelenburg-Duchenne was not strictly accurate as in Trendelenburg gait the contralateral pelvis dips while in Duchenne gait it remains level or elevated (Metaxiotis et al., 2000, Westhoff et al., 2006). With this in mind, the term “complex Trendelenburg-Duchenne” was applied to this pattern type.

When the kinematic presentation of this complex Trendelenburg–Duchenne pattern was considered, a similar pelvic position to the Trendelenburg pattern was demonstrated.

However, as a consequence of the increased pelvic obliquity, trunk side flexion with respect to the pelvis was therefore increased compared to Duchenne only pattern where the pelvis remained flat. Peak trunk flexion in the global frame was also increased compared to Duchenne only pattern suggesting that those children with CP with combined Trendelenburg–Duchenne were more involved at the trunk when compared to Duchenne only.

When all 3 movement types were considered, the resultant effects at the lower lumbar spine were most evident for complex Trendelenburg-Duchenne type gait. Similar to Trendelenburg only pattern, there was an increased force towards the contralateral side at initial swing. However, this force was greater in magnitude compared to Trendelenburg only. As pelvic position was similar, the increase in force must therefore be attributed to the increased side flexion of the trunk.

L5/S1 peak lateral bend moments were increased for complex Trendelenburg-Duchenne compared to TD and marginally increased for complex Trendelenburg-Duchenne compared to Duchenne only pattern. Consequently, it would appear that greater levels of loading were placed on the lower lumbar spine as the trunk and pelvis maintained suitably compensatory positions during complex Trendelenburg–Duchenne type gait compared to TD. Due to only a small increase in moments compared to Duchenne only pattern, results suggested that the contralateral drop of the pelvis (Trendelenburg pattern) had a relatively small impact on demands at the lower spine. Instead, it was primarily the excessive trunk lean (Duchenne pattern) that contributed mainly to increased lumbar spinal loading in CP subjects who presented with a complex Trendelenburg–Duchenne type pattern during gait. This further highlighted that loading at the lumbar spine in those subjects who presented with either Duchenne or complex Trendelenburg–Duchenne type patterns during gait also needs to be given consideration during clinical decision making.

11.5 Conclusions

A proportion of children with CP in this cohort presented with a complex Trendelenburg–Duchenne walking pattern. This was the first study to specifically describe the associated trunk and pelvic kinematics of this pattern and the phrase “complex Trendelenburg–Duchenne” appeared suitable to describe this pattern. Those children with CP who presented with a complex Trendelenburg-Duchenne type pattern demonstrated the greatest increase in loading at the lower lumbar spine compared to TD controls. Trunk position was a critical factor with only a small contribution as a result of the contralateral drop of the pelvis. For those children with CP who presented with a Duchenne type pattern, loading at the lumbar spine was increased. However, while the position of the trunk was also important, numbers in this group were low and only descriptive statistics were reported. Finally, the Trendelenburg only gait pattern had the least impact at the lower lumbar spine with only small differences in lower lumbar spinal loading compared to TD controls. Consequently, clinicians need to be aware of the resultant effects at the lower spine when presented with these types of walking patterns. Specifically, promotion of a Duchenne or complex Trendelenburg-Duchenne type pattern as a non-invasive rehabilitative or conservative treatment should be considered with caution due to the potential for negative effects at the lumbar spine. More investigation as to the effects of increased loading at the lower lumbar spine during gait in CP, possibly by means of a longitudinal study, maybe an area worthy of further study.

Chapter 12: Discussion

12.1 Introduction

The overall goal of this thesis was to investigate levels of loading at the lower lumbar spine during gait in children with CP, with a view to determine whether a relationship existed between pathological movement of the upper and lower trunk and kinetic profiles at the lower lumbar spine, and to investigate whether children with CP presenting with Trendelenburg and Duchenne type gait patterns demonstrated altered patterns of lower spinal loading compared to controls. A secondary goal was to assess the kinematic and kinetic models before use in this study.

There were a number of major contributions of this thesis. Firstly, this was the first study to report levels of loading at the lower lumbar spine during CP gait. This thesis has identified typical patterns of 3-dimensional reactive forces and moments at the lower lumbar spine in children with CP and assessed the group according to level of functional impairment (assessment according to principle diagnosis was also reported in Appendices 10.1 to 10.5) and according to clinical presentation of Trendelenburg or Duchenne type gait. Additionally, comparisons were made to lower lumbar spinal loading in TD children. Secondly, this thesis identified differences in thorax movement in children with CP that further supports those reported in the literature and it was the first study to specifically identify differences between CP children and typically developed for lumbar segment movement. The thesis highlighted that treating the lumbar region as a single segment can be useful to differentiate between normal and pathological function. Finally, this thesis identified areas of the kinematic and inverse dynamic models that warranted further investigation. Differences in choice of BSP set and regression equation set were assessed from a clinical perspective, two lumbar segment protocols were assessed during gait and a new thorax kinematic protocol was proposed.

12.2 Preparatory Studies

In Chapter 1, reference was made to the role of movement analysis in CP followed by a review of common gait patterns associated with this population and the possible role of the trunk. At commencement of this project, studies on trunk movement in this population were limited but results suggested that children with CP experienced greater range of motion of the thorax in all 3 planes during gait compared to typically developed controls (Romkes et al., 2007, Pratt et al., 2012, Heyrman et al., 2013a). More recent studies assessing trunk movement supported these findings (Attias et al., 2015). As the position of the trunk changes with respect to the pelvis, mechanical loads at the spine change and a prolonged exposure of the lumbar spine to pathological changes in the mechanics of motion of the trunk may result in adaptations of the structural tissue surrounding this area (Bogduk and Twomey, 1991). While the role of the trunk in manipulating lower limb kinetics during gait had been highlighted in the literature (Õunpuu et al., 1996), the extent to which pathological trunk movement affects loading at the lumbar spine during CP gait was unclear. Consequently, the need for an assessment of reactive forces and moments at the lower lumbar spine during CP gait compared to TD controls was warranted. As Trendelenburg and Duchenne type movements affect motion of the trunk and pelvis, and are often demonstrated during CP gait, an investigation into the affect of these movements on lower lumbar spinal loading was considered necessary.

Chapter 2 reviewed the role of gait analysis in the assessment of thoracic and lumbar kinematics and lower lumbar spinal loading and highlighted challenges faced with the use of the associated kinematic and kinetic models. Accordingly, before addressing the primary goals of this study, the following model aspects were assessed: (1) BSP set; (2) HJC position; (3) Thoracic kinematic protocol and (4) Lumbar segment protocol. In essence, it would have been possible to achieve the primary aims of this thesis without considering the underlying mathematical models. However, it is important for clinicians to have a solid understanding of

the kinematic and kinetic models before clinical data can be correctly understood. Chapter 3 highlighted areas of the data capture procedure where errors could occur (e.g. CoP alignment, SMA, choice of HJC regression equation set etc.). With some of these uncertainties, for example CoP alignment error, the clinician can only account for it by applying best practice in terms of quality assurance procedures. Other uncertainties, for example choice of HJC regression equation set, can be investigated by the clinician before data capture to better understand the implications of any related error. With this in mind, the choice of BSP set and HJC regression equations set were further investigated.

In relation to BSP set, it would be unlikely that differences relating to the use of specific BSP sets could be considered clinically meaningful if different sets were used during gait analysis. With this in mind, the BSP set of Jensen and colleagues was chosen for the purposes of this thesis and used in the inverse dynamic calculations in Chapters 10 and 11. The results of this investigation have implications not only for this thesis but for the wider gait analysis community. The majority of gait laboratories use BSP in their inverse dynamic calculations and the results presented here provide a new perspective that will allow clinicians or researchers to assess impact from a clinical point of view in order to determine whether current models are adequate or if changes are needed. When HJC position was considered, results demonstrated differences primarily in kinetic output and it was concluded that these differences could be considered clinical meaningful when in fact the change was solely due to the choice of set. The use of the Davis set should most likely be avoided if inverse dynamic calculations are required and the set of Bell and colleagues was almost identical the Harrington reference. For the purposes of this thesis, the set of Bell and colleagues was implemented in the kinematic and kinetic models used in Chapters 10 and 11. Similarly to the choice of BSP set, taking a clinical perspective on the choice of HJC will have implications outside of this thesis. Most gait laboratories use HJC regression equations on a day-to-day basis and, as previously mentioned, the choice of most accurate method is currently a topic of

debate, evidenced by the large number of studies in this area over the last few years. This investigation demonstrated that some of the older equations were close in kinematic and kinetic output to those of Harrington. For a standard gait laboratory, a change of HJC set can be easily implemented in terms of the underlying mathematical model. However, there may be issues relating to historical databases or indeed standards accreditation that may make such a change a substantial amount of work. The results presented here will help provide clinicians and researchers using those equations additional confidence in their data.

Clinical experience was the driving force for Chapter 8 where an alternative thorax protocol was proposed and benchmarked against the reference standard. Issues associated with various thoracic kinematic protocols were highlighted in Chapter 2. The proposed protocol addressed some of the practical issues experienced during the assessment procedure. An advantage of the proposed protocol is that it is not system specific and could be used by other researchers or clinicians. Some adjustment may be required depending on sensor design or size but in general the protocol is transferable across laboratories. In the situation where standard thorax protocols are not suitable, the proposed thorax protocol of this research may provide an alternative solution. Thorax kinematics reported in Chapters 10 and 12 were recorded using this proposed protocol. As a rigid cluster placed on the thorax does not account for movement at the lumbar spine, it was decided to place a kinematic protocol on the area to assess movement during CP gait. However, unlike the thorax, no reference standards exist and it was necessary to assess kinematic protocols used in the literature. Consequently, lumbar segment motion reported in Chapter 10 was recorded using a skin surface protocol. While the skin surface protocol was not without its limitations, when applied in the clinical setting it was possible to distinguish pathological movement from normal and, as a consequence of this, it may be a useful addition to other clinicians or researchers wishing to measure similar movement during gait. Similar to the thorax protocol, the lumbar protocol was applied in this thesis in Chapter 11.

12.3 Estimates of lower lumbar spinal loads during gait

The next step after assessing the kinematic and kinetic models was to investigate levels of loading at the lower lumbar spine during gait in children with CP, with a view to determine whether a relationship existed between pathological movement of the upper and lower trunk and kinetic profiles at the lower lumbar spine. Chapter 1 made reference to the potential for altered mechanical loads at the spine in the presence of excessive trunk movement. Previously reported excessive movement of the trunk during CP gait thus provided the rationale for this investigation (Heyrman et al., 2013a, Romkes et al., 2007). In general, reactive forces and moments at the lower lumbar spine were increased for children with CP compared to TD and the impact of excessive thorax movement was directly evident. At peak points, these increases were up to 21% higher than normal for GMFCS I children and up to 90% higher than normal for GMFCS II children for moment data. A moderate to strong and highly significant positive correlation of this movement with reactive forces and moments ($r = 0.39$ to 0.52) helped support the theory that increased lower lumbar spinal loading was influenced by the position of the thorax. The assessment of lumbar segment movement during CP gait was another novel aspect of this thesis with differences most obvious in the sagittal plane (children with CP demonstrating more flexion compared to TD). However, in the coronal plane, mean increases were only in the magnitude of 4^{o}. A low correlation between movement and loading in this plane ($r = 0.24$ to 0.35), suggested that, while there was some impact of this pathological movement on loading in this area, movement of the thorax was more likely the dominant factor.

When the investigation was further applied to a specific clinical presentation during gait, children with a Duchenne type movement, whether it is a Duchenne or complex Trendelenburg-Duchenne type gait, demonstrate increased reactive forces and moments at the lower lumbar spine. The complex Trendelenburg-Duchenne type of movement had the biggest impact at the lower lumbar spine and it appeared that the drop of the pelvis had little

impact here and instead it was more likely the increased lean of the thorax that contributed to the increased loading. Overall, the results of this investigation highlighted that caution is needed when presented with a child with CP displaying a Duchenne type pattern compared to a Trendelenburg type pattern during gait. Results of Chapter 10 help support the theory that position of the trunk was a critical factor. Additionally, this was the first study to specifically describe the associated trunk and pelvic kinematics of a "complex Trendelenburg–Duchenne" type pattern. It was concluded that promotion of a walking pattern where a Duchenne type movement was present, whether it be as a conservative or rehabilitative treatment (Schröter et al., 1999, Svehlik et al., 2012), should be considered with caution as there exists the potential for negative effects at the spine. From a clinical perspective, it appears from results described in this chapter and also Chapter 10 that a first step in this situation would be to attempt to reduce excessive movement of the thorax. How this is achieved will of course depend on the clinical situation. Some children with CP may benefit from specifically directed hip abductor strengthening program to potentially reduce the need for a compensatory movement of the trunk. A core trunk strengthening program may benefit others. An assessment of such interventions, using the approach described in this thesis, would help improve our knowledge relating to the impact of excessive movement of the trunk during CP gait.

12.4 Clinical Implications

It is difficult to identify exactly what the impact of pathological reactive forces and moments will be at the spine over time. No studies have specifically examined lumbar stresses and strains specifically related to altered trunk motion during CP gait. Radiographic studies have highlighted changes in the lumbar spine of children with CP (Harada et al., 1993). Whether these changes are a consequence of altered movement of the trunk is unclear. Wolff's law states that bone tissue will respond by deposition of new bone in response to

cyclic high stresses (Wolff, 1892). In relation to the spine, it has been suggested that pathological changes in the mechanics of motion of the spine, which ultimately alter stresses applied to the spine, can result in the formation of osteophytes along the junction of the vertebral bodies and intervertebral discs (Bogduk and Twomey, 1991). Based on this, it is a reasonable assumption that altered trunk movement will have some impact on the health of the spine over time. However, this is an assumption at best and cannot be concluded from the results of this study. The corresponding clinical implications are also unclear. The next obvious question is whether this altered movement plays a role in low back pain (LBP) in CP? Occurrences of LBP in children with CP have not been reported in the literature. However, incidents of LBP have been reported in adults with CP (Jahnsen et al., 2004). LBP in itself is notoriously multi-factorial and it was not the purpose of this thesis to link LBP with increased reactive forces and moments at the spine. However, this thesis does highlight another potential risk factor for possible problems at the spine in later life, one of those risk factors being a potential contribution to LBP. As a starting point, this thesis provides a foundation for further exploration. A longitudinal study of low back pain in CP from childhood into adulthood, where reactive forces and moments at the spine are assessed at regular intervals, may shed further light as to the impact of excessive thoracic, lumbar and pelvic movements on the lower lumbar spine over time during CP gait.

Based on the results of this thesis, and taking into account the previously reported moderate to strong relationship between thorax movement and lower lumbar joint loading as reported in Chapter 10, it is suggested that therapy is aimed at reducing thorax movement in the CP child, in particular when presented with a Duchenne or complex Trendelenburg-Duchenne type pattern. However, as altered thorax movement is usually a compensation for a lower limb deficiency (e.g. weak hip abductors or dysfunction of the affected hip) (Stief et al., 2014), the optimal thorax lean for the best trade-off between reduced reactive forces and moments at the lower lumbar spine and minimising the effects of lower limb problems is

unknown. Hip abductor muscle strengthening may be beneficial to reduce excessive medial/lateral thorax sway and thus reduce reactive forces and moments at the spine. Alternatively, adjustable walking poles have been shown to result in less lateral trunk lean (Bechard et al., 2012), and may be a consideration for children with CP presenting with excessive trunk patterns. However, as discussed, more investigation is warranted as to the long term effects of increased reactive forces and moments at the lower lumbar spine during CP gait over time.

12.5 Limitations of the thesis

As discussed in Section 5.13, the forces produced by the inverse dynamic approach employed in this study were the net inter-segmental reactive forces between segments. These net inter-segmental forces represent the effects of external loads and, as a result of this, corresponding forces from muscles and soft tissue acting across the joints were not considered. When these additional forces have been considered in the literature, the total force has been shown to be larger. Due to a continuously changing muscle moment arm and a dynamic line of action of the various muscles, it can be difficult to determine their exact contribution to total force. A further limitation of this study is that stiffness or spasticity acting across specific joints was not taken into account in the final inverse dynamic estimation. However, as the purpose of this study was to assess the impact of excessive trunk movement on lower lumbar spinal loading, the use of the inverse dynamic approach was considered acceptable.

As highlighted in Chapter 11, the original group of 52 children with CP were spilt according to clinical presentation of Trendelenburg, Duchenne or complex Trendelenburg–Duchenne gait. This resulted in a small number of subjects presenting with a Duchenne type pattern (Type 2). Consequently, results relating to this pattern may need to be interpreted with caution. However, as it was the purpose of the study to also examine the effects of a

Duchenne only type pattern on lower lumbar spinal during CP gait, descriptive statistics and ensemble average profiles were discussed.

This study has demonstrated clear differences in both thorax and lumbar segment kinematics and reactive forces and moments at the lower lumbar spine between CP and TD. Previous studies have attempted to quantify repeatability of trunk kinematics during walking in children with CP (Heyrman et al., 2013b). However, as this is the first study to report L5/S1 reactive forces and moments in a CP population, no repeatability data exists for these measures. This thesis does not present an in-depth repeatability analysis of these measures. As a preliminary assessment of test-retest repeatability, 8 children with CP were assessed using a test-retest approach with data presented using the approach of Schwartz et al (Schwartz et al., 2004). Mean inter-subject and intra-subject data based on the protocol of Schwartz et al are reported graphically in Appendices 13.1 to 13.4. Initial analysis suggested good levels of repeatability across all measures with inter/intra ratios ranging from 1.26 to 3.54 (Appendix 13.4). If these values are considered in relation to previously reported values for lower limb kinematic data using the same approach, they appear reasonable (ranges of 1.4 to 5.0 and 1.2 to 2.8 have previously been reported (Kiernan et al., 2014b, Schwartz et al., 2004)). However, while this preliminary examination gave some indication of levels of repeatability of the measures of interest of this study, a further in-depth examination of the measures used in this thesis is warranted in both CP and normal subjects.

Chapter 13: Conclusions

This thesis demonstrated for the first time that children with CP experienced increased reactive forces and moments during gait at the L5/S1 joint compared to TD children. These increased reactive forces and moments were strongly linked to excessive thorax motion. In addition, reactive forces and moments increased according to GMFCS level. Changes in lumbar segment position were also evident for children with CP. However, movement of the thorax appeared to be a critical factor contributing to lower lumbar spinal loading. Similar results were demonstrated when children were grouped according to principal diagnosis with dipelgic children with CP demonstrating more involvement. When a further clinical application of these measures was performed, children with CP with a Duchenne or a complex Trendelenburg-Duchenne type gait pattern demonstrated increases in loading at the lumbar spine compared to TD controls. Thorax position was again highlighted as a critical factor. The thesis has highlighted that additional demands are present at the lower lumbar spine during gait in children with CP. It is important that clinicians are aware that pathological movement demonstrated during CP gait may result in pathological loading at the lower lumbar spine.

An assessment of the kinematic and kinetic models highlighted that no clinically significant differences were recorded between BSPs sets. However, use of the Davis set for HJC location should be avoided if inverse dynamics are a consideration. With this in mind, the BSP set of Jensen and the HJC set described by Bell and colleagues were used in this thesis. Both of these investigations have implications for the wider gait analysis community. The proposed thorax kinematic protocol was another significant contribution of this thesis and worked well for this study demonstrating a number of practical advantages to other protocols in the literature. The preliminary validation against two reference protocols helped provide confidence in the protocol for use in the clinical setting. The mount was also straightforward to apply and stood proud of the back and so marker occlusion was not an issue. This protocol is readily transferable to other systems and laboratories and may provide an alternative choice

for some clinicians or researchers depending on the clinical investigation. The remaining preparatory chapter, examining choice of lumbar segment protocol, identified the skin surface protocol as sufficient to distinguish pathological movement from normal and, in the absence of reference standard, may also be useful to other clinicians or researchers wishing to examine similar movement during gait.

This thesis is a first step at measuring and understanding the additional levels of loading placed on the lower lumbar spine during CP gait. For clinical engineers, physiotherapists and surgeons, this thesis confirms that children with CP experience abnormal high loading at the lower lumbar spine during gait and that a link does exists between this aberrant loading and excessive movement of the trunk. Often children with CP will present for gait analysis with lower limb deficits that clearly affect movement of the trunk during gait. While these compensatory movements of the trunk may reduce loads at the hip for example, whether achieved by means of a Duchenne or complex Trendelenburg-Duchenne pattern, this thesis has demonstrated that this movement may negatively affect loading further up the kinematic chain. At the very least, the results of this thesis suggest that an assessment of loading at the lower lumbar spine should be considered when clinicians are presented with the child with CP who demonstrates excessive trunk movement during gait.

As a result of the findings of this thesis, the assessment of thorax and lumbar segment motion has become a regular addition to the standard gait analysis in the CRC gait laboratory. The laboratory has expanded the 3-dimensional CODA cx1 camera system from a 4 camera system to a 6 camera system in order to incorporate a full 360 degree capture volume area. Prior to this work, cameras were placed only parallel to the direction of the walkway (sagittal plane) making it difficult to actively follow markers placed on the coronal plane of the subject. The additional cameras are suspended from rails looking directly up and down the laboratory walkway. Additionally, the CRC gait laboratory is in the process of permanently incorporating

two additional force platforms into the lab floor to allow for lumbar spinal kinetics to be captured without the need for a raised walkway.

To summarise, it is common practice to measure and report kinetics of the lower limbs during gait analysis of children with CP. This study is a first step towards expanding kinetic measurements upwards towards the trunk in this population. There is no doubt that further work is necessary to understand the individual components of these increased loads and this thesis lays the basis upon which further work can be conducted. Based on results to date, it is important that any interventions relating to movement of the trunk, or specifically related to Duchenne or complex Trendelenburg-Duchenne type gait, whether conservative or surgical, are aimed at reducing trunk motion specifically in the coronal plane in order to reduce abnormal loading which could, in turn, impact the health of the spine in this population.

Chapter 14: Future Work

An inverse dynamic analysis approach was used in this thesis and the roles of individual muscles and soft tissue acting across the L5/S1 joint were not considered. Additionally, a moderate to strong correlation between excessive thorax movement and increased loading suggested other factors may have contributed to these altered loads. With this in mind, future studies could attempt to further assess the contribution of various muscles acting across the joint, possibly by means of an electromyographic (EMG) analysis.

Clear differences in measures at the trunk and lower lumbar spine were present between CP and TD children. Future studies could establish reliability and measurement error in order to further aid clinical interpretation. An understanding of the magnitude by which these variables must change, in order to ensure the change is real, is required. The minimal detectable change (MDC) in the case of kinetics at the lumbar spine during CP gait has not been reported.

The current study was a cross-sectional study taken at a single time point for both children with CP and TD children. Future work may incorporate a longitudinal approach of assessing reactive forces and moments at the lumbar spine in this population to determine how measures of loading change as the child progress from early childhood into adolescence. Additionally, a pre and post assessment of different interventions to address excessive trunk movement in this population could be considered for future work.

References

Akbarshahi, M., Schache, A. G., Fernandez, J. W., Baker, R., Banks, S. & Pandy, M. G. 2010. Non-invasive assessment of soft-tissue artifact and its effect on knee joint kinematics during functional activity. *J Biomech,* 43**,** 1292-301.

Alexander, E. J. & Andriacchi, T. P. 2001. Correcting for deformation in skin-based marker systems. *Journal of Biomechanics,* 34**,** 355-361.

Amar, J. 1916. Trottoir dynamographique. *Comptes rendus hebdomadaires des seances de l Academie des Sciences,* 163**,** 130-133.

Andersen, M. S., Mellon, S., Grammatopoulos, G. & Gill, H. S. 2013. Evaluation of the accuracy of three popular regression equations for hip joint centre estimation using computerised tomography measurements for metal-on-metal hip resurfacing arthroplasty patients. *Gait Posture,* 38**,** 1044-7.

Armand, S., Sangeux, M. & Baker, R. 2014. Optimal markers' placement on the thorax for clinical gait analysis. *Gait Posture,* 39**,** 147-53.

Attias, M., Bonnefoy-Mazure, A., Lempereur, M., Lascombes, P., De Coulon, G. & Armand, S. 2015. Trunk movements during gait in cerebral palsy. *Clin Biomech (Bristol, Avon),* 30**,** 28-32.

Baker, R. 1997. The "Poker" Test: A Spot Check to confirm the accuracy of Kinetic Gait Data. *Gait and Posture,* 5**,** 177-178.

Baker, R. 2001. Pelvic angles: a mathematically rigorous definition which is consistent with a conventional clinical understanding of the terms. *Gait & Posture,* 13**,** 1-6.

Baker, R. 2007. The history of gait analysis before the advent of modern computers. *Gait & Posture,* 26**,** 331-342.

Baker, R. 2013. *Measuring Walking: A Handbook of Clinical Gait Analysis,* London, Mac Keith Press.

Baker, R., Finney, L. & Orr, J. 1999. A new approach to determine the hip rotation profile from clinical gait analysis data. *Human Movement Science,* 18**,** 655-667.

Baker, R., Mcginley, J. L., Schwartz, M., Thomason, P., Rodda, J. & Graham, H. K. 2012. The minimal clinically important difference for the Gait Profile Score. *Gait Posture,* 35**,** 612-5.

Baker, R., Mcginley, J. L., Schwartz, M. H., Beynon, S., Rozumalski, A., Graham, H. K. & Tirosh, O. 2009. The gait profile score and movement analysis profile. *Gait Posture,* 30**,** 265-9.

Bartonek, Å., Saraste, H., Eriksson, M., Knutson, L. & Cresswell, A. G. 2002. Upper body movement during walking in children with lumbo–sacral myelomeningocele. *Gait & Posture,* 15**,** 120-129.

Bax, M. 1964. Terminology and Classification of Cerebral Palsy. *Dev Med Child Neurol,* 6**,** 295-307.

Bax, M., Goldstein, M., Rosenbaum, P., Leviton, A. & Paneth, N. 2005. Proposed definition and classification of cerebral palsy, April 2005. *Dev Med Child Neurol,* 47**,** 571-576.

Bechard, D. J., Birmingham, T. B., Zecevic, A. A., Jones, I. C., Leitch, K. M., Giffin, J. R. & Jenkyn, T. R. 2012. The effect of walking poles on the knee adduction moment in patients with varus gonarthrosis. *Osteoarthritis and Cartilage,* 20**,** 1500-1506.

Bell, A. L., Brand, R. A. & Pedersen, D. R. 1989. Prediction of hip joint centre location from external landmarks. *Human Movement Science,* 8**,** 3-16.

Benoit, D. L., Ramsey, D. K., Lamontagne, M., Xu, L., Wretenberg, P. & Renström, P. 2006. Effect of skin movement artifact on knee kinematics during gait and cutting motions measured in vivo. *Gait & Posture,* 24**,** 152-164.

Bland, J. M. & Altman, D. G. 1986. Statistical methods for assessing agreement between two methods of clinical measurement. *Lancet,* 1**,** 307-10.

Bogduk, N. & Twomey, L. T. 1991. Clinical Anatomy of the Lumbar Spine. Churchill Livingstone.

Bohm, H., Dussa, C. U., Multerer, C. & Doderlein, L. 2013. Pathological trunk motion during walking in children with amyoplasia: is it caused by muscular weakness or joint contractures? *Res Dev Disabil,* 34**,** 4286-92.

Brinckmann, P., Frobin, W. & Hierholzer, E. 1981. Stress on the articular surface of the hip joint in healthy adults and persons with idiopathic osteoarthrosis of the hip joint. *J Biomech,* 14**,** 149-56.

Callaghan, J. P., Patla, A. E. & Mcgill, S. M. 1999. Low back three-dimensional joint forces, kinematics, and kinetics during walking. *Clin Biomech (Bristol, Avon),* 14**,** 203-216.

Camargo-Junior, F., Ackermann, M., Loss, J. F. & Sacco, I. C. 2013. Influence of Center of Pressure Estimation Errors on 3D Inverse Dynamics Solutions During Gait at Different Velocities. *J Appl Biomech*.

Camomilla, V., Cereatti, A., Vannozzi, G. & Cappozzo, A. 2006. An optimized protocol for hip joint centre determination using the functional method. *J Biomech,* 39**,** 1096-106.

Cans, C. 2000. Surveillance of cerebral palsy in Europe: a collaboration of cerebral palsy surveys and registers. *Dev Med Child Neurol,* 42**,** 816-824.

Cappello, A., Stagni, R., Fantozzi, S. & Leardini, A. 2005. Soft tissue artifact compensation in knee kinematics by double anatomical landmark calibration: performance of a novel method during selected motor tasks. *IEEE Trans Biomed Eng,* 52**,** 992-8.

Chang, F. M. M. D., Seidl, A. J. B. S., Muthusamy, K. M., Meininger, A. K. M. & Carollo, J. J. 2006. Effectiveness of Instrumented Gait Analysis in Children With Cerebral Palsy - Comparison of Outcomes. *Journal of Paediatric Orthopaedics,* 26**,** 612-616.

Chen, S. C., Hsieh, H. J., Lu, T. W. & Tseng, C. H. 2011. A method for estimating subject-specific body segment inertial parameters in human movement analysis. *Gait Posture,* 33**,** 695-700.

Clement, J., Dumas, R., Hagemeister, N. & De Guise, J. A. 2015. Soft tissue artifact compensation in knee kinematics by multi-body optimization: Performance of subject-specific knee joint models. *J Biomech,* 48**,** 3796-802.

Collins, T. D., Ghoussayni, S. N., Ewins, D. J. & Kent, J. A. 2009. A six degrees-of-freedom marker set for gait analysis: repeatability and comparison with a modified Helen Hayes set. *Gait Posture,* 30**,** 173-80.

Crosbie, J., Vachalathiti, R. & Smith, R. 1997. Patterns of spinal motion during walking. *Gait Posture,* 5**,** 6-12.

Damavandi, M., Farahpour, N. & Allard, P. 2009. Determination of body segment masses and centers of mass using a force plate method in individuals of different morphology. *Med Eng Phys,* 31**,** 1187-94.

Davis, R., Ounpuu, S., Tyburski, D. & Gage, J. 1991. A gait analysis data collection and reduction technique. *Human Movement Science,* 10**,** 575-587.

Della Croce, U., Leardini, A., Chiari, L. & Cappozzo, A. 2005. Human movement analysis using stereophotogrammetry: Part 4: assessment of anatomical landmark misplacement and its effects on joint kinematics. *Gait & Posture,* 21**,** 226-237.

Dempster, W. 1955. Space requirements for the seated operator. *WADC Technical Report 55-159.Wright Patterson Air Force Base, OH; 1955.* .

Dodd, K. J., Taylor, N. F. & Damiano, D. L. 2002. A systematic review of the effectiveness of strength-training programs for people with cerebral palsy. *Arch Phys Med Rehabil,* 83**,** 1157-64.

Du Plessis, A. J. 2009. Mechanisms and Manifestations of Neonatal Brain Injury. *In:* GAGE, J. R., SCHWARTZ, M. H., KOOP, S. & NOVACHECK, T. F. (eds.) *The Identification and Treatment of Gait Problems in Cerebral Palsy* 2nd ed. London: Mac Keith Press.

Duchenne, G. B. 1949. *Physiologie des Mouvements,* Philadelphia, Lip-pincott.

Essex, C. 2003. Hyperbaric oxygen and cerebral palsy: No proven benefit and potentially harmful. *Developmental Medicine and Child Neurology,* 45**,** 213-5.

Fernandes, R., Armada-Da-Silva, P., Pool-Goudaazward, A., Moniz-Pereira, V. & Veloso, A. P. 2016. Three dimensional multi-segmental trunk kinematics and kinetics during gait: Test-retest reliability and minimal detectable change. *Gait & Posture,* 46**,** 18-25.

Ferrari, A., Benedetti, M. G., Pavan, E., Frigo, C., Bettinelli, D., Rabuffetti, M., Crenna, P. & Leardini, A. 2008. Quantitative comparison of five current protocols in gait analysis. *Gait Posture,* 28**,** 207-16.

Ferrari, A., Cutti, A. G. & Cappello, A. 2010. A new formulation of the coefficient of multiple correlation to assess the similarity of waveforms measured synchronously by different motion analysis protocols. *Gait Posture,* 31**,** 540-2.

Gage, J. 1993. Gait Analysis. An Essential Tool in the Treatment of Cerebral Palsy. *Clin Orthop Related Res,* 288**,** 136-134.

Gage, J. R. & Novacheck, T. F. 2001. An update on the treatment of gait problems in cerebral palsy. *J Pediatr Orthop B,* 10**,** 265-74.

Ganley, K. J. & Powers, C. M. 2004. Anthropometric parameters in children: a comparison of values obtained from dual energy x-ray absorptiometry and cadaver-based estimates. *Gait & Posture,* 19**,** 133-140.

Gillet, C., Duboy, J., Barbier, F., Armand, S., Jeddi, R., Lepoutre, F. X. & Allard, P. 2003. Contribution of accelerated body masses to able-bodied gait. *Am J Phys Med Rehabil,* 82**,** 101-9.

Gough, M. & Shortland, A. P. 2008. Can clinical gait analysis guide the management of ambulant children with bilateral spastic cerebral palsy? *J Pediatr Orthop,* 28**,** 879-83.

Gutierrez, E. M., Bartonek, Å., Haglund-Åkerlind, Y. & Saraste, H. 2003. Characteristic gait kinematics in persons with lumbosacral myelomeningocele. *Gait & Posture,* 18**,** 170-177.

Hara, R., Mcginley, J., Briggs, C., Baker, R. & Sangeux, M. 2016. Predicting the location of the hip joint centres, impact of age group and sex. *Scientific Reports,* 6**,** 37707.

Harada, T., Ebara, S., Anwar, M. M., Kajiura, I., Oshita, S., Hiroshima, K. & Ono, K. 1993. The lumbar spine in spastic diplegia. A radiographic study. *J Bone Joint Surg Br,* 75**,** 534-7.

Harrington, M. E., Zavatsky, A. B., Lawson, S. E., Yuan, Z. & Theologis, T. N. 2007. Prediction of the hip joint centre in adults, children, and patients with cerebral palsy based on magnetic resonance imaging. *J Biomech,* 40**,** 595-602.

Hashish, R., Samarawickrame, S. D. & Salem, G. J. 2014. A comparison of dorsal and heel plate foot tracking methods on lower extremity dynamics. *J Biomech,* 47**,** 1211-4.

Hendershot, B. D. & Wolf, E. J. 2014. Three-dimensional joint reaction forces and moments at the low back during over-ground walking in persons with unilateral lower-extremity amputation. *Clin Biomech (Bristol, Avon),* 29**,** 235-42.

Heyrman, L., Feys, H., Molenaers, G., Jaspers, E., Monari, D., Meyns, P. & Desloovere, K. 2013a. Three-dimensional head and trunk movement characteristics during gait in children with spastic diplegia. *Gait & Posture,* 38**,** 770-776.

Heyrman, L., Feys, H., Molenaers, G., Jaspers, E., Monari, D., Nieuwenhuys, A. & Desloovere, K. 2014. Altered trunk movements during gait in children with spastic diplegia: compensatory or underlying trunk control deficit? *Res Dev Disabil,* 35**,** 2044-52.

Heyrman, L., Feys, H., Molenaers, G., Jaspers, E., Van De Walle, P., Monari, D., Aertbeliën, E. & Desloovere, K. 2013b. Reliability of head and trunk kinematics during gait in children with spastic diplegia. *Gait & Posture,* 37**,** 424-429.

Holden, J. P., Orsini, J. A., Lohmann Siegel, K., Kepple, T. M., Gerber, L. H. & Stanhope, S. J. 1997. Surface movement errors in shank kinematics and knee kinetics during gait. *Gait Posture,* 5**,** 217-227.

Holden, J. P., Selbie, W. S. & Stanhope, S. J. 2003. A proposed test to support the clinical movement analysis laboratory accreditation process. *Gait & Posture,* 17**,** 205-213.

Houck, J. R., Duncan, A. & De Haven, K. E. 2006. Comparison of frontal plane trunk kinematics and hip and knee moments during anticipated and unanticipated walking and side step cutting tasks. *Gait Posture,* 24**,** 314-22.

Jahnsen, R., Villien, L., Aamodt, G., Stanghelle, J. K. & Holm, I. 2004. Musculoskeletal pain in adults with cerebral palsy compared with the general population. *J Rehabil Med,* 36**,** 78-84.

Jensen., R. 1989. Changes in segment inertia proportions between 4 and 20 years. *J Biomech,* 22**,** 529-536.

Johnson, M. B., Goldstein, L., Thomas, S. S., Piatt, J., Aiona, M. & Sussman, M. 2004. Spinal deformity after selective dorsal rhizotomy in ambulatory patients with cerebral palsy. *J Pediatr Orthop,* 24**,** 529-36.

Kapandji, I. 1974. *The Physiology of the Joints: the trunk and the vertebral column,* New York, Churchill Livingstone

Khoo, B., Goh, J. & Bose, K. 1995. A biomechanical model to determine lumbosacral loads during single stance phase in normal gait. *Medical Engineering and Physics***,** 27-35.

Kiernan, D., Malone, A., Obrien, T. & Simms, C. K. 2014a. A 3-dimensional rigid cluster thorax model for kinematic measurements during gait. *J Biomech,* 47**,** 1499-1505.

Kiernan, D., Walsh, M., O'sullivan, R., Fitzgerald, D. & O'brien, T. 2014b. Reliability of the CODA cx1 motion analyser for 3-dimensional gait analysis. *Gait & Posture,* 39**,** S99-S100.

Kiernan, D., Walsh, M., O'sullivan, R., O'brien, T. & Simms, C. K. 2014c. The influence of estimated body segment parameters on predicted joint kinetics during diplegic cerebral palsy gait. *J Biomech,* 47**,** 284-8.

Kingma, I., Toussaint, H. M., Delooza, M. P. & Van Dieen, J. H. 1996. Segment inertial parameter evaluation in two anthropometric models by application of a dynamic linked segment model. *J Biomech,* 29**,** 693-704.

Kirkwood, R., Culham, E. & Costigan, P. 1999. Radiographic and non-invasive determination of the hip joint centre location: effect on hip joint moments. *Clin Biomech (Bristol, Avon),* 14**,** 227-235.

Koman, L. A., Smith, B. P. & Shilt, J. S. 2004. Cerebral palsy. *The Lancet,* 363**,** 1619-1631.

Koman, L. a. M. D., Mooney, J. F. I. I. I. M. D., Smith, B. P. D., Goodman, A. R. N. & Mulvaney, T. L. P. T. 1993. Management of Cerebral Palsy with Botulinum-A Toxin: Preliminary Investigation. *Journal of Pediatric Orthopaedics July/August,* 13**,** 489-495.

Konz, R., Fatone, S., Stine, R., Ganju, A., Gard, S. & Ondra, S. 2006. A Kinematic Model to Assess Spinal Motion During Walking. *Spine,* 31**,** E898-E906.

Krach, L. 2009. Treatment of Spasticity with Intrathecal Baclofen. *In:* GAGE, J. R., SCHWARTZ, M. H., KOOP, S. & NOVACHECK, T. F. (eds.) *The Identification and Treatment of Gait Problems in Cerebral Palsy.* 2nd ed. London: Mac Keith Press.

Krautwurst, B. K., Wolf, S. I., Heitzmann, D. W., Gantz, S., Braatz, F. & Dreher, T. 2013. The influence of hip abductor weakness on frontal plane motion of the trunk and pelvis in patients with cerebral palsy. *Res Dev Disabil,* 34**,** 1198-203.

Krebs, D., Wong, D., Jevsevar, D., Oriley, P. & Hodge, A. 1992. Trunk Kinematics During Locomotor Activities. *Phys Ther,* 72**,** 505-514.

Kuban, K. C. K. & Leviton, A. 1994. Cerebral Palsy. *The New England Journal of Medicine,* 330**,** 188-195.

Lamoth, C., Beek, P. & Meijer, O. 2002. Pelvis-thorax coordination in the transverse plane during gait. *Gait and Posture,* 16**,** 101-114.

Lampe, R., Grassl, S., Mitternacht, J., Gerdesmeyer, L. & Gradinger, R. 2006. MRT-measurements of muscle volumes of the lower extremities of youths with spastic hemiplegia caused by cerebral palsy. *Brain and Development,* 28**,** 500-506.

Lariviere, C. & Gagnon, D. 1999. The L5/S1 joint moment sensitivity to measurement errors in dynamic 3D multisegment lifting models. *Human Movement Science,* 18**,** 573-587.

Leardini, A., Biagi, F., Belvedere, C. & Benedetti, M. G. 2009. Quantitative comparison of current models for trunk motion in human movement analysis. *Clin Biomech (Bristol, Avon),* 24**,** 542-50.

Leardini, A., Biagi, F., Merlo, A., Belvedere, C. & Benedetti, M. G. 2011. Multi-segment trunk kinematics during locomotion and elementary exercises. *Clin Biomech (Bristol, Avon),* 26**,** 562-71.

Leardini, A., Cappazzo, A., Catani, F., Toksvig-Larsen, S., Petitto, A., Sforza, V., Cassanelli, G. & Giannini, S. 1999. Validation of a functional method for the estimation of hip joint centre location. *J Biomech,* 32**,** 99-103.

Leardini, A., Chiari, L., Della Croce, U. & Cappozzo, A. 2005. Human movement analysis using stereophotogrammetry. Part 3. Soft tissue artifact assessment and compensation. *Gait Posture,* 21**,** 212-25.

Leteneur, S., Gillet, C., Sadeghi, H., Allard, P. & Barbier, F. 2009. Effect of trunk inclination on lower limb joint and lumbar moments in able men during the stance phase of gait. *Clin Biomech (Bristol, Avon),* 24**,** 190-5.

Levine, D. & Whittle, M. W. 1996. The effects of pelvic movement on lumbar lordosis in the standing position. *J Orthop Sports Phys Ther,* 24**,** 130-5.

Lewis, A., Stewart, C., Postans, N. & Trevelyan, J. 2007. Development of an instrumented pole test for use as a gait laboratory quality check. *Gait Posture,* 26**,** 317-22.

Little, W. J. 1844. COURSE OF LECTURES ON THE DEFORMITIES OF THE HUMAN FRAME. *The Lancet,* 41**,** 809-815.

Liu, J., Li, S., Lin, Q. & Li, Z. 1999. Prevalence of cerebral palsy in China. *International Journal of Epidemiology,* 28**,** 949-954.

Lu, T. W. & O'connor, J. J. 1999. Bone position estimation from skin marker co-ordinates using global optimisation with joint constraints. *J Biomech,* 32**,** 129-34.

Lucchetti, L., Cappozzo, A., Cappello, A. & Croce, U. D. 1998. Skin movement artefact assessment and compensation in the estimation of knee-joint kinematics. *Journal of Biomechanics,* 31**,** 977-984.

Mac Keith, R., Mackenzie, I. & Polani, P. 1959. Definition of Cerebral Palsy. *Dev Med Child Neurol,* 1**,** 23.

Marey, E. J. 1874. *Animal mechanism: a treatise on terrestrial and aerial locomotion,* London, HS King.

Marey, E. J. 1883. De la mesure dans les differents acts de la locomotion. *Comptes Rendues de l'Academie des Sciences de Paris,* 97**,** 820-825.

Mason, D. L., Preece, S. J., Bramah, C. A. & Herrington, L. C. 2014. Reproducibility of kinematic measures of the thoracic spine, lumbar spine and pelvis during fast running. *Gait & Posture*.

Mccarthy, J. J. & Betz, R. R. 2000. The relationship between tight hamstrings and lumbar hypolordosis in children with cerebral palsy. *Spine (Phila Pa 1976),* 25**,** 211-3.

Mccaw, S. & Devita, P. 1995. Errors in alignment of centre of pressure and foot coordinates affect predicted lower extremity torques. *Journal of Biomechanics,* 28**,** 985-988.

Metaxiotis, D., Accles, W., Siebel, A. & Doederlein, L. 2000. Hip deformities in walking patients with cerebral palsy. *Gait & Posture,* 11**,** 86-91.

Minear, W. 1956. A classification of Cerebral Palsy. *Pediatrics,* 18**,** 841-852.

Mitnitski, A., Yahia, L., Newman, N., Gracovetsky, S. & Feldman, A. 1998. Coordination between the lumbar spine lordosis and trunk angle during weight lifting. *Clin Biomech (Bristol, Avon),* 13**,** 121-127.

Molenaers, G. & Desloovere, K. 2009. Pharmacologic Treatment with Botulinum Toxin. *In:* GAGE, J. R., SCHWARTZ, M. H., KOOP, S. & NOVACHECK, T. F. (eds.) *The Identification and Treatment of Gait Problems in Cerebral Palsy.* 2nd ed. London: Mac Keith Press.

Molloy, M., Mcdowell, B. C., Kerr, C. & Cosgrove, A. P. 2010. Further evidence of validity of the Gait Deviation Index. *Gait Posture,* 31**,** 479-82.

Moreau, N. G., Teefey, S. A. & Damiano, D. L. 2009. In vivo muscle architecture and size of the rectus femoris and vastus lateralis in children and adolescents with cerebral palsy. *Developmental Medicine & Child Neurology,* 51**,** 800-806.

Murr, S. & Walt, K. 2009. Physical Therapy. *In:* GAGE, J. R., SCHWARTZ, M. H., KOOP, S. & NOVACHECK, T. F. (eds.) *The Identification and Treatment of Gait Problems in Cerebral Palsy.* 2nd ed. London: Mac Keith Press.

Mutch, L., Alberman, E., Hagberg, B., Kodama, K. & Velickovic, M. 1992. Cerebral Palsy Epidemiology: Where are we now and where are we going? *Dev Med Child Neurol,* 34**,** 547-555.

Needham, R., Naemi, R. & Chockalingam, N. 2014. Quantifying lumbar-pelvis coordination during gait using a modified vector coding technique. *J Biomech,* 47**,** 1020-6.

Nguyen, T. C. & Baker, R. 2004. Two methods of calculating thorax kinematics in children with myelomeningocele. *Clin Biomech (Bristol, Avon),* 19**,** 1060-5.

Niiler, T. & Riad, J. 2012. A comparison of shank segment parameters between hemi-plegic and typically developing individuals. *Gait & Posture,* 36**,** s1-s101.

Novacheck, T. F., Kroll, G. J., Gent, G., Rozumalski, A., Beattie, C. & Schwartz, M. H. 2009. Orthoses. *In:* GAGE, J. R., SCHWARTZ, M. H., KOOP, S. & NOVACHECK, T. F. (eds.) *The Identification and Treatment of Gait Problems in Cerebral Palsy.* 2nd ed. London: Mac Keith Press.

O'byrne, J., Jenkinson, A. & O'brien, T. 1998. Quantitative analysis and classification of gait patterns in cerebral palsy using a three-dimensional motion analyser. *J Child Neurol,* 13**,** 101-108.

O'sullivan, K., Clifford, A. & Hughes, L. 2010a. The reliability of the CODA motion analysis system for lumbar spine analysis: a pilot study. *Physiotherapy Ireland,* 31**,** 16-22.

O'sullivan, R., Walsh, M., Jenkinson, A. & O'brien, T. 2007. Factors associated with pelvic retraction during gait in cerebral palsy. *Gait Posture,* 25**,** 425-31.

O'sullivan, R., Walsh, M., Kiernan, D. & O'brien, T. 2010b. The knee kinematic pattern associated with disruption of the knee extensor mechanism in ambulant patients with diplegic cerebral palsy. *Clin Anat,* 23**,** 586-92.

Olsen, E., Pfau, T. & Ritz, C. 2013. Functional limits of agreement applied as a novel method comparison tool for accuracy and precision of inertial measurement unit derived displacement of the distal limb in horses. *J Biomech,* 46**,** 2320-5.

Õunpuu, S., Davis, R. B. & Deluca, P. A. 1996. Joint kinetics: methods, interpretation and treatment decision-making in children with cerebral palsy and myelomeningocele. *Gait & Posture,* 4**,** 62-78.

Ounpuu, S., Thomason, P., Harvey, A. & Graham, H. K. 2009. Classification of Cerebral Palsy and patterns of gait pathology. *In:* GAGE, J. R., SCHWARTZ, M. H., KOOP, S. & NOVACHECK, T. F. (eds.) *The Identification and Treatment of Gait Problems in Cerebral Palsy.* 2nd ed. London: Mac Keith Press.

Palisano, R., Rosenbaum, P., Walter, S., Russell, D., Wood, E. & Galuppi, B. 1997. Development and reliability of a system to classify gross motor function in children with cerebral palsy. *Dev Med Child Neurol,* 39**,** 214-23.

Patrick, J. H. 1991. Use of movement analysis in understanding abnormalities of gait in cerebral palsy. *Arch Dis Child,* 66**,** 900-3.

Patrick, J. H. 2003. Case for gait analysis as part of the management of incomplete spinal cord injury. *Spinal Cord,* 41**,** 479-82.

Paul, J. P. 1966. Paper 8: Forces Transmitted by Joints in the Human Body. *Proceedings of the Institution of Mechanical Engineers, Conference Proceedings,* 181**,** 8-15.

Pearsall, D. & Costigan, P. 1999. The effect of segment parameter error on gait analysis results. *Gait & Posture,* 9**,** 173-183.

Perry, J. 1992. *Gait analysis,* Thornofare, NJ, SLACK.

Peters, A., Baker, R., Morris, M. E. & Sangeux, M. 2012. A comparison of hip joint centre localisation techniques with 3-DUS for clinical gait analysis in children with cerebral palsy. *Gait Posture,* 36**,** 282-6.

Peters, A., Galna, B., Sangeux, M., Morris, M. & Baker, R. 2010. Quantification of soft tissue artifact in lower limb human motion analysis: a systematic review. *Gait Posture,* 31**,** 1-8.

Pharoah, P., Cooke, T., Johnson, M., King, R. & Mutch, L. 1998. Epidemiology of cerebral palsy in England and Scotland, 1984–9. *Arch Dis Child Fetal Neonatal Ed,* 79**,** F21-F25.

Piazza, S., N., O. & Cavanagh, P. 2001. Accuracy of the functional method of hip joint center location: effect of limited motion and varied implementation. *J Biomech,* 34**,** 967-973.

Pin, T., Dyke, P. & Chan, M. 2006. The effectiveness of passive stretching in children with cerebral palsy. *Dev Med Child Neurol,* 48**,** 855-62.

Pratt, E. J., Dickens, W. & Bell, M. 2012. 3D thorax kinematics during gait in children with cerebral palsy (Abstract). *Gait Posture,* 36**,** S1-S101.

Rao, G., Amarantini, D., Berton, E. & Favier, D. 2006. Influence of body segments' parameters estimation models on inverse dynamics solutions during gait. *J Biomech,* 39**,** 1531-6.

Reed, M., Manary, M. & Schneider, L. 1999. Method for measuring and representing automobile occupant posture. *SAE Technical Paper Series* 1999-01-0959**,** 1-15.

Rice, J., Kaliszer, M., Walsh, M., Jenkinson, A. & O'brien, T. 2004. Movements at the low back during normal walking. *Clin Anat,* 17**,** 662-6.

Rice, J., Walsh, M., Jenkinson, A. & O'brien, T. 2002. Measuring movement at the low back. *Clinical Anatomy,* 15**,** 88-92.

Riemer, R., Hsiao-Wecksler, E. T. & Zhang, X. 2008. Uncertainties in inverse dynamics solutions: a comprehensive analysis and an application to gait. *Gait & Posture,* 27**,** 578-88.

Rivest, L. P. 2005. A correction for axis misalignment in the joint angle curves representing knee movement in gait analysis. *J Biomech,* 38**,** 1604-11.

Roislien, J., Rennie, L. & Skaaret, I. 2012a. Functional limits of agreement: a method for assessing agreement between measurements of gait curves. *Gait & Posture,* 36**,** 495-9.

Roislien, J., Skare, O., Opheim, A. & Rennie, L. 2012b. Evaluating the properties of the coefficient of multiple correlation (CMC) for kinematic gait data. *J Biomech,* 45**,** 2014-8.

Romkes, J., Peeters, W., Oosterom, A., Molenaar, S., Bakels, I. & Brunner, R. 2007. Evaluating upper body movements during gait in healthy children and children with diplegic cerebral palsy. *J Pediatr Orthop B,* 16**,** 175-180.

Rosenbaum, P., Paneth, N., Leviton, A., Goldstein, M., Bax, M., Damiano, D., Dan, B. & Jacobsson, B. 2007. A report: the definition and classification of cerebral palsy April 2006. *Dev Med Child Neurol,* 49**,** 8-14.

Rozumalski, A. & Schwartz, M. H. 2011. The GDI-Kinetic: a new index for quantifying kinetic deviations from normal gait. *Gait Posture,* 33**,** 730-2.

Salazar-Torres, J. J., Mcdowell, B. C., Kerr, C. & Cosgrove, A. P. 2011. Pelvic kinematics and their relationship to gait type in hemiplegic cerebral palsy. *Gait Posture,* 33**,** 620-4.

Sangeux, M. 2015. On the implementation of predictive methods to locate the hip joint centres. *Gait Posture*.

Sangeux, M., Peters, A. & Baker, R. 2011. Hip joint centre localization: Evaluation on normal subjects in the context of gait analysis. *Gait Posture,* 34**,** 324-8.

Sangeux, M., Pillet, H. & Skalli, W. 2014. Which method of hip joint centre localisation should be used in gait analysis? *Gait Posture,* 40**,** 20-5.

Schache, A., Blanch, P., Rath, D., Wrigley, T., Starr, R. & Bennell, K. 2002. Intra-subject repeatability of the three dimensional angular kinematics within the lumbo-pelvic-hip complex during running. *Gait & Posture,* 15**,** 136-145.

Schmiedmayer, H. B. & Kastner, J. 1999. Parameters influencing the accuracy of the point of force application determined with piezoelectric force plates. *J Biomech,* 32**,** 1237-42.

Schröter, J., Güth, V., Overbeck, M., Rosenbaum, D. & Winkelmann, W. 1999. The 'Entlastungsgang'. A hip unloading gait as a new conservative therapy for hip pain in the adult. *Gait & Posture,* 9**,** 151-157.

Schutte, L. M., Narayanan, U., Stout, J. L., Selber, P., Gage, J. & Schwartz, M. 2000. An index for quantifying deviations from normal gait. *Gait and Posture,* 11**,** 25-31.

Schwartz, M. H. & Rozumalski, A. 2008. The Gait Deviation Index: a new comprehensive index of gait pathology. *Gait Posture,* 28**,** 351-7.

Schwartz, M. H., Trost, J. P. & Wervey, R. A. 2004. Measurement and management of errors in quantitative gait data. *Gait & Posture,* 20**,** 196-203.

Seay, J., Selbie, W. S. & Hamill, J. 2008. In vivo lumbo-sacral forces and moments during constant speed running at different stride lengths. *J Sports Sci,* 26**,** 1519-29.

Shortland, A. 2009. Muscle deficits in cerebral palsy and early loss of mobility: can we learn something from our elders? *Dev Med Child Neurol,* 51 Suppl 4**,** 59-63.

Silva, M. P. T. & Ambrósio, J. a. C. 2004. Sensitivity of the results produced by the inverse dynamic analysis of a human stride to perturbed input data. *Gait & Posture,* 19**,** 35-49.

Soderkvist, I. & Wedin, P. A. 1993. Determining the movements of the skeleton using well-configured markers. *J Biomech,* 26**,** 1473-7.
Soul, J. S., Hammer, P. E., Tsuji, M., Saul, J. P., Bassan, H., Limperopoulos, C., Disalvo, D. N., Moore, M., Akins, P., Ringer, S., Volpe, J. J., Trachtenberg, F. & Du Plessis, A. J. 2007. Fluctuating pressure-passivity is common in the cerebral circulation of sick premature infants. *Pediatr Res,* 61**,** 467-73.
Stagni, R., Leardini, A., Cappazzo, A., Benedetti, M. G. & Cappello, A. 2000. Effects of hip joint centre mislocation on gait analysis results. *J Biomech,* 33**,** 1479-1487.
Stanley, F., Blair, E. & Alberman, E. 2000. *Cerebral palsies: epidemology and causal pathways,* London, Mac Keith Press.
Stief, F., Bohm, H., Ebert, C., Doderlein, L. & Meurer, A. 2014. Effect of compensatory trunk movements on knee and hip joint loading during gait in children with different orthopedic pathologies. *Gait Posture,* 39**,** 859-64.
Su, F. C., Lai, K. A. & Hong, W. H. 1998. Rising from chair after total knee arthroplasty. *Clin Biomech (Bristol, Avon),* 13**,** 176-181.
Sutherland, D. H. 2001. The evolution of clinical gait analysis part 1: kinesiological EMG. *Gait & Posture,* 14**,** 61-70.
Sutherland, D. H. 2002. The evolution of clinical gait analysis -Part II Kinematics. *Gait & Posture,* 16**,** 159-179.
Sutherland, D. H., Kaufman, K. R., Wyatt, M. P., Chambers, H. G. & Mubarak, S. J. 1999. Double-blind study of botulinum A toxin injections into the gastrocnemius muscle in patients with cerebral palsy. *Gait & Posture,* 10**,** 1-9.
Svehlik, M., Kraus, T., Steinwender, G., Zwick, E. B. & Linhart, W. E. 2012. Pathological gait in children with Legg-Calve-Perthes disease and proposal for gait modification to decrease the hip joint loading. *Int Orthop,* 36**,** 1235-41.
Thorngren-Jerneck, K. & Herbst, A. 2006. Perinatal Factors Associated With Cerebral Palsy in Children Born in Sweden. *Obstet Gynecol,* 108**,** 1499-1505.
Trendelenburg, F. 1895. Ueber denGang bei angeborener Huftgelenksluxation (On the gait of people with congenital dislocation of the hip). *Deutsche medizinische wochenschrift,* 2**,** 21-24.
Ward, M. 2009. Pharmacologic Treatment with Oral Medications. *In:* GAGE, J. R., SCHWARTZ, M. H., KOOP, S. & NOVACHECK, T. F. (eds.) *The Identification and Treatment of Gait Problems in Cerebral Palsy.* 2nd ed. London: Mac Keith Press.
Westhoff, B., Petermann, A., Hirsch, M. A., Willers, R. & Krauspe, R. 2006. Computerized gait analysis in Legg Calve Perthes disease--analysis of the frontal plane. *Gait Posture,* 24**,** 196-202.
Whittle, M. & Levine, D. 1999. Three-dimensional relationships between the movements of the pelvis and the lumbar spine during normal gait. *Human Movement Science,* 18**,** 681-692.
Willoughby, K. L., Dodd, K. J. & Shields, N. 2009. A systematic review of the effectiveness of treadmill training for children with cerebral palsy. *Disabil Rehabil,* 31**,** 1971-9.
Winter, D. 2009. Biomechanics and motor control of human movement. *Wiley: New Jersey,* 4th ed.
Winters, T., Gage, J. & Hicks, R. 1987. Gait patterns in spastic hemiplegia in children and young adults. *J Bone Joint Surg Am,* 69**,** 437-441.
Wolff, J. 1892. *Das Gesetz der Transformation der Knoche,* Hirschwald, Berlin.

Wren, T., Rethlefsen, S. & Kay, R. 2005. Prevalence of Specific Gait Abnormalities in Children with Cerebral Palsy. *J Pediatr Orthop* 25**,** 79-83.

Wu, G., Siegler, S., Allard, P., Kirtley.C., Leardini, A., Rosenbaum, D., Whittle, M., D'lima, D., Cristofolini, L., Witte, H., Schmid, O. & Stokes, I. 2002. ISB recommendation on definitions of joint coordinate system of various joints for the reporting of human joint motion—part I: ankle, hip, and spine. *J Biomech,* 35**,** 543-548.

Wu, G., Van Der Helm, F. C., Veeger, H., Makhsous, M., Van Roy, P., Anglin, C., Nagels, J., Karduna, A., Mcquade, K., Wang, X., Werner, F. & Buchholz, B. 2005. ISB recommendations on definitions of joint coordinate systems of various joints for the reporting of human joint motion - Part II: shoulder, elbow, wrist and hand. *Journal of Biomechanics,* 38**,** 981-992.

Wu, W., Meijer, O. G., Lamoth, C. J., Uegaki, K., Van Dieen, J. H., Wuisman, P. I., De Vries, J. I. & Beek, P. J. 2004. Gait coordination in pregnancy: transverse pelvic and thoracic rotations and their relative phase. *Clin Biomech (Bristol, Avon),* 19**,** 480-8.

Appendices

Appendix 5.1: Approval letter from CRC Ethics Committee

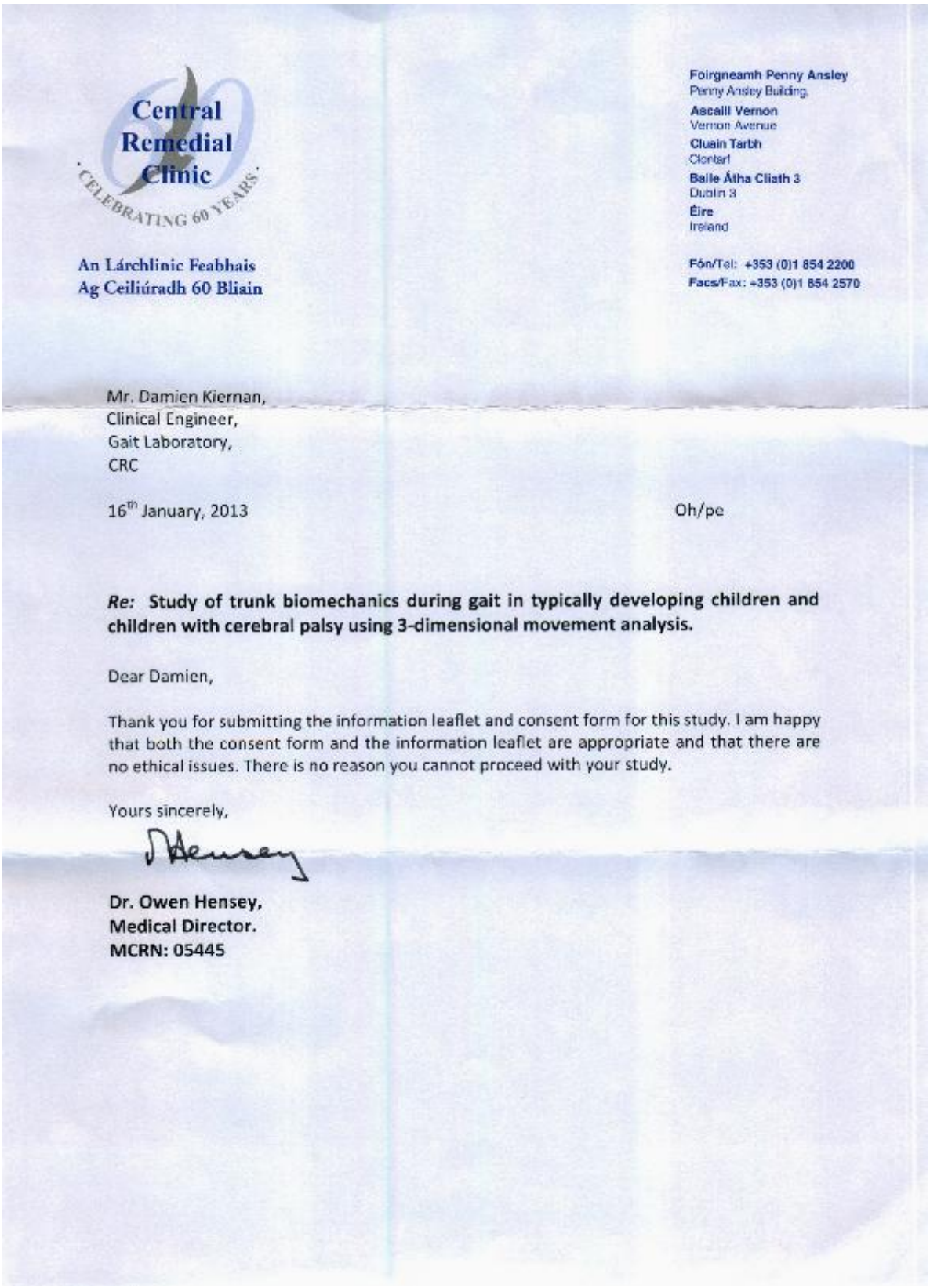

Central Remedial Clinic
CELEBRATING 60 YEARS

An Lárchlinic Feabhais
Ag Ceiliúradh 60 Bliain

Foirgneamh Penny Ansley
Penny Ansley Building
Ascaill Vernon
Vernon Avenue
Cluain Tarbh
Clontarf
Baile Átha Cliath 3
Dublin 3
Éire
Ireland

Fón/Tel: +353 (0)1 854 2200
Facs/Fax: +353 (0)1 854 2570

Mr. Damien Kiernan,
Clinical Engineer,
Gait Laboratory,
CRC

16th January, 2013

Oh/pe

Re: **Study of trunk biomechanics during gait in typically developing children and children with cerebral palsy using 3-dimensional movement analysis.**

Dear Damien,

Thank you for submitting the information leaflet and consent form for this study. I am happy that both the consent form and the information leaflet are appropriate and that there are no ethical issues. There is no reason you cannot proceed with your study.

Yours sincerely,

Dr. Owen Hensey,
Medical Director.
MCRN: 05445

Appendix 5.2: Participant Information Leaflet

Gait Laboratory Trunk Project

Participant Information Leaflet

Study Title

A study of trunk biomechanics during gait in typically developing children and children with cerebral palsy using 3-dimensional movement analysis

Investigators

Mr. Damien Kiernan, Clinical Engineer, Gait Laboratory, CRC.
Prof. Tim O'Brien, Consultant Orthopaedic Surgeon & Gait Laboratory Director
Dr. Ciaran Simms, Bioengineer, Trinity Centre for Bioengineering, Trinity College Dublin.

Contact Details

Mr. Damien Kiernan, Gait Laboratory, Central Remedial Clinic, Vernon Ave, Clontarf, Dublin 3
Email: dkiernan@crc.ie. Tel: 01-8542467

Introduction

Your child is invited to take part in a clinical research study at the Gait Laboratory in the Central Remedial Clinic (CRC). Before you decide whether he or she will take part, please read the information provided below carefully and, if you wish, discuss it with your family. Take time to ask questions.

You should clearly understand the risks and benefits of taking part in this study so that you can make a decision that is right for your child. This process is known as 'Informed Consent'.

Your child does not have to take part in this study. If you decide not to take part it will not affect your child's future care at the CRC.

Why is this study taking place?

Children with Cerebral Palsy (CP) often experience difficulties walking and as a result of this their upper body can move in unexpected ways. This study will assess how the trunk (the part of the body between the waist and the neck, excluding the arms) moves in children with CP, compared to children who do not have CP. The information will help healthcare professionals who work with children with CP to understand and manage these unexpected movements.

Who is organising and funding this study?

This study is organised by the staff members of the Gait Laboratory in the CRC in conjunction with the Trinity Centre for Bioengineering, Trinity College Dublin as part of the requirements for a PhD undertaken by Damien Kiernan. Damien Kiernan has received funding from the CRC Scientific and Research Trust to conduct this project as part of his PhD.

Why has my child been invited to take part?

Your child has been invited to take part because:

- your child has CP and may have compensatory trunk movements that would benefit from this assessment,

OR

- your child has normal gait and their abilities will be a valuable comparison for children with CP.

How will the study be carried out?

This study will be carried out in the Gait Laboratory at the CRC. Children with CP and children without CP will be invited to participate.

CP children will attend the Gait Laboratory as part of their scheduled assessment and on arrival the child and their parents will be asked if they would like to participate in the study.

If they agree, the assessment will continue as normal and the data captured during the assessment will be used as part of the research study.

Children without CP will be recruited through staff members in the CRC. This assessment will take approximately 45 minutes. The assessment will consist of:

1. Measurement of height, weight, leg length and width of the pelvis, knees and ankles.
2. Placement of markers consisting of small light-emitting diodes (LEDs) on the child's legs and upper back (these will be placed with sticky tape).
3. Walking up and down the lab walkway.

Finally, the markers will be removed. Your child will have close supervision at all times in case he or she becomes unsteady. A video will be recorded during the assessment for quality.

What are the benefits of taking part in the study?

If your child has CP, the information from this assessment will help to measure his or her trunk movements in detail. This will guide your child's physiotherapist in choosing the best strategies to improve movement and make progress in therapy, both for your child and for children with similar problems.

Children without CP will not gain a direct benefit for themselves however their participation will help to provide better care for other children with CP who do have movement problems.

What are the risks of taking part in the study?

This study has no significant risks however the markers for the analysis system are applied with sticky tape, similar to a "Band-Aid", and your child may find them a little uncomfortable when they are removed.

Is the study confidential?

When your child participates in the study, his or her identity and diagnosis (if any) will be known to only the research staff. Any information arising from the assessment that may help your child, for example, information on balance for his or her physiotherapist, will be shared only with your permission and only for the purpose of improving your child's care.
Your child's data (information on their trunk movements) will be stored securely on a database. Their details will be linked to a confidential code instead of their name. Their identity (including any other identifying details, such as address or date of birth) will not be revealed to people outside the study. When the results of the study are published or presented, your child will not be identified. Instead, summaries of the results for all children with and without CP will be presented and compared.

A video of your child performing walking will be recorded. This is to help with the interpretation of the results afterwards. This video will be stored securely, with a code instead of your child's name to protect their identity. Videos will only be viewed by the research team and will not be released to people outside the study.

In some cases, we may request permission to present your child's video to other healthcare professionals for teaching at conferences or courses where there is a learning benefit to these people. We will seek your permission specifically for this purpose. You have the right to decline this request.

Where can I get further information?

Please contact Damien Kiernan, Clinical Engineer at dkiernan@crc.ie 01-8542467 if you have any questions.

Appendix 5.3: Participant Consent Form

Gait Laboratory Trunk Project

Participant Consent Form

Study title: A study of trunk biomechanics during gait in typically developing children and children with cerebral palsy using 3-dimensional movement analysis

I have read and understood the **Information Leaflet** about this research project. The information has been fully explained to me and I have been able to ask questions, all of which have been answered to my satisfaction.	**Yes** ☐	**No** ☐
I understand that my child doesn't have to take part in this study and can opt out at any time. I understand that I don't have to give a reason for opting out and I understand that opting out won't affect my child's future care.	**Yes** ☐	**No** ☐
I am aware of any potential risks of this research study.	**Yes** ☐	**No** ☐
I have been assured that information about my child will be kept private and confidential.	**Yes** ☐	**No** ☐
I have been given a copy of the Information Leaflet for my records.	**Yes** ☐	**No** ☐
Storage and future use of information: I give my permission for information collected about my child to be used in *related studies in the future* but only if the research is approved by a Research Ethics Committee.	**Yes** ☐	**No** ☐

Child's name	**Parent / guardian name**	**Parent / guardian signature**	**Date**

To be completed by the Principal Investigator or nominee.
I, the undersigned, have taken the time to fully explain to the above participant the nature and purpose of this study. I have explained the risks involved as well as the possible benefits. I have invited them to ask questions on any aspect of the study that concerned them.

Name (Block Capitals)	**Qualifications**	**Signature**	**Date**

Participant Consent Form v1.1 dKiernan 14/01/2013

Appendix 5.4: Visual 3D Pipeline Script for Model Calculations

Left Side Computations	*Right Side Computations*
Compute_Model_Based_Data /RESULT_NAME=LeftPelvis /FUNCTION=JOINT_ANGLE /SEGMENT=RPV /REFERENCE_SEGMENT=Virtual Lab /RESOLUTION_COORDINATE_SYSTEM= ! /USE_CARDAN_SEQUENCE=FALSE ! /NORMALIZATION=FALSE ! /NORMALIZATION_METHOD= ! /NORMALIZATION_METRIC= /NEGATEX=TRUE ! /NEGATEY=FALSE /NEGATEZ=TRUE ! /AXIS1=X ! /AXIS2=Y ! /AXIS3=Z ;	Compute_Model_Based_Data /RESULT_NAME=RightPelvis /FUNCTION=JOINT_ANGLE /SEGMENT=RPV /REFERENCE_SEGMENT=Virtual Lab /RESOLUTION_COORDINATE_SYSTEM= ! /USE_CARDAN_SEQUENCE=FALSE ! /NORMALIZATION=FALSE ! /NORMALIZATION_METHOD= ! /NORMALIZATION_METRIC= /NEGATEX=TRUE /NEGATEY=TRUE ! /NEGATEZ=FALSE ! /AXIS1=X ! /AXIS2=Y ! /AXIS3=Z ;
Compute_Model_Based_Data /RESULT_NAME=LeftHip /FUNCTION=JOINT_ANGLE /SEGMENT=LTH /REFERENCE_SEGMENT=RPV /RESOLUTION_COORDINATE_SYSTEM= ! /USE_CARDAN_SEQUENCE=FALSE ! /NORMALIZATION=FALSE ! /NORMALIZATION_METHOD= ! /NORMALIZATION_METRIC= ! /NEGATEX=FALSE /NEGATEY=TRUE /NEGATEZ=TRUE /AXIS1=Z ! /AXIS2=Y /AXIS3=X ;	Compute_Model_Based_Data /RESULT_NAME=RightHip /FUNCTION=JOINT_ANGLE /SEGMENT=RTH /REFERENCE_SEGMENT=RPV /RESOLUTION_COORDINATE_SYSTEM= ! /USE_CARDAN_SEQUENCE=FALSE ! /NORMALIZATION=FALSE ! /NORMALIZATION_METHOD= ! /NORMALIZATION_METRIC= ! /NEGATEX=FALSE ! /NEGATEY=FALSE ! /NEGATEZ=FALSE /AXIS1=Z ! /AXIS2=Y /AXIS3=X ;
Compute_Model_Based_Data /RESULT_NAME=LeftKnee /FUNCTION=JOINT_ANGLE /SEGMENT=LSK /REFERENCE_SEGMENT=LTH /RESOLUTION_COORDINATE_SYSTEM= ! /USE_CARDAN_SEQUENCE=FALSE ! /NORMALIZATION=FALSE ! /NORMALIZATION_METHOD= ! /NORMALIZATION_METRIC= /NEGATEX=TRUE /NEGATEY=TRUE	Compute_Model_Based_Data /RESULT_NAME=RightKnee /FUNCTION=JOINT_ANGLE /SEGMENT=RSK /REFERENCE_SEGMENT=RTH /RESOLUTION_COORDINATE_SYSTEM= ! /USE_CARDAN_SEQUENCE=FALSE ! /NORMALIZATION=FALSE ! /NORMALIZATION_METHOD= ! /NORMALIZATION_METRIC= /NEGATEX=TRUE ! /NEGATEY=FALSE

/NEGATEZ=TRUE /AXIS1=Z ! /AXIS2=Y /AXIS3=X ;	! /NEGATEZ=FALSE /AXIS1=Z ! /AXIS2=Y /AXIS3=X ;
Compute_Model_Based_Data /RESULT_NAME=LeftFoot /FUNCTION=JOINT_ANGLE /SEGMENT=LMF /REFERENCE_SEGMENT=LSK /RESOLUTION_COORDINATE_SYSTEM= ! /USE_CARDAN_SEQUENCE=FALSE ! /NORMALIZATION=FALSE ! /NORMALIZATION_METHOD= ! /NORMALIZATION_METRIC= ! /NEGATEX=FALSE /NEGATEY=TRUE /NEGATEZ=TRUE /AXIS1=Y /AXIS2=Z /AXIS3=X ;	Compute_Model_Based_Data /RESULT_NAME=RightFoot /FUNCTION=JOINT_ANGLE /SEGMENT=RMF /REFERENCE_SEGMENT=RSK /RESOLUTION_COORDINATE_SYSTEM= ! /USE_CARDAN_SEQUENCE=FALSE ! /NORMALIZATION=FALSE ! /NORMALIZATION_METHOD= ! /NORMALIZATION_METRIC= ! /NEGATEX=FALSE ! /NEGATEY=FALSE ! /NEGATEZ=FALSE /AXIS1=Y /AXIS2=Z /AXIS3=X ;
Compute_Model_Based_Data /RESULT_NAME=Left Hip Moment /FUNCTION=JOINT_MOMENT /SEGMENT=LTH /REFERENCE_SEGMENT= /RESOLUTION_COORDINATE_SYSTEM=RPV ! /USE_CARDAN_SEQUENCE=FALSE /NORMALIZATION=TRUE /NORMALIZATION_METHOD=DEFAULT_NOR MALIZATION ! /NORMALIZATION_METRIC= /NEGATEX=TRUE ! /NEGATEY=FALSE ! /NEGATEZ=FALSE ! /AXIS1=X ! /AXIS2=Y ! /AXIS3=Z ;	Compute_Model_Based_Data /RESULT_NAME=Right Hip Moment /FUNCTION=JOINT_MOMENT /SEGMENT=RTH /REFERENCE_SEGMENT= /RESOLUTION_COORDINATE_SYSTEM=RPV ! /USE_CARDAN_SEQUENCE=FALSE /NORMALIZATION=TRUE /NORMALIZATION_METHOD=DEFAULT_NOR MALIZATION ! /NORMALIZATION_METRIC= /NEGATEX=TRUE /NEGATEY=TRUE /NEGATEZ=TRUE ! /AXIS1=X ! /AXIS2=Y ! /AXIS3=Z ;
Compute_Model_Based_Data /RESULT_NAME=Left Knee Moment /FUNCTION=JOINT_MOMENT /SEGMENT=LSK /REFERENCE_SEGMENT= /RESOLUTION_COORDINATE_SYSTEM=LTH ! /USE_CARDAN_SEQUENCE=FALSE /NORMALIZATION=TRUE /NORMALIZATION_METHOD=DEFAULT_NOR MALIZATION ! /NORMALIZATION_METRIC= ! /NEGATEX=FALSE	Compute_Model_Based_Data /RESULT_NAME=Right Knee Moment /FUNCTION=JOINT_MOMENT /SEGMENT=RSK /REFERENCE_SEGMENT= /RESOLUTION_COORDINATE_SYSTEM=RTH ! /USE_CARDAN_SEQUENCE=FALSE /NORMALIZATION=TRUE /NORMALIZATION_METHOD=DEFAULT_NOR MALIZATION ! /NORMALIZATION_METRIC= ! /NEGATEX=FALSE

! /NEGATEY=FALSE /NEGATEZ=TRUE ! /AXIS1=X ! /AXIS2=Y ! /AXIS3=Z ;	/NEGATEY=TRUE ! /NEGATEZ=FALSE ! /AXIS1=X ! /AXIS2=Y ! /AXIS3=Z ;
Compute_Model_Based_Data /RESULT_NAME=Left Ankle Moment /FUNCTION=JOINT_MOMENT /SEGMENT=LFT /REFERENCE_SEGMENT= /RESOLUTION_COORDINATE_SYSTEM=LSK ! /USE_CARDAN_SEQUENCE=FALSE /NORMALIZATION=TRUE /NORMALIZATION_METHOD=DEFAULT_NOR MALIZATION ! /NORMALIZATION_METRIC= /NEGATEX=TRUE ! /NEGATEY=FALSE /NEGATEZ=TRUE ! /AXIS1=X ! /AXIS2=Y ! /AXIS3=Z ;	Compute_Model_Based_Data /RESULT_NAME=Right Ankle Moment /FUNCTION=JOINT_MOMENT /SEGMENT=RFT /REFERENCE_SEGMENT= /RESOLUTION_COORDINATE_SYSTEM=RSK ! /USE_CARDAN_SEQUENCE=FALSE /NORMALIZATION=TRUE /NORMALIZATION_METHOD=DEFAULT_NOR MALIZATION ! /NORMALIZATION_METRIC= /NEGATEX=TRUE /NEGATEY=TRUE ! /NEGATEZ=FALSE ! /AXIS1=X ! /AXIS2=Y ! /AXIS3=Z ;
Compute_Model_Based_Data /RESULT_NAME=Left Trunk_Pel /FUNCTION=JOINT_ANGLE /SEGMENT=Trunk /REFERENCE_SEGMENT=RPV /RESOLUTION_COORDINATE_SYSTEM= ! /USE_CARDAN_SEQUENCE=FALSE ! /NORMALIZATION=FALSE ! /NORMALIZATION_METHOD= ! /NORMALIZATION_METRIC= /NEGATEX=TRUE /NEGATEY=TRUE /NEGATEZ=TRUE ! /AXIS1=X ! /AXIS2=Y ! /AXIS3=Z ;	Compute_Model_Based_Data /RESULT_NAME=Right Trunk_Pel /FUNCTION=JOINT_ANGLE /SEGMENT=Trunk /REFERENCE_SEGMENT=RPV /RESOLUTION_COORDINATE_SYSTEM= ! /USE_CARDAN_SEQUENCE=FALSE ! /NORMALIZATION=FALSE ! /NORMALIZATION_METHOD= ! /NORMALIZATION_METRIC= /NEGATEX=TRUE ! /NEGATEY=FALSE ! /NEGATEZ=FALSE ! /AXIS1=X ! /AXIS2=Y ! /AXIS3=Z ;
Compute_Model_Based_Data /RESULT_NAME=Left Trunk_Lab /FUNCTION=JOINT_ANGLE /SEGMENT=Trunk /REFERENCE_SEGMENT=Virtual Lab /RESOLUTION_COORDINATE_SYSTEM= ! /USE_CARDAN_SEQUENCE=FALSE ! /NORMALIZATION=FALSE ! /NORMALIZATION_METHOD= ! /NORMALIZATION_METRIC=	Compute_Model_Based_Data /RESULT_NAME=Right Trunk_Lab /FUNCTION=JOINT_ANGLE /SEGMENT=Trunk /REFERENCE_SEGMENT=Virtual Lab /RESOLUTION_COORDINATE_SYSTEM= ! /USE_CARDAN_SEQUENCE=FALSE ! /NORMALIZATION=FALSE ! /NORMALIZATION_METHOD= ! /NORMALIZATION_METRIC=

/NEGATEX=TRUE /NEGATEY=TRUE /NEGATEZ=TRUE ! /AXIS1=X ! /AXIS2=Y ! /AXIS3=Z ;	/NEGATEX=TRUE ! /NEGATEY=FALSE ! /NEGATEZ=FALSE ! /AXIS1=X ! /AXIS2=Y ! /AXIS3=Z ;
Compute_Model_Based_Data /RESULT_NAME=Left L5S1_Moment /FUNCTION=JOINT_MOMENT /SEGMENT=RPV_2 /REFERENCE_SEGMENT= /RESOLUTION_COORDINATE_SYSTEM=RPV_3 ! /USE_CARDAN_SEQUENCE=FALSE /NORMALIZATION=TRUE /NORMALIZATION_METHOD=DEFAULT_NOR MALIZATION ! /NORMALIZATION_METRIC= /NEGATEX=TRUE ! /NEGATEY=FALSE ! /NEGATEZ=FALSE ! /AXIS1=X ! /AXIS2=Y ! /AXIS3=Z ;	Compute_Model_Based_Data /RESULT_NAME=Right L5S1 Moment /FUNCTION=JOINT_MOMENT /SEGMENT=RPV_2 /REFERENCE_SEGMENT= /RESOLUTION_COORDINATE_SYSTEM=RPV_3 ! /USE_CARDAN_SEQUENCE=FALSE /NORMALIZATION=TRUE /NORMALIZATION_METHOD=DEFAULT_NOR MALIZATION ! /NORMALIZATION_METRIC= /NEGATEX=TRUE /NEGATEY=TRUE /NEGATEZ=TRUE ! /AXIS1=X ! /AXIS2=Y ! /AXIS3=Z ;
Compute_Model_Based_Data /RESULT_NAME=Left RF w.r.t Trunk /FUNCTION=JOINT_FORCE /SEGMENT=RPV_2 /REFERENCE_SEGMENT= /RESOLUTION_COORDINATE_SYSTEM=RPV_3 ! /USE_CARDAN_SEQUENCE=FALSE /NORMALIZATION=TRUE /NORMALIZATION_METHOD=DEFAULT_NOR MALIZATION ! /NORMALIZATION_METRIC= /NEGATEX=TRUE ! /NEGATEY=FALSE /NEGATEZ=TRUE ! /AXIS1=X ! /AXIS2=Y ! /AXIS3=Z ;	Compute_Model_Based_Data /RESULT_NAME=Right RF w.r.t Trunk /FUNCTION=JOINT_FORCE /SEGMENT=RPV_2 /REFERENCE_SEGMENT= /RESOLUTION_COORDINATE_SYSTEM=RPV_3 ! /USE_CARDAN_SEQUENCE=FALSE /NORMALIZATION=TRUE /NORMALIZATION_METHOD=DEFAULT_NOR MALIZATION ! /NORMALIZATION_METRIC= ! /NEGATEX=FALSE ! /NEGATEY=FALSE /NEGATEZ=TRUE ! /AXIS1=X ! /AXIS2=Y ! /AXIS3=Z ;
Compute_Model_Based_Data /RESULT_NAME=Left Lumbar w.r.t Lab /FUNCTION=JOINT_ANGLE /SEGMENT=Back Lumbar /REFERENCE_SEGMENT=Virtual Lab /RESOLUTION_COORDINATE_SYSTEM= ! /USE_CARDAN_SEQUENCE=FALSE ! /NORMALIZATION=FALSE ! /NORMALIZATION_METHOD=	Compute_Model_Based_Data /RESULT_NAME=Right Lumbar w.r.t Lab /FUNCTION=JOINT_ANGLE /SEGMENT=Back Lumbar /REFERENCE_SEGMENT=Virtual Lab /RESOLUTION_COORDINATE_SYSTEM= ! /USE_CARDAN_SEQUENCE=FALSE ! /NORMALIZATION=FALSE ! /NORMALIZATION_METHOD=

! /NORMALIZATION_METRIC= /NEGATEX=TRUE /NEGATEY=TRUE /NEGATEZ=TRUE ! /AXIS1=X ! /AXIS2=Y ! /AXIS3=Z ;	! /NORMALIZATION_METRIC= /NEGATEX=TRUE ! /NEGATEY=FALSE ! /NEGATEZ=FALSE ! /AXIS1=X ! /AXIS2=Y ! /AXIS3=Z ;
Compute_Model_Based_Data /RESULT_NAME=Left Lumbar w.r.t Pel /FUNCTION=JOINT_ANGLE /SEGMENT=Back Lumbar /REFERENCE_SEGMENT=RPV /RESOLUTION_COORDINATE_SYSTEM= ! /USE_CARDAN_SEQUENCE=FALSE ! /NORMALIZATION=FALSE ! /NORMALIZATION_METHOD= ! /NORMALIZATION_METRIC= /NEGATEX=TRUE /NEGATEY=TRUE /NEGATEZ=TRUE ! /AXIS1=X ! /AXIS2=Y ! /AXIS3=Z ;	Compute_Model_Based_Data /RESULT_NAME=Right Lumbar w.r.t Pel /FUNCTION=JOINT_ANGLE /SEGMENT=Back Lumbar /REFERENCE_SEGMENT=RPV /RESOLUTION_COORDINATE_SYSTEM= ! /USE_CARDAN_SEQUENCE=FALSE ! /NORMALIZATION=FALSE ! /NORMALIZATION_METHOD= ! /NORMALIZATION_METRIC= /NEGATEX=TRUE ! /NEGATEY=FALSE ! /NEGATEZ=FALSE ! /AXIS1=X ! /AXIS2=Y ! /AXIS3=Z ;

Appendix 5.5: Segment Definitions in Visual 3D

The following describes the segment definitions in Visual 3d for the model used in this thesis. The LED placement protocol was as described in Chapter 5.

(1) <u>Pelvic Segments Definition:</u>

A number of definitions of the pelvis were required to calculate the kinematic and kinetic variables of interest. Firstly, to measure pelvic kinematics, the CODA pelvis was defined.

- **Coda Pelvis:**

In order to define the CODA pelvis, a belt was placed around the pelvis of the subject on the PSISs and ASISs. A rigid frame containing 4 LEDs was attached to the belt. A sacral offset measure was then taken using a depth gauge to measure the distance between the frame and the actual PSISs. The position of the LEDs was then offset forward, as defined by the pelvic frame, by this offset measure to define the actual or real position of the PSISs. A measure of the depth of the pelvis, taken during clinical exam using a tape measure, was then used to locate the position of the ASISs. The PSIS LEDs were offset forward by the pelvic depth distance, as defined by the pelvic frame, to locate the actual or real ASISs. The LEDs located on the pelvic frame were used as tracking targets. The CODA pelvis was then defined as follows:

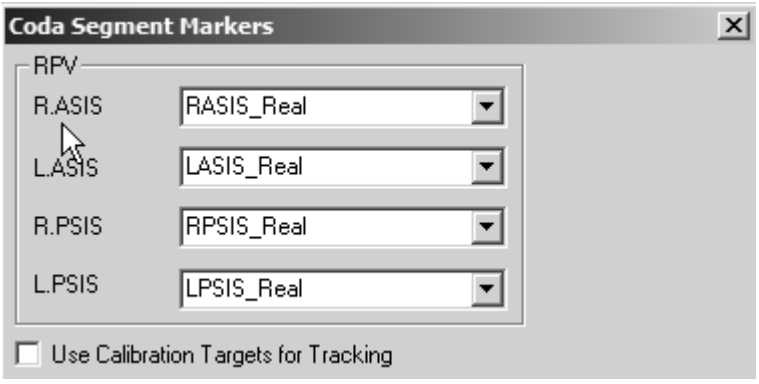

Figure 5.5 -1: CODA pelvis definition in V3d.

Once the CODA pelvis was defined, the Hip Joint Centres (HJCs) and the L5/S1 joint were then defined.

- **Hip Joint Centres (HJCs):**

RIGHT_Hip and LEFT_HIP were defined according to the regression equations of Bell et al as described in chapter X. A landmark (Pelvic_Front) was created. This was defined as the mid-point of RASIS_Real and LASIS_Real. Pelvic_Front was the point at which regression equations were realised based on the definition of the CODA pelvis.

- ML: 0.36*PelWidth*RPV_ML_Direction
- AP: 0.19*PelWidth*RPV_AP_Direction
- Ax: 0.3*PelWidth*RPV_Axial_Direction

(RPV_ML_Direction, RPV_AP_Direction, and RPV_Axial_Direction define the pelvic segment).

- **L5/S1 Joint:**

A tracking LED (L5/S1) was placed on the L5/S1 joint space. A virtual marker (L5/S1_Virtual) was then created, based on the study of Seay et al., as follows:

- Starting Point: L5/S1
- Ending Point: Pelvis_Front
- Offset using the following ML/AP/AXIAL offsets: 0, 0, 0.05.

This corresponded to 5% along the length of the line between the L5/S1 tracking marker and the front of the pelvis.

In order to estimate kinetics at the L5/S1 joint, it was necessary to create a second pelvic segment definition (referenced as RPV_2). This pelvic segment was not used for kinematic calculations. Instead it was required to connect the proximal end of the thigh segments to the distal end of the L5/S1 joint.

- **Pelvis Segment RPV_2:**

This pelvis was defined using L5/S1_Virtual and the right and left HJCs as follows:

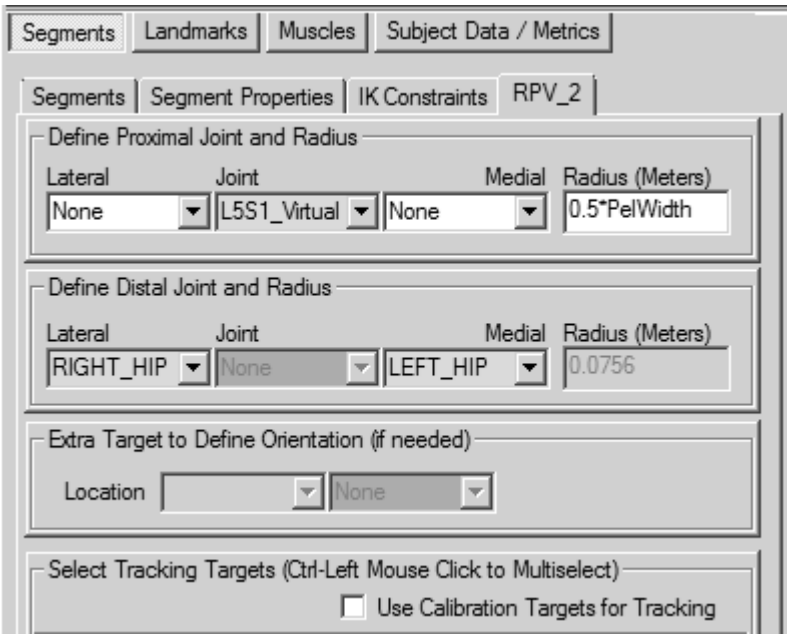

Figure 5.5 -2: V3d pelvic definition required for L5/S1 kinetic calculations

Once this pelvic segment was defined, it was then possible to calculate kinetics at the L5/S1_Virtual point.

As the CODA pelvis was defined to tilt anteriorly, it was felt that this pelvic definition did not reflect the orientation of the lumbar spine. Consequently, L5/S1 kinetics were not resolved in the CODA pelvic segment. Instead, a third pelvis definition was required in order to provide a coordinate system with more anatomical meaning than the CODA pelvic segment or the pelvic segment that originated from L5/S1 (referenced as RPV_3).

- **Pelvis Segment RPV_3:**

The third pelvic segment, a Visual 3D pelvis, was created and orientated vertically to the laboratory frame so that L5/S1 kinetics could be resolved into this coordinate system. This was defined using two virtual landmarks (RT.ILIAC and LT.ILIAC) and the right and left HJCs. The virtual landmarks were defined as follows:

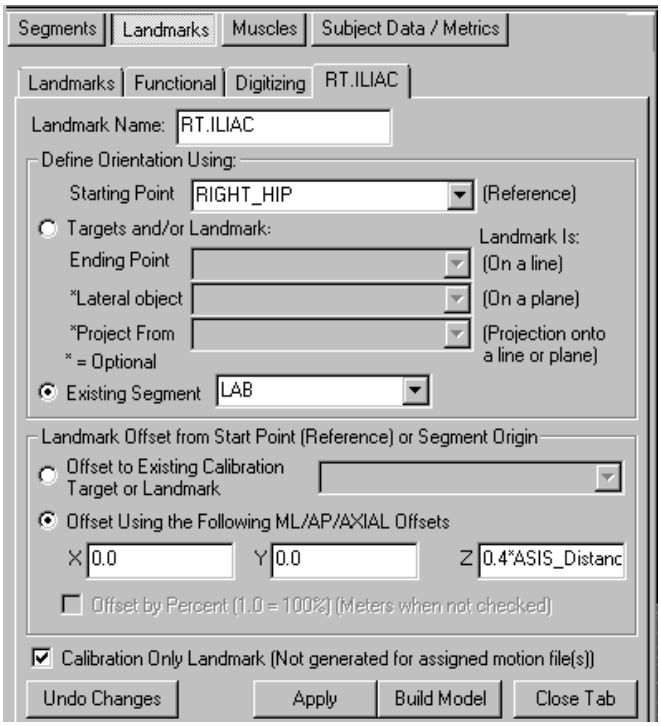

Figure 5.5 -3: Definition of the virtual ILIAC markers for Visual 3D pelvic definition

The Z-offset contained the subject metric 0.4*ASIS_Distance. As there were no strict dimensions, it was decided to base the offset partly on subject size. This measure was then the depth of the virtual pelvic segment. LT.ILIAC was then created as above.

Once the ILIAC virtual markers were created, it was then possible to define the Visual 3D segment. The segment was defined as follows:

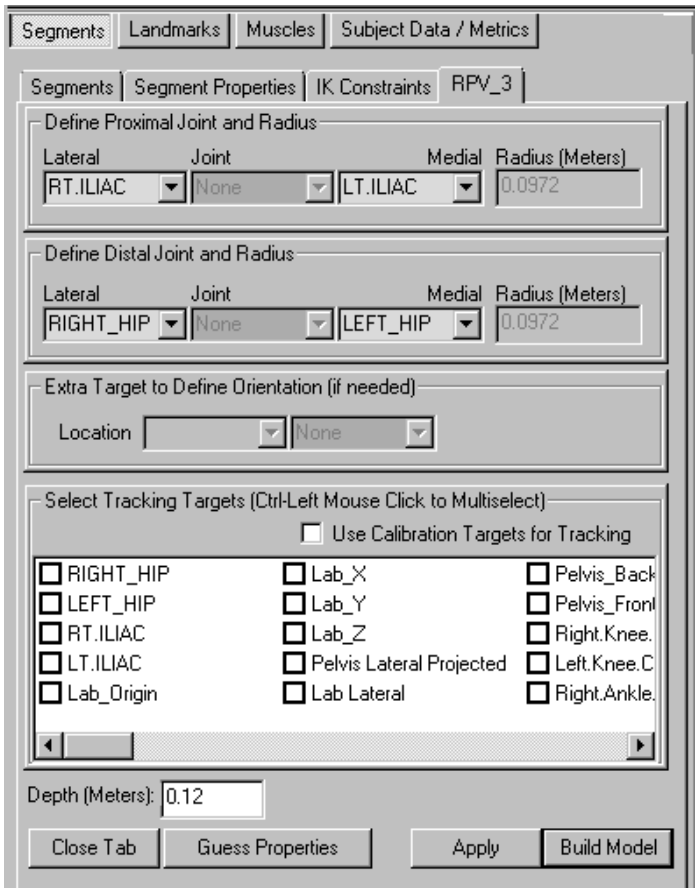

Figure 5.5 -4: Definition of the Visual 3D pelvis segment

L5/S1 kinetics were then resolved into this segment using the "Compute model Based Data" dialogue box.

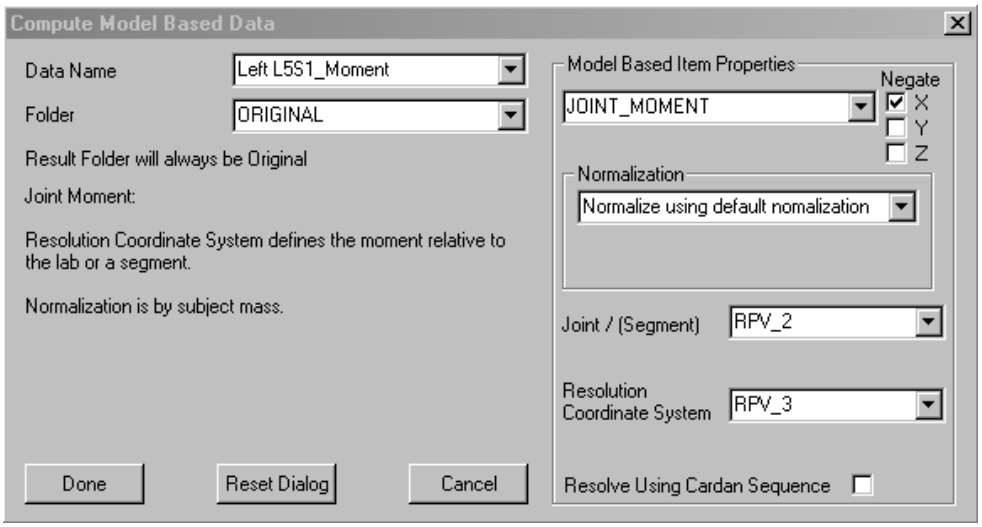

Figure 5.5 - 5: L5/S1 kinetics resolved into RPV_3 pelvic segment

(2) <u>Thigh Segment Definition:</u>

Before the thigh segments could be defined, both the HJCs and the Knee Joint Centres (KJCs) needed to be defined. The HJCs were defined as above. For the KJCs, a number of landmarks were first needed.

- Right.Fem.LM01 / Left.Fem.LM01: The purpose of these landmarks was to create a virtual point that projected from the Knee LED so that the line between the knee LED and this virtual point was equal in orientation to the line defined by the femoral wand markers. This virtual point was then used in the final step to create the actual KJC.
    - Starting point: R.KNEE
    - End point: R.POST.FEM
    - Lateral Obj.: R.ANT.FEM
    - ML: -0.2 (arbitrary), AP: 0.0, Ax. 0.0
- Right.Fem.LM02/ Left.Fem.LM02: These landmarks refer to the virtual hip joint centre (VirtHJC) virtual marker. This was used to define the knee joint centre (next step). CODA state that the purpose of this adjustment to the thigh wand plane is to align it more accurately with the femur for an improved perpendicular medio-lateral knee axis. This was implemented as follows:
    - Starting point: RIGHT_HIP
    - End point: R.POST.FEM
    - Lateral Obj.: R.ANT.FEM
    - ML: 0.0 AP: 0.5*RightKW, Ax. 0.0
- Right.Fem.LM03/ Left.Fem.LM03: These landmarks refer to the lateral aspect of the knee joint. The line between the R.KNEE marker and these virtual points define the axis of the knee. They are used later used to define the thigh segment.
    - Starting point: R.KNEE
    - End point: Right.Fem.LM02
    - Lateral Obj.: Right.Fem.LM01
    - ML: 0.0 AP: RightKW, Ax. 0.0

- Definition of the Thigh Segment:
    - Proximal Joint: RIGHT_HIP (lateral/medial None), Radius: 0.5*PelWidth
    - Distal Joint: Lateral: R.KNEE, Medial: Right.Fem.LM03

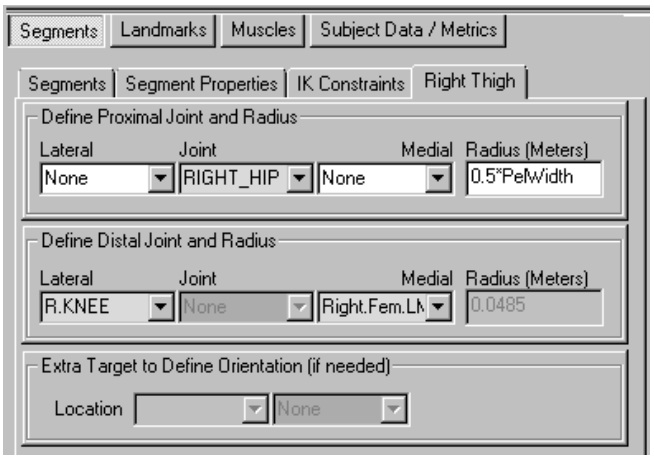

Figure 5.5 -6: Final definition of the thigh segment in v3d

Right.Knee.Centre is defined as half way between R.KNEE and Right.Fem.LM03. The same process was followed for the left KJC.

(3) <u>Shank Segment Definition:</u>

Before the shank segments could be defined, the KJCs and the Ankle Joint Centres (AJCs) needed to be defined. The KJCs were defined as above. A number of tibial landmarks were needed before the shank segment could be defined.

- Right.Tib.LM01 / Left.Tib.LM01: Used to define a virtual point that projected from the Ankle LED so that the line between the Ankle LED and this virtual point was the same orientation as the line between the Tibial wand LEDs.
    - Starting point: R.ANKLE
    - End point: R.POST.TIB
    - Lateral Obj.: R.ANT.TIB
    - ML: -0.2 (arbitrary), AP: 0.0, Ax. 0.0
- Right.Tib.LM02 / Left.Tib.LM02: These points refer to the medial ankle markers. They are projected medially by the ankle width. The projection was defined by the plane using the knee LED, the ankle LED and the previously defined landmark (Right.Tib.LM01).

- Starting point: R.ANKLE
- End point: R.KNEE
- Lateral Obj.: Right.Tib.LM01
- ML: 0.0, AP: RightAW, Ax. 0.0

- Right.Tib.LM03 / Left.Tib.LM03: This point is a projection of the Right.Tib.LM01 in by half ankle width defined by the plane R.KNEE, R.ANKLE and Right.Tib.LM01. This will then be used with knee joint centre and ankle joint centre to define the shank segment orientation. (Essentially it is coincident with the orientation of the tibial wand: R.POST.TIB → R.ANT.TIB).

  - Starting point: Right.Tib.LM01
  - End point: R.KNEE
  - Lateral Obj.: R.ANKLE
  - ML: 0.0, AP: -0.5*RightAW, Ax. 0.0

  Right.Ankle.centre was defined as half way between R.ANKLE and Right.Tib.LM02.

Definition of the Shank segment:

- Proximal Joint: Right.Knee.Centre (lateral/medial None), Radius: 0.05
- Distal Joint: Lateral: Right.Ankle.centre (lateral/medial None), Radius: 0.03
- Extra target: Anterior, Right.Tib.LM03

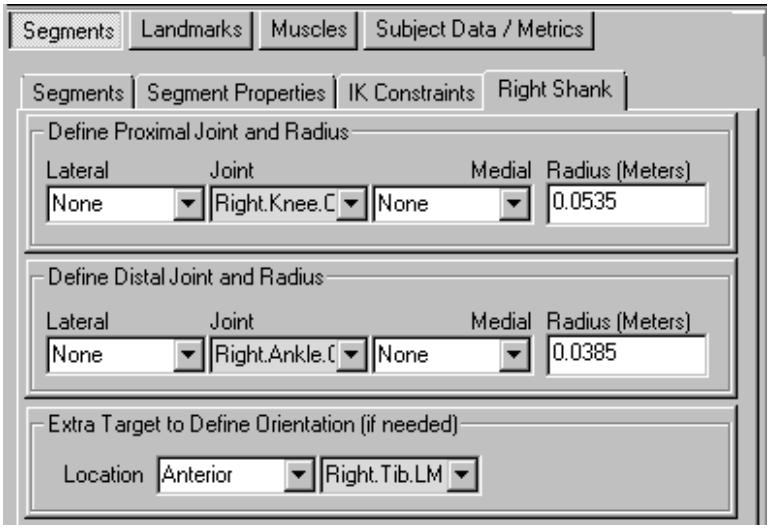

Figure 5.5 -7: Final definition of the shank segment in v3d

(4) Foot Segment Definition:

It was necessary to define two segments for each foot. The "Right Foot" and "Left Foot" segments are needed to correctly compute kinetics while the "Right Virtual Foot" and "Left Virtual Foot" segments are required to compute ankle angles.

Right Foot/Left Foot:

The method used to create the foot segment is sufficient to compute kinetics. The ankle joint centre is needed along with the ANKLE and TOE markers. The segment is defined as follows:

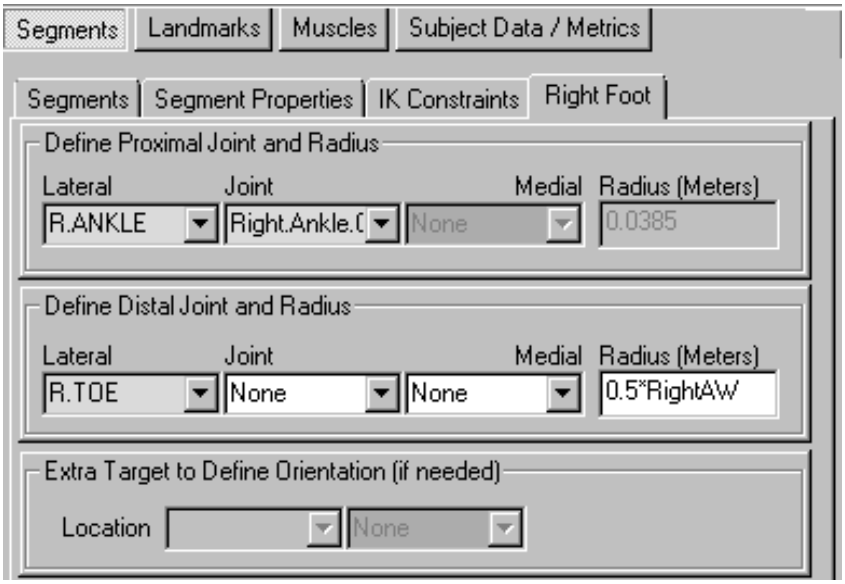

Figure 5.5 -8: Final definition of the (Kinetic) foot segment in v3d

Right Virtual Foot/Left Virtual Foot:

The method used to create the virtual foot segments is referred to as heel to toe. The definition assumes that the heel, toe and ankle centre define the sagittal plane of the foot. Before the virtual foot segments could be defined, additional landmarks were needed. Right.Heel.Centre was defined as a virtual point offset from the R.HEEL LED perpendicular to the plane formed by the R.HEEL, R.TOE and R.ANKLE LEDs. The offset was set at half the ankle width.

- Starting point: R.HEEL
- End point: R.TOE

- Lateral Obj.: R.ANKLE
- ML: 0.0, AP: -0.5*RightAW, Ax. 0.0

Right.Toe.Centre was defined as a virtual point offset from the R.TOE LED using the same process.

- Starting point: R.TOE
- End point: R.HEEL
- Lateral Obj.: R.ANKLE
- ML: 0.0, AP: 0.5*RightAW, Ax. 0.0

The foot segment was defined as follows:

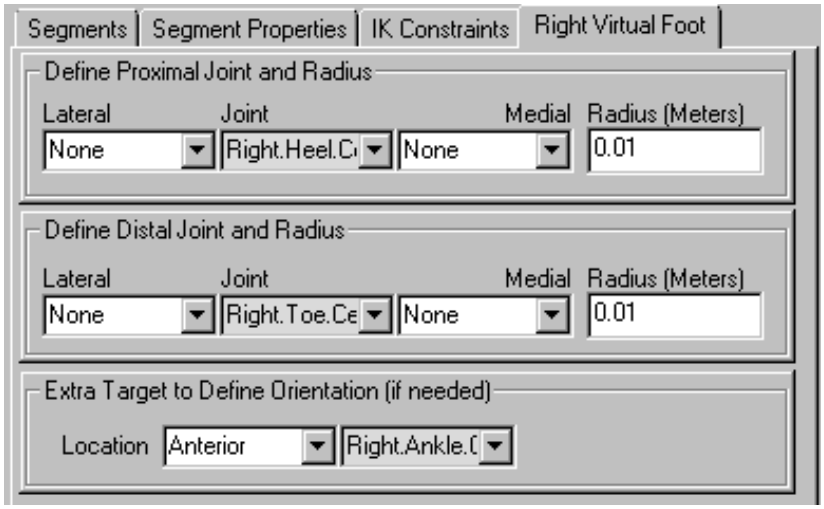

Figure 5.5 -9: Final definition of the (kinematic) foot segment in V3d

The virtual foot segments will need to be rotated so that the coordinate system follows the convention: x-axis → red (flexion/extension), y-axis → green (inversion/eversion) and z-axis → blue (internal/external). All output data are based on the Right Hand Rule.

(5) <u>Lumbar Segment Definition:</u>

The lumbar segment was tracked by means of 5 LEDs placed at set points around the lumbar spine as described in chapter X (Fig X.x). Two virtual points were created as the mid-point of between the T12-L1 LED and the Lumbar01 LED (Mid.L1.T12) and the mid-point of the T12-L1 LED and the Lumbar02 LED (Mid.L2.T12). A least square plane was then fit to the two virtual points and LEDs Lumbar03 and Lumbar04 to define the lumbar segment. This was implemented in v3d as follows:

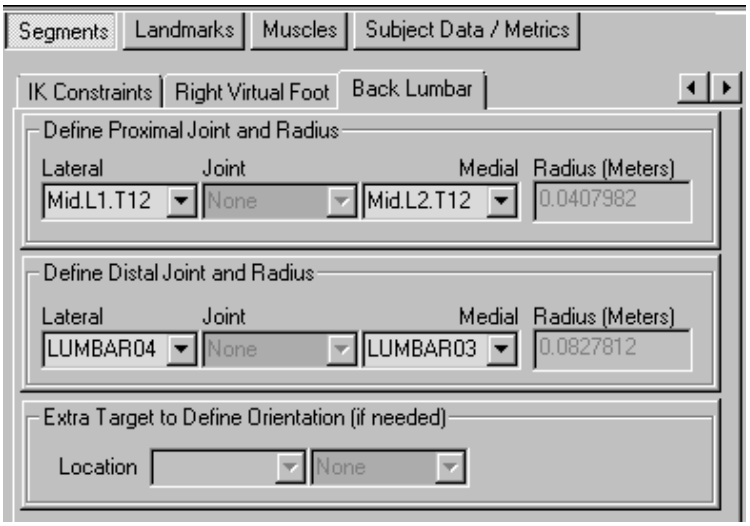

Figure 5.5 -10: Final definition of the lumbar segment in V3d

(6) <u>Thorax Segment Definition:</u>

The thorax segment was tracked using the rigid cluster mount described in chapter X (Fig X.x). The mid-point of LEDs m1 and m2 was defined. This virtual point (MidLowUp) was used along with the m1 and m3 markers to define a lateral virtual marker (Trunk.Lateral) as follows:

- Starting point: MidLowUp
- End point: BACKLOW(m2 LED)
- Lateral Obj.: BACKOUT (m3 LED)
- ML: 0.0, AP: 0.1 (arbitrary), Ax. 0.0

This virtual point (Trunk.Lateral) was then used with LEDs m1 and m3 to define the thorax segment as follows:

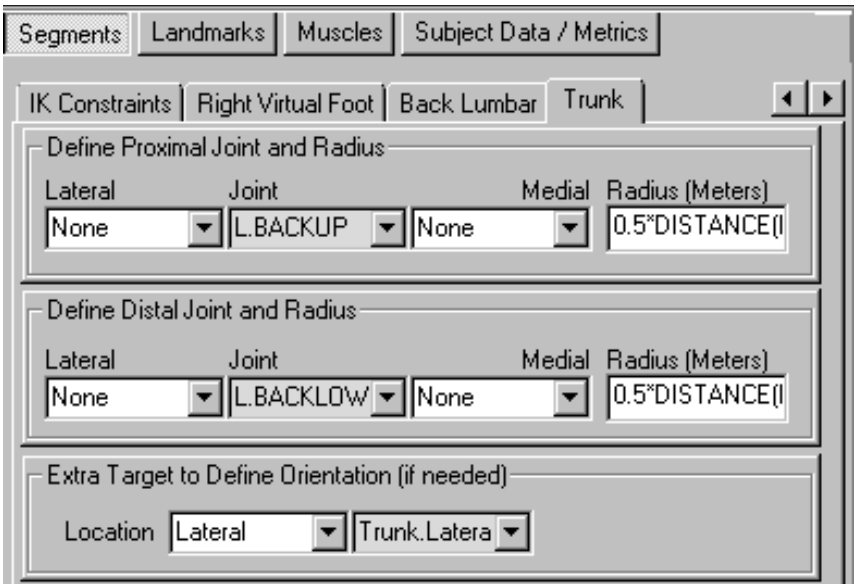

Figure 5.5 -11: Final definition of the thorax segment in V3d

Appendix 8.1: Bland and Altman plots for Thorax protocol study

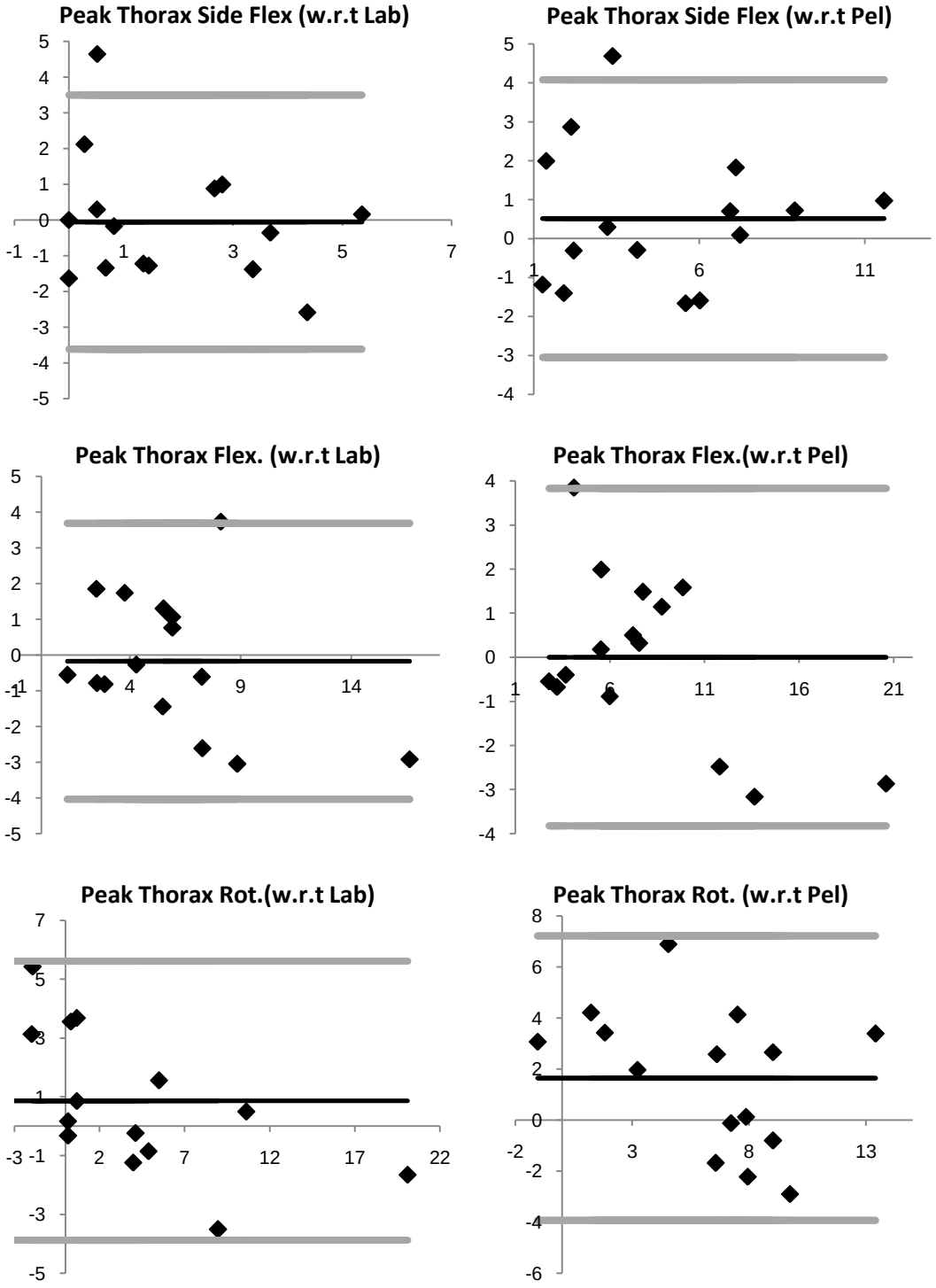

Figure 8.1: Bland and Altman plots for peak kinematic parameters between CRCTM and ISB

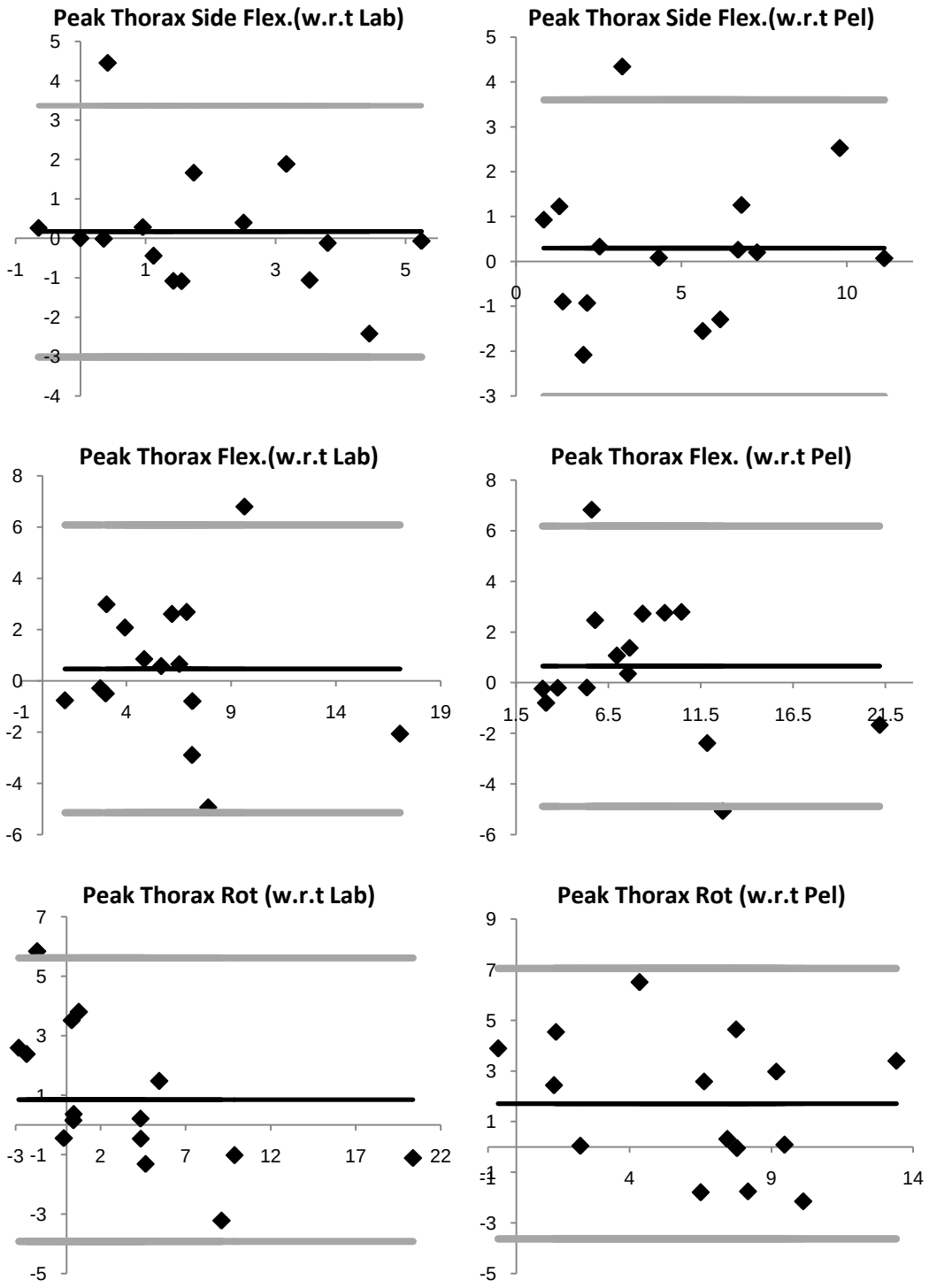

Figure 8-2: Bland and Altman plots for peak kinematic parameters between CRCTM and Armand.

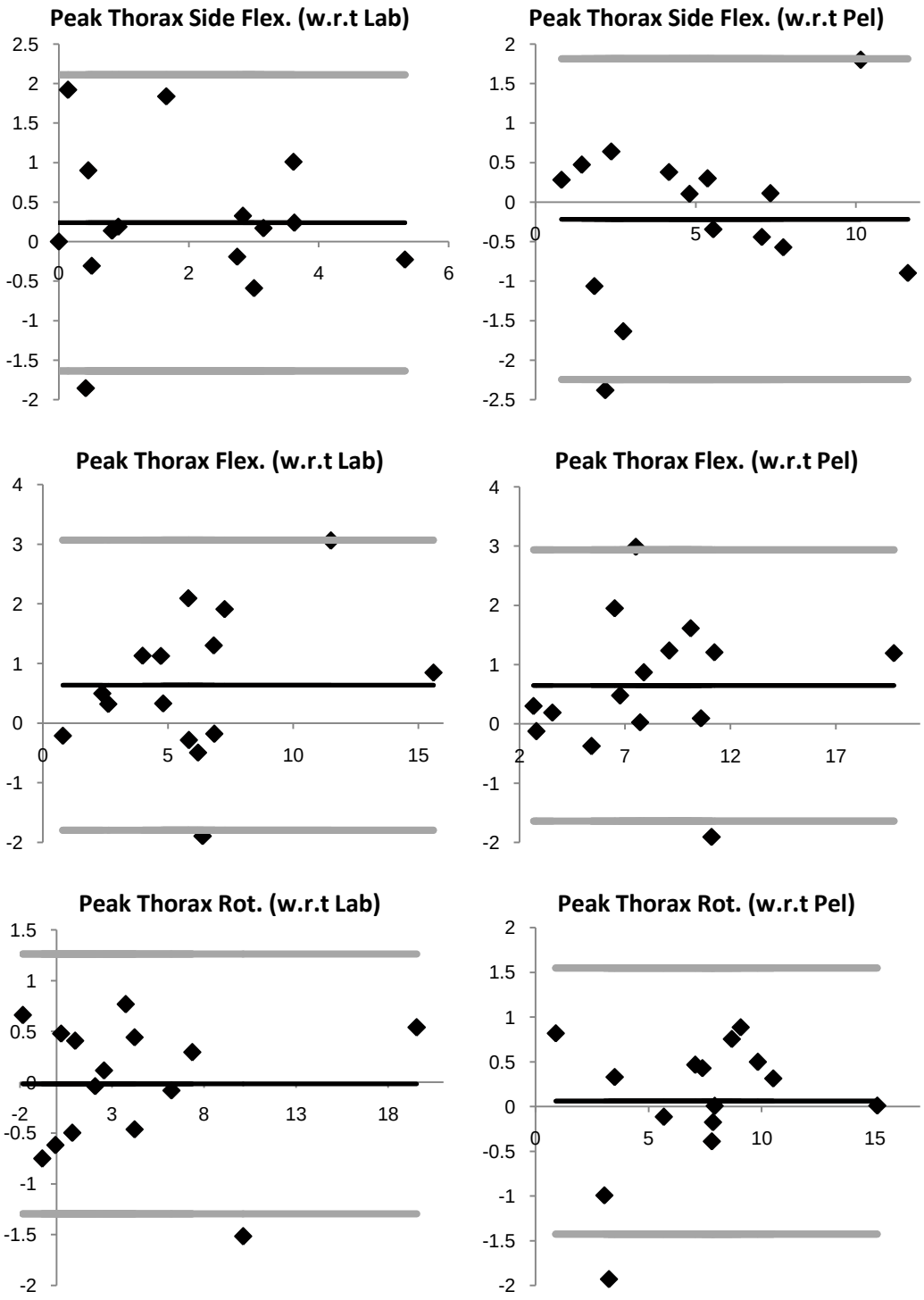

Figure 8-3: Bland and Altman plots for peak kinematic parameters between ISB and Armand

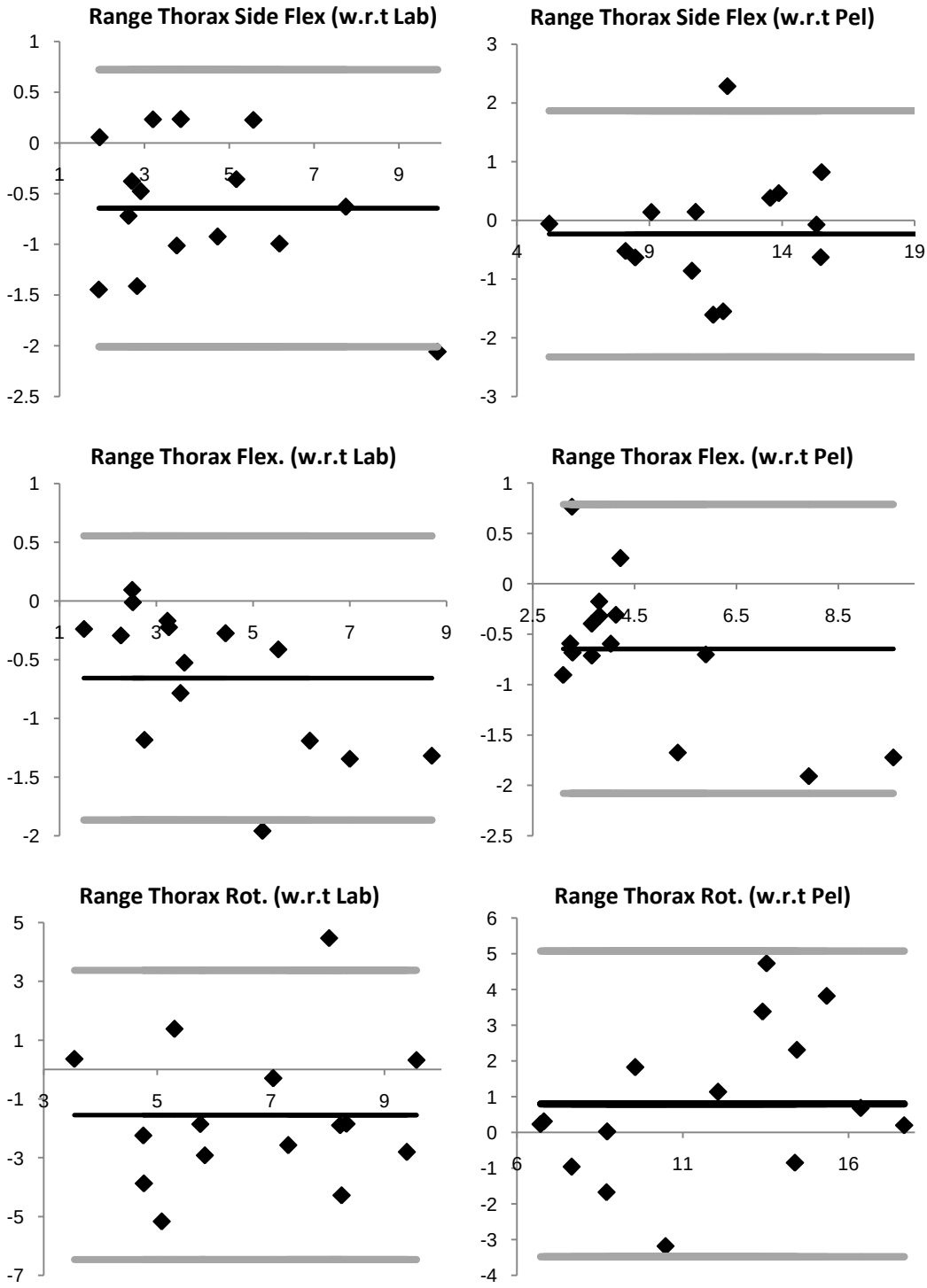

Figure 8-4: Bland and Altman plots for range kinematic parameters between CRCTM and ISB

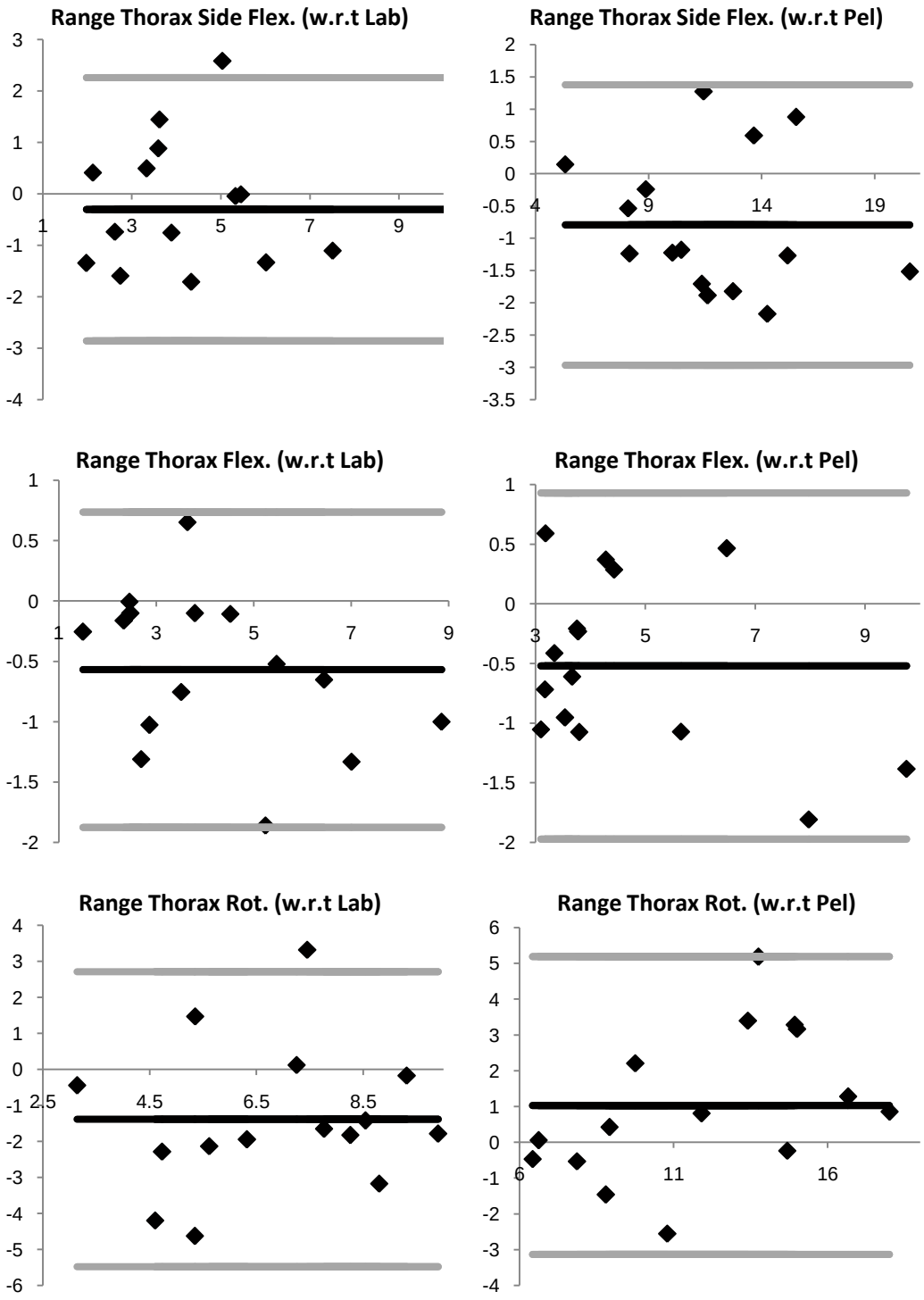

Figure 8-5: Bland and Altman plots for range kinematic parameters between CRCTM and Armand

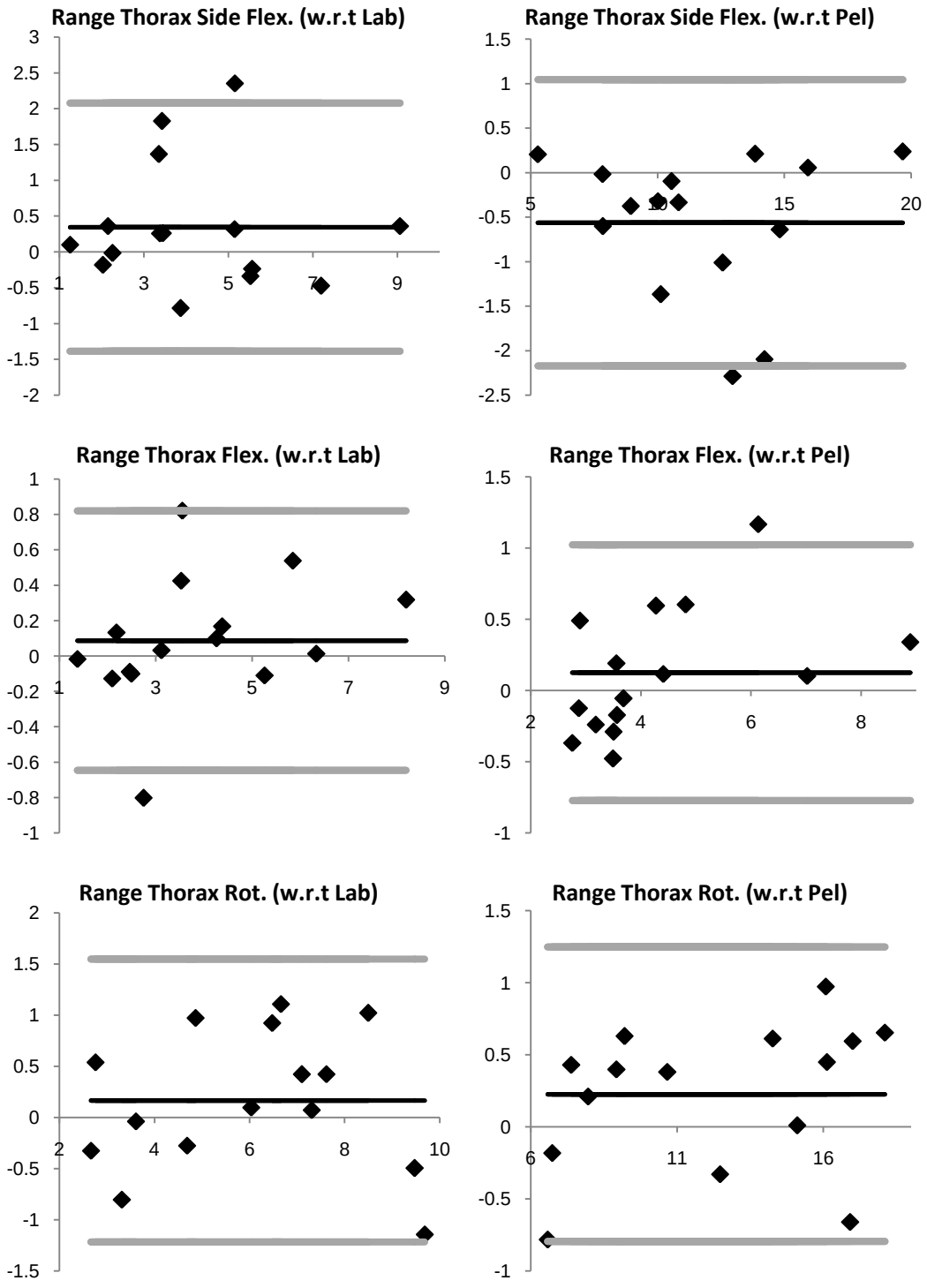

Figure 8-6: Bland and Altman plots for range kinematic parameters between ISB and Armand

Appendix 10.1: Participant Data according to Diagnosis

Table 10-1: Mean (SD) participant data for typically developed (TD), Hemiplegia and Diplegia groups.

Parameter	**TD (*n = 26*)**	**Hemiplegia (*n = 21*)**	**Diplegia (*n = 31*)**	***p*-Value**
Age (years)	10.15 (3.17)	11.81(3.12)	10.49 (2.86)	0.120
Male / Female	15 / 11	11 / 10	22 / 9	------
Height (m)	1.40 (0.18)	1.51 (0.17)	1.43 (0.16)	0.098
Weight (kg)	35.31 (12.85)	42.99 (15.10)	37.68 (14.09)	0.201
Walking Speed (m/s)	1.19 (0.13)	1.13 (0.15)	1.03 (0.14)	0.015*

Appendix 10.2: Thorax Kinematics and L5/S1 Kinetics according to diagnosis

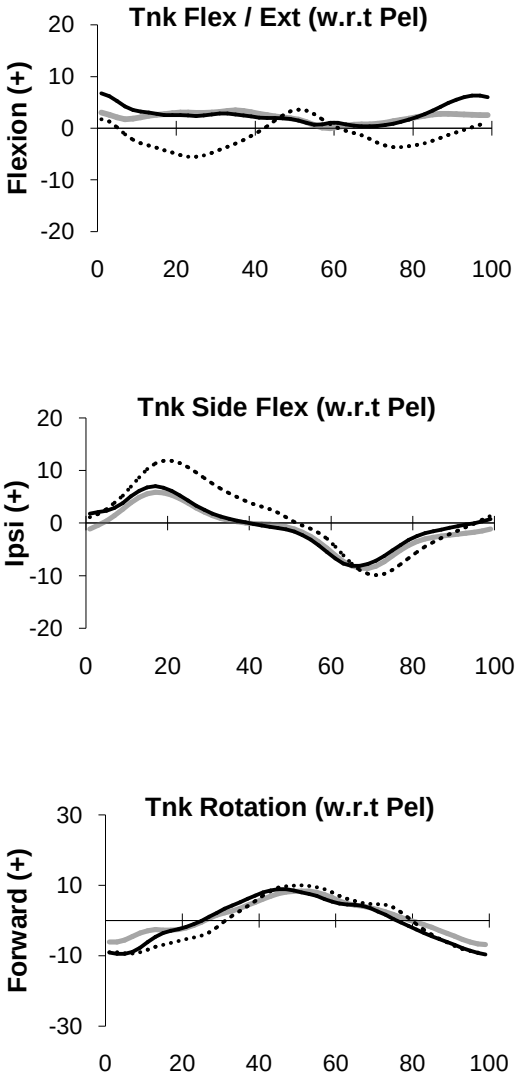

Figure 10-1: Ensemble average profiles for the thorax in all 3 planes (w.r.t Pelvis) (Gray – Typically Developed, Black – Hemiplegia , Dotted – Diplegia).

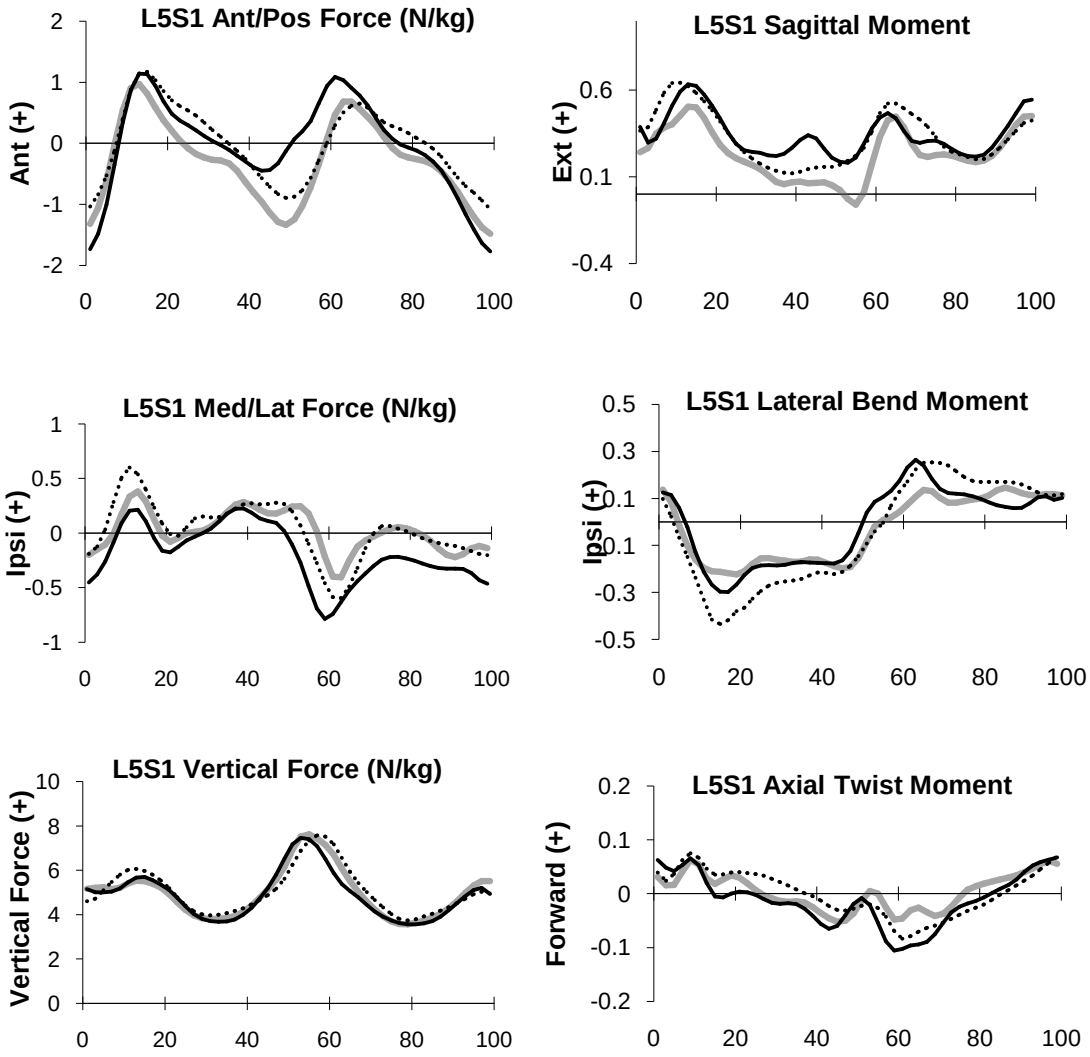

Figure 10-2: Ensemble average profiles for L5/S1 reactive forces in all 3 directions (left column) and L5/S1 moments in all 3 planes (right column). (Gray – Typically Developed, Black – Hemiplegia , Dotted – Diplegia).

Appendix 10.3: Mean (SD) thorax kinematic data according to diagnosis

Parameters	TD Mean (SD)	Hemiplegia Mean (SD)	Diplegia Mean (SD)	ANOVA *p*-Value
Tnk Flex / Ext (Sag) (deg)				
RMS*	6.31 (14.9)	10.95 (17.4)	9.28 (20.02)	0.069
Peak value (Flexion)	5.93 (7.54)	8.68 (12.27)	5.91 (11.05)	0.584
Time To Peak Flexion (%GC)*	39.0 (98.0)	44.0 (78.0)	38.0 (98.0)	0.835
Peak value (Extension)	-2.30 (7.97)	-2.32 (11.94)	-7.85 (11.27)	0.080
Time to Peak Ext. (%GC)*	61.0 (94.0)	56.0 (88.0)	26.0 (88.0)	0.297
RoM*	8.27 (12.03)	10.59 (15.73)	12.25 (47.5)	0.001(a)(b)
Tnk Side Flex (Cor) (deg)				
RMS*	5.55 (10.64)	5.60 (12.9)	8.52(11.73)	<0.001(b)
Peak Value (Ipsi)	6.47 (4.59)	8.07 (7.48)	12.88 (7.27)	0.001(a)(b)(c)
Time To Peak Ipsi (%GC)*	17.0 (98.0)	22.0 (98.0)	22.0 (98.0)	0.312
Peak Value (Contra)	-9.33 (5.13)	-8.84 (7.15)	-10.84 (8.77)	0.577
Time To Peak Contra (%GC)*	68.0 (72.0)	68.0 (16.0)	72.0 (16.0)	0.002(c)
RoM	15.79 (4.75)	16.91 (4.96)	23.73 (8.84)	<0.001(b)(c)
Tnk Rot (Trans) (deg)				
RMS*	7.6 (10.94)	9.89 (13.54)	10.15 (19.3)	0.197
Peak value	9.22 (7.41)	10.53 (7.64)	12.91 (9.29)	0.238
Time To Peak (%GC)*	43.0 (90.0)	38.0 (80.0)	42.0 (92.0)	0.209
RoM*	18.56 (18.6)	21.64 (29.5)	23.54 (70.2)	0.025(b)

Table 10-2: Mean (SD) thorax kinematic values (w.r.t Pelvis) for TD, Hemiplegia and Diplegia groups with concurrent p-values. Distribution of data was assessed using a Shipiro-Wilk normality test (*Median and Range for non-normally distributed data). Results of post-hoc tests are indicated as follows: (a) Hemiplegia and TD; (b) Diplegia and TD; (c) Hemiplegia and Diplegia.

Appendix 10.4: Mean (SD) L5/S1 force data according to diagnosis

Parameters	TD Mean (SD)	Hemiplegia Mean (SD)	Diplegia Mean (SD)	ANOVA *p*-Value
L5/S1 Ant/Pos Force (N/kg)				
RMS	0.833 (0.141)	0.91 (0.186)	0.85 (0.198)	0.346
Peak Anterior value (stance)	1.109 (0.508)	1.33 (0.574)	1.33 (0.641)	0.302
Time To Peak (stance) (%GC)*	12.0 (8.0)	14.0 (14.0)	14.0 (14.0)	0.001(a)(b)
Peak Posterior value	-1.453 (0.393)	-0.68 (0.554)	-1.20 (0.605)	<0.001(a)(c)
Time To Peak Posterior (%GC)*	52.0 (10.0)	46.0 (14.0)	52.0 (26.0)	<0.001(a)(c)
Peak anterior value (swing)*	0.82 (1.573)	1.16 (2.67)	1.02 (4.068)	0.043(a)
Time To Peak (swing) (%GC)*	68.0 (10.0)	64.0 (12.0)	68.0 (36.0)	<0.001(a)(c)
RoM	2.83 (0.489)	3.49 (0.597)	2.97 (0.643)	0.001(a)(c)
L5/S1 Med/Lat Force (N/kg)				
RMS*	0.325(0.496)	0.496 (0.527)	0.513 (0.714)	0.003(a)(b)
Peak Ipsilateral value*	0.465 (1.654)	0.487 (1.126)	0.706 (1.863)	0.010(b)(c)
Time To Peak Ipsilateral (%GC)*	14.0 (30.0)	16.0 (32.0)	12.0 (38.0)	0.040(b)(c)
Peak Contralateral value	-0.542 (0.407)	-1.044 (0.450)	-0.883 (1.850)	0.001(a)(b)
Time To Peak Contra (%GC)*	64.0 (28.0)	62.0 (18.0)	66.0 (30.0)	0.054
RoM	1.232 (0.33)	1.650 (0.39)	1.770 (0.50)	<0.001(a)(b)
L5/S1 Vertical Force (N/kg)				
RMS*	5.01 (3.82)	5.03 (2.21)	5.11 (2.14)	0.694
Peak value*	8.23 (5.17)	7.96 (4.51)	8.24 (5.78)	0.656
Time To Peak (%GC)*	56.0 (98.0)	54.0 (42.0)	56.0 (58.0)	0.190
RoM*	4.833 (4.479)	4.596 (5.839)	5.184 (7.422)	0.614

Table 10-3: Mean (SD) L5/S1 reactive force values for TD, Hemiplegia and Diplegia groups with concurrent p-values. Distribution of data was assessed using a Shipiro-Wilk normality test (*Median and Range for non-normally distributed data). Results of post-hoc tests are indicated as follows: (a) Hemiplegia and TD; (b) Diplegia and TD; (c) Hemiplegia and Diplegia.

Appendix 10.5: Mean (SD) L5/S1 moment data according to diagnosis

Parameters	TD Mean (SD)	Hemiplegia Mean (SD)	Diplegia Mean (SD)	ANOVA *p*-Value
L5/S1 Sagittal Mom (Nm/kg)				
RMS	0.328 (0.126)	0.423 (0.104)	0.414 (0.111)	0.007(a)(b)
Peak value (stance)*	0.573 (1.019)	0.779 (1.598)	0.769 (1.381)	0.032(a)(b)
Time To Peak (stance) (%GC)*	12.0 (16.0)	5.0 (19.0)	5.0 (10.0)	0.001(a)(b)
Peak value (swing)*	0.381 (1.329)	0.546 (0.628)	0.615 (0.765)	0.005(a)(b)
Time To Peak (swing) (%GC)*	68.0 (16.0)	62.0 (28.0)	66.0 (32.0)	<0.001(a)(c)
RoM*	0.874 (0.972)	1.005 (1.802)	0.873 (2.308)	0.196
L5/S1 Lat Bend Mom (Nm/kg)				
RMS	0.172 (0.038)	0.198 (0.055)	0.267 (0.071)	<0.001(b)(c)
Peak Ipsilateral value*	0.228 (0.466)	0.332 (0.525)	0.375 (0.847)	0.002(a)(b)
Time To Peak Ipsilat (%GC)*	66.0 (36.0)	64.0 (28.0)	68.0 (36.0)	0.037(c)
Peak Contralateral value*	-0.291 (0.410)	-0.355 (0.683)	-0.491 (0.851)	<0.001(b)(c)
Time to Peak Contra (%GC)*	22.0 (40.0)	20.0 (46.0)	16.0 (56.0)	0.099
RoM*	0.555 (0.574)	0.672 (1.033)	0.870 (1.056)	<0.001(a)(b)(c)
L5/S1 Axial Twist Mom (Nm/kg)				
RMS*	0.045(0.084)	0.062 (0.092)	0.064(0.091)	<0.001(a)(b)
Peak Forward Value*	0.089 (0.234)	0.113 (0.196)	0.131 (0.200)	<0.001(a)(b)
Time To Peak Forward (%GC)*	16.0 (98.0)	24.0 (98.0)	18.0 (98.0)	0.745
Peak Backward Value	-0.086 (0.03)	-0.148 (0.04)	-0.127 (0.042)	<0.001(a)(b)
Time to Peak Back (%GC)	59.0 (70.0)	58.0 (52.0)	60.0 (74.0)	0.292
RoM*	0.162 (0.331)	0.257 (0.285)	0.245 (0.284)	<0.001(a)(b)

Table 10-4: Mean (SD) L5/S1 moment values for TD, Hemiplegia and Diplegia groups with concurrent p-values. Distribution of data was assessed using a Shipiro-Wilk normality test (*Median and Range for non-normally distributed data). Results of post-hoc tests are indicated as follows: (a) Hemiplegia and TD; (b) Diplegia and TD; (c) Hemiplegia and Diplegia.

Appendix 10.6: Ensemble average pelvic data for children with CP

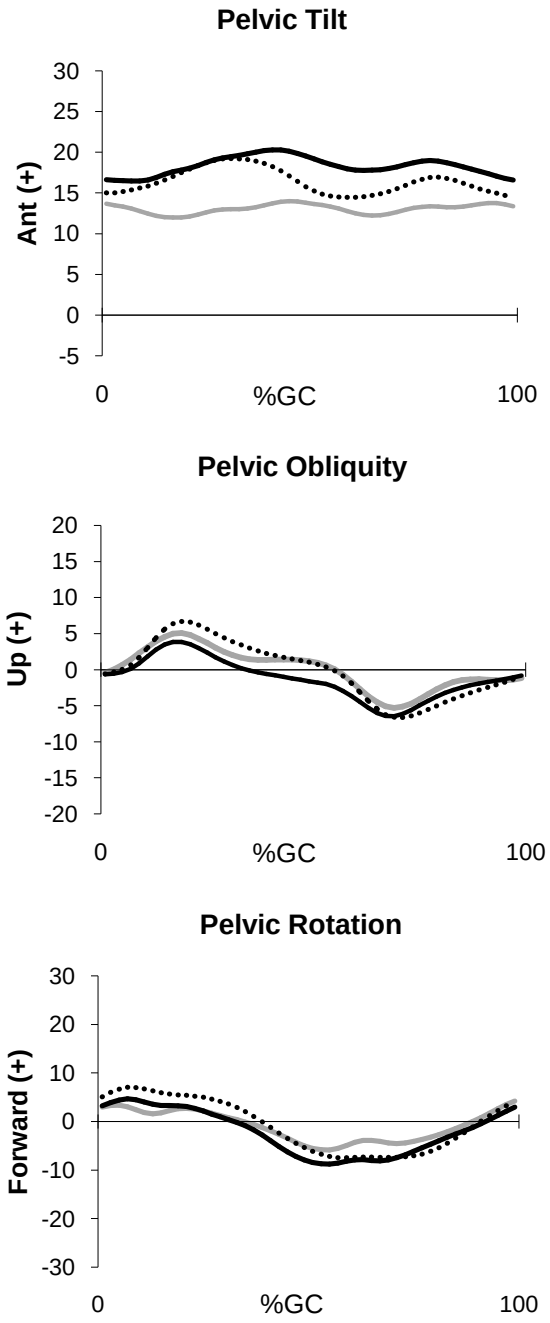

Figure 10-2: Ensemble average kinematic profiles for the pelvis in all 3 planes (Gray – Typically Developed, Black – CP GMFCS I, Dotted – CP GMFCS II).

Appendix 10.7: Mean and SD profiles for Thorax and L5/S1 loading data for GMFCS I and GMFCS II groups compared to TD

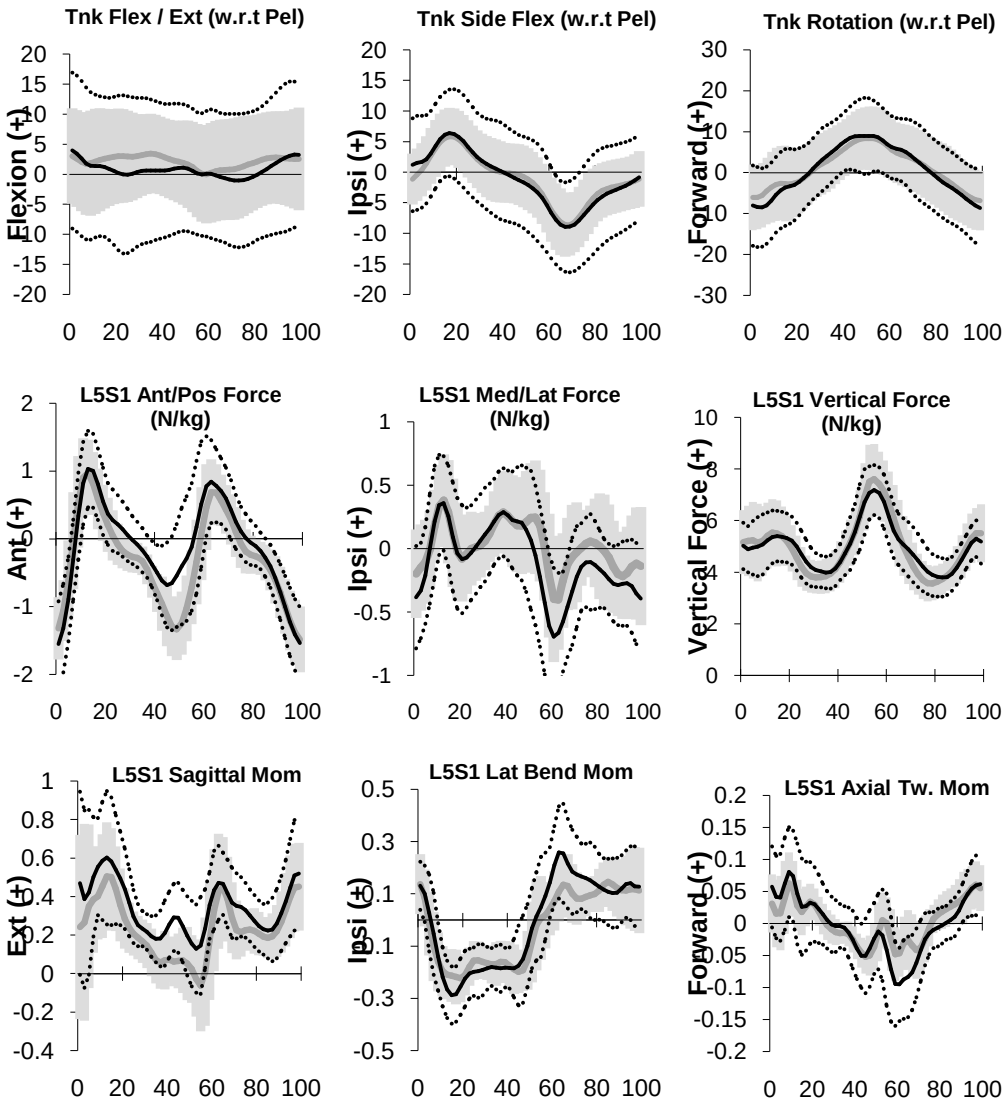

Figure 10-3: Mean and SD profiles for GMFCS I children compared to TD for Thorax kinematics and L5/S1 loading (TD – Gray; GMFCS I – Black).

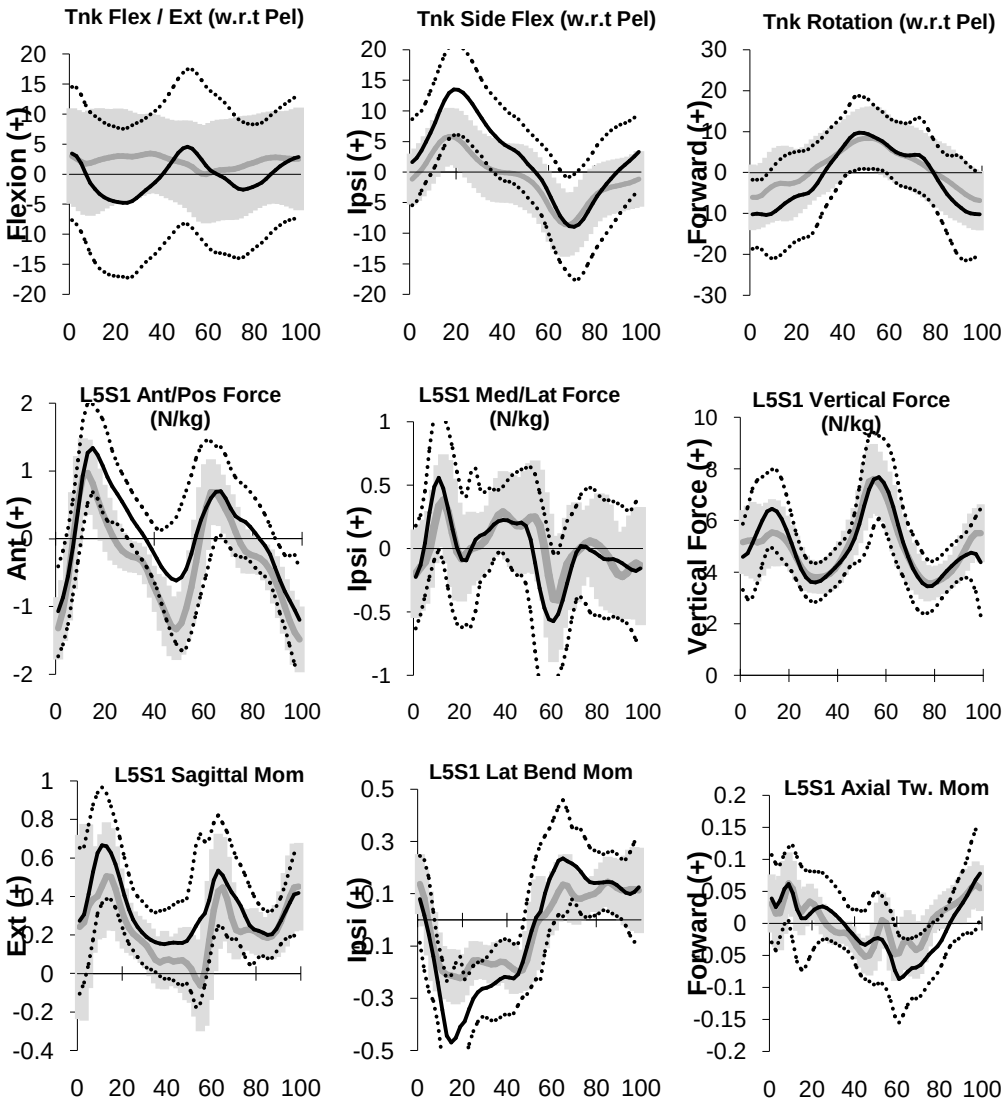

Figure 10-4: Mean and SD profiles for GMFCS II children compared to TD for Thorax kinematics and L5/S1 loading (TD – Gray; GMFCS I – Black).

Appendix 13.1: Reliability Profiles for Thorax Kinematics

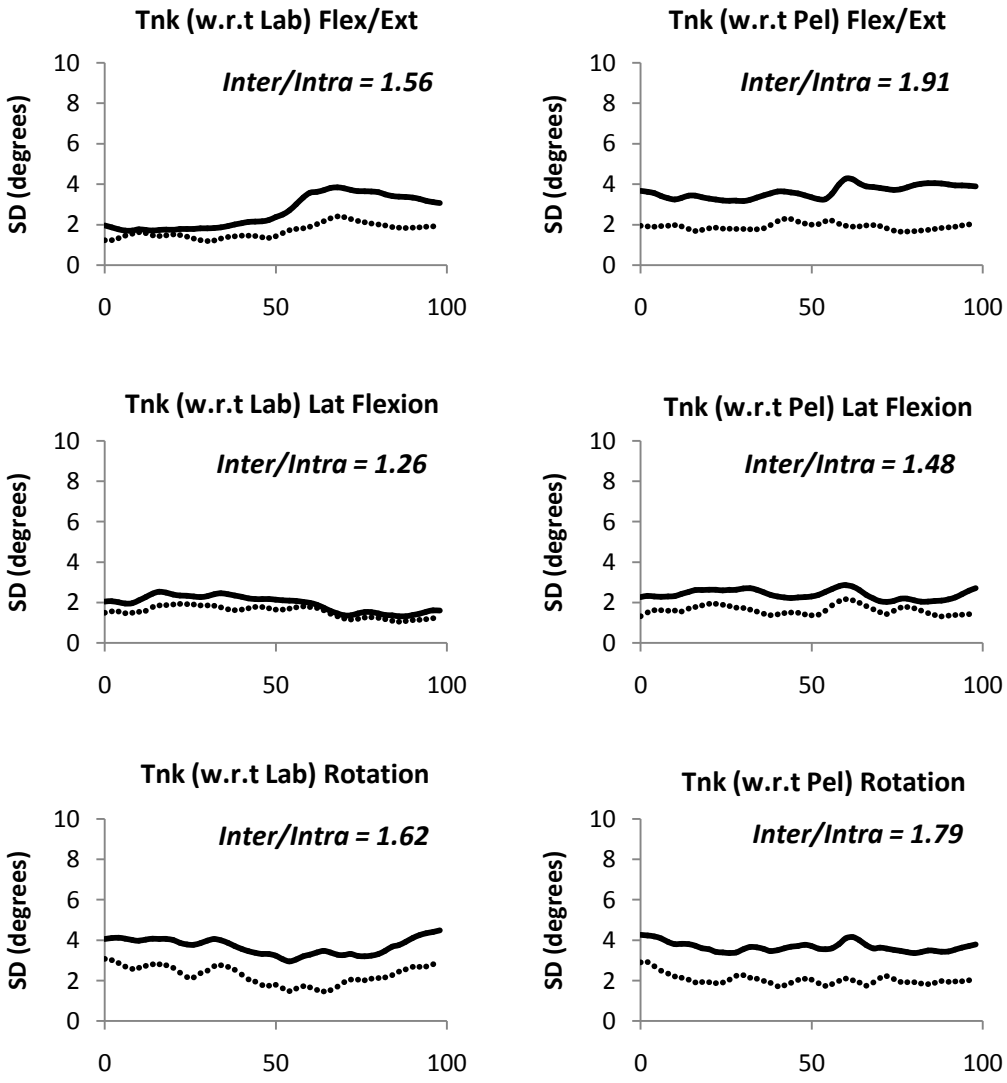

Figure 13-1: Reliability profiles for Thorax kinematic data based on 8 repeat assessments using the approach of Schwartz et al (Schwartz et al., 2004). Dotted – Intra Subject, Black – Inter Subject. Ratio of inter-subject error to intra-subject error is provided (Inter/Intra).

Appendix 13.2: Reliability Profiles for Lumbar Segment Kinematics

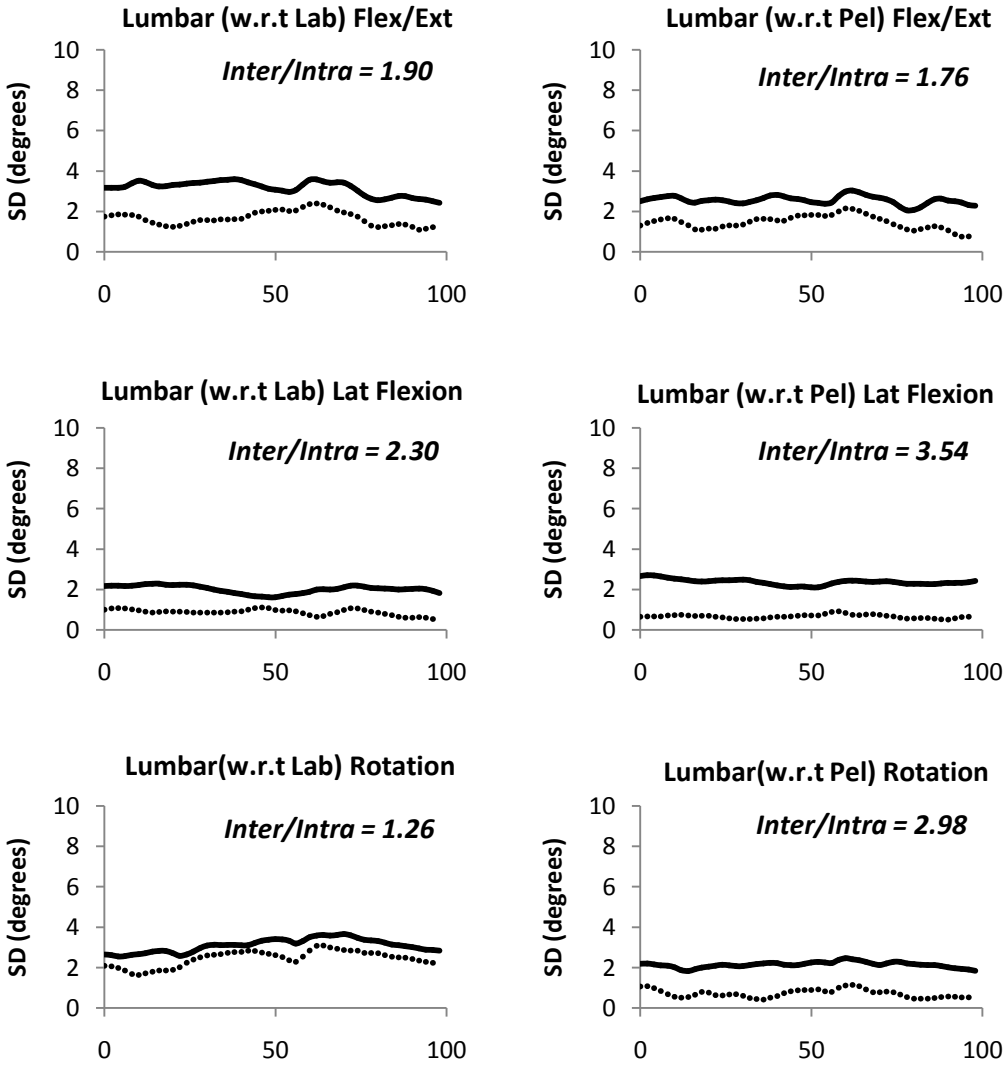

Figure 13-2: Reliability profiles for Lumbar segment kinematic data based on 8 repeat assessments using the approach of Schwartz et al (Schwartz et al., 2004). Dotted – Intra Subject, Black – Inter Subject. Ratio of inter-subject error to intra-subject error is provided (Inter/Intra).

Appendix 13.3: Reliability Profiles for L5/S1 Reactive Force and Moment data

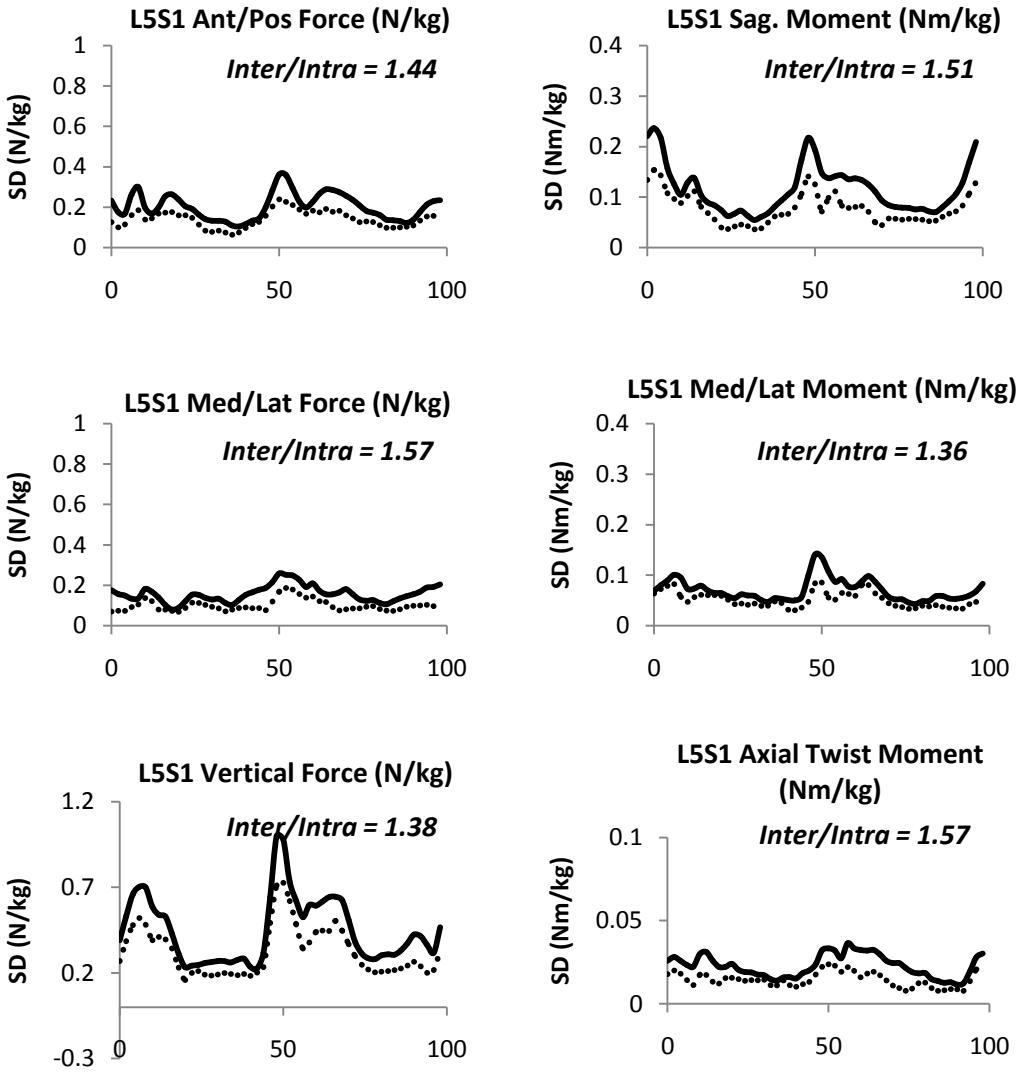

Figure 13-3: Reliability profiles for L5/S1 reactive force data (column 1) and L5/S1 moment data (column 2) based on 8 repeat assessments using the approach of Schwartz et al (Schwartz et al., 2004). Dotted – Intra Subject, Black – Inter Subject. Ratio of inter-subject error to intra-subject error is provided (Inter/Intra).

Appendix 13.4: Mean intra and inter-subject error for thorax and lumbar kinematics and L5/S1 reactive force and moment data

Table 13-1: Mean inter and intra subject error for variables of interest in this study.

Parameter		Mean Intra-subject	Mean Inter-subject	Inter/Intra ratio
Thorax Kinematics	Tnk (w.r.t Lab) Flex/Ext	1.68°	2.62°	1.56
	Tnk (w.r.t Pel) Flex/Ext	1.90°	3.63°	1.91
	Tnk (w.r.t Lab) Lat. Flexion	1.55°	1.95°	1.26
	Tnk (w.r.t Pel) Lat. Flexion	1.63°	2.40°	1.48
	Tnk (w.r.t Lab) Rot.	2.29°	3.70°	1.62
	Tnk (w.r.t Pel) Rot.	2.05°	3.67°	1.79
Lumbar Kinematics	Lumbar (w.r.t Lab) Flex/Ext	1.67°	3.17°	1.90
	Lumbar (w.r.t Pel) Flex/Ext	1.46°	2.56°	1.76
	Lumbar (w.r.t Lab) Lat. Flex	0.88°	2.02°	2.30
	Lumbar (w.r.t Pel) Lat. Flex	0.67°	2.38°	3.54
	Lumbar (w.r.t Lab) Rot.	2.45°	3.10°	1.26
	Lumbar (w.r.t Pel) Rot.	0.72°	2.15°	2.98
L5/S1 Forces	L5/S1 Ant/Pos Force	0.14N/kg	0.20N/kg	1.44
	L5/S1 Med/Lat Force	0.10N/kg	0.16N/kg	1.57
	L5/S1 Vertical Force	0.32N/kg	0.45N/kg	1.38
L5/S1 Moments	L5/S1 Sag. Moment	0.07Nm/kg	0.12Nm/kg	1.51
	L5/S1 Med/Lat Moment	0.05Nm/kg	0.07Nm/kg	1.36
	L5/S1 Axial Twist Moment	0.015Nm/kg	0.023Nm/kg	1.57